THE JOURNAL
OF
CHEMICAL PHYSICS

VOLUME 8 SEPTEMBER, 1940 NUMBER 9

Studies of Equilibrium Solid Solutions in Ionic Lattices[1]

Systems: $KMnO_4-KClO_4-H_2O$ and $NH_4Cl-MnCl_2-H_2O$

ALEXANDER L. GREENBERG AND GEORGE H. WALDEN, JR.
Columbia University, New York, New York

(Received June 20, 1940)

1. The systems, potassium permanganate-potassium perchlorate-water and ammonium chloride-manganous chloride-water, have been studied at equilibrium conditions by phase rule and x-ray diffraction methods. 2. The system potassium permanganate-potassium perchlorate-water yields a continuous series of solid solutions having orthorhombic crystal symmetry. For these, the components of which are of similar crystal and chemical structure and of identical valence type, Vegard's additivity law is followed by the a_0 and c_0 lattice constants, but the b_0 constant shows a definite deviation. 3. A method is described of obtaining homogeneous crystals with a particle size which gives excellent powder diffraction photograms in cases where heat annealing is not feasible. 4. A method of analyzing for ClO_4^- is given. 5. The danger of making serious errors is pointed out in the use of rapid precipitation by chemical reaction or from supersaturated solutions as a method of preparing solid solutions for the study of the relationship between their lattice constants and composition. 6. The system ammonium chloride-manganous chloride-water shows three solid solution series; the crystals obtained in the first series have cubic symmetry, while in the others the symmetry is tetragonal. 7. The mechanism of the formation of the "anomalous" solid solutions between ammonium chloride and manganous chloride is given. Experimental and other considerations verify it. 8. It is shown that Vegard's law is not followed by the first solid solution series in which the components are of dissimilar chemical and crystal structure and dissimilar valence types. The curve for the relationship between the lattice constants and composition rises to a maximum and then falls off. Reasons to explain why this law does not apply to these solid solutions are given. 9. The existence of a new "compound," $6NH_4Cl \cdot MnCl_2 \cdot 2H_2O$, is demonstrated. This and the known compound, $2NH_4Cl \cdot MnCl_2 \cdot 2H_2O$, are considered to be examples of "compounds of variable composition." They are tetragonal with $a_0=15.256 \pm 0.004$A, $c_0=16.008 \pm 0.007$A and $a_0=7.5139 \pm 0.0005$A. $c_0=8.245 \pm 0.003$A, respectively. The structure of the latter is that of $2NH_4Cl \cdot CuCl_2 \cdot 2H_2O$ which belongs to space group $D_4^{14}h$ or $P4mnm$.

INTRODUCTION

EXPERIMENTAL demonstration of the existence of solid solutions rests mainly upon two different kinds of evidence: (1) phase rule investigations, and (2) the determination of the variation of the lattice dimensions of crystalline solid phases with change in composition by x-ray diffraction methods. Numerous experimental investigations have been made by both methods.

One result of the x-ray investigations is Vegard's additivity law,[2a] which states that the unit cell dimensions in a continuous solid solution series vary linearly with the mole fraction of solute present. The validity of this rule rests upon measurements made by Vegard[2a,c] and others,[3]

[1] Dissertation submitted by Alexander L. Greenberg in partial fulfillment of the requirements for the degree of Doctor of Philosophy in the Faculty of Pure Science, Columbia University. Publication assisted by the Ernest Kempton Adams Fund for Physical Research of Columbia University.

[2] (a) L. Vegard, Zeits. f. Physik **5**, 17 (1921); (b) L. Vegard, Zeits. f. Physik **43**, 299 (1927); (c) L. Vegard and H. Dale, Zeits. f. Krist. **67**, 148 (1928).

[3] R. J. Havighurst, E. Mack and F. C. Blake, J. Am. Chem. Soc. **47**, 29 (1925).

almost exclusively on crystals of cubic symmetry. Many deviations from this law have been observed in alloys.[4] The only deviations, in the literature, among ionic lattice crystals are those observed by Walden and Cohen,[5a] and by Walden and Averell[5b] in precipitates of barium sulphate with barium nitrate and with permanganic acid. Since the proof that these precipitates were contaminated through solid solution formation rests upon the observed change in the unit cell dimensions which did not follow Vegard's law,[6] we have investigated by the x-ray method some systems of both isomorphic and nonisomorphic mixing where the solid solution nature of the solid phases could be demonstrated by simultaneously carried out phase rule studies to obtain further data on Vegard's law in ionic lattice crystals.

Precision x-ray data on solid solutions formed in equilibrium with their aqueous solutions has been lacking up to the present time. The work done in recent years by Vegard and his coworkers,[2] Grimm and his associates[7] and others too numerous to mention, in which the solid solutions were formed from water solution either (1) by precipitation of insoluble substances by chemical reaction or (2) by crystallization from supersaturated solutions with little or no attempt at equilibrating the solid phase thus obtained, can safely be called nonequilibrium studies. Coupling this with the statement by Vegard[2b] that "the additivity law is the limiting case of slowly precipitated solid solutions," showed the necessity for studies of solid solutions formed in equilibrium systems so that the experimental conditions would be reproducible. We have attempted to choose systems for investigation resembling as closely as possible the barium sulphate precipitates referred to above. The nearest approach would be a system with components of identical space group symmetry as barium sulphate, limited range of solid miscibility, and with a sufficiently high solubility in water to permit accurate phase rule study. We have not been able to find such a system. Therefore two systems were investigated one of which $KClO_4-KMnO_4-H_2O$, will serve to show how isomorphic crystals behave in forming a complete series of solid solutions, and the other $NH_4Cl-MnCl_2-H_2O$ will demonstrate the behavior of two nonisomorphic solids in a limited series of solid solutions.

This work will concern itself, then, with one of each of the main types of solid solution possible (1) complete miscibility (2) incomplete miscibility. Under (1) the system has components in the solid solutions of similar crystal and chemical structure, of identical valence type and not too different lattice constants. Under (2) the system studied has components of dissimilar valence type, chemical structure, and crystal system; of the type whose solid solutions have been termed "anomalous."

The $KMnO_4-KClO_4-H_2O$ system, for (1), had been described by Muthman and Kuntze[8] and Barker[9] as a system which yields a complete series of solid solutions. Muthman and Kuntze worked out the isotherm at 7° while Barker showed by crystallographic methods that as the weight percent of potassium permanganate in the solid phase increased, the interfacial angles for the crystals increased in a fairly linear fashion. The two salts are orthorhombic and belong to the same space group $V^{16}h$.

Except for qualitative studies by Vegard[2a] on one sample of potassium sulphate-ammonium sulphate orthorhombic solid solutions, the low precision x-ray studies of Wagner[7b] on the nonequilibrium barium sulphate-potassium permanganate complete series of solid solutions and the precision studies on limited, nonequilibrium solid solutions of barium sulphate-barium nitrate and barium sulphate-permanganic acid mentioned above no other x-ray data are available for solid solutions one or more of whose components is orthorhombic.

For (2) the classic system of $NH_4Cl-MnCl_2-H_2O$ was selected. This system has been the

[4] E. R. Jette, Trans. Am. Inst. Mining Met. Eng. **111**, 75 (1934).

[5] (a) G. H. Walden, Jr. and M. U. Cohen, J. Am. Chem. Soc. **57**, 259 (1935); (b) G. H. Walden, Jr. and P. R. Averell, J. Am. Chem. Soc. **59**, 906 (1937).

[6] F. Schneider and W. Rieman, J. Am. Chem. Soc. **59**, 354 (1937).

[7] (a) H. G. Grimm and G. Wagner, Zeits. f. physik. Chemie **132**, 131 (1928); (b) G. Wagner, Zeits. f. physik. Chemie **2B**, 27 (1929); (c) H. G. Grimm and G. Wagner, Zeits. f. anorg. allgem. Chemie **220**, 31 (1934); (d) H. G. Grimm, C. Peters and H. Wolff, Zeits. f. anorg. allgem. Chemie **236**, 57 (1938).

[8] Muthman and Kuntze, Zeits. f. Krist. **23**, 375 (1894).

[9] T. V. Barker, Zeits. f. Krist. **43**, 529 (1907).

subject of much controversy. The formation of "anomalous" solid solutions between the cubic ammonium chloride and the monoclinic $MnCl_2 \cdot 4H_2O$ has interested investigators for the last sixty odd years. Lehman[10] first showed the solid solution character of the solid phase separating from the mother liquor in the ammonium chloride region of the system. Foote and Saxton,[11] by means of phase rule studies of the 25° isotherm and calorimetric data on the solid solutions formed, check this. Clendinnen and Rivett[12] extending this work at 60°C and repeating the 25° isotherm, agreed as to the solid solutions formed.

Benrath and Shackman[13] state that no solid solutions are obtained when ammonium chloride solid is shaken together with a saturated solution of ammonium chloride and manganous chloride; that furthermore if the solid phase is formed by precipitation from the supersaturated solution the percentage of manganous chloride in the solid will decrease to zero if the solid is shaken with the mother liquor for a sufficient length of time. Kuznecov[14] concludes from x-ray data that a contraction in the unit cell size of ammonium chloride takes place when this and manganous chloride form a solid solution.

Experimental: $KClO_4 - KMnO_4 - H_2O$

The x-ray apparatus was essentially the same as described by Walden and Cohen,[5a] the precision focusing cameras were the same as described by them. The method of computing the lattice constants from the films is that described by Cohen.[15]

Chromium radiation was used in taking the x-ray photograms. The values of the wavelengths[16] of the $K\alpha_1$ and $K\alpha_2$ used in the computations are $K_{\alpha 1} = 2.285{,}03$A, $K_{\alpha 2} = 2.288{,}91$.

Each of materials used in the preparation of the solid solutions was recrystallized twice. This precaution was taken because of the large amount of manganese dioxide in the reagent grade potassium permanganate and the presence of chloride ion in the potassium perchlorate. After this treatment the permanganate when dissolved and filtered through a sintered glass funnel showed no sign of manganese dioxide, while the perchlorate showed no trace of chloride ion (against silver nitrate in nitric acid).

The thermostat used in equilibrating the samples was held at 25.000°±.055°. The thermometer used was checked against a platinum resistance thermometer calibrated by the National Bureau of Standards.

The samples were prepared by making solutions at an elevated temperature of such concentration as to be supersaturated at 25°C. These solutions were placed in glass stoppered bottles, allowed to cool to room temperature, sealed with paraffin, and brought to equilibrium at 25°C in a thermostat while being continuously tumbled end over end. The approach to equilibrium was followed by determining the MnO_4^- content of the liquid phase at intervals. The process required about $1\frac{1}{2}$ months and produced a solid phase which was coarsely crystalline and did not give sharp x-ray diffraction patterns. Grinding the solid made matters much worse in this latter respect. Annealing at temperatures sufficiently low to avoid decomposition was found to be without effect. The following procedure was found to produce solid phases which gave satisfactory x-ray patterns, and at the same time to accelerate greatly the approach to equilibrium. By this procedure samples were prepared as above and allowed to equilibrate for a few days, after which time the solid phases were filtered off on sintered glass filters, dried by drawing air through them, crushed in an agate mortar to below 100 mesh and returned to the mother liquor. The bottles were then replaced in the equilibrating machine. Equilibrium was found to be established within two weeks.

Sampling of the liquid and solid phase

For removing samples of the liquid phase for analysis, a modified form of the weight-pipette described by Kiehl and Manfriedo[17] was used.

[10] O. Lehman, Zeits. f. Krist. **8**, 438 (1883).
[11] H. W. Foote and B. Saxton, J. Am. Chem. Soc. **36**, 1695 (1914).
[12] F. W. J. Clendinnen and A. C. D. Rivett, J. Chem. Soc. **119**, 1329 (1921).
[13] A. Benrath and H. Schachman, Zeits. f. anorg. allgem. Chemie **221**, 418 (1935).
[14] V. G. Kuznecov, Comptes rendus Acad. Sci. U. R. S. S. **15**, 469 (1937).
[15] M. U. Cohen, Rev. Sci. Inst. **6**, 68 (1935); M. U. Cohen, Zeits. f. Krist. **A94**, 288 (1936).
[16] Int. Tab. Kryst. Best. Vol. 11, p. 586.
[17] S. J. Kiehl and E. J. Manfriedo, J. Am. Chem. Soc. **59**, 2118 (1937).

This permits the taking of a sample of the solution without removing the bottle from the thermostat; to prevent the solid phase from being drawn into the pipette, a sintered-glass filter plug was sealed on to the tube used for sucking up the sample.

Schreinemakers' wet residue method[18] was used in the analysis of the solid phase which was separated from the mother liquor by filtration through a sintered glass funnel but not dried. A portion of the wet solid was transferred to a weighing tube and delivered from there to flasks by means of a platinum spatula. The remaining solid was dried on the funnel by sucking air over it for x-ray analysis.

Methods of analysis

The determination of the MnO_4^- was carried out by adding 0.1 *M* ferrous sulphate solution to a slight excess and back-titrating with standard 0.1 *M* ceric ammonium sulfate solution to the *o*-phenanthroline ferrous complex end point.

After trial of many of the methods given in the literature, a modification of the method proposed by Rosenberg[19] was evolved for the determination of ClO_4^-. The ClO_4^- was reduced by passing sulphur dioxide over the surface of a solution of the sample in 25 ml of water containing 2–3 ml of 1 *M* sulphuric acid. The excess sulphur dioxide was boiled off by evaporating to a small volume, the sample was then diluted to a volume of 25 ml and 50 ml of concentration. Sulphuric acid was added and the air displaced with carbon dioxide. Blank runs were made at the same time as the sample runs (with 25 ml of distilled water and 50 ml concentrated sulphuric acid). After the air was removed, approximately 25 ml of titanous chloride solution (approximately 0.25 *M*, made up in 1 *M* sulphuric acid) was added to the sample and 15 ml to the blank (approximately the amount to be determined in the sample flasks after the reduction of the ClO_4^-). The flask was heated for two hours so that there was gentle refluxing, during which time carbon dioxide was continuously passed through at a slow rate. After this time, the flask was allowed to cool to room temperature with a stream of carbon dioxide going through.

Table I.

Sample No.	Weight % $KMnO_4$		Weight % $KClO_4$		Weight % $KMnO_4$ in Solid Phase (extrap. on ternary diagram)
	Liquid Phase	Solid Phase	Liquid Phase	Solid Phase	
1	0.4712	1.032	1.868	76.21	1.2
2	2.065	7.075	1.381	82.15	7.7
3	2.651	10.59	1.230	77.64	11.8
4	2.628	10.71	1.245	75.77	12.0
5	4.009	22.28	0.9777	58.49	26.8
6	4.573	32.76	0.8434	52.07	38.2
7	4.864	38.12	0.7816	46.83	44.4
8	5.698	60.29	0.5872	28.21	68.0
9	5.732	62.70	0.5548	26.48	70.2
10	6.333	76.94	0.3582	13.96	84.5

The sample was then diluted with 25 ml of air-free distilled water and standard 0.1 *M* ceric ammonium sulphate solution was added to a slight excess, while a current of carbon dioxide was passed over the surface of the solution in the flask. The excess was back-titrated with 0.1 *M* ferrous sulphate solution, by using *o*-phenanthroline ferrous complex indicator. The end point is extremely sharp at the concentration of sulphuric acid present in the solution (approximately 9 *M*). The reason for making up the titanous chloride solution in sulphuric acid rather than in hydrochloric acid is to avoid the large amount of HCl which boils off from the solutions during the heating and which, when used, gave us erratic results.

All volumetric apparatus and weights used in the analytical work was calibrated. The ceric ammonium sulfate solution was standardized against National Bureau of Standards sodium oxalate according to the method described by Walden, Hammett and Chapman.[20]

Results of analysis

The results of the analysis are given in Table I. Each value is the mean of two analyses on each sample of the liquid and of the wet residues for both MnO_4^- and ClO_4^-. The precision measures for the deviation from the mean of the liquid phase determinations were 2 parts per 1000 for MnO_4^- and ClO_4^-, for the solid phase 5 parts per 1000.

[18] F. A. H. Schreinemakers, Zeits. f. physik. Chemie **11**, 81 (1893).

[19] A. Rosenberg, Zeits. f. anal. Chemie **90**, 103 (1932).

[20] G. H. Walden, L. P. Hammett and R. P. Chapman, J. Am. Chem. Soc. **55**, 2649 (1933).

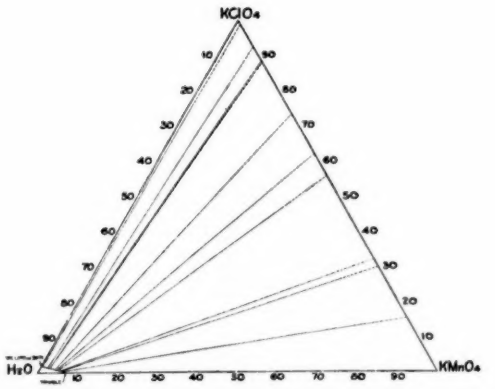

FIG. 1. The values for the solubility at 25°C of pure potassium perchlorate and potassium permanganate, which are plotted are given by H. H. Willard and G. F. Smith (J. Am. Chem. Soc. **45**, 286 (1923)) and H. M. Trimble (J. Am. Chem. Soc. **44**, 451 (1922)), respectively.

These results are plotted on the triangular diagram Fig. 1, weight percentage is used in order to show the tie-lines to better advantage; and by weight percent of potassium permanganate in the liquid phase against weight percent of potassium permanganate in the solid phase (obtained by extrapolation on the ternary diagram) in Fig. 2.

X-ray results

Every measurable line on the x-ray photograms was used in the computation of the lattice constants of the solid solutions, but no fewer than ten and as many as twenty-six pairs of lines were used in any one case. The range of the probable errors on the individual films was:

$$a_0 = \pm 0.004 - 0.03\%, \quad b_0 = \pm 0.005 - 0.04\%,$$
$$c_0 = \pm 0.003 - 0.02\%.$$

However, since the values of the lattice constants obtained from different films for a single substance did not always check within these probable errors, the values given in Table II are mean values of all films taken on each sample and the a. d. given is the average deviation from the mean of the lattice constants obtained from the different films.

These results are plotted against weight percent of potassium permanganate in the solid phase (extrapolated from the ternary diagram) in Fig. 3.

Discussion of results

From the ternary plot Fig. 1, is seen that a complete series of solid solutions of potassium

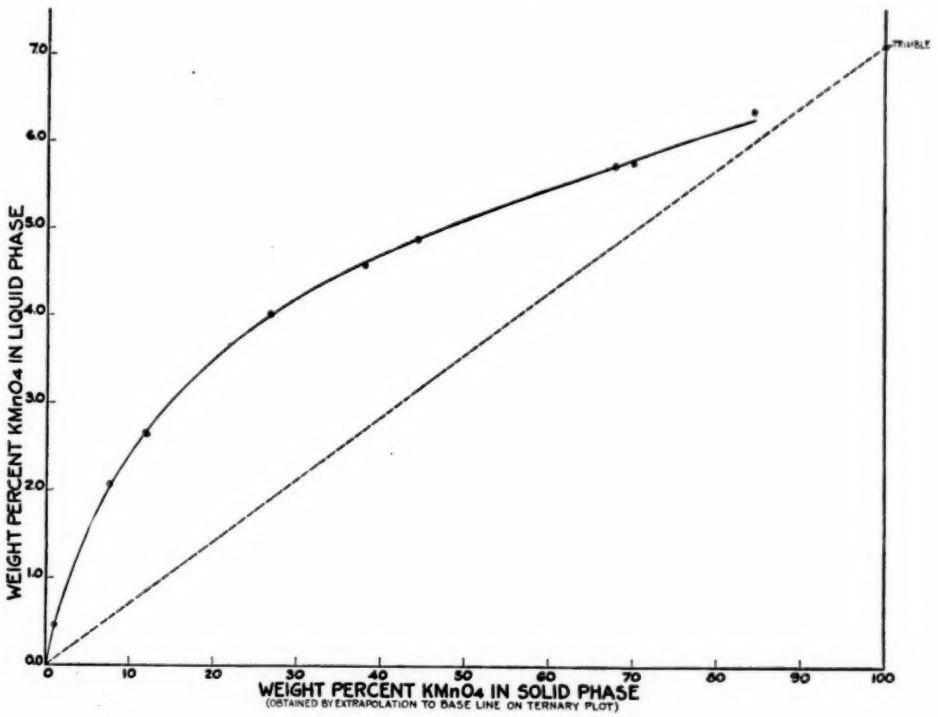
WEIGHT PERCENT KMnO4 IN LIQUID PHASE
WEIGHT PERCENT KMnO4 IN SOLID PHASE
(OBTAINED BY EXTRAPOLATION TO BASE LINE ON TERNARY PLOT)
TRIMBLE

FIG. 2. $KMnO_4 - KClO_4 - H_2O$.

TABLE II. *Lattice constants (A). Mean values 23–29°C.*

SAMPLE NO.	MEAN OF	a_0	b_0	c_0
$KClO_4$	3 films	8.837±.003	5.6521±.0004	7.240±.002
1	5 films	8.843±.003	5.6531±.0007	7.243±.001
2	2 films	8.859±.007	5.6574±.0008	7.255±.001
3	2 films	8.866±.003	5.6590±.0005	7.260±.001
4	2 films	8.865±.000	5.6596±.0006	7.265±.002
5	1 film	8.902	5.6690	7.294
6	1 film	8.931	5.6777	7.311
7	1 film	8.955	5.6803	7.320
8	2 films	9.007±.001	5.6940±.0016	7.360±.000
9	2 films	9.015±.001	5.6958±.0013	7.363±.001
10	3 films	9.054±.001	5.7030±.0008	7.389±.001
$KMnO_4$	3 films	9.099±.002	5.7076±.0003	7.411±.001

permanganate and potassium perchlorate are formed. This is also shown by plotting the results differently, as in Fig. 2. Also, from Fig. 2 we see that the liquid phase always contains a larger percentage by weight of potassium permanganate than the solid which, according to Roozeboom's[21] classification of solid solutions, places the system under Type I.

Our work at 25°C does not show the presence of either a congruent point or of a definite crystallization end point as shown in the paper by Muthman and Kunzte[8] at 90 mole percent potassium permanganate on their 7° isotherm for the system, but since this region was not investigated thoroughly our evidence does not eliminate the possibility of its existence.

Figure 3 demonstrates conclusively that the solid solutions formed in this equilibrium system follow Vegard's additivity law quite exactly in the case of the a_0 and c_0 constants but for the b_0 constants a small deviation is observed, the curve being slightly convex.

It may be pointed out that there is great danger of making serious errors in studying solid solutions prepared by rapid precipitation through chemical reaction or from supersaturated solutions to determine the relationship between the lattice constants and composition. In such solid solutions, homogeneous distribution of the components is not to be expected, as shown by Hahn's discussion[22] of the results obtained by his coworkers. In our work it was shown that the crystals, which were first formed on cooling the supersaturated solution while this was being tumbled in the thermostat, gave very poor x-ray diffraction patterns, the lines being broad and diffuse. But after being crushed and returned to the mother liquor for equilibration over a period of two weeks or more, the crystals obtained gave sharp x-ray diffraction lines. This is in complete accord with the results given in the papers by Mumbrauer *et al.*,[22] which describe the conditions for obtaining homogeneous solid solutions.

In rapidly formed solid solutions which are not further treated to homogenize the components, then, the best that can be expected is to get experimental indications that the lattice is expanded in a more or less regular fashion by the entrance of contaminent. Inhomogeneous crystals will, of course, never give a true relationship between the weight percentage composition (as determined by analysis of the entire crystal) and the lattice constant (determined by x-ray reflection from the first few hundred surface layers). This seems to be indicated by the work

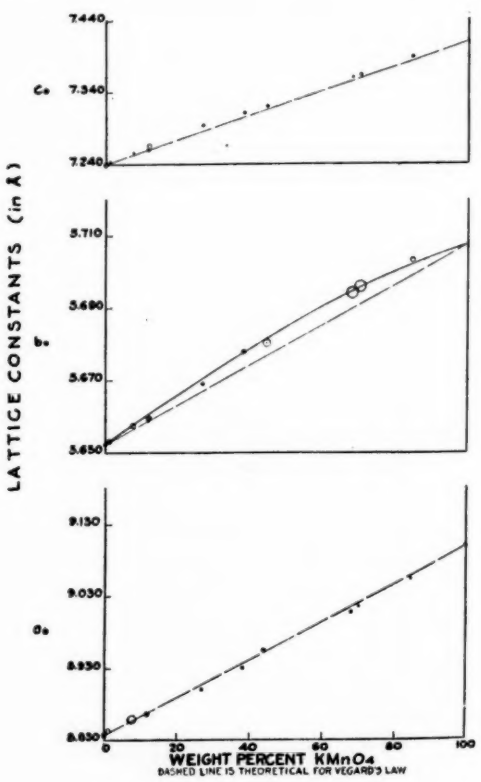

FIG. 3. $KMnO_4-KClO_4-H_2O$.

[21] H. W. B. Roozeboom, Zeits. f. physik. Chemie **8**, 521 (1891).

[22] (a) O. Hahn, *Applied Radio Activity* (Cornell University Press, Ithaca, N. Y., 1936), p. 70 on, for complete discussion and bibliography.

TABLE III.

SAMPLE NO.	TIME IN THERMOSTAT	% Cl^-		% NH_4Cl		% $MnCl_2$ (CALC.)	
		LIQUID	SOLID	LIQUID	SOLID	LIQUID	SOLID
2	3 weeks	19.28	53.02	26.22	78.31	3.365	1.968
4	4 "	20.12	43.74	23.53	61.49	8.026	5.292
5	5 "	20.67	46.71	22.04	63.43	10.76	8.267
6	2 "	21.35	43.22	20.89	56.58	13.32	10.14
7*	8 "	21.43	50.74	20.27	65.54	14.19	12.94
7–3	3 "	21.51	41.40	20.25	45.60	14.36	19.82
7–2	3 "	21.30	39.89	19.81	43.26	14.50	19.90
7–1	3 "	21.34	38.88	19.72	41.30	14.66	20.41
7–A	3 "	21.33	43.98	19.51	47.52	14.91	22.15
8	5 months	21.32	44.55	19.07	48.13	15.40	22.44
10	4 "	21.42	47.42	18.09	50.64	16.73	24.58
12	3½ "	21.60	42.70	17.10	44.03	18.21	23.98
14	3½ "	21.78	42.08	16.31	41.13	19.46	26.28
16	3½ "	22.18	38.19	15.94	34.70	20.62	26.94
18	3½ "	22.32	44.59	15.04	38.93	21.91	33.33
22	3½ "	22.41	48.35	13.90	39.30	23.42	39.57
26	2 weeks	22.52	42.06	10.22	29.30	27.95	40.16
29	2 "	23.44	45.43	5.860	30.62	34.70	44.61
31	2 "	24.81	46.72	3.977	31.05	39.34	46.38
33	2 "	26.29	33.66	2.978	1.387	43.16	58.11

* Sample No. 7 was shown to consist of two solid phases, one isotropic and the other birefringent, when examined under the microscope between crossed Nicols. The second solid phase was present in so small an amount that no new lines were observed on x-ray photograms of this sample, only lines corresponding to the ammonium chloride structure were found. This sample fixes the invariant point on the liquidus curve (marked *b*, Fig. 4) for the condensed system at constant temperature.

of Walden and Averell[5b] where rapid precipitation was the method used for the preparation of the solid solutions. Furthermore, in Vegard's paper[2(b)] on the mercuric bromide-mercuric chloride solid solution series is presented evidence for this hypothesis, in that the crystals formed by rapid precipitation gave lattice constants which scattered badly when plotted against the weight percentage composition, while crystals prepared by slow precipitation gave consistent values for the lattice constants which corresponded almost exactly with those predicted by the additivity law. Vegard explained the discrepancy of the results for the rapidly precipitated crystals, on the basis of "uncompensated" surface atoms in the much finer solids obtained in this way. He attributed the increase in line width on the x-ray diffraction patterns given by these crystals to smaller particle size. From consideration of the above, we are inclined to explain the deviation from the additivity law and the line broadening on the x-ray films for these crystals to inhomogeneity of the solid solutions.

EXPERIMENTAL: $NH_4Cl-MnCl_2-H_2O$

Using the triangular phase diagram of the 25° isotherm of the $NH_4Cl-MnCl_2-H_2O$ system as given by Clendinnen and Rivett,[12] supersaturated solutions of ammonium chloride and manganese chloride in water were prepared to give approximately 8 g of solid phase to 400 ml of liquid phase when cooled to 25°C. The points chosen were well spaced to cover the entire range of the first two solid solution regions as shown by their diagram. Analytical reagent grade ammonium chloride and $MnCl_2 \cdot 4H_2O$ were of sufficient purity for the work without recrystallization.

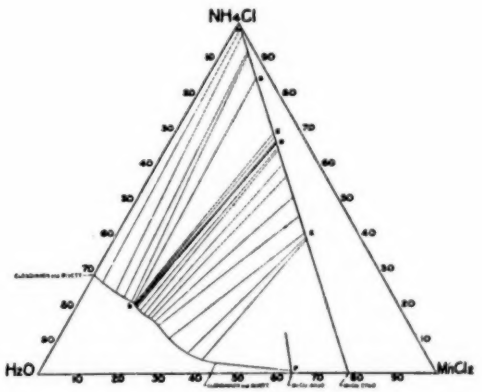

FIG. 4.

The same procedure, used for the $KMnO_4-KClO_4-H_2O$ system, was followed in regard to thermostating the samples, crushing the solid phases to below 100 mesh and then replacing in the mother liquor, determination of achievement of equilibrium, methods of sampling and so forth.

Only one change in the procedure under sampling was adopted; after removing sufficient moist solid phase for analysis by the Schreinemakers method, the remaining solid was washed with alcohol and then with ether (which had no effect on the x-ray photograms obtained as shown by films taken on air-dried samples and the same samples dried by alcohol and ether) and then quickly dried by sucking air through the filter.

For studies of the compounds and the low angle reflections of the first solid solution series in this system, a vacuum type Debye-Scherrer camera was used.

Methods of analysis

Manganese was determined by the bismuthate method of Park.[23] The permanganate was titrated to a slight excess of 0.1*M* ferrous sulphate solu-

[23] B. Park, J. Ind. Eng. Chem. **18**, 597 (1926).

tion and this in turn back-titrated with standard 0.1*M* ceric ammonium sulphate solution using *o*-phenanthroline ferrous complex indicator. Ammonia was determined by distillation from strong alkali solution into standard 0.1*M* hydrochloric acid solution. The total amount of chloride was determined by the Volhard method as modified by Caldwell and Moyer.[24] The determinations were always run in duplicate for Mn^{++} and NH_4^+ while triplicate samples were used in the Cl^- determination.

Results of analysis

It was found that the analysis of the samples for all three ions; Cl^-, NH_4^+, and Mn^{++}, was unnecessary since the checks were good, so the analysis for Mn^{++} was not continued and only NH_4^+ and Cl^- were determined except in the case of the compounds formed where complete analysis was desired. Table III gives the results obtained for the analysis of liquid and moist solid phases.

Figure 4 shows these results plotted on a triangular diagram. In Fig. 5 is plotted weight percent ammonium chloride in the solid phase (obtained by extrapolation to the $MnCl_2 \cdot 2H_2O$ base line on the ternary plot) against weight percent ammonium chloride in the liquid phase (from analysis).

To establish the state of hydration of the compounds shown on the phase diagram, Fig. 5, namely *D*, *E* and *F*, complete analyses were run in duplicate on the solid phases of samples 7*A*, 26 and 33, respectively (dried by washing with alcohol and ether and then sucking air over them). Table IV gives the results of these analyses in weight percent.

The results shown in Tables III and IV and plotted in Figs. 4 and 5 demonstrate the following features of the system:

1. Starting with pure ammonium chloride (point *A*) there is a solid solution range which terminates at point *B*. At point *B* a second solid phase appears and initiates a new short solid solution range at point *C* which terminates at point *D*. This series belongs to Type IV, Roozeboom's classification,[21] *BC* (Fig. 5) being the boundary between the two conjugate solid solutions.

[24] J. R. Caldwell and H. V. Moyer, Ind. and Eng. Chem. Anal. Ed. **7**, 38 (1935).

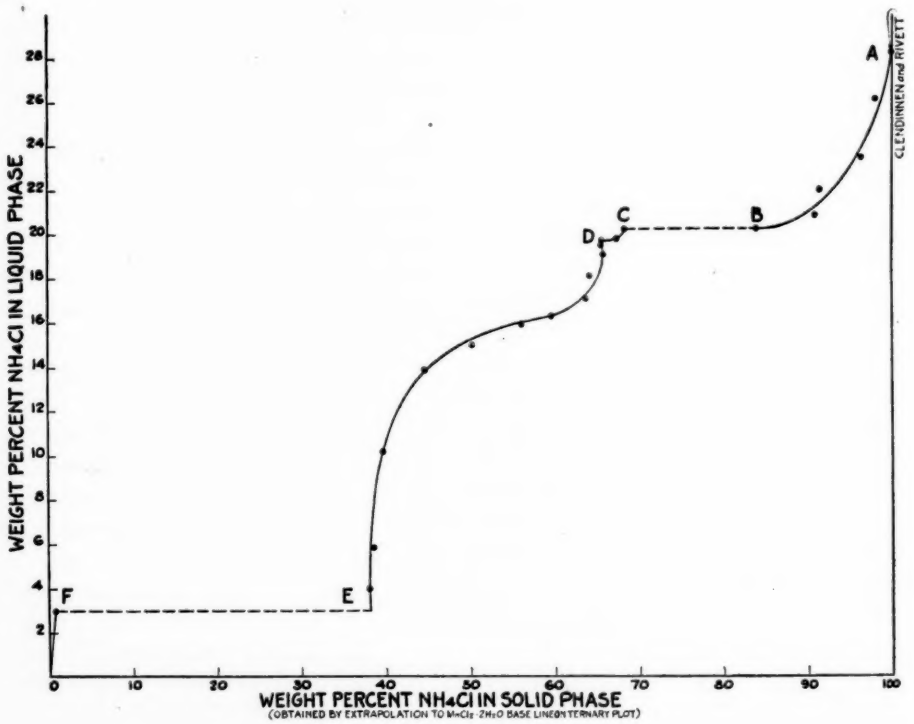

FIG. 5. $NH_4Cl - MnCl_2 - H_2O$.

TABLE IV. *Complete analysis of the substances at D, E and F.**

POINT ON PLOT	SAMPLE NO.	WT. % Cl^-	WT. % NH_4^+	WT. % Mn^{++}	TOTAL WT. % FOUND	% H_2O BY DIFFERENCE	THEORETICAL FOR THE COMPOUND
D	7*A*	58.60±.14	22.21±.03	11.43±.001	92.24	7.76	$6NH_4Cl \cdot MnCl_2 \cdot 2H_2O = 7.46$
E	26	52.99±.06	13.74±.01	19.89±.01	86.62	13.38	$2NH_4Cl \cdot MnCl_2 \cdot 2H_2O = 13.40$
F	33	37.51±.01		28.31±.04	65.82	34.18	$MnCl_2 \cdot 4H_2O = 36.42$

* The analytical data of Foote and Saxton, reference 11, have been accepted as fully proving that whenever a mole of manganous ion enters the solid solutions (*A–B*, Fig. 5), 2 moles of water go in also. This situation holds across the 25° diagram from point *A* to point *E*, as shown by the analysis of the solid phases at *D* and *E*, given in the table above.

2. The solid phase at point *D* is a double salt having the formula $6NH_4Cl \cdot MnCl_2 \cdot 2H_2O$. This compound exhibits incongruent solubility.

3. Between points *D* and *E* is a third solid solution range. This series belongs to Type II, Roozeboom's classification.[21]

4. The solid phase at *E* is a second double salt having the composition $2NH_4Cl \cdot MnCl_2 \cdot 2H_2O$. This compound also exhibits incongruent solubility.

5. At point *F* the solid phase is the hydrate $MnCl_2 \cdot 4H_2O$.

Our phase diagram while bearing great similarity to Foote and Saxton's,[11] and Clendinnen and Rivett's[12] exhibits certain marked differences. Our boundary (*B–C*) between the first two series of solid solutions is shifted towards the ammonium chloride end. Then there is the recognition of a short series of solid solutions (*C–D*) and the hitherto unobserved compound at *D*, $6NH_4Cl \cdot MnCl_2 \cdot 2H_2O$ which the previous workers missed. The solid solution series, *D–E*, is a complete one between the $6NH_4Cl \cdot MnCl_2 \cdot 2H_2O$ and the $2NH_4Cl \cdot MnCl_2 \cdot 2H_2O$. The remainder of the diagram checks very closely with that of Clendinnen and Rivett[12] at 25°C. The solubilities of ammonium chloride and $MnCl_2 \cdot 4H_2O$ as determined by them are used on our plots and, as can be seen, fit in extremely well on the liquidus curve, Fig. 4.

All the solid phases prepared in the phase rule investigation were studied by means of x-ray powder diffraction methods described above. This investigation disclosed the following facts:

1. The solid phases in the solid solution range *AB* have an ammonium chloride lattice, no other lines appearing on any of the films. The lattice constants as computed from precision camera films are shown in Table V and are plotted in Fig. 6 against the weight percent of $MnCl_2 \cdot 2H_2O$ (obtained by extrapolation on the ternary plot). This shows that the change in the lattice constants does not follow Vegard's law but increases with addition of $MnCl_2 \cdot 2H_2O$ to a maximum and then decreases slightly. The variation of lattice constant with composition is small, 0.08 percent maximum at a concentration of 13 weight percent $MnCl_2 \cdot 2H_2O$.

The range of the probable errors on the individual films is $a_0 = \pm 0.0015$ percent to ± 0.008 percent. As in the case of the $KMnO_4 - KClO_4$ solid solutions, the values for the lattice constants obtained from all the films on any one sample were averaged and the mean values are those given in Table V. The average deviation given is the a.d. of the mean lattice constant and not the probable error. The radii of the circles on Fig. 6 gives the a.d. of the mean.

2. The solid phase appearing at *C* has a lattice of lower than cubic symmetry. Visual examination of the films shows no differences between any of the solid phases from *C* to *D*.

3. The compound *D* is tetragonal, $a_0 = 15.256 \pm 0.004$, $c_0 = 16.008 \pm 0.007$, $c_0/a_0 = 1.05$ from a Debye-Scherrer film taken with calcium radiation. Further elucidation of the structure must

TABLE V. *Mean values of the lattice constants of first solid solution series. Temp. 25°–29°.*

SAMPLE NO.	a_0 (MEAN VALUE)	MEAN OF	WT. % $MnCl_2 \cdot 2H_2O$ (PLOT)
NH_4Cl	3.8680±.0003	6 films	
No. 2	3.8687±.0003	5 films	1.9
No. 4	3.8691±.0003	15 films	3.7
No. 5	3.8699±.0005	2 films	8.5
No. 6	3.8714±.0001	2 films	9.1
No. 7	3.8708±.0007	4 films	16.0

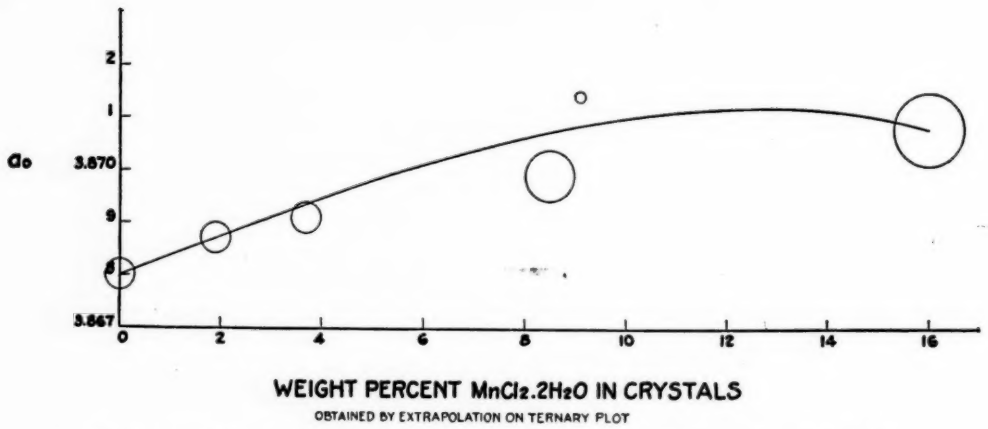

FIG. 6. Lattice constants of solid solutions $A-B$ against weight percent $MnCl_2 \cdot 2H_2O$.

await the preparation of single crystal diffraction films. We were unable to prepare these since we could never obtain single crystals. All attempts to grow single crystals resulted in samples which, while they resembled crystals macroscopically, were found to be complicated structures resulting from multiple twinning when examined under the microscope between crossed Nichols.

4. Samples in the solid solution range between D and E gave rather unsatisfactory films with weak and diffuse lines. They appear to exhibit a gradual transition from the diffraction pattern of the compound $6NH_4Cl \cdot MnCl_2 \cdot 2H_2O$ to that of the compound $2NH_4Cl \cdot MnCl_2 \cdot 2H_2O$.

5. The compound $2NH_4Cl \cdot MnCl_2 \cdot 2H_2O$ is tetragonal, $a_0 = 7.5139 \pm 0.0005$, $c_0 = 8.245 \pm 0.003$, $c_0/a_0 = 1.09$ from a precision camera film taken with chromium radiation. The compound is isomorphic with and has the same structure as the compound $2NH_4Cl \cdot CuCl_2 \cdot 2H_2O$ as is shown by the comparison data in Table VI, obtained from Debye-Scherrer films taken with calcium radiation.

Interpretation of results

A very revealing light is shed upon the complexities of this system by consideration of the structure of the compound $2NH_4Cl \cdot MnCl_2 \cdot 2H_2O$. As noted above the structure is undoubtedly that of the corresponding cupric compound which was determined by Hendricks and Dickinson,[25] and is shown in Fig. 7. It will be seen that this structure is obtained from that of ammonium chloride in the following manner: Consider two ammonium chloride unit cubes having a common face and with chloride ions at the corners. A manganous ion is placed in the common face in the center of the four chloride ions. Water molecules are substituted for the ammonium ions in the body centers. This arrangement is shown in Fig. 8. The structure in Fig. 7 will be seen to be an alternation of this arrangement with the unmodified ammonium chloride arrangement. In such a unit the Mn^{++} would have a coordination number of six.

TABLE VI.

CALCIUM RADIATION							
$2NH_4Cl \cdot CuCl_2 \cdot 2H_2O$ $a_0 = 7.583 \pm 0.002$ $c_0 = 7.950 \pm 0.002$*				$2NH_4Cl \cdot MnCl_2 \cdot 2H_2O$ $a_0 = 7.514 \pm 0.001$ $c_0 = 8.247 \pm 0.002$ (SAMPLE NO. 26)			
LINE NO.	PLANE AND SOURCE	EXP. $\sin^2\theta$	REL. INTENSITY	LINE NO.	PLANE AND SOURCE	EXP. $\sin^2\theta$	REL. INTENSITY
1	101α	0.09272	9	3	101α	0.09105	8
2	110α	.09722	6	4	110α	.09881	4
3	002α	.1772	5	5	002α	.1654	6
5	112α	.2755	6	6	112α	.2643	4
6	121α	.2888	6	7	121α	.2907	4
7†	$202\beta \rightarrow 202\alpha$	.3732	4	8	$202\beta \rightarrow 202\alpha$	.3640	5
8	$220\beta \rightarrow 220\alpha$	.3902	5	9	$220\beta \rightarrow 220\alpha$	.3990	6
9	202α	.3731	10	10	202α	.3642	10
10	220α	.3914	10	11	220α	.3980	10
13	222α	.5697	8	15	222α	.5638	9
14	123α	.6453	6	16	123α	.6197	5
15	231α	.6810	8	19	231α	.6885	8
17	400α	.7827	10	21	400α	.7958	10

* Our values for the lattice constants of this substance obtained from this film agree with those given by Hendricks and Dickinson as $a_0 = 7.58$ and $c_0 = 7.96$.

† In all such tables in this paper the $K\beta$ reflections have been converted to the equivalent $K\alpha$, by multiplying $\sin^2\theta$ by $(\lambda K\alpha/\lambda K\beta)^2$, which for calcium radiation is 1.18 157.

[25] S. B. Hendricks and R. G. Dickinson, J. Am. Chem. Soc. **49**, 2149 (1927).

The structure of this compound points clearly to the mechanism by means of which increasing amounts of $MnCl_2 \cdot 2H_2O$ are taken up by ammonium chloride. In the solid solution series *A–B*, the interstitial inclusion of Mn^{++} in the ammonium chloride lattice and the simultaneous substitution of H_2O for NH_4^+ occurs at random. After the phase boundary *BC* is crossed the solid phase gives a new diffraction pattern corresponding to tetragonal symmetry and greatly increased cell size. It should be noted, however, that the axial ratio is very close to unity and that the length of the cell edge is very closely four times that of ammonium chloride. While we are not able to give a definite structure for this solid phase, the change in symmetry must be due to the appearance of an ordered arrangement of the altered ammonium chloride cubes.

The continuous solid solution series between *D* and *E* is very interesting because of the very large

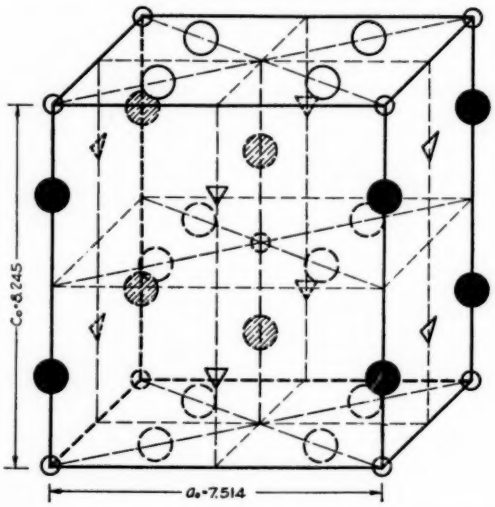

FIG. 7. Small open circle, Mn^{++}; triangle, NH_4^+; solid circle, oxygen (water); large open circle, Cl^-. Hidden and interior atoms are designated by dashed lines.

changes in the diffraction pattern due to the fact that the edges of the unit cell at *D* have twice the lengths of the corresponding edges at *E*. We can see no explanation for what happens except the assumption that, as more and more manganous chloride is included, an ordered arrangement of the altered ammonium chloride cubes having tetragonal symmetry is maintained and this basic pattern contracts as the proportion of ammonium chloride decreases.

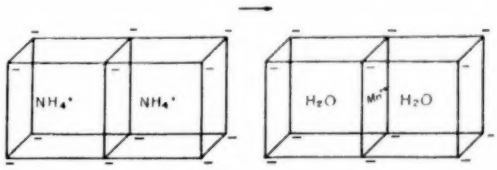

FIG. 8.

That the process described above would be expected to cause little change in the chloride ion lattice is apparent from the following considerations:

(a) The value for the radius of Cl^-, 1.86A, in ammonium chloride where each Cl^- is coordinated with 8 NH_4^+, is obtained by increasing the value, 1.81A, for the radius of Cl^- with a coordination number of six[26] by a factor[27] of 3 percent. Figure 9, showing the Cl^- positions on the unit cell side of pure ammonium chloride is drawn to scale using $a_0 = 3.868$A obtained above, and this radius for Cl^-. The space available at the face center between the chloride ions would accommodate an ion having a radius of approximately 0.87A. The value[26] for the radius of Mn^{++} with a coordination number of six is 0.80A and is drawn on Fig. 9 in a dashed line circle. No great change in the chloride ion lattice is to be expected from this source.

(b) The radius of NH_4^+ with a coordination number of 8 is 1.52A, calculated, as above, from the 6 coordination numbered radius given[26] as 1.48A. In ice, the positions assigned to each oxygen atom, from crystal structure work[28] is such that each oxygen atom is tetrahedrally surrounded by four other oxygen atoms at a distance of 2.76A. This holds for water of crystallization as shown by the work of Beevers and Lipson[29] on $BeSO_4 \cdot 4H_2O$, the work of Keggin[30] and of Bradley and Illingworth[31] on $H_3PW_{12}O_{40} \cdot 5H_2O$, $H_3PW_{12}O_{40} \cdot 29H_2O$ and related substances. The radius of a water molecule is, therefore, 1.38A at a coordination number of 4.

[26] Linus Pauling, *Nature of the Chemical Bond* (Cornell University Press, 1939), pp. 326 and 330.
[27] L. Pauling, reference 26, p. 334. Also see V. M. Goldschmidt *Geochemische Verteilungsgesetze der Elemente.*
[28] L. Pauling, reference 26, p. 281; see also J. O. Bernal and R. H. Fowler, J. Chem. Phys. **1**, 515 (1933).
[29] C. A. Beevers and H. Lipson, Zeits. f. Krist **82**, 297 (1932).
[30] J. F. Keggin, Proc. Roy. Soc. London **A144**, 75 (1934).
[31] A. J. Bradley and J. W. Illingworth, Proc. Roy. Soc. London **A157**, 113 (1936).

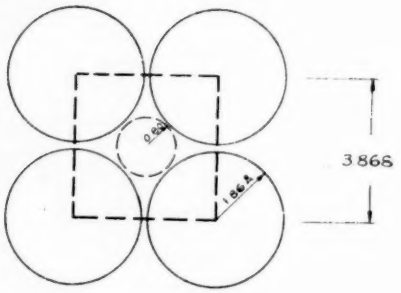

FIG. 9. NH_4Cl.

Increasing this by a factor of 5.8 percent, and then by 3 percent (Goldschmidt[27]) there is obtained 1.50A, the value for the radius of water having a coordination number of 8. The radius of the NH_4^+ and of water are then practically the same and substitution of NH_4^+ by water in the unit above should give only very small changes in the chloride ion lattice.

These considerations of ionic size alone should not be taken as exact as is shown by the fact that the body diagonal distance between NH_4^+ and Cl^- in NH_4Cl calculated from the x-ray data from the relationship $(\sqrt{3}/2)a_0$ gives 3.35A while the sum of the ionic radii gives 3.38A. Consideration of the changes in the electrostatic fields of force when NH_4^+ is replaced by a water molecule and the polarization effects when Mn^{++} is inserted between the chloride ions would be necessary for a complete picture of all that happens. Such an analysis will not be attempted here.

Densities of the solid solutions, A–B, and the compounds at A, D, and E

To provide further evidence for this mechanism, density determinations on the solid phases in the series *A–B* and of the substances at *A*, *D* and *E* were made. The method used was that of Jette and Foote.[32] Duplicate determinations were performed in three instances to determine the precision of the results. This is indicated in Table VII and Table VIII where the data obtained are summarized. The densities for the solid solutions were calculated from the x-ray data given in Table V for the cases of substitutional solid solution of $MnCl_2 \cdot 2H_2O$ in the lattice of NH_4Cl, of interstitial solid solutions and for the case where the water molecules substitute for the ammonium ions, while the manganous ion is inserted interstitially. These values are shown in Table VII under the heading Density calc. I, II and III, respectively.

The calculated densities of the compounds at *D* and *E* given in Table VIII were computed for the unit cell size given above with 8 molecules to the unit cell of the $6NH_4Cl \cdot MnCl_2 \cdot 2H_2O$ compound and with 2 molecules to the unit cell of the $2NH_4Cl \cdot MnCl_2 \cdot 2H_2O$ compound.

The mechanism of solid solution postulated above, where a substitution of water molecules takes place for NH_4^+ while Mn^{++} is interstitially inserted, is borne out by the experimental determination of the densities of the solid solutions in the range *A–B*, see Table VII. For when these values are compared with the densities calculated from the x-ray data for this mechanism they are found to be in good agreement (Table VII, column III) while the densities calculated on other postulates (columns I and II) are not.

The densities for the compounds found experimentally are checked by the values calculated from the x-ray and analytical results obtained above as shown in Table VIII.

Discussion of results

The results given by our investigation show that solid solutions are formed in the NH_4Cl region of this system, see Fig. 4 and 5, points *A* to

TABLE VII. *Solid solutions A–B.*

SAMPLE	DENSITY[a] (EXPERIMENTAL)	DENSITY (CALCULATED FROM X-RAY DATA) I	II	III
NH_4Cl[b]	1.519±.001	1.525	1.525	1.525
No. 2	1.508±.004	1.546	1.557	1.535
No. 4	1.528	1.563	1.583	1.543
No. 5	1.557	1.616	1.667	1.569
No. 6	1.586±.007	1.621	1.676	1.571
No. 7	1.610	1.706	1.814	1.610

[a] The density determinations were made at temperatures between 25.0° and 28.0° while the x-ray films were exposed at temperatures between 25° and 29°.

[b] The I. C. T. give the density of NH_4Cl calculated from x-ray studies as 1.528 and from experiment as $d_4^{30}=1.536$, $=1.526$ (Vol. 1, p. 108; Vol. III, p. 43). Our results check these values.

TABLE VIII. *Compounds at D and E.*

SAMPLE	DENSITY (EXP.)	DENSITY (CALC. FROM X-RAY DATA)
No. 8 ($6NH_4Cl \cdot MnCl_2 \cdot 2H_2O$)	1.701	1.711
No. 31 ($2NH_4Cl \cdot MnCl_2 \cdot 2H_2O$)	1.913	1.906

[32] E. R. Jette and F. Foote, J. Chem. Phys. **1**, 29 (1933).

TABLE IX. *Relative intensities of lines on Debye-Scherrer films for solid solution series No. 1.*

SAMPLE	LINE NO. 1 PLANE 100α	2 110β	3 110α	4 111α	5 200β	6 200α	7 210β	8 210α	9 211β
NH_4Cl	4	6	10	3	3	9	2	9	9
4	3	5	10	3	2	8	2	9	9
5	3	5	10	2	1	8	1	8	8
6	3	5	10	3	2	9	0	7	7
7	2	5	10	3	1	9	1	7	7

B, which is in complete agreement with the work of Foote and Saxton,[11] and Clendinnen and Rivett.[12] The solid phases obtained were homogenous, as shown by x-ray diffraction studies, after being rotated for a minimum of two weeks and as long as 8 weeks (see Table III for time in thermostat) in contact with the liquid phase till equilibrium was established. The results do not, therefore, bear out the contention of Benrath and Schackman[13] that these solid solutions eventually rid themselves of all the $MnCl_2 \cdot 2H_2O$ if shaken for a sufficient length of time.

As can be seen from Fig. 6, the lattice of ammonium chloride is expanded very slightly from one sample to the next in the first solid solution series, *A–B*, but the trend is marked and there is no doubt that the expansion takes place. The plot does not exhibit a linear relationship between weight percent composition and the lattice constant. The curve reaches a maximum and then begins to fall off between point 6 and 7 at about 13 weight percent $MnCl_2 \cdot 2H_2O$ in the solid phase. This phenomenon has been observed in metallic solid solutions[33] but this is the first time that it has been reported in crystal systems.

The solid solution series, *A* to *B* Fig. 5, does not follow Vegard's additivity law, nor should it be expected to, for as shown by Jette[34] this law may be considered analogous to Raoult's law of liquid solutions. It has been well established that Raoult's law holds for solutions only when the molecular species involved are very much alike chemically and physically. Therefore, Vegard's law should be applied only to cases of solid solution in which the components are similar in chemical and crystal structure. This is borne out by the previous work of Walden and Cohen,[5a] in which the solid solutions formed did not follow this law.

If the $MnCl_2 \cdot 2H_2O$ is in an ordered arrangement in the ammonium chloride lattice, new reflection lines should be observed on the x-ray films for these solid solutions or at least the relative intensities of the reflection lines should change.[35] Debye-Scherrer and precision camera films taken for each sample in this solid solution series showed no new lines. Furthermore visual examination of the films revealed no marked change in relative intensities of the lines, see Table IX. Therefore, the distribution of

TABLE X.

CALCIUM RADIATION							
NH_4Cl				$6NH_4Cl \cdot MnCl_2 \cdot 2H_2O$ (SAMPLE NO. 8)			
LINE NO.	PLANE AND SOURCE	EXP. $\sin^2\theta$	REL. INTENSITY	LINE NO.	PLANE AND SOURCE	EXP. $\sin^2\theta$	REL. INTENSITY
1	100α	0.1859	4	8	004α	0.1744	3
				9	400α	.1931	2
2	110β→110α	.3754	6	13	404β→α	.3676	6
				14	440β→α	.3854	6
3	110α	.3756	10	15	404α	.3684	10
				16	440α	.3859	10
4	111α	.5627	3	17	444α	.5615	8
6	200α	.7505	9	22	008α	.7019	8
				23	800α	.7733	10

TABLE XI.

CALCIUM RADIATION							
NH_4Cl				$2NH_4Cl \cdot MnCl_2 \cdot 2H_2O$ (SAMPLE NO. 26)			
LINE NO.	PLANE AND SOURCE	EXP. $\sin^2\theta$	REL. INTENSITY	LINE NO.	PLANE AND SOURCE	EXP. $\sin^2\theta$	REL. INTENSITY
1	100α	0.1859	4	5	002α	0.1654	6
				8	202β→α	.3640	5
2	110β→110α	.3754	6	9	220β→α	.3990	6
				10	202α	.3642	10
3	110α	.3756	10	11	220α	.3980	10
4	111α	.5627	3	15	222α	.5638	9
5	200β→200α	.7509	3	18	400β→α	.7958	3
6	200α	.7505	9	21	400α	.7958	10
				22	204α	.8602	5
8	210α	.9388	9	25	402α	.9599	10

[33] E. R. Jette and F. Foote, Am. Inst. Mining Met. Eng. No. 670 (1936).

[34] E. R. Jette, Trans. Am. Inst. Mining Met. Eng. **111**, 75 (1934).

[35] M. von Laue, Ann. d. Physik **78**, 167 (1925).

$MnCl_2 \cdot 2H_2O$ must be entirely random in the solid solutions.

Much has been written in regard to double salts as to whether or not they were "true" compounds or merely a portion of a solid solution series which corresponds to a stoichiometric relationship, e.g., Clendinnen and Rivett[12,36] concluded from their work that these double salts are really solid solutions. In line with this, the results of our investigation on the substances present at *D* and *E*, Fig. 5, indicate that there exists grounds for reasonable doubt for calling these "true" compounds. The existance of the complete series of solid solutions between *D* and *E* makes it impossible to definitely demonstrate a finite existence range for either end member. If such an existence range is to be used as the criterion of a true compound then these end members cannot be definitely so designated on the basis of the existing data. We have, nevertheless, used the term compound for these substances throughout this paper on the basis that they correspond to simple formulae (see Table IV for complete chemical analysis), that they give distinctly different x-ray diffraction patterns from $NH_4Cl \cdot MnCl_2 \cdot 4H_2O$ and each other, and that they do appear to have existence ranges as indicated by the somewhat vertical portions of the curve at the corresponding compositions of these substances. It would perhaps be better to call these "compounds of variable compositions"[37] in accordance with a similar procedure used in the metallic systems where the formation of superstructure lines is now attributed to "intermediate phases" rather than intermetallic compounds. Many examples are now listed in the literature of compounds having variable compositions.[37] This has been discussed by Hägg in a general way.[38] The picture of such compounds has been extremely useful in explaining the structure of silicates, as for example, the formation of $NaAlSiO_4$ from SiO_2 by the substitution of aluminum for silicon and the interstitial addition of sodium.[39]

The regular distribution of the $MnCl_2 \cdot 2H_2O$ in the ammonium chloride lattice increases the axial ratio of the unit cell from 1.00 to 1.05 and then to 1.09 which are just off-cubic. The unit cell is then tetragonal and the diffraction lines of ammonium chloride are split into two for planer indices containing (*hkl*) with two unlike numbers, such as 100, 110, 120, etc., but remains single for (*hkl*) all similar, (111) planes. This is apparent from Tables X and XI in which ammonium chloride diffraction lines are compared with those of the two "compounds." Kusnecov[14] undoubtedly made the mistake of using one set of these tetragonal lines from which he computed the lattice constants and found a contraction of the ammonium chloride unit cell. For, if one systematically picks out all the lines which appear displaced from those of ammonium chloride towards higher angles of reflection (larger $\sin^2\theta$ values), it will be found that these can be indexed on the assumption of cubic symmetry and there will be shown a contraction of the ammonium chloride lattice. Thus, in Table X or XI, if we used the 400, 440, 800 plane reflections or the 220, 400, 402 plane reflections, respectively, for the $6NH_4Cl \cdot MnCl_2 \cdot 2H_2O$ and $2NH_4Cl \cdot MnCl_2 \cdot 2H_2O$ we could calculate out a unit cell side which is smaller than that of ammonium chloride. However, if we chose the other set of lines, 004, 404, 008 and 202, 204, respectively, we could equally well demonstrate an increase in the unit cell side.

Kusnecov[14] in his x-ray studies missed completely the slight expansion of the ammonium chloride lattice with entrance of $MnCl_2 \cdot 2H_2O$ which exists in the solid solution series *A–B*. The decrease in lattice constant of ammonium chloride that he found at concentrations 11.6, 27.6, 32.8, 47.0 weight percent manganous chloride are undoubtedly due to measurements, at least from 27.6 weight percent and up, on diffraction lines of the tetragonal compounds and their solid solutions, on the mistaken assumption that they were ammonium chloride diffraction lines. The possibility of making such an error has been pointed out above. It illustrates quite clearly the danger of using only a few of the diffraction lines on an x-ray photogram for the purpose of computing lattice constants.

We wish to thank Professor Paul F. Kerr of Columbia University for his invaluable help in the microscopic examination of several of our samples, and Mr. Morris Krasnoff for his assistance in drawing the plots and diagrams.

[36] F. W. J. Clendinnen and A. C. O. Rivett, J. Chem. Soc. **123**, 1634 (1923).
[37] C. W. Stillwell, *Crystal Chemistry* (McGraw-Hill, 1938), pp. 154–157, 201–203, 330–333.
[38] G. Hägg, Zeits. f. Krist. **91**, 114 (1935).
[39] T. F. W. Barth and E. Posnjak, Zeits. f. Krist. **81**, 376 (1932).

Application of the Theory of Absolute Reaction Rates to Heterogeneous Processes

I. The Adsorption and Desorption of Gases

K. J. LAIDLER,* S. GLASSTONE AND H. EYRING
Frick Chemical Laboratory, Princeton University, Princeton, New Jersey

(Received June 24, 1940)

By regarding the process of adsorption as involving a reaction between a molecule of gas and an adsorbing center on the solid surface, it has been possible, with the aid of the theory of absolute reaction rates, to derive for the rates of adsorption and desorption of gases simple equations which can be tested experimentally. Different results are obtained according as the adsorbed gas forms an immobile or a mobile layer on the surface: in the latter circumstance, which does not appear to be common, the rate of adsorption would be given by the Hertz-Knudsen equation, provided there were no activation energy for adsorption. Combination of the expressions for the rates of adsorption and desorption gives an adsorption isotherm of the same form as that originally derived by Langmuir. Various cases of adsorption accompanied by dissociation of the adsorbed molecule are considered and the appropriate rate equations are deduced. If the molecule undergoes dissociation in the course of adsorption and the atoms remain on neighboring sites, these equations and the isotherm are the same as if there had been no dissociation, but if the molecule is adsorbed as such and then dissociation occurs as the result of an atom jumping from one adsorption center to another, the rate equations and isotherm differ from those obtained previously. The isotherm involves $p^{\frac{1}{2}}$ instead of p, but the form of the rate equation depends on whether the adsorption of the molecule or the jump of the atom is the slow stage. The possibility of interaction between adsorbed atoms or molecules in an immobile film on the surface is considered, and a modified isotherm which makes allowance for such interaction is derived. Equations have also been deduced for adsorption on covered surfaces.

INTRODUCTION

AN application of the theory of absolute reaction rates to adsorption processes has been made by G. E. Kimball,[1] and M. Temkin[2] has independently applied the same theory to the adsorption and desorption of gases and to simple heterogeneous chemical reactions. It is the object of the present paper and the succeeding one to show that such processes, involving solids and gases, may be profitably treated in a somewhat different manner by regarding the active points on the surface of the solid as constituting one of the reactants; the treatment is extended to a number of cases of different types, and it is shown that provided the accessible area of the surface is known it is possible to calculate reaction rates which are in excellent agreement with those found by experiment.

RATE OF ADSORPTION

According to the theory of absolute reaction rates,[3] a reaction takes place by the union of two or more molecules to form an activated complex which is assumed to be always in equilibrium with the reactants, and the rate of reaction is then given by the rate of passage of this complex over a potential energy barrier: the height of the barrier gives the energy of activation of the process. In the simplest case of adsorption, the reaction may be considered as involving a molecule (or atom) from the gas phase and an atom or, in general, an active point, occupying a fixed position on the adsorbing surface. In general, the adsorbing centers on the surface will not all have the same activity, and hence may be regarded as consisting of several types; centers belonging to each type will have their own characteristic heat and entropy of adsorption.

Consider the adsorption sites of a particular type: at any given instant in the course of adsorption their number is supposed to be N_s, and this will diminish as the surface becomes covered to an increasing extent. Let N_g be the number of molecules in the gas phase, and $N^{\ddagger}$ the number of activated complexes on the sites under consideration; if V cc is the volume of the gas phase and S sq. cm the area of the surface, then concentration in gas phase, $c_g = N_g/V$ molecules per cc; concentration of adsorption centers,

* Commonwealth Fund Fellow, 1938–40.
[1] G. E. Kimball, J. Chem. Phys. **6**, 447 (1938).
[2] M. Temkin, Acta Physicochimica U. R. S. S. **8**, 141 (1938).
[3] For reviews, see H. Eyring, Chem. Rev. **17**, 65 (1935); Trans. Faraday Soc. **34**, 41 (1938).

$c_s = N_s/S$ sites per sq. cm; concentration of activated complexes, $c^{\ddagger} = N^{\ddagger}/S$ molecules per sq. cm. According to the postulates of the theory of absolute reaction rates an equilibrium may be supposed to exist between molecules of gas, adsorption centers and activated complexes, so that, provided the various components of the system behave ideally,

$$K = \frac{c^{\ddagger}}{c_g c_s} = \frac{N^{\ddagger}}{(N_g/V)N_s} \tag{1}$$

$$= f^{\ddagger\prime}/(f_g/V)f_s, \tag{2}$$

where the f terms are the complete partition functions of the indicated species. If F_g represents the partition function for unit volume of the gas undergoing adsorption, i.e.,

$$F_g = f_g/V, \tag{3}$$

then it follows from (1) and (2) that

$$c^{\ddagger}/c_g c_s = f^{\ddagger\prime}/F_g f_s \tag{4}$$

and hence

$$c^{\ddagger} = c_g c_s f^{\ddagger\prime}/F_g f_s. \tag{5}$$

According to the theory of absolute reaction rates, the rate of adsorption of gas on sites of the ith kind per sq. cm of surface is given by

$$v_{1(i)} = c_g c_{s(i)} \frac{kT}{h} \cdot \frac{f^{\ddagger}}{F_g f_s}, \tag{6}$$

where $f^{\ddagger}$ differs from $f^{\ddagger\prime}$ by the removal from the latter of the contribution to the partition function of the degree of translational freedom in the reaction coordinate. If the surface were uniform and all the adsorbing centers had equal activity, c_s would represent the *total* number of bare sites per sq. cm, and $f^{\ddagger}$ and f_s would be applicable to all activated complexes and adsorbing centers, respectively; the resultant rate of adsorption over the whole surface would then be

$$v_1 = c_g c_s \frac{kT}{h} \cdot \frac{f^{\ddagger}}{F_g f_s}. \tag{7}$$

If the zero-point energy contribution is extracted from the partition functions, Eq. (7) becomes

$$v_1 = c_g c_s \frac{kT}{h} \cdot \frac{f^{\ddagger}}{F_g f_s} e^{-\epsilon_1/kT}, \tag{8}$$

where ϵ_1 is the energy of activation for adsorption per single molecule at the absolute zero; the value of the energy in the partition function for each species is now reckoned from its own zero-point level. If the surface is non-uniform, Eq. (8) may still be regarded as applicable, but $f^{\ddagger}$, f_s and ϵ_1 are now weighted averages for all the types of adsorbing centers on the surface: it will be seen later that $f^{\ddagger}/f_s$ is approximately unity for an immobile adsorbed layer, and so the only effective correction necessary is in the activation energy.

Immobile Adsorbed Layers

In the above treatment the adsorption centers on the surface have been regarded as reactants and hence it is implied that every adsorbed molecule uses up one active center: this is equivalent to saying that the gas adsorbed on the surface forms an immobile layer, i.e., a molecule is assumed to stay wherever it is adsorbed until it is desorbed. The translational contribution to the partition function of the activated state $f^{\ddagger}$ is thus unity, and the remainder, due to vibration and rotation, may be represented by $b^{\ddagger}$. Further, the adsorption centers are presumably atoms of the metal, or other substance, constituting the surface, and these probably have vibrational energy only; hence the partition function f_s may be taken as unity. Substitution of these values in Eq. (8) gives

$$v_1 = c_g c_s \frac{kT}{h} \cdot \frac{b^{\ddagger}}{F_g} e^{-\epsilon_1/kT} \tag{9}$$

$$= c_g c_s \frac{kT}{h} \cdot \frac{b^{\ddagger}}{(2\pi mkT)^{\frac{1}{2}} b_g/h^3} e^{-\epsilon_1/kT}, \tag{10}$$

where F_g, the partition function of the gas for unit volume, is split up into the translation contribution, for three degrees of freedom, $(2\pi mkT)^{\frac{1}{2}}/h^3$, and the vibrational and rotational factors, represented by b_g. It is probable, in view of the immobility of the activated complex, that there will be no rotation in this state; hence $b^{\ddagger}$ will be virtually a vibrational partition function and its value may be taken as unity, apart from a symmetry factor. Similarly the vibrational part of b_g will not differ greatly from unity, and hence b_g can be replaced by the rotational contribution; Eq. (10) then becomes

$$v_1 = c_g c_s \frac{kT}{h} \cdot \frac{1/\sigma^{\ddagger}}{\dfrac{(2\pi mkT)^{\frac{1}{2}}}{h^3} \cdot \dfrac{8\pi^2 IkT}{h^2\sigma}} e^{-\epsilon_1/kT}, \tag{11}$$

where $\sigma\ddagger$ is the symmetry factor of the activated complex and σ is that of the gas, or

$$v_1 = c_g c_s \frac{\sigma}{\sigma\ddagger} \cdot \frac{h^4}{8\pi^2 I (2\pi mkT)^{\frac{1}{2}}} e^{-\epsilon_1/kT}. \qquad (12)$$

So far it has been assumed that in the formation of the activated state the gas molecule attaches itself to one adsorption center only; this will be the case for monatomic molecules, and possibly for more complicated molecules in certain instances, but in many cases two adjacent sites are required for adsorption. Under these circumstances Eq. (12) will still give the rate of adsorption if c_s now represents the number of such dual sites per square cm, and this may be related to the number of single adsorption centers in the following manner. Each site will have a certain number, say s, adjacent sites, so that the total number of dual sites will be $\frac{1}{2}sc_s$, the $\frac{1}{2}$ arising from the fact that otherwise each pair is counted twice. The initial rate of adsorption of a gas molecule requiring two centers is thus $\frac{1}{2}s$ times the rate given by Eq. (12), i.e.,

$$v_1 = \tfrac{1}{2}s \cdot c_g c_s \frac{\sigma}{\sigma\ddagger} \cdot \frac{h^4}{8\pi^2 I (2\pi mkT)^{\frac{1}{2}}} e^{-\epsilon_1/kT}, \qquad (13)$$

where c_s still represents the number of single adsorption centers per square cm. It will be shown later that this equation may also be valid when dissociation accompanies adsorption.

Mobile Adsorbed Layer

It is of interest to compare this result with that which would be obtained if the molecules were mobile in the adsorbed state, and hence presumably also in the activated state. The adsorption centers need no longer be regarded as reactants, the activated complex being the gas molecule just before it strikes the surface. The equilibrium between initial and activated states may thus be represented (cf. Eqs. (1) and (2)) by

$$K = \frac{c\ddagger}{c_g} = \frac{N\ddagger/S}{N_g/V} = \frac{F\ddagger'}{F_g}, \qquad (14)$$

where F_g and $F\ddagger'$ are the partition functions for unit volume of gas and per sq. cm of activated state, respectively; hence, by the same methods as used in the case of immobile molecules, it follows that

$$v_1 = c_g \frac{kT}{h} \cdot \frac{F\ddagger}{F_g} e^{-\epsilon_1/kT}. \qquad (15)$$

Since the activated complex is still in the gaseous state, it will have vibrational and rotational degrees of freedom similar to the initial gas molecules; hence the ratio of the partition functions $F\ddagger/F_g$ reduces to the ratio of the translational terms. In the activated state the molecule has only two degrees of translational freedom, i.e., over the surface, while in the gaseous state it has three such degrees of freedom; it follows, therefore, that

$$v_1 = c_g \frac{kT}{h} \cdot \frac{h}{(2\pi mkT)^{\frac{1}{2}}} e^{-\epsilon_1/kT}. \qquad (16)$$

If $c_g kT$ is replaced by the pressure p of the gas, to which it is equivalent if the latter is ideal, then in the special case of adsorption requiring no activation energy, Eq. (16) becomes

$$v_1 = \frac{p}{(2\pi mkT)^{\frac{1}{2}}}. \qquad (17)$$

This result is identical with the classical Hertz-Knudsen equation for the number of gas molecules striking 1 sq. cm of a surface in unit time; it would also give the rate of adsorption provided the adsorbed layer were mobile and there was no activation energy of adsorption.

Test of Adsorption Equations

In order to test the validity of the equations based on the theory of absolute reaction rates, it would be necessary to have reliable data for the rates of adsorption of gases on surfaces of known area; unfortunately such data are very scanty. All of the examples which will here be considered refer to adsorption processes which involve the dissociation of the diatomic gas on adsorption, but it will be shown later that Eq. (13) is generally applicable to such processes.

An approximate comparison of observed and calculated rates of adsorption has been made by M. Temkin,[2] who derived an expression similar to (13); he showed that the measurements of O. I.

TABLE I.

GAS	TEMP.	E_1 KCAL.	RATE OF ADSORPTION	
			CALC.	OBS.
N_2	544°K	14.4	35.8×10^{16}	3.4×10^{16}
H_2	194.5°K	10.4	5.7×10^{15}	1.8×10^{17}

Leypunsky[4] were in general agreement with those to be expected from the theory of absolute reaction rates for an immobile adsorbed layer. A more precise comparison can be made using Emmett's data for the adsorption of nitrogen[5] and hydrogen[6] on an iron-aluminum oxide catalyst (the so-called "catalyst 931"). The surface area of such a catalyst cannot be determined by direct measurement, but a reliable estimate can be made by examination of the curve showing the amount of gas adsorbed against time. In Table I are given the observed and calculated initial rates, expressed as molecules per second on the surface present in the experiment. The agreement is seen to be satisfactory on the whole; it is probable that the recorded activation energy (E_1 kcal. per mole) for the adsorption of hydrogen is too high, and a value of 8.9 kcal. would give almost exact correspondence between observed and calculated rates of adsorption.

It appeared possible, at first sight, that the data obtained by J. K. Roberts[7] for the rate of adsorption of hydrogen on a clean tungsten wire of known area might provide a satisfactory test of Eq. (13), but there may be some doubt concerning the reliability of the results obtained. Application of the equation, assuming each molecule of hydrogen to become adsorbed on two centers and taking s as equal to 4 and c_s as 10^{15} sites per square cm, gives the rate of adsorption as $9.84\times10^{17}e^{-E_1/RT}$ molecules per square cm per second for a pressure of 10^{-4} mm at 79°K; this value may be compared with the maximum rate of adsorption of 5.9×10^{12} molecules per square cm per second derived from the measurements of Roberts. The calculated and observed rates would agree if the activation energy for adsorption were about 2.0 kcal., but since the experiments show that the rates of adsorption are almost the same at 79°K and 295°K, the activation energy should be zero. Another possibility is that only one site in about 10^5 can act as an adsorption center in the rate-determining stage, but this would seem to be unlikely. The discrepancy of 10^5 between calculated and experimental rates of adsorption is, therefore, difficult to understand, particularly in view of the satisfactory agreement obtained in other instances. It is possible, however, that in the work with hydrogen on tungsten the rate measured was not that of adsorption, but of another process, such as the rate of access of hydrogen to the surface under the experimental conditions.* If this is so, the conclusion that the rate of adsorption is independent of temperature, and that the activation energy for adsorption is thus zero, is open to doubt; the activation energy for adsorption might be as high as 2 kcal. and the adsorption process still be faster than the over-all observed rate.

RATE OF DESORPTION

The variation with pressure of the amount of gas adsorbed by a solid at constant temperature has been represented by the empirical classical isotherm or by the familiar equation first deduced by I. Langmuir[8] on the basis of a kinetic interpretation of adsorption of a single layer of gas molecules. The same result has been obtained by M. Volmer,[9] who assumed the adsorbed molecules to be mobile, and by R. H. Fowler[10] using statistical methods. It will be shown that the same isotherm can be derived from the theory of absolute reaction rates.

Desorption from an immobile layer may be regarded as involving an activated state in which a molecule attached to an adsorption center acquires the necessary configuration and activation energy to permit it to escape from the surface. As a result of the equilibrium between

[4] O. I. Leypunsky, Acta Physicochimica U. R. S. S. **2**, 737 (1935); J. Chem. Phys. Russ. **9**, 143 (1937).
[5] P. H. Emmett and S. Brunauer, J. Am. Chem. Soc. **56**, 35 (1934).
[6] P. H. Emmett and R. W. Harkness, J. Am. Chem. Soc. **57**, 1631 (1935).
[7] J. K. Roberts, Proc. Roy. Soc. **A152**, 445 (1935).

* Somewhat similar possibilities were considered in a footnote to p. 76 of a preliminary paper by J. K. Roberts, Proc. Camb. Phil. Soc. **30**, 74 (1933–4).
[8] I. Langmuir, J. Am. Chem. Soc. **38**, 2221 (1916); **40**, 1361 (1918).
[9] M. Volmer, Zeits. f. physik. Chemie **115**, 253 (1925).
[10] R. H. Fowler, Proc. Camb. Phil. Soc. **31**, 260 (1935); cf. R. H. Fowler and E. A. Guggenheim, *Statistical Thermodynamics* (Cambridge Univ. Press, 1939), p. 426.

adsorbed and activated molecules, it follows that if N_a and $N_\ddagger$ are the numbers of adsorbed molecules and of activated complexes, and c_a and $c_\ddagger$ are their respective concentrations, in molecules per sq. cm, then

$$K=\frac{c_\ddagger}{c_a}=\frac{N_\ddagger/S}{N_a/S}=\frac{f_\ddagger'}{f_a} \tag{18}$$

and hence

$$c_\ddagger=c_a f_\ddagger'/f_a, \tag{19}$$

the f terms being the complete partition functions. According to the theory of absolute reaction rates, the rate of desorption, v_2, per sq. cm of surface per sec., is given by

$$v_2=c_a\frac{kT}{h}\cdot\frac{f_\ddagger}{f_a}, \tag{20}$$

where $f_\ddagger$ no longer includes the partition function for translation across the potential energy barrier. If the zero-point energy term is extracted, it follows that

$$v_2=c_a\frac{kT}{h}\cdot\frac{f_\ddagger}{f_a}e^{-\epsilon_2/kT}, \tag{21}$$

where ϵ_2 represents the energy of activation for the desorption of a single molecule at the absolute zero.

This equation may be tested by the data on the rates of desorption of carbon monoxide from platinum[11] and of oxygen from tungsten.[12] If both the activated complexes and adsorbed molecules are assumed to be immobile, the ratio of the partition functions $f_\ddagger/f_a$ should be approximately equal to unity, and hence if the rate of desorption is expressed in the general form $v_2=Ae^{-E_2/RT}$, where E_2 is the activation energy for desorption per mole of gas, A should be equal to $c_a(kT/h)$, by Eq. (21). For a surface which is almost completely covered, c_a may be taken as 10^{15} molecules per sq. cm, and so the rate of desorption may be calculated; the values of A obtained in this manner are compared in Table II with those derived experimentally, the rates being expressed as molecules becoming desorbed per sq. cm per second. The difference between observed and calculated values for carbon monoxide is not serious, but with oxygen it is greater than would be expected. It must be remembered that there may well be more rotational and vibrational freedom in the activated than in the adsorbed state and this would tend to make the partition function factor greater than unity; the calculated rate of desorption would then be larger than given in Table II.

TABLE II.

Gas	Surface	Temp.	E kcal.	Rate of Desorption	
				A (calc.)	A (obs.)
CO	Pt	600°K	32.0	1.25×10^{28}	2.79×10^{29}
O_2	W	2000°K	165.0	4.16×10^{28}	13.4×10^{30}

[11] I. Langmuir, Trans. Faraday Soc. **17**, 641 (1922).
[12] I. Langmuir and D. S. Villars, J. Am. Chem. Soc. **51**, 486 (1931).

The Adsorption Isotherm

For adsorption equilibrium at any temperature, the rates of adsorption and of desorption, as given by Eqs. (8) and (21) must be equal; hence

$$c_g c_s\frac{kT}{h}\cdot\frac{f_\ddagger}{F_g f_s}e^{-\epsilon_1/kT}=c_a\frac{kT}{h}\cdot\frac{f_\ddagger}{f_a}e^{-\epsilon_2/kT}; \tag{22}$$

$$\therefore\quad \frac{c_a}{c_s}=c_g\frac{f_a}{F_g f_s}e^{\epsilon/kT}, \tag{23}$$

where ϵ, which is equal to $\epsilon_2-\epsilon_1$, is the heat of adsorption per single molecule at 0°K. If θ is the fraction of the adsorption centers which are covered by adsorbed molecules, $1-\theta$ is the fraction still bare at any instant, and

$$c_a/c_s=\theta/(1-\theta); \tag{24}$$

hence by (23),

$$\frac{\theta}{1-\theta}=c_g\frac{f_a}{F_g f_s}e^{\epsilon/kT}. \tag{25}$$

As seen above, f_s may be taken as unity, and F_g may be represented by

$$F_g=(2\pi mkT)^{\frac{3}{2}}b_g/h^3. \tag{26}$$

Further, since the adsorbed molecules are supposed to be immobile, the partition function f_a may be replaced by b_a, the contribution of the internal degrees of freedom. Finally, writing p/kT for c_g in Eq. (25), the latter becomes

$$\frac{\theta}{1-\theta}=p\frac{h^3}{(2\pi m)^{3/2}(kT)^{5/2}}\cdot\frac{b_a}{b_g}e^{\epsilon/kT}, \tag{27}$$

which is identical with the expression derived by

Fowler.[10] This relationship may be written as

$$\theta/(1-\theta)=ap, \tag{28}$$

where, for a given system, a is a function of the temperature only; Eq. (28) is, in fact, an isotherm which is identical with that of Langmuir, as may be seen by rewriting it in the form

$$\theta=ap/(1+ap). \tag{29}$$

If the surface is covered to a small extent only, then $1-\theta\approx 1$, and hence (28) reduces to

$$\theta=ap, \tag{30}$$

the extent of adsorption being proportional to the pressure.

Although Eqs. (29) and (30) were derived from (7), which was based on the assumption that each adsorbed molecule occupies only one center, a similar result would be obtained from Eq. (13), for the case of a gas molecule requiring two adjacent sites for adsorption.

Adsorption with Dissociation

The application of quantum mechanics to the system consisting of a molecule of hydrogen and two surface atoms of carbon or nickel has led to the conclusion that in the most stable configuration the distance between the adsorbed hydrogen atoms is much greater than in a normal molecule.[13] It follows, therefore, that in these instances adsorption is accompanied by dissociation of the adsorbed molecule. It is probable that many cases of activated adsorption involve dissociation, and hence it is necessary to consider what effect this will have on the equations for the rates of adsorption and desorption and on the adsorption isotherm. Two main types of behavior may be distinguished: one in which the molecule undergoes dissociation in the course of adsorption but the atoms remain on adjacent sites; and the second, in which dissociation results from the jump of one or both of the atoms constituting the molecule from one site to another. In the first case equilibrium between initial, activated and final states may be written as

$$\underset{\text{gas}}{G_2}+\underset{\text{surface}}{S_2}\rightleftharpoons\underset{\text{activated state}}{(G_2S_2)^{\ddagger}}\rightleftharpoons\underset{\text{adsorbed atoms}}{G-S\text{——}S-G}.$$

The rate of adsorption is given by an equation similar to (7), or by any of the succeeding equations which are equivalent to it, and that of desorption by one identical with Eqs. (20) and (21); the adsorption isotherm will then be identical with Eqs. (27), (28) and (29).

When dissociation results from the jump of an atom from one site to another, two possibilities may arise: the actual adsorption of the molecule may be rapid and the jump of the atom slow, or the adsorption of the molecule may be the rate-determining stage. In the former case, the adsorption and desorption equilibrium can be represented as

$$\underset{\text{gas}}{\tfrac{1}{2}G_2}+\underset{\text{surface}}{S_2}\rightleftharpoons\underset{\text{activated state}}{(GS_2)^{\ddagger}}\rightleftharpoons\underset{\text{adsorbed atoms}}{G-S_2}.$$

The rate of adsorption can be readily shown, by the method used in deriving Eqs. (7), etc., to be given by

$$v_1=c_g^{\frac{1}{2}}c_s\frac{kT}{h}\cdot\frac{f_{\ddagger}}{F_g^{\frac{1}{2}}f_s}e^{-\epsilon_1/kT}, \tag{31}$$

where the symbols have the same significance as previously. Similarly, the rate of desorption is

$$v_2=c_a\frac{kT}{h}\cdot\frac{f_{\ddagger}}{f_a}e^{-\epsilon_2/kT}. \tag{32}$$

When equilibrium is attained v_1 is equal to v_2, and hence

$$\frac{c_a}{c_s}=c_g^{\frac{1}{2}}\frac{f_a}{f_sF_g^{\frac{1}{2}}}e^{\epsilon/kT}. \tag{33}$$

If, as before, θ is the fraction of the surface covered, now by adsorbed atoms, it follows from (33), by the arguments used in deriving (27) and (28), that

$$\frac{\theta}{1-\theta}=p^{\frac{1}{2}}\frac{h^{\frac{1}{2}}}{(2\pi m)^{3/4}(kT)^{5/4}}\cdot\frac{b_a}{b_g^{\frac{1}{2}}}e^{\epsilon/kT}, \tag{34}$$

or

$$\frac{\theta}{1-\theta}=ap^{\frac{1}{2}}. \tag{35}$$

$$\therefore\quad \theta=\frac{ap^{\frac{1}{2}}}{1+ap^{\frac{1}{2}}}. \tag{36}$$

At low pressures, or in general when the surface is sparely covered,

$$\theta=ap^{\frac{1}{2}}. \tag{37}$$

[13] A. Sherman and H. Eyring, J. Am. Chem. Soc. **54**, 2661 (1932); A. Sherman, C. E. Sun and H. Eyring, J. Chem. Phys. **3**, 49 (1935); G. Okamoto, J. Horiuti and S. Ikehara, Sci. Papers Inst. Phys. Chem. Res. Tokyo **29**, 223 (1936).

In the second type of dissociation, when the adsorption of the molecule is rate determining, the process may be represented by

$$G_2+S_2\rightleftarrows(G_2S_2)^{\ddagger},$$

$$(G_2S_2)^{\ddagger}+2S'\rightarrow 2GS'+S_2,$$

where S_2 is a dual site on which the molecule of G_2 is first adsorbed, and S′ represents a site to which each atom finally jumps. The over-all change is seen to be, as before, the adsorption of G_2 on two S′ sites in the form of atoms. By considering the equilibrium between initial and activated states it is found that the rate of adsorption is given by

$$v_1=c_g c_s\frac{kT}{h}\cdot\frac{f_{\ddagger}}{F_g f_s}e^{-\epsilon_1/kT}, \qquad (38)$$

where c_s is the concentration of dual sites. Similarly the rate of desorption is

$$v_2=\frac{c_a c_s}{c_{s'}{}^2}\cdot\frac{kT}{h}\cdot\frac{f_{\ddagger}f_{s'}{}^2}{f_a{}^2 f_s}e^{-\epsilon_2/kT}, \qquad (39)$$

where $c_{s'}$ is the concentration of single S′ sites. By equating (38) and (39), the adsorption isotherm is seen to be

$$\frac{c_a}{c_{s'}}=c_g{}^{\frac{1}{2}}\frac{f_a}{f_{s'}F_g{}^{\frac{1}{2}}}e^{\epsilon/kT}. \qquad (40)$$

This equation is identical in form, as is necessary, with (33), and hence leads to equations of the same type as (34) to (37). However, the expressions for the rates of adsorption and desorption are different: thus according to (31) the rate is proportional to the square-root of the gas pressure, while according to (38) it is proportional to its first power. In most of the examples which have been studied the exponent is unity rather than one-half, so that the second mechanism, in which the adsorption of the molecule is rate determining, appears to be the more common. That this is so is confirmed by the agreement between calculated and observed values for adsorption rates in Table I. Agreement was obtained by the use of Eq. (13), which is equivalent to (38), whereas if Eq. (31) had been used there would have been large discrepancies between the calculated and observed values. It may be noted in particular that the application of Eq. (31) to Roberts's data on the adsorption of hydrogen on tungsten (p. 662) leads to rates which are faster than those derived from (13), and therefore still more in disagreement with the experimental values.

Adsorption with Interaction

In the foregoing treatment the possibility of interaction between adsorbed molecules or atoms has been ignored, and this may account for the deviations frequently observed from the behavior to be expected from the adsorption isotherms given above. In particular it has been found that the variation of the constant a with temperature is in the opposite direction to that expected. Such deviations can be explained in two ways; in the first place they may be due to interaction between the adsorbed particles, and in the second place, the variability of the surface may be responsible. Both these factors probably play an important part in adsorption processes.

Allowance may be made in a number of ways for the interaction between adsorbed molecules and the following is analogous to the treatment adopted in the study of electrode processes.[14] It has been shown[15] that for an immobile layer the heat of adsorption may be expected to vary in a linear manner with the fraction (θ) of the surface covered, thus

$$\text{Heat of adsorption}=\epsilon-s\theta V \qquad (41)$$

where ϵ is the heat evolved in the adsorption of a molecule of gas on a bare surface; s, as before, is the number of adsorption sites adjacent to any given one, and V is the repulsive interaction energy between neighboring adsorbed molecules. Since the molecular interaction decreases the heat evolved in adsorption by an amount $s\theta V$, it is reasonable to suppose that the energy of activation for adsorption will be increased by a definite fraction α of this quantity. This represents the fraction of the repulsive force operative between the initial and activated states: any subsequent interaction effects will not influence the activation energy. The activation energy per molecule ϵ_1 for adsorption will thus be increased

[14] H. Eyring, S. Glasstone and K. J. Laidler, J. Chem. Phys. **7**, 1053 (1939); G. E. Kimball, *ibid.* **8**, 199 (1940).
[15] J. K. Roberts, reference 7; Ann. Rep. Chem. Soc. **35**, 59 (1938).

by an amount $\alpha s\theta V$, so that the total is $\epsilon_1+\alpha s\theta V$. Molecular repulsions will, on the other hand, tend to diminish the activation energy for desorption by a fraction $1-\alpha$ of the total interaction effect, and so the activation energy for this process becomes $\epsilon_2-(1-\alpha)s\theta V$. The rates of adsorption (v_1) and desorption (v_2) obtained by making the appropriate alterations in the activation energies in Eqs. (8) and (21) are thus

$$v_1=c_g c_s\frac{kT}{h}\cdot\frac{f_{\ddagger}}{F_g f_s}e^{-(\epsilon_1+\alpha s\theta V)/kT} \tag{42}$$

and

$$v_2=c_a\frac{kT}{h}\cdot\frac{f_{\ddagger}}{f_a}e^{-[\epsilon_2-(1-\alpha)s\theta V]/kT}. \tag{43}$$

At equilibrium, when the two rates are equal, the ratio of covered to uncovered surface is given by the method used in deriving Eq. (27) as

$$\frac{\theta}{1-\theta}=p\frac{h^3}{(2\pi m)^{3/2}(kT)^{5/2}}\cdot\frac{b_a}{b_g}e^{(\epsilon-s\theta V)/kT}, \tag{44}$$

where ϵ, as before, is equal to $\epsilon_2-\epsilon_1$. It may be pointed out that this argument involves the tacit assumption that for an immobile film the energy of activation, like the heat of adsorption, varies in a linear manner with the fraction of surface covered.

Adsorption on a Covered Surface

For certain purposes (see Part II, succeeding paper) it is desirable to consider adsorption of a gas on a surface already covered to a large extent by another substance, e.g., a poison. In the simplest case the adsorption of gas and poison may be supposed to occur on the same sites, which may be dual or single, and hence Eq. (8) is applicable. If the adsorption isotherm, Eq. (23), is written in the abbreviated form

$$c_a/c_s=Ac_g, \tag{45}$$

where A is $(f_a/F_g f_s)e^{\epsilon/kT}$, then using the suffix p to indicate the poison, we also have

$$c_{ap}/c_s=A_p c_{gp}, \tag{45a}$$

where A_p is $(f_{ap}/F_{gp}f_s)e^{\epsilon_p/kT}$. Let L be the total number of adsorption sites on 1 sq. cm of bare surface; this is equal to $c_s+c_a+c_{ap}$, but if the poison covers the larger part of the surface c_a may be neglected, so that L is approximately equal to c_s+c_{ap}. Substituting the value of c_{ap} given by Eq. (45a), it is seen that

$$c_s=L/(1+A_p c_{gp}) \tag{46}$$

and hence Eq. (8) for the rate of adsorption of gas becomes

$$v_1=\frac{Lc_g}{1+A_p c_{gp}}\cdot\frac{kT}{h}\cdot\frac{f_{\ddagger}}{F_g f_s}e^{-\epsilon_1/kT}. \tag{47}$$

For a strongly adsorbed poison, unity may be neglected in comparison with $A_p c_{gp}$, and substituting the value for A_p given above,

$$v_1=L\frac{c_g}{c_{gp}}\cdot\frac{kT}{h}\cdot\frac{f_{\ddagger}F_{gp}}{f_{ap}F_g}e^{-(\epsilon_1+\epsilon_p)/kT}. \tag{48}$$

The rate of adsorption is seen to vary as the pressure of the gas and inversely as the pressure of the strongly adsorbed poison, and the heat of activation for adsorption is increased from ϵ_1 to $\epsilon_1+\epsilon_p$, where ϵ_p is the heat (evolved) of adsorption of the poison.

It may be pointed out that the rate of adsorption is not decreased as much as might be supposed from the increase in the heat of activation, because the adsorption of a gas molecule is accompanied by the transfer of a poison molecule from the surface to the gas phase: there is consequently a gain of entropy compared with that for adsorption on a bare surface. It can be readily shown that A_p is equal to $e^{-\Delta F_p^0/kT}$, where ΔF_p^0 is the standard entropy of adsorption of the poison, and writing Eq. (8) in the alternative form

$$v_1=c_g c_s\frac{kT}{h}e^{-\Delta F_1^{\ddagger}/kT}, \tag{49}$$

where $\Delta F_1^{\ddagger}$ is the entropy of activation for adsorption on a bare surface, it follows that for a surface covered by a poison

$$v_1=L\frac{c_g}{c_{gp}}\cdot\frac{kT}{h}e^{-(\Delta F_1^{\ddagger}-\Delta F_p^0)/kT}. \tag{50}$$

In view of the large change of entropy accompanying adsorption and desorption, ΔF_p^0 is often a small negative quantity, and hence $\Delta F_1^{\ddagger}-\Delta F_p^0$ may be little different from $\Delta F_1^{\ddagger}$. For a strongly

adsorbed poison, however, ΔF_p^0 will have a large negative value and the rate of adsorption of the gas will be markedly decreased.

The rate of desorption of gas from a poisoned surface is still given by Eq. (21), and so from this and Eq. (48), it follows that

$$c_a = L\frac{c_g}{c_{gp}}\cdot\frac{F_{gp}f_a}{F_g f_{ap}}e^{(\epsilon-\epsilon_p)/kT}, \qquad (51)$$

where ϵ, as before, is $\epsilon_2-\epsilon_1$, the heat of adsorption of the gas.

By utilizing the methods developed in this and the succeeding paper, equations analogous to (48) and (51) can be derived for various types of adsorption, e.g., involving dual sites or dissociation, of both gas and poison; an illustration is provided in Part II by the treatment of the decomposition of ammonia, adsorbed on a dual site, on a surface poisoned by hydrogen in the form of atoms.

The authors wish to express their thanks to Professor Hugh S. Taylor for a number of helpful suggestions in connection with this paper.

SEPTEMBER, 1940 JOURNAL OF CHEMICAL PHYSICS VOLUME 8

Application of the Theory of Absolute Reaction Rates to Heterogeneous Processes

II. Chemical Reactions on Surfaces

K. J. LAIDLER,* S. GLASSTONE AND H. EYRING
Frick Chemical Laboratory, Princeton University, Princeton, New Jersey

(Received June 24, 1940)

The method developed in the preceding paper is used to derive equations for the rates of unimolecular and bimolecular heterogeneous gas reactions under various conditions of surface coverage by either reactants or poisons. The resulting equations are of the same form as those previously deduced by Langmuir and others, but they are more explicit; provided the activation energy is known they can be utilized to calculate rates of surface reactions which are in good agreement with the observed values. In the case of the dissociation of hydrogen on a tungsten surface, the simple assumption that the activated state consists of hydrogen atoms permits the absolute rate of the reaction to be calculated with an accuracy which is at least as good as that attained by direct experimental measurement. The factors responsible for the difference in rates of the same reaction taking place homogeneously or heterogeneously are considered; it is shown that adsorption of the activated complex lowers the over-all activation energy, and this has the most important influence in favoring the surface reaction. If one of the products, or any other substance acting as a poison, is strongly adsorbed, the effective activation energy is increased, but there is some compensation resulting from the increase of entropy accompanying the desorption of the poison.

INTRODUCTION

FROM the point of view of the theory of absolute reaction rates a chemical reaction taking place on a surface is formally the same as an adsorption, the initial state being a molecule, or molecules, in the gas phase while the activated state is an adsorbed molecular species. The question, frequently discussed, as to whether the adsorption process or the reaction on the surface is slow, and hence rate determining, is for present purposes of no importance, since the essential point is the equilibrium between reactants and the activated complex, whatever the latter may be. Equations for the rates of surface reactions were derived by I. Langmuir and others[1] from kinetic considerations, and it will be shown that analogous, but more explicit, equations may be obtained by using the method described in the preceding paper (Part I) of regarding the surface

* Commonwealth Fund Fellow, 1938–40.

[1] I. Langmuir, Trans. Faraday Soc. **17**, 621 (1922); C. N. Hinshelwood, *Kinetics of Chemical Change* (Oxford University Press, 1926, p. 145; 1940, p. 187); cf. H. S. Taylor, *Treatise on Physical Chemistry* (Van Nostrand Company, New York, 1931), p. 1074.

as one of the reactants. By means of these equations the rates of a number of heterogeneous gas reactions have been calculated and found to be in agreement with the experimental values. For present purposes it is convenient to consider various reactions according to the number of molecules, *viz.*, one or two, involved in the chemical change.

Unimolecular Reactions

Suppose the reaction involves one molecule of the gaseous reactant A, and S represents the active center on which reaction occurs. The activated complex consists of an adsorbed molecule which has acquired the appropriate amount of energy and the proper configuration: the equilibrium between initial and activated states may be written as

$$A+S \rightleftharpoons (A-S)^{\ddagger} \rightarrow \text{products},$$

and hence

$$\frac{c^{\ddagger}}{c_g c_s} = \frac{f_{\ddagger}}{F_g f_s} e^{-\epsilon_0/kT}, \tag{1}$$

where ϵ_0 is the energy of activation per molecule at 0°K, and the other symbols have the same significance as in the preceding paper. The rate of reaction according to the theory of absolute reaction rates is then

$$v = c_g c_s \frac{kT}{h} \cdot \frac{f_{\ddagger}}{F_g f_s} e^{-\epsilon_0/kT}. \tag{2}$$

It may be noted that this expression is formally identical with Eq. (8) of Part I for the rate of adsorption; the activated states are, however, different in the two cases, although since both consist of immobile molecules attached to the surface their partition functions will be of the order of unity, in each case, at ordinary temperatures.

First-order kinetics

The application of Eq. (2) may be considered under two sets of conditions. In the first place, if the surface is sparsely covered by adsorbed molecules, c_s, the concentration of bare sites on the surface, is practically constant and is almost identical with the number of sites per sq. cm of completely bare surface. In these circumstances c_s in Eq. (2) may be taken as constant, and the rate of reaction, for a given surface, is seen to be directly proportional to the concentration of the reacting material in the gas phase: the process is thus kinetically of the first order. Numerous examples of this type of behavior are known.

Introducing the expressions for the partition functions into Eq. (2), it follows that the rate equation for a unimolecular, first-order, reaction involving a diatomic molecule is

$$v = c_g c_s \frac{\sigma}{\sigma_{\ddagger}} \cdot \frac{\frac{1}{2}sh^4}{8\pi^2 I(2\pi mkT)^{\frac{1}{2}}} e^{-\epsilon_0/kT}, \tag{3}$$

where s is the total number of possible sites adjacent to any reaction center, σ and $\sigma_{\ddagger}$ are the symmetry numbers of the molecules of reactant and of activated complex, respectively, and I and m are the moment of inertia and mass of the reacting molecule. For a nonlinear polyatomic molecule, the rate is

$$v = c_g c_s \frac{\sigma}{\sigma_{\ddagger}} \cdot \frac{\frac{1}{2}sh^5}{8\pi^2(8\pi^3 ABC)^{1/2}(2\pi m)^{3/2}(kT)^{5/2}} e^{-\epsilon_0/kT}, \tag{4}$$

where A, B and C are the three moments of inertia of the reactant. In both these equations c_s is the number of reaction sites per sq. cm of surface, and the factor $\frac{1}{2}s$ is introduced when the reacting molecules are attached to two sites in the activated state. Using known, or reasonable, values for the moments of inertia and taking s to be 4 in each case, the specific reaction rates for the surface decomposition of phosphine,[2] hydrogen iodide[3] and nitrous oxide[4] have been evaluated, the assumption being made that in each case the surface is smooth and sparsely covered, so that there are about 10^{15} individual sites per sq. cm. In Table I the calculated re-

Table I. *Observed and calculated first-order surface reaction rates.*

Decomposition of:	Surface	Temperature	Specific Reaction Rates	
			Obs.	Calc.
PH_3	Glass	684°K	4.7×10^{-7}	2.2×10^{-8}
HI	Platinum	836°	1.0×10^{-3}	1.2×10^{-3}
N_2O	Gold	1211°	12.3×10^{-5}	3.4×10^{-6}

[2] J. H. van't Hoff and D. M. Kooij, Zeits. f. physik. Chemie **12** (1893); cf. M. Temkin, Acta Physicochimica U. R. S. S. **8**, 141 (1938).

[3] C. N. Hinshelwood and R. E. Burk, J. Chem. Soc. **127**, 2896 (1925).

[4] C. N. Hinshelwood and C. R. Prichard, Proc. Roy. Soc. **A108**, 211 (1925).

sults are compared with those observed, which are for relatively even surfaces, the values given being the ordinary first-order rate constants which refer to the particular amount of surface used in the experiment. Although the calculated and observed rates are in satisfactory agreement, it will be noted that the former are somewhat too small for the decomposition of phosphine and nitrous oxide. This may be due partly to the roughness of the surface, which would make the number of reaction centers greater than the value employed, and partly to the fact that there is some freedom of movement in the activated state. By taking the partition function for the latter to be unity it is assumed that there is no movement of any kind in the activated state; with relatively complex molecules such as phosphine and nitrous oxide rotation or libration in the activated state may well be appreciable and the inclusion of the appropriate contribution to the partition function would increase the calculated reaction rates.

Zero-order kinetics

When the surface is covered by adsorbed molecules to an appreciable extent, the value of c_s varies with the pressure of the gas, and the behavior to be expected is apparent from a combination of Eq. (2) and the adsorption isotherm; substituting the following value for $c_g c_s$ obtained from Eq. (23) of Part I, *viz.*,

$$c_g c_s = c_a(F_g f_s/f_a)e^{-\epsilon/kT} \tag{5}$$

in (2), it follows that

$$v = c_a \frac{kT}{h} \cdot \frac{f_{\pm}}{f_a} e^{-(\epsilon_0+\epsilon)/kT}, \tag{6}$$

where ϵ is the heat evolved in the adsorption of one molecule of reactant. If the surface is almost completely covered by adsorbed molecules, c_a may be taken as constant, and the rate of reaction as given by Eq. (6) is seen to be virtually independent of the pressure of the reactant: the process is then said to obey zero-order kinetics. It will be apparent that Eq. (6) treats the reaction from the standpoint of adsorbed molecules, instead of gas molecules, as the initial reactant: the "surface activation energy," i.e., the difference in energy between the activated state and the *adsorbed* reactants, is $\epsilon_0+\epsilon$.[9]

Table II. *Observed and calculated zero-order surface reaction rates*

Decomposition of:	Surface	E kcal.	T	k_{obs}	k_{calc}
NH_3[5]	W	38	904°K	4×10^{17}	8.0×10^{18}
NH_3[6]	W	41.5	1316	2×10^{19}	3.4×10^{21}
NH_3[7]	Mo	53.2	1228	$5\text{–}20\times10^{18}$	8.5×10^{18}
HI[8]	Au	25.0	978	5.2×10^{22}	1.6×10^{17}

Since both $f_{\pm}$ and f_a may be taken as unity, it follows that (6) may be written as

$$v = c_a(kT/h)e^{-E/RT}, \tag{7}$$

where E is the observed activation energy per mole. An equation of the same form as (7), with a frequency factor assumed to be 10^{12} per sec., in place of kT/h, was proposed from general considerations by Topley.[10]

When the surface is almost entirely covered, c_a is equal to the number of active centers per sq. cm of surface, which may be taken as 10^{15}. In Table II are given a number of calculated and observed rate constants expressed as molecules per sq. cm per second, for zero-order reactions calculated from (7), making use of the data collected by Topley. The agreement is seen to be satisfactory except for the decomposition of hydrogen iodide on gold; the discrepancy may be due to the adsorption of hydrogen on the surface, for this would have the effect, as explained later, of increasing the activation energy and so would make the calculated reaction rate too low.

Bimolecular Reactions

In a surface reaction between two molecules it is presumably necessary that the molecules shall be adsorbed on adjacent sites; the reaction may thus be considered as occurring between one molecule of each of the reactants A and B and a dual site S_2 on the surface of the catalyst: thus

$$A+B+S_2 \rightleftharpoons (A-B-S_2)^{\ddagger} \rightarrow \text{products}.$$

[5] C. N. Hinshelwood and R. E. Burk, J. Chem. Soc. **127**, 1105 (1925).
[6] C. H. Kunsman, E. S. Lamar and W. E. Deming, Phil. Mag. **10**, 1015 (1930).
[7] R. E. Burk, Proc. Nat. Acad. Sci. **13**, 67 (1927).
[8] C. N. Hinshelwood and C. R. Prichard, J. Chem. Soc. **127**, 806 (1925).
[9] Cf. C. N. Hinshelwood and B. Topley, J. Chem. Soc. **123**, 1014 (1923).
[10] B. Topley, Nature **128**, 115 (1931).

It is first required to determine the number of dual sites in terms of the number of available single sites per sq. cm (c_s) and other factors. If the fraction of the surface covered by reactant A is θ, and that covered by B is θ', then the number of bare sites adjacent to any given site will be $s(1-\theta-\theta')$ where s, as before, is the total number of possible sites adjacent to any given site. The number of dual sites per sq. cm is thus $\frac{1}{2}c_s s(1-\theta-\theta')$, the factor one-half arising from the fact that in the above treatment each dual site is counted twice. The fractions θ and θ' may be expressed in terms of the concentrations of surface adsorbed molecules, or atoms, of A, i.e., c_a, and of B, i.e., $c_{a'}$, as follows,

$$\theta = c_a/(c_a+c_{a'}+c_s) \tag{8}$$

and

$$\theta' = c_{a'}/(c_a+c_{a'}+c_s), \tag{9}$$

and so the number of dual sites per sq. cm may be written in the form

$$\text{Conc. of dual sites} = \tfrac{1}{2}sc_s^2/L, \tag{10}$$

where L stands for $c_a+c_{a'}+c_s$, the total number of sites per sq. cm of bare surface. The theory of absolute reaction rates then gives the velocity of the bimolecular surface reaction as

$$v = \tfrac{1}{2}s\frac{c_g c_{g'} c_s^2}{L}\cdot\frac{kT}{h}\cdot\frac{f_\ddagger}{F_g F_{g'} f_s}e^{-\epsilon_0/kT}, \tag{11}$$

where c_g and $c_{g'}$ are the concentrations of A and B in the gas phase, and F_g and $F_{g'}$ are their partition functions for unit volume; $f_\ddagger$ and f_s are the partition functions, for the whole surface, of the activated complex and of reaction sites, respectively. Since L is the sum of c_a, $c_{a'}$ and c_s, it is possible to express Eq. (11) in terms of c_g, $c_{g'}$, and c_s by substituting the appropriate values of c_a and $c_{a'}$ given by the adsorption isotherm, Eq. (5). It is convenient, in this connection, to consider a number of special cases.

(a) *Sparsely covered surface.*—When the surface is sparsely covered, i.e., the sum of c_a and $c_{a'}$ is small, L is practically equal to c_s and hence Eq. (11) becomes

$$v = \tfrac{1}{2}sc_g c_{g'} c_s\frac{kT}{h}\cdot\frac{f_\ddagger}{F_g F_{g'} f_s}e^{-\epsilon_0/kT}. \tag{12}$$

This represents the simplest type of second-order kinetics, the rate of the heterogeneous reaction being directly proportional to the concentration of each of the reactants: provided c_s is known, e.g., for a smooth sparsely covered surface, it is possible to calculate the reaction rate from Eq. (12).

The velocity of the reaction between nitric oxide and oxygen on a glass surface has been measured[11] at 85°K and found to be represented by the expression

$$v = 9.4\times10^{-27} c_{NO}c_{O_2}e^{-\epsilon_0/kT} \text{ molecules cm}^{-2}\text{ sec.}^{-1}$$

with concentrations in molecules per cc. In this equation ϵ_0 is the activation energy at 0°K, a slight adjustment having been made, by means of the theoretical Eq. (12), to the experimental activation energy observed at 85°K. The dependence of the rate on the product of the concentrations of the reactants suggests that the activated complex consists of a molecule of NO and one of O_2 adsorbed on neighboring sites on the surface, so that Eq. (12) should be applicable. The ratio of the partition functions for the adsorbed, immobile, activated complex and for the adsorption centers, i.e., $f_\ddagger/f_s$, may be taken as unity, while F_{NO} and F_{O_2} may be calculated in the usual manner for diatomic molecules, the vibrational contributions being very little different from unity at the experimental temperature. Both nitric oxide and oxygen have multiplet ground states and allowance should be made for these in deriving the partition functions, but since the electron multiplicity of the activated complex is unknown it may be assumed that the values cancel each other; this approximation cannot be in error by a factor of more than two or three.[12] Since the experimental results suggest a sparsely covered surface, the number of individual reaction sites, c_s, is about 10^{15} per sq. cm. If every site is surrounded by four others, i.e., s is 4, and if two adjacent sites are involved, it is found from Eq. (12) that

$$v = 14.8\times10^{-27}\, c_{NO}c_{O_2}e^{-\epsilon_0/kT}$$

in good agreement with the experimental result.

(b) *One reactant more strongly adsorbed than the other.*—If the reactant A is more strongly ad-

[11] M. Temkin and W. Pyzhow, Acta Physicochimica U. R. S. S. **2**, 473 (1935).

[12] Cf. H. Gershinowitz and H. Eyring, J. Am. Chem. Soc. **57**, 985 (1935).

sorbed than B, then $c_{a'}$ may be neglected in comparison with c_a, and L may be put equal to c_a+c_s; Eq. (11) then becomes

$$v=\tfrac{1}{2}s\frac{c_g c_{g'} c_s^2}{c_a+c_s}\cdot\frac{kT}{h}\cdot\frac{f_{\ddagger}}{F_g F_{g'} f_s}e^{-\epsilon_0/kT}. \qquad (13)$$

Writing the adsorption isotherm, as in Part I, in the abbreviated form $c_a/c_s=Ac_g$ where A is equal to $(f_a/F_g f_s)e^{\epsilon/kT}$, and using this relationship to eliminate c_a from Eq. (13), it is found that

$$v=\tfrac{1}{2}s\frac{c_g c_{g'} c_s}{1+Ac_g}\cdot\frac{kT}{h}\cdot\frac{f_{\ddagger}}{F_g F_{g'} f_s}e^{-\epsilon_0/kT}. \qquad (14)$$

Further, since L is approximately equal to c_a+c_s, as already seen, it follows (cf. Eq. (46), Part I) that $c_s=L/(1+Ac_g)$, and substitution for c_s in (14) gives

$$v=\tfrac{1}{2}s\frac{Lc_g c_{g'}}{(1+Ac_g)^2}\cdot\frac{kT}{h}\cdot\frac{f_{\ddagger}}{F_g F_{g'} f_s}e^{-\epsilon_0/kT}, \qquad (15)$$

which is equivalent to the more familiar form[13]

$$v=k'p_A p_B/(1+Bp_A)^2, \qquad (16)$$

where k' and B are constants at a definite temperature. It is of interest to note that if $c_{g'}$, or p_B, is kept constant as c_g, or p_A is increased, the reaction velocity should pass through a maximum: behavior of this kind has been observed in the reaction between hydrogen and carbon dioxide on platinum.[13]

(c) *One reactant very strongly adsorbed.*—If the reactant A is so strongly adsorbed that it occupies most of the available surface, the fraction c_a/c_s, which is equal to Ac_g, is much greater than unity: in Eq. (15) therefore unity may be neglected in comparison with Ac_g, and hence

$$v=\tfrac{1}{2}s\frac{L}{A^2}\cdot\frac{c_{g'}}{c_g}\cdot\frac{kT}{h}\cdot\frac{f_{\ddagger}}{F_g F_{g'} f_s}e^{-\epsilon_0/kT}. \qquad (17)$$

Expressing A as $(f_a/F_g f_s)e^{\epsilon/kT}$ Eq. (17) becomes

$$v=\tfrac{1}{2}sL\frac{c_{g'}}{c_g}\cdot\frac{kT}{h}\cdot\frac{F_g f_{\ddagger} f_s}{F_{g'} f_a}e^{-\epsilon_0'/kT}, \qquad (18)$$

where ϵ_0' is equal to $\epsilon_0+2\epsilon$. The experimental activation energy will thus be greater by 2ϵ than the value for a sparsely covered surface of the same material. Equation (18) is equivalent to the expression derived by the method of Langmuir, $v=k'p_B/p_A$ where p_A and p_B are the partial pressures of the reactants A and B, which are proportional to c_g and $c_{g'}$, respectively. Several instances of this type of kinetics have been reported.[14]

Equation (18) may be applied quantitatively to the reaction between carbon monoxide and oxygen on the surface of platinum.[15] At 572°K the observed rate is equal to

$$7.10\times10^{14}\frac{c_{O_2}}{c_{CO}}\text{ molecules cm}^{-2}\text{ sec.}^{-1}$$

The temperature coefficient corresponds to an activation energy of 33.3 kcal. in this temperature region; the use of this value in Eq. (18) gives a calculated rate of

$$4.33\times10^{15}\frac{c_{O_2}}{c_{CO}}\text{ molecules cm}^{-2}\text{ sec.}^{-1}$$

in satisfactory agreement with experiment. The reaction between hydrogen and oxygen on platinum[15] shows a similar behavior but the data are not sufficiently precise to permit an application of the theory.

Bimolecular Reaction with a Single Reactant

When both reacting molecules are the same, it can be readily seen that the general Eq. (11) simplifies to the form

$$v=\tfrac{1}{2}s\frac{c_g^2 c_s^2}{L}\cdot\frac{kT}{h}\cdot\frac{f_{\ddagger}}{F_g^2 f_s}e^{-\epsilon_0/kT}, \qquad (19)$$

where L is equal to c_s+c_a. If the surface is sparsely covered, $L\approx c_s$, and (19) reduces to

$$v=\tfrac{1}{2}sc_g^2 c_s\frac{kT}{h}\cdot\frac{f_{\ddagger}}{F_g^2 f_s}e^{-\epsilon_0/kT}, \qquad (20)$$

and the reaction behaves kinetically as a straightforward second-order process. At the other extreme, when the surface is almost completely

[13] C. N. Hinshelwood and C. R. Prichard, J. Chem. Soc. 127, 806 (1925).

[14] For examples, see G.-M. Schwab, *Catalysis* (Translated by H. S. Taylor and R. Spence, Van Nostrand Company, New York, 1937), p. 227.

[15] I. Langmuir, Trans. Faraday Soc. 17, 621 (1922).

covered, L is approximately equal to c_a, and hence $L=Ac_0c_s$, and insertion of L/A for c_0c_s in (19) gives

$$v=\tfrac{1}{2}s\frac{L}{A^2}\cdot\frac{kT}{h}\cdot\frac{f_{\pm}}{F_0^2f_s}e^{-\epsilon_0/kT}. \qquad (21)$$

The reaction is clearly of zero order, since it is independent of the concentration, or pressure, of the reacting gas. Alternatively, if L is replaced by c_a, then

$$v=\tfrac{1}{2}s\frac{c_a}{A^2}\cdot\frac{kT}{h}\cdot\frac{f_{\pm}}{F_0^2f_s}e^{-\epsilon_0/kT}. \qquad (22)$$

In this equation, as in (6), the reaction is treated from the standpoint of the adsorbed molecules; if the value of A, given above, is inserted in Eq. (22), the result is

$$v=\tfrac{1}{2}sc_a\frac{kT}{h}\cdot\frac{f_{\pm}f_s}{f_a^2}e^{-(\epsilon_0+2\epsilon)/kT}, \qquad (23)$$

which may be compared with (6) for a unimolecular reaction. In the present case c_a is also constant, since the surface is almost fully covered, and the velocity of the reaction is independent of the pressure of the reactant, as already recorded. The "surface activation energy" is seen from Eq. (23) to be $\epsilon_0+2\epsilon$.

Retardation by Poisons

Unimolecular reactions.—When the product of a reaction, or other substance, e.g., a poison which may be present in the system, is strongly adsorbed, the process is retarded. For a unimolecular reaction occurring on a single site, the poison also being adsorbed on a single site, the problem is similar to adsorption on a covered surface considered in Part I. An equation exactly analogous to (47) is applicable, except that $f_{\pm}$ is the partition function for the activated state of the reaction and ϵ_1 is the corresponding heat of activation; the rate equation may then be written in the more familiar form

$$v=k'p_A/(1+Bp_P), \qquad (24)$$

where p_P is the partial pressure of the poisoning substance. If the poison is very strongly adsorbed and virtually covers the whole surface, this becomes

$$v=k'p_A/p_P. \qquad (25)$$

For such a surface an equation similar to (48) of Part I is applicable; by utilizing the adsorption isotherms (45) and (45*a*) of Part I, and putting L equal to c_{ap} since the surface is almost completely covered by poison, this equation takes the form

$$v=c_a\frac{kT}{h}\cdot\frac{f_{\pm}}{f_a}e^{-(\epsilon_0+\epsilon)/kT}, \qquad (26)$$

where ϵ_0 is the heat of activation for the reaction on a clean surface and ϵ is the heat of adsorption of the reactant. This equation again considers the reaction from the standpoint of adsorbed molecules of reactant, and the surface activation energy is seen to be $\epsilon_0+\epsilon$. The experimental heat of activation, the gas being considered as the reactant, is $\epsilon_0+\epsilon_p$, where ϵ_p is the heat of adsorption of the product, and if this is represented by $\epsilon_{exp.}$ it is seen that the surface activation energy is $\epsilon_{exp.}+\epsilon-\epsilon_p$.[16]

In Eq. (2) the quantity c_s represents the concentration of reaction centers, irrespective of whether they are single or dual sites; for the present purpose, however, it is necessary to restrict c_s to the concentration of single sites, and then the concentration of dual sites is given by Eq. (10). Inserting this value into Eq. (2), the rate of a unimolecular reaction on dual sites becomes

$$v=\tfrac{1}{2}s\frac{c_0c_s^2}{L}\cdot\frac{kT}{h}\cdot\frac{f_{\pm}}{F_0f_s}e^{-\epsilon_0/kT}. \qquad (27)$$

If the surface is almost completely covered by a reaction product or other substance acting as a poison, then L can be replaced by c_{ap}, the surface concentration of poison, which may be adsorbed either as molecules or as atoms. Since the latter case is of experimental interest, it alone will be considered; according to Eq. (33) of Part I,

$$c_{ap}/c_s=c_{0p}^{\frac{1}{2}}\frac{f_{ap}}{f_sF_{0p}^{\frac{1}{2}}}e^{\epsilon_p/kT}, \qquad (28)$$

and hence (27) may be written

$$v=\tfrac{1}{2}sL\frac{c_0}{c_{ap}}\cdot\frac{kT}{h}\cdot\frac{F_{0p}f_{\pm}f_s}{F_0f_{ap}^2}e^{-(\epsilon_0+2\epsilon_p)/kT} \qquad (29)$$

$$=k'p_A/p_P, \qquad (30)$$

[16] Cf. C. N. Hinshelwood, *Kinetics of Chemical Change* (Oxford University Press, 1926, p. 178; 1940, p. 245).

where c_g and c_{gp} are the concentrations of reactant and poison, respectively, in the gas phase, and p_A and p_P are their partial pressures. The heat of activation is seen to be $\epsilon_0+2\epsilon_p$.

The rate of decomposition of ammonia at low pressures on a platinum surface varies as the pressure of the reactant and inversely as that of hydrogen, which acts as a poison;[17] both Eqs. (25) and (30) satisfy these conditions, but the latter is probably applicable, since hydrogen is adsorbed atomically on platinum at high temperatures. It should, therefore, be possible to calculate the rate of reaction by means of Eq. (29). According to the experiments of Schwab and Schmidt the observed rate at 1423°K is $2.60\times10^{22}\ c_{NH_3}/c_{H_2}$ molecules per sq. cm and the energy of activation is 44.3 kcal.[18] Taking this value as equivalent to $\epsilon_0+2\epsilon$, and considering $f\pm$, f_s and f_{ap} to be unity, as usual, the rate of reaction for a smooth surface ($L=10^{15}$ per sq. cm, $s=4$) is calculated from Eq. (29) to be $0.92\times10^{22}\ c_{NH_3}/c_{H_2}$ molecules per sq. cm at 1423°K. Equally good agreement is, of course, obtained at other temperatures, since the experimental activation energy is employed in the calculations.

Bimolecular reactions.—If two molecules of a single reactant are involved, Eq. (19) is still applicable, but L is equal to $c_s+c_a+c_{ap}$. If the poison is fairly strongly adsorbed c_a may be neglected in comparison with c_{ap}, and so L will be given by c_s+c_{ap}; inserting this value in (19), it is seen that

$$v=\tfrac{1}{2}s\frac{c_g^2c_s^2}{c_s+c_{ap}}\cdot\frac{kT}{h}\cdot\frac{f_\pm}{F_g^2f_s}e^{-\epsilon_0/kT}. \qquad (31)$$

Substituting the value $A_pc_sc_{gp}$ for c_{ap}, Eq. (31) becomes

$$v=\tfrac{1}{2}s\frac{c_g^2c_s}{1+A_pc_{gp}}\cdot\frac{kT}{h}\cdot\frac{f_\pm}{F_g^2f_s}e^{-\epsilon_0/kT}. \qquad (32)$$

Utilizing the relationship $c_s=L/(1+A_pc_{gp})$, i.e., Eq. (46) of Part I, it follows that

$$v=\tfrac{1}{2}s\frac{Lc_g^2}{(1+A_pc_{gp})^2}\cdot\frac{kT}{h}\cdot\frac{f_\pm}{F_g^2f_s}e^{-\epsilon_0/kT} \qquad (33)$$

or

$$v=k'\frac{p_A^2}{(1+Bp_P)^2}, \qquad (34)$$

where p_A and p_P are the pressures of reactant and poison, respectively, the latter being preferentially adsorbed.

If the product is very strongly adsorbed, so that c_s can be neglected in comparison with c_{ap}, L becomes virtually equal to c_{ap}: it is then found that

$$v=\tfrac{1}{2}s\frac{L}{A_p^2}\cdot\frac{c_g^2}{c_{gp}^2}\cdot\frac{kT}{h}\cdot\frac{f_\pm}{F_g^2f_s}e^{-\epsilon_0/kT}, \qquad (35)$$

where A_p is $(f_{ap}/F_{gp}f_s)e^{\epsilon_p/kT}$. The same result may, of course, be obtained by neglecting unity in comparison with A_pc_{gp}, since A_p will be large for a strongly adsorbed substance, in Eq. (33). The general form of this equation is equivalent to $v=k'p_A^2/p_P^2$ where A denotes the reacting substance, and P the retarding material; the latter retards a bimolecular reaction according to the second power of its pressure, and not to the first, as has frequently been assumed. However, if the retarding gas is composed of diatomic molecules which are adsorbed in the form of atoms the equation takes the form

$$v=\tfrac{1}{2}s\frac{L}{A_p^2}\cdot\frac{c_g^2}{c_{gp}}\cdot\frac{kT}{h}\cdot\frac{f_\pm}{F_g^2f_s}e^{-\epsilon_0/kT}, \qquad (36)$$

where A_p has the value $(f_{ap}/F_{gp}{}^{\frac{1}{2}}f_s)e^{\epsilon/kT}$. The reaction rate now varies inversely as the first power of the poison pressure. The quantity $A_p{}^2$, which appears in both Eqs. (35) and (36), involves $e^{2\epsilon_p/kT}$ and so the heat of activation is in each case $\epsilon_0+2\epsilon_p$, where ϵ_p is the heat of adsorption of a molecule of poison in the former case and an atom in the latter.

Behavior of the type represented by Eq. (36) has been recorded[19] for the decomposition of nitric oxide on platinum and on a platinum-rhodium alloy surface, which is retarded by

[17] G.-M. Schwab and H. Schmidt, Zeits. f. physik. Chemie **B3**, 337 (1929).

[18] The figure 140 kcal. given by C. N. Hinshelwood and R. E. Burk, J. Chem. Soc. **127**, 1114 (1925) appears to apply at higher pressures when the reaction kinetics are more complicated, as found by G.-M. Schwab and H. Schmidt, reference 14. The high temperature coefficient obtained under these conditions may be due to the operation of a chain reaction [cf. reference 14, p. 316].

[19] P. W. Bachman and G. B. Taylor, J. Phys. Chem. **33**, 447 (1929).

oxygen. At 1483°K on pure platinum the rate is given as

$$v = 2.2\times10^{-4}\frac{c_{NO}^2}{c_{O_2}} \text{ molecules cm}^{-2}\text{ sec.}^{-1}.$$

Since the oxygen is adsorbed atomically on platinum Eq. (36) should be applicable. Assuming $f_\pm$, f_s and f_{ap} to be unity, and taking the activation energy to be 14 kcal.,[20] the calculated rate is found to be

$$v = 2.9\times10^{-4}\frac{c_{NO}^2}{c_{O_2}} \text{ molecules cm}^{-2}\text{ sec.}^{-1},$$

in excellent agreement with experiment.

Similar equations may be deduced for the cases in which the two reacting molecules are different: these are analogous to (33) and (34), except that $c_g c_{g'}$ replaces c_g^2, where c_g and $c_{g'}$ are the concentrations of the two reacting gases, and $F_g F_{g'}$ is used instead of F_g^2. No cases appear to be known in which equations of the resulting type are applicable, but the reaction between sulfur dioxide and oxygen on platinum is the nearest approach. The product, i.e., sulfur trioxide, undoubtedly retards the reaction, but the reaction rate is not inversely proportional to the square of its pressure as the theoretical treatment predicts.

Dissociation of Hydrogen on Tungsten

When a tungsten filament is heated in an atmosphere of hydrogen, the latter is converted into the atomic form which evaporates off from the surface of the tungsten and is generally adsorbed by the glass walls of the reaction vessel.[21] The rate of formation of atomic hydrogen has been found,[22] over a range of temperature (1148° to 1420°K) and pressure (3×10^{-3} to 3.7×10^{-2} mm of mercury) to be proportional to the square-root of the pressure. This result indicates clearly that the activated complex of the reaction consists of hydrogen atoms, and not molecules (cf. Part I), and hence the rate equation should be

$$v = c_{H_2}{}^{\frac{1}{2}} c_s \frac{kT}{h}\cdot\frac{f_\pm}{F_{H_2}{}^{\frac{1}{2}} f_s} e^{-\epsilon_0/kT}. \qquad (37)$$

The partition functions of the activated state and of the reaction centers on the surface may both be taken as unity, for even if the former consisted of a free hydrogen atom it would be hemmed in by its neighbors and so have no freedom of movement. Equation (37) may thus be written in the form

$$v = c_{H_2}{}^{\frac{1}{2}} c_s \frac{kT}{h}\cdot\frac{1}{\frac{(2\pi mkT)^{\frac{1}{2}}}{h^{\frac{1}{2}}}\left(\frac{8\pi IkT}{2h^2}\right)^{\frac{1}{2}}} e^{-E_0/RT}. \qquad (38)$$

The mechanism of the formation of atomic hydrogen on a tungsten surface appears to be the adsorption of a molecule, then an atom jumps to another site, becomes detached from the surface—this constitutes the activated state—and finally escapes into the gas phase. Since the initial state in the reaction is $\frac{1}{2}H_2$ and the final state is H, the process is endothermic to the extent of one-half the heat of dissociation of molecular hydrogen, i.e., 51.5 kcal. at 0°K. The activation energy of the process under consideration should thus have at least this value, and if E_0 is assumed to be 51.5 kcal. it is possible to calculate the rate of the reaction, at various temperatures, by means of Eq. (38); the surface is assumed to be sparsely covered, so that c_s may be taken as 10^{15} per sq. cm. The results, expressed as atoms cm^{-2} $sec.^{-1}$, are compared with the experimental rates[21] in Table III, the pressure being in mm of mercury. It is of interest to call attention to the fact that in this particular reaction the simple assumption that the activated state consists of hydrogen atoms permits the absolute rate of dissociation of hydrogen on a tungsten surface to be calculated with an accuracy which is probably as good as that attained by experiment.

According to the observations of R. C. L. Bosworth[23] the surface is almost fully covered

Table III.

Temp.	Rate of Dissociation Obs.	Calc.
1148°K	$6.6\times10^{15}\sqrt{p}$	$3.3\times10^{15}\sqrt{p}$
1243	3.0×10^{16}	1.8×10^{16}
1378	1.1×10^{17}	8.0×10^{16}
1420	2.9×10^{17}	2.4×10^{17}

[20] G. E. Green and C. N. Hinshelwood, J. Chem. Soc. 1709 (1936).
[21] I. Langmuir, J. Am. Chem. Soc. **34**, 1310 (1912); **37**, 417 (1915).
[22] G. Bryce, Proc. Camb. Phil. Soc. **32**, 648 (1936).
[23] R. C. L. Bosworth, Proc. Camb. Phil. Soc. **33**, 394 (1937).

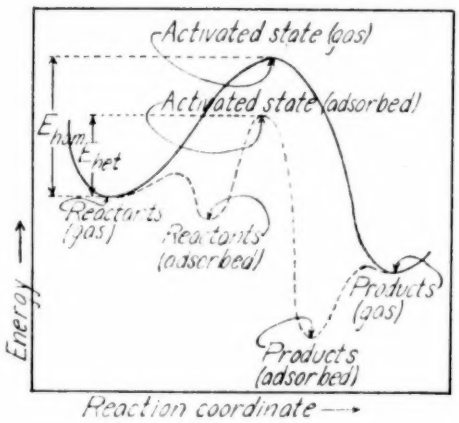

FIG. 1.

with hydrogen under the conditions employed in obtaining the data in Table III. Since the formation of atomic hydrogen is not of zero order, it is apparent that even if the surface as a whole were largely covered, the active centers on which reaction occurs can be only sparsely covered. If the experiments on the extent of coverage of the surface are correct, therefore, the active centers must constitute a fraction only of the total number of tungsten atoms on the surface. In view of the agreement between observed and calculated rates in Table III, the latter being based on the assumption of a bare surface, this fraction must be relatively large.

COMPARISON OF HOMOGENEOUS AND HETEROGENEOUS REACTIONS

The reaction rate per sq. cm of surface for a second-order heterogeneous reaction may be written (cf. Eq. (12)) as

$$v_{het.} = c_A c_B c_s \frac{kT}{h} \cdot \frac{1}{F_A F_B} e^{-E_{het.}/RT}, \qquad (39)$$

where the reactants are designated by A and B; the partition functions of the activated complex and of the reaction centers have been taken as unity. For the corresponding process occurring entirely in the gas phase, the rate equation, according to the theory of absolute reaction rates, is given by

$$v_{hom.} = c_A c_B \frac{kT}{h} \cdot \frac{F_{\ddagger}}{F_A F_B} e^{-E_{hom.}/RT}. \qquad (40)$$

It follows, therefore, that

$$\frac{v_{het.}}{v_{hom.}} = \frac{c_s}{F_{\ddagger}} e^{\Delta E/RT}, \qquad (41)$$

where ΔE is equal to $E_{hom.} - E_{het.}$, i.e., the amount that the activation energy of the homogeneous reaction is greater than that of the heterogeneous process. For one sq. cm of smooth surface, c_s is about 10^{15} whereas the partition function $F_{\ddagger}$ for the activated complex of the homogeneous gas reaction is at least 10^{24} (for hydrogen) and is often of the order of 10^{30} per cc; taking 10^{27} as a mean value for $F_{\ddagger}$, it follows that

$$v_{het.}/v_{hom.} \approx 10^{-12} e^{\Delta E/RT}, \qquad (42)$$

the heterogeneous rate being that for one sq. cm of surface, and the homogeneous rate for one cc of the gaseous reactants. It is obvious, therefore, that if a heterogeneous reaction is to be as fast as a homogeneous one involving the same reactants at the same pressures, either a very large surface, *viz.*, 10^{12} sq. cm, must be employed, or alternatively the activation energy for the heterogeneous reaction must be considerably less than that for the homogeneous process. At a temperature of 500°K, for example, the reaction per sq. cm of surface will have the same rate as the gas reaction per cc, only if the activation energy of the former is about 27.6 kcal. less than that of the latter. At lower temperatures the difference would need to be smaller, e.g., 16.5 kcal. at 300°K.

It may appear surprising, at first sight, in view of the much smaller activation energy necessary for a heterogeneous reaction to have the same rate as the corresponding homogeneous one, that catalyzed reactions are frequently so much faster than those which take place entirely in the gas phase. The reason is twofold: in the first place the surface area of the catalyst is very large, so that the reaction is not restricted to one sq. cm as has been assumed in the above calculations; and in the second place, the activation energy for a heterogeneous reaction is generally less than for the same process in the gas phase.[24]

It is of interest to inquire next into the circum-

[24] Cf. C. N. Hinshelwood, reference 16 (1940), p. 224.

stances which make it possible for the activation energy of the heterogeneous reaction to be less than for that occurring wholly in the gas phase: this may be most easily seen with the aid of a potential energy diagram. The full line in Fig. 1 represents the variation of potential energy in the decomposition coordinate for the homogeneous reaction, while the dotted curve represents the change during the course of the heterogeneous reaction. It will be seen that the surface reaction involves first the adsorption of the reactants, then the formation of an adsorbed activated complex which decomposes to give adsorbed resultants, and finally the latter must be desorbed. The difference between $E_{\text{hom.}}$ and $E_{\text{het.}}$ is seen to be equal to the difference in potential energy between the activated state in the gas phase and on the surface, and hence is equal to the heat of adsorption of the activated complex. If the reactants undergo activated adsorption, it is very probable that the activated complex for the reaction on the surface will consist virtually of atoms or free radicals, and these are likely to have a high energy of adsorption. Under these circumstances $E_{\text{het.}}$ is likely to be very much lower than $E_{\text{hom.}}$. The decrease in the activation energy for the hydrogen-oxygen reaction and the decompositions of hydrogen iodide and methane on surfaces, as compared with the same homogeneous reactions, has been explained[25] somewhat in this manner.

If all the active centers of the surface are covered by one of the products of the reaction or by some other material which is strongly adsorbed and so acts as a poison, then since these must be desorbed before an activated complex can be formed on the surface, the heat of activation is increased by an amount equal to the heat of adsorption of the poison, as seen above. There is some compensation for this increase, however, by the increase of entropy accompanying the desorption of the poison, and the situation is very similar to that considered in Part I in connection with the rate of adsorption on a poisoned surface. As in that instance, the free energy of activation for reaction on such a surface is greater than the value for an unpoisoned surface by an amount equal to the standard free energy of desorption of the poison. It will be noted that in all poisoned reactions, a function of the concentration (or pressure) of the poison in the gas phase appears in the denominator of the rate equation, so that the greater the pressure of the retarding gas the slower the reaction rate.

The authors wish to thank Professor Hugh S. Taylor for valuable comments and discussion.

[25] M. Polanyi, Zeits. f. Elektrochemie **27**, 143 (1921); G.-M. Schwab and E. Pietsch, *ibid.*, **32**, 430 (1926); Zeits. f. physik. Chemie **121**, 189 (1926); **126**, 473 (1927); H. S. Taylor, J. Phys. Chem. **30**, 145 (1926).

Directed Valence in Chemical Reactions

JOHN L. MAGEE*
Department of Chemistry, University of Wisconsin, Madison, Wisconsin
(Received March 30, 1940)

The potential energy surfaces for the reactions of two hydrogen atoms with another hydrogen-like atom having a single valence electron in a $2p$ orbital are investigated. The simple Heitler-London approximation is used in the calculations. The calculated activation energies for the reactions:

$$H_2+X\rightarrow H+HX(^2\Sigma)$$
$$HX(^2\Sigma)+H\rightarrow H+XH(^2\Sigma),$$

where X is the atom having the $2p$ valence electron, are quite low, ~1 Calorie. This is in good agreement with the experimental results for X=halogen, and the general principle that directed valence lowers activation energies. The symmetrical configurations for the H_2X complex are found to have the lowest energy. In fact, a triangular complex was found to be stable with respect to dissociation into either HX+H or H_2+X. The mechanism of the reactions between hydrogen and the halogens is discussed.

INTRODUCTION

ELECTRONS in higher than s atomic orbitals taking part in chemical reactions introduce two features in the reaction potential energy surfaces. (1) The number of surfaces is increased by the orbital degeneracy. (2) Each surface has directional properties due to the directed nature of the higher valence states.

In this paper the most simple example in which directed valence occurs in chemical reactions is considered, namely, the reactions of three hydrogen-like atoms with one electron apiece, two being in s atomic orbitals and one in a p orbital. The simple Heitler-London method is used for the calculations.

Triatomic systems which are formed from two atoms in S states with one atom in a P state are of considerable importance in chemistry. Such a complex is the intermediate in the reactions of hydrogen and deuterium with the halogens.

$$H_2+X\rightarrow H+HX, \quad (1)$$
$$HX+D\rightarrow H+XD \text{ etc.} \quad (2)$$

Other common examples include the reactions of the halogens with the alkali metals. Since the majority of the elements are in S or P states, a great many examples might be given. In all these actual examples the problem is much more complicated than the one considered in this paper, since there are usually many electrons, rather than only three. Polar states, which are neglected in this work, frequently play an important part. The valence forces characterized by the directional property of the atomic states should, however, be similar in all cases. It is this feature which is of interest in the present work.

II. CALCULATION

Three atoms (see Fig. 1) a and c with one s electron each and b with a p electron interact to form six doublet states and three quartet states. We shall be concerned only with the doublet states. The diatomic molecules, ab and ac, which are formed from the quartet state are in triplet states. These are repulsive with the exception of

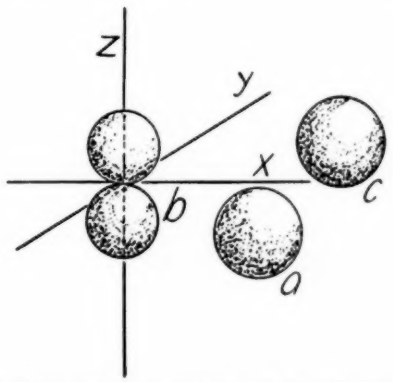

FIG. 1. Schematic representation of the charge distributions of the atoms for isosceles triangular configurations. This scheme of representation is that used in Pauling and Wilson (*Introduction to Quantum Mechanics* (McGraw-Hill, New York, 1935), p. 150). This figure shows the situation for the A_2 and B_2 states. The other states have the p valence in the plane of the atoms and cannot be shown in such a simple figure since they are made up of a linear combination of P_x and P_y.

* Present address: Chemistry Department, Princeton University.

the $^3\Pi$ state of ab which is weakly attractive. This latter is the first excited state of the molecule, the normal state being the $^1\Sigma$ state. Thus the quartet states are really of little chemical interest.

Two special cases have been considered in which the secular equation is reduced by symmetry. These are isosceles triangular and linear configurations.

We shall now consider the eigenfunctions of the systems.

A. Isosceles triangle configurations

The Z axis (Fig. 1) is taken perpendicular to the plane of the three atoms and b, the p atom is placed at the origin. The point symmetry group for the problem is C_{2v}, using Schoenflies notation.[1] Two of the doublet eigenfunctions belong to the identical representation A_1, which means that they are unchanged by any symmetry operation. Two eigenfunctions belong to B_1, and are antisymmetric with respect to rotation about the X axis and reflection in the XZ plane. The other two eigenfunctions are antisymmetric with respect to reflection in the XY plane; one (A_2) is also antisymmetric with respect to reflection in the XZ plane; the other (B_2) is antisymmetric on rotation about the X axis.

These eigenfunctions have been formed as linear combinations of the following real atomic orbitals.

$$a(1)=\left(\frac{1}{\pi}\right)^{\frac{1}{2}}\exp(-r_{a1}),$$

$$c(1)=\left(\frac{1}{\pi}\right)^{\frac{1}{2}}\exp(-r_{c1}),$$

$$b_x(1)=\left(\frac{1}{\pi}\right)^{\frac{1}{2}}x_1\exp(-r_{a1}),$$

$$b_y(1)=\left(\frac{1}{\pi}\right)^{\frac{1}{2}}y_1\exp(-r_{b1}),$$

$$b_z(1)=\left(\frac{1}{\pi}\right)^{\frac{1}{2}}z_1\exp(-r_{b1}).$$

[1] Discussions of the applications of group theory to molecular structure may be found in these references: Mulliken, Phys. Rev. **41**, 49 (1932); Rosenthal and Murphy, Rev. Mod. Phys. **8**, 317 (1936); Eyring, Frost and Turkevich, J. Chem. Phys. **1**, 777 (1933). Other references in group theory: E. Wigner, *Gruppentheorie* (Viewey, Braunschweig, 1931); Van der Waerden, *Gruppentheoretische Methode in der Quantenmechanik* (Julius Springer, Berlin, 1932).

$r_{\beta i}$ is the distance of the ith electron from the βth nucleus in units of a_0, the first Bohr radius (0.53A). x_i, y_i, z_i are the Cartesian coordinates of the ith electron.

The eigenfunctions are:

$$\Psi_{1y}(A_1)=2\begin{pmatrix}a & b_y & c\\ \alpha & \beta & \alpha\end{pmatrix}-\begin{pmatrix}a & b_y & c\\ \alpha & \alpha & \beta\end{pmatrix}-\begin{pmatrix}a & b_y & c\\ \beta & \alpha & \alpha\end{pmatrix},$$

$$\Psi_{2y}(B_1)=\begin{pmatrix}a & b_y & c\\ \alpha & \alpha & \beta\end{pmatrix}-\begin{pmatrix}a & b_y & c\\ \beta & \alpha & \alpha\end{pmatrix},$$

$$\Psi_{1x}(B_1)=2\begin{pmatrix}a & b_x & c\\ \alpha & \beta & \alpha\end{pmatrix}-\begin{pmatrix}a & b_x & c\\ \alpha & \alpha & \beta\end{pmatrix}-\begin{pmatrix}a & b_x & c\\ \beta & \alpha & \alpha\end{pmatrix},$$

$$\Psi_{2x}(A_1)=\begin{pmatrix}a & b_x & c\\ \alpha & \alpha & \beta\end{pmatrix}-\begin{pmatrix}a & b_x & c\\ \beta & \alpha & \alpha\end{pmatrix},$$

$$\Psi_{1z}(A_2)=2\begin{pmatrix}a & b_z & c\\ \alpha & \beta & \alpha\end{pmatrix}-\begin{pmatrix}a & b_z & c\\ \alpha & \alpha & \beta\end{pmatrix}-\begin{pmatrix}a & b_z & c\\ \beta & \alpha & \alpha\end{pmatrix},$$

$$\Psi_{2z}(B_2)=\begin{pmatrix}a & b_z & c\\ \alpha & \alpha & \beta\end{pmatrix}\quad\begin{pmatrix}a & b_z & c\\ \beta & \alpha & \alpha\end{pmatrix}.$$

Here $\begin{pmatrix}a & b_i & c\\ \alpha & \beta & \alpha\end{pmatrix}$, etc. are the usual Slater determinants;[2] $i=x, y, z$. The eigenfunctions are recognized as bond eigenfunctions; those with subscript 1 can be thought of as giving a chemical bond between a and b alternating with a bond between b and c; those with subscript 2 correspond to the bond $a-c$. The letter in parenthesis following each Ψ gives the representation of the symmetry group to which it belongs.

Since there are matrix elements only between eigenfunctions of the same symmetry (same A_i), the secular equation is reduced to two quadratic and two linear factors.

1. Linear factors.—

$$A_2\quad H_{1z,1z}-S_{1z,1z}E=0,$$

$$B_2\quad H_{2z,2z}-S_{2z,2z}E=0.$$

2. Quadratic factors.—

$$A_1\quad\begin{vmatrix}H_{1y,1y}-S_{1y,1y}E & H_{1y,2x}-S_{1y,2x}E\\ H_{1y,2x}-S_{1y,2x}E & H_{2x,2x}-S_{2x,2x}E\end{vmatrix}=0,$$

$$B_1\quad\begin{vmatrix}H_{1x,1x}-S_{1x,1x}E & H_{1x,2y}-S_{1x,2y}E\\ H_{1x,2y}-S_{1x,2y}E & H_{2y,2y}-S_{2y,2y}E\end{vmatrix}=0.$$

[2] Slater, Phys. Rev. **38**, 1109 (1931). For a discussion of bond eigenfunctions see Eyring and Kimball, J. Chem. Phys. **1**, 239 (1933).

The subscripts on the matrix elements are the same as the wave functions which they connect. The S's are the matrix elements for unity.

B. Linear configurations

The linear states are classified as Σ and Π. The Y axis (Fig. 1) is taken as the line of centers which makes the eigenfunctions containing $b_y(i)$ give the Σ states and those containing $b_x(i)$ and $b_z(i)$, the Π states. Since the orbitals b_x and b_z are orthogonal, the secular equation will contain three quadratic factors, two of which are identical.

$$\begin{vmatrix} H_{1x,1x}-S_{1x,1x}E & H_{1x,2x}-S_{1x,2x}E \\ H_{1x,2x}-S_{1x,2x}E & H_{2x,2x}-S_{2y,2x}E \end{vmatrix}=0,$$

$$\begin{vmatrix} H_{1y,1y}-S_{1y,2y}E & H_{1y,2y}-S_{1y,2y}E \\ H_{1y,2y}-S_{1y,2y}E & H_{2y,2y}-S_{2y,2y}E \end{vmatrix}=0,$$

$$\begin{vmatrix} H_{1z,1z}-S_{1z,1z}E & H_{1z,2z}-S_{1z,2z}E \\ H_{1z,2z}-S_{1z,2z}E & H_{2z,2z}-S_{2z,2z}E \end{vmatrix}=0.$$

The symmetric linear configuration is also a special case of the isosceles triangle. All non-diagonal elements vanish and there are only linear factors in the secular equation.

At this point it is well to notice that the p atomic orbital on the atom b corresponds to a hydrogen-like atom of nuclear charge 2. According to the work of Brown[3] on the Hartree-Fock consistent field for fluorine, the effective nuclear charge on this nucleus for the valence electron is 1.8 for distances greater than about one Bohr radius. Thus the present calculation should describe the interaction of F with H_2 insofar as electrons other than valence electrons do not matter, and polar states are unimportant. Of course, the ground state for HF is ionic; so this last assumption is certainly not valid and we are dealing with excited HF.

The atom b will be referred to as X since it is halogen-like.

Values of the energy reported are average values of the perturbation Hamiltonian for $a(1)\ b(2)\ c(3)$:

$$H'=\frac{1}{r_{ab}}+\frac{1}{r_{bc}}+\frac{1}{r_{ac}}+\frac{1}{r_{12}}+\frac{1}{r_{23}}+\frac{1}{r_{13}}+\frac{1}{r_{a2}}+\frac{1}{r_{a3}}+\frac{1}{r_{b1}}+\frac{1}{r_{b2}}+\frac{1}{r_{c1}}+\frac{1}{r_{c2}}.$$

[3] Brown, Phys. Rev. **44**, 214 (1933).

The arguments for obtaining such a Hamiltonian are familiar.[4]

The matrix elements which are needed for the special cases treated fall into three classes.

$$H_{1i,1i}=a^2b_i^2c^2+\tfrac{1}{2}ab_iab_ic^2+\tfrac{1}{2}a^2b_icb_ic-acacb_i^2-ab_ib_icac,$$

$$H_{2i,2i}=a^2b_i^2c^2-\tfrac{1}{2}ab_iab_ic^2-\tfrac{1}{2}a^2b_icb_ic+acacb_i^2-ab_ib_icac,$$

$$H_{1i,2j}=\frac{\sqrt{3}}{2}\{ab_iab_jc^2-a^2b_icb_jc\}.$$

Here $i=x, y, z$.

$$ab_iab_ic^2=\int a(1)b_i(2)c(3)H'b_i(1)a(2)c(3)d\tau, \quad \text{etc.}$$

The matrix elements for unity are of course obtained by replacing H' by 1.

The customary procedure of neglecting the triple exchange integrals has been adopted. Three center integrals which involve integration over the p function have been approximated. Thus in $ab_iab_ic^2$ the integral

$$\int \frac{a(1)b_i(1)c^2(2)}{r_{12}}d\tau_1d\tau_2$$

has been set equal to

$$\int \frac{a(1)b_i(1)}{r_{c1}}d\tau_1.$$

In $acacb_i^2$, $\int a(1)c(1)b_i^2(2)d\tau_1d\tau_2$ has been replaced by $\int a(3)c(3)d\tau_3\int b_i^2(1)d^2(2)d\tau_1d\tau_2$ when d is a hydrogen-like orbital midway between a and c.

These are the only approximations used in the calculations. The use of these probably leads to results for all configurations of the atoms which are closer to the Heitler-London prediction than the latter is to reality. Needless to say this simple theory cannot give very good results for very small configurations, but should be quite good for large separations.

[4] See for example Kemble and Zener, Phys. Rev. **33**, 512 (1929).

III. Results

Figures 2 and 3 show the contour surfaces for the linear reactions

$$H+HX(^1\Sigma)\rightarrow H_2(^1\Sigma)+X(^2P), \quad (3)$$

$$H+XH(^1\Sigma)\rightarrow HX(^1\Sigma)+H. \quad (4)$$

These surfaces are the lowest since they lead from one stable molecule to the formation of another. The first surface (Fig. 2) is similar to the semi-empirical HHCl surface calculated by Kimball and Eyring.[5] These linear cases of the present calculation should very nearly compare with the actual HHCl surfaces at fairly large distances. The effects of the other than valence electrons in the outermost chlorine shell should be small since they are in orbitals orthogonal to the hydrogen electrons; the inner shell electrons are far removed. These results may be taken as indicating that the Heitler-London predicted activation energy for reaction 3 and 4 should be very small, X being an actual halogen atom.

The formation of a stable intermediate complex for linear HHCl is not given by Kimball and Eyring's calculation. The regions of low potential energy are more pronounced for configurations of small dimensions in the isosceles triangle case and will be discussed in more detail later.

Figure 3 gives an unsymmetrical activated state for the symmetrical reaction 4. The symmetrical configurations are in fact the most stable of the linear configurations. This is very similar to the semi-empirical result for the H_3 linear molecule.[6] Application of the variational procedure,[7] however, predicted that the activated state would be symmetrical. In view of the results for isosceles triangle configuration, it is not likely that a variational procedure would yield a similar change in this case.

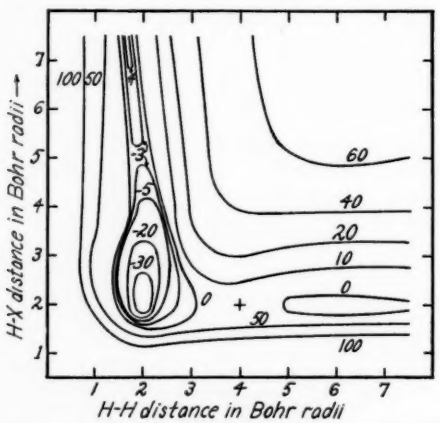

Fig. 2. Contour surface for the reaction $H_2+X\rightarrow H+HX$ with energy in Cal. The activated state at + has an energy of about one-half Cal. The zero of energy is that of the HX molecule. The calculated heat of reaction is 4.2 Cal.

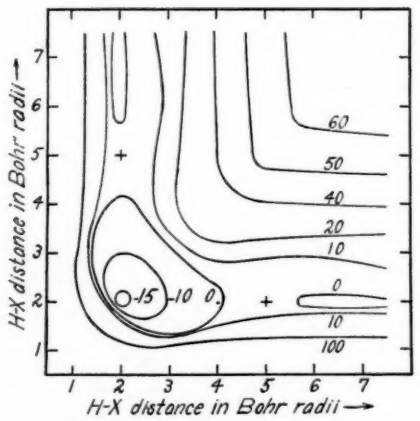

Fig. 3. Contour surface (in Cal.) for symmetrical reaction $HX+H\rightarrow H+XH$. The point + is the activated state; the activation energy, 1 Cal.

The actual value of the activation energy for the reaction $H_2+H\rightarrow H+H_2$ obtained by the most refined calculation of Hirschfelder, Diamond and Eyring was 25 Cal. to be compared with the experimental value 7 Cal. The activation energy obtained for this reaction by a crude calculation such as used in this work is 18 Cal. While the variation of a scale factor and the inclusion of polar states increases the binding energy of H_2 by twenty Calories, that of the activated state is relatively poorer by seven Calories. Results such as this suggest that the rough approximations made in work of this type are practically as good as one can do at present.

It is interesting to note that the predicted activation energies are low. Most of the semi-empirical results (using a 20 percent Coulombic term) as well as the value reported immediately above for H_2+H are too high. Directed valence appears to be effective in lowering activation energies.

[5] Kimball and Eyring, J. Am. Chem. Soc. **54**, 3881 (1932).

[6] Eyring and Polanyi, Zeits. f. physik. Chemie **B12**, 279 (1931).

[7] Hirschfelder, Diamond and Eyring, J. Chem. Phys. **5**, 695 (1937).

The relative positions of the calculated surfaces are more interesting than their absolute values. Figure 4 gives the effect of the presence of the X atom on a line with the H_2 molecule on the potential energy curve of the latter. In 4*a* the Sugiura[8] result for H_2 is given. In 4*b* the X atom is $5a_0$ distant and the H_2 curves are somewhat altered. The Σ and Π surfaces have definitely separated, the former lower and the latter higher than the energy of H_2. In 4*c* for an X−H distance of $3a_0$ the effect is more pronounced. The higher Σ surface develops a minimum as X approaches. This result is to be expected from general considerations. The surfaces are made up from resonance between two states which have these properties: I forms the bond H−X and II forms the bond H−H. For infinite separation of H−H the bond H−X exists (unless of course H−X is also infinite); for finite H−X distance and small H−H separation the bond H−H is lowest in energy. The diagonal matrix elements for the Σ states are shown in the dashed lines and demonstrate this resonance. The nonorthogonality of the eigenfunctions for small distances is shown quite well by the displacement of the center of gravity of the levels by the solution of the secular equation. This nonorthogonality makes it impossible to say that the diagonal elements represent the energy of pure bonds.

Figure 5 gives the effect on the energy of HX

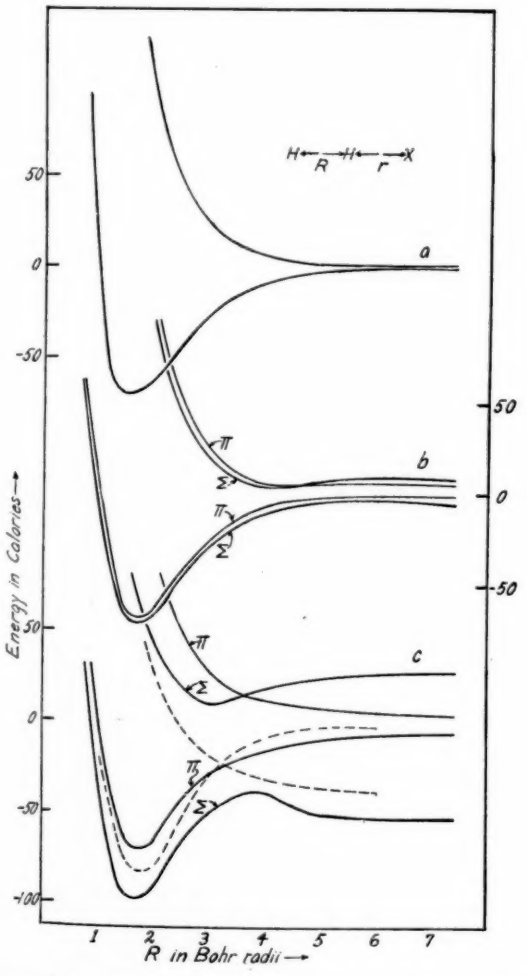

FIG. 4. Linear configuration. *a*, $r=\infty$; *b*, $r=5a_0$; *c*, $r=3a_0$.

[8] Sugiura, Zeits. f. Physik **45**, 484 (1927).

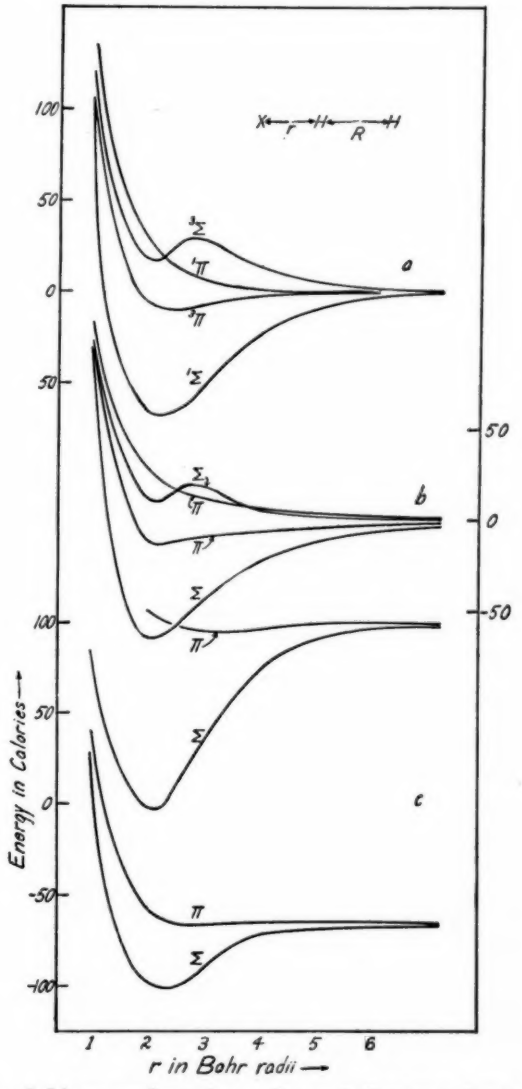

FIG. 5. Linear configuration. *a*, $R=\infty$; *b*, $R=4a_0$; *c*, $R=2a_0$.

of H on a line. In 5*a* the result for H−X which is equivalent to the Sugiura result for H_2 is shown i.e., the H atom is at infinite separation.

The $^3\Sigma$ state surprisingly shows a minimum. The cause of this minimum is of course quite different from the one occurring in 4*c* and discussed above. This result is directly traced to the behavior of the normalization term. The energy of the state is given by the expression $-(J-K)/(1-I^2)$ where J is the Heitler-London Coulomb integral, K the exchange integral and I the overlap integral. $J-K$ is a monotonic function decreasing with the internuclear separation, while $1-I^2$ goes through a minimum. Thus E also goes through a minimum. Of course there is a physical meaning to the behavior of the normalization. In the triplet state the electrons tend to keep further apart. Although they are kept away from the regions of lowest potential energy there is some compensation for the lessened repulsion. Presumably the division by $1-I^2$ makes this correction. If the eigenfunctions are not good in this region large errors may be introduced since I^2 gets quite large. It is not known whether there really is such a minimum in this repulsive curve for such molecules as HCl etc. This behavior of the overlap integral I is responsible in large part for the low energies occurring in this work for small separations. Rosen[9] observed a similar phenomenon in calculations with *s* electrons. He found that as the principal quantum number, n, increases, the repulsive curve ($^3\Sigma$) developed a minimum similar to the one observed here. For $n=6$ the $^3\Sigma$ state actually has a stable minimum. This occurs because of the decrease in importance of the exchange energy as n increases.

It is to be noted that the $^3\Pi$ state lies below the $^1\Pi$ state and forms a shallow minimum while the latter is always repulsive. The reason for the reversal of these states is due to the positive exchange integral. In the spectra of the hydrogen halides there is a continuum in the region corresponding to the transition $^1\Sigma \rightarrow {}^1\Pi$ indicating that the latter state is really repulsive.

In 5*b* the H−H separation is $4a_0$ and both of the Σ states are slightly lowered while the Π states are practically unaffected. In 5*c* for H−H separation of $2a_0$ there is strong interaction. The upper Π state develops a minimum due to resonance with the lower. The upper Σ state becomes slightly negative at one point.

Figure 6 continues the description of the effect of H on a line with HX. This time the H atom is next to the X atom.

The linear symmetric states are shown in Fig. 7. For this particular configuration there is a *g* and *u* property (gerade and ungerade). The Σ_u is the lower of the Σ states because it forms the bonds H−X while the Σ_g state forms the bond H−H. For small distances the H−H attraction is great enough to overcome the H−X repulsion and the Σ_g state is very low.

The triangular configurations are quite interesting because they give the unexpected result of a very low energy. In Fig. 8 the energy in contours for the A_1 surface is given. This is the surface which gives the Σ linear state and is to

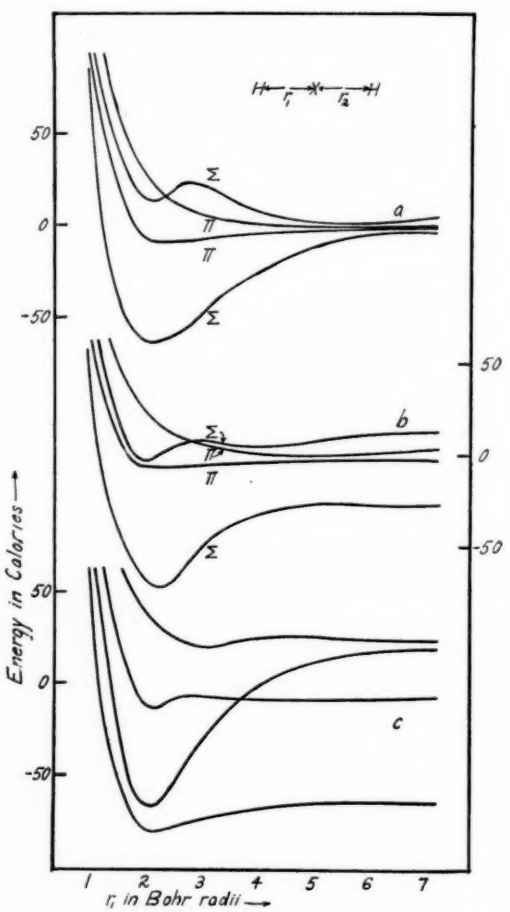

FIG. 6. Linear configuration. *a*, $r_2=5$; *b*, $r_2=4$; *c*, $r_2=2$.

[9] Rosen, Phys. Rev. **43**, 671 (1933).

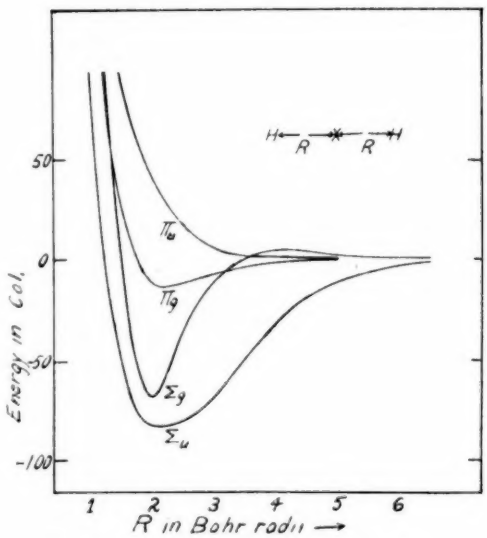

FIG. 7. Symmetrical linear configurations.

be compared with Figs. 2 and 3. It is to be noticed first that there is no activation energy for the approach of X perpendicular to the line of centers of H_2. Then also there is a very stable triatomic system formed. It is quite certain that this stable system exists for H_2X in the Heitler-London approximation. This is a system which has only three electrons and of course it is not possible to predict the reality of a stable triatomic molecule H_2Cl from this calculation since the effects of the neglected electrons are most important in this region. The results of this calculation would indicate that the equilibrium for the reaction $2H_2X \rightleftharpoons H_2+2HX$ is displaced to the left. If, however, the actual binding energy of H_2 is used, this condition is no longer true.

It is probably not because the eigenfunctions which were used are better in this region than for larger separations that the energy becomes low as it does. It is rather more likely that the neglect of the triple exchange integrals is not permissible and the error which is thus introduced works in the direction such as to give this result. The qualitative results of this calculation are probably correct, i.e., the existence of a region of low potential energy for triangular configurations. This point will be discussed later.

Figure 9 gives the angular dependence of the triangular configurations. The extreme right with $\theta=90$ corresponds to the symmetric linear case. It is apparent that the linear system is very unstable with respect to the formation of a triangular system. It was found from Fig. 3 that the symmetric linear systems were the most stable of the linear configurations.

In the calculation no points were obtained quite near the linear system, i.e., for the slightly bent condition and so the exact behavior of the surfaces is not known in that region. The figure is not quite exact since of course all of the surfaces must have zero slope for $\theta=90°$, since they

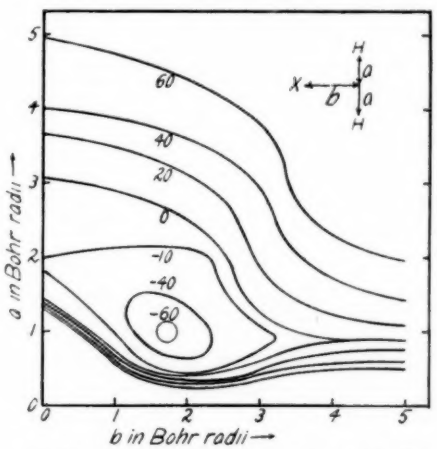

FIG. 8. Triangular configuration A_1 surface. Energy is in Cal. The actual physical situation is obtained from the figure directly; the atom X is at the origin and one H atom is at a point on the figure; the other H atom is symmetrically located below the figure.

cannot have two slopes at a point. In some cases the curvature in this region may be quite great.

The low energies of the A_1 and B_1 states are somewhat surprising. One can understand this better by examining the charge distribution for these states. The A_1 surface is the lower. It arises from the resonance of two bond functions. One of these forms the bond $a-c$ with the orbital of X directed midway between these two atoms. This strongly overlapping charge distribution is responsible for the low energy for the triangle when θ is small. The second A_1 function is responsible for the low energy of the linear system. It forms the bonds ab and bc with the p orbital directed toward these nuclei. Thus the charge distribution is always favorable to the formation of a stable system.

The B_1 surface has good overlapping of the charge for small values of θ, but forms II linear states, which are of course not very low.

These low energies are also favored by another

factor. The Coulombic interaction of a p orbital with an s orbital is greater than the exchange interaction.[4,10] Thus the overlap of the p charge distribution always tends to lower the energy rather than raise it, even when the exchange interaction is unfavorable.

These considerations make the stable triangular molecule more reasonable. It is probably a reality, although the energy is undoubtedly not as low as this calculation would predict.

IV. Discussion

The most interesting results of this calculation are the low values obtained for the activation energies of reactions 1 and 2. This is a direct consequence of the relatively small importance of the exchange energy. It is of course the exchange interaction which gives rise to activation energy. The Coulombic term is always attractive. This means that the potential is decreased for the electrons between a molecule and an approaching reactant. However, due to saturated valence of the molecule the Pauli exclusion principle prevents the valence electrons of the reacting atom or molecule from occupying this region of low potential unless they increase their momentum simultaneously. This condition is called unfavorable exchange interaction; it is the "promotion" of valence electrons of the reactant.

As pointed out previously, the activation energy for the ortho–parahydrogen conversion calculated by this method is far above the experimental value. The semi-empirical calculation (using a Coulombic term 14–20 percent of the total binding energy) also tends to give activation energies too high. It has been already pointed out[11] that larger Coulombic terms will improve these results. In the present calculation it was found that at the activated state the Coulombic energy was approximately half the total. This question has been discussed again by Hirschfelder and Daniels.[12] In calculating the binding energy of atoms in s states Rosen and Ikehara[13] observed that the fraction of Coulombic energy increased rapidly with the principal quantum number. It has been observed[10] that for electrons in p states the Coulombic energy is much more important than the exchange energy.

From these considerations it is to be expected that the activation energy for atomic reactions of the type

$$A+BC\rightarrow AB+C$$

should decrease with increasing atomic weight of the reactants. One might expect that the true activation energies for all reactions of this type should be less than 7 cal., the value for the ortho–parahydrogen conversion. It has been pointed out[14] that the condition for large exchange interaction is the approximate equality

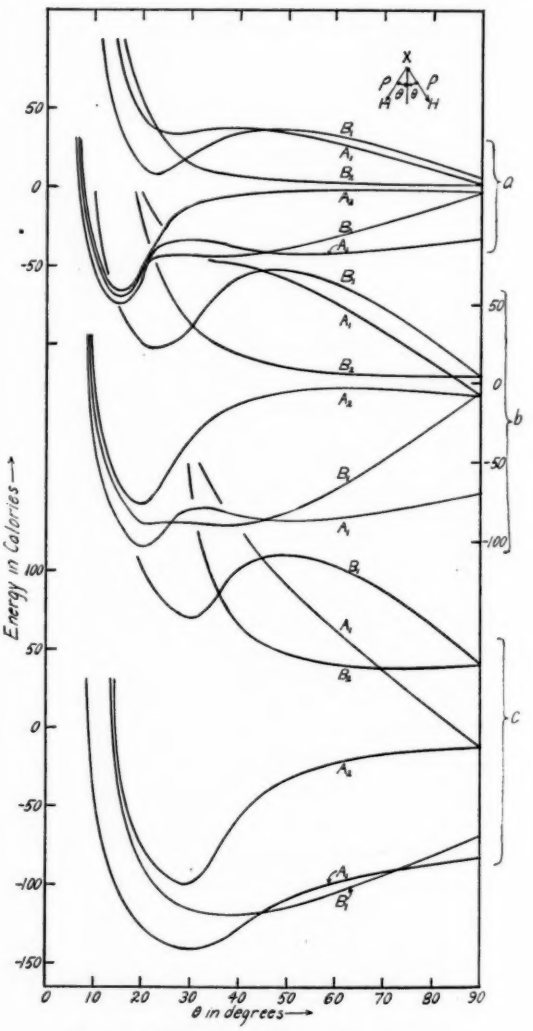

Fig. 9. Isosceles triangle configurations. a, $\rho=4$; b, $\rho=3$; c, $\rho=2$.

[10] Bartlet, Phys. Rev. **37**, 507 (1931).
[11] Wheeler, Topley and Eyring, J. Chem. Phys. **4**, 178 (1936).
[12] Hirschfelder and Daniels, J. Chem. Phys. forthcoming.
[13] Rosen and Ikehara, Phys. Rev. **43**, 5 (1932).
[14] See for example, Pauling, *The Nature of the Chemical Bond* (Cornell University Press, Ithaca, 1939).

of the energies of the two atomic orbitals involved. Thus one should expect activation energy to decrease with difference in principal quantum numbers of the valence electrons. The general experimental results seem to confirm these observations.

The above discussion applies to the linear reactions which are described by the contour surfaces of Figs. 2 and 3. There is, however, doubt that the reactions are this simple. It is shown (Fig. 8) that there is no activation energy for the formation of the triangular complex H_2X from H_2 and X, the approach of X being made perpendicular to the H_2 molecule. The approach of H perpendicular to HX was not investigated but there is reason to believe that such an approach would involve less energy than the linear one (see below). If this is true the reaction 1. does not proceed by a linear mechanism but in such a way that a triangle is formed by the three molecules at all times. A proposed mechanism is shown in Fig. 10.

At present it is not possible to prove from calculation just what the structure of the activated state really is. The activation energy calculation for any given reaction is uncertain by such a large amount that it is impossible to distinguish between two forms by a theoretical calculation of rate. Wheeler, Topley and Eyring[11] calculated the absolute rate for the reaction of chlorine and bromine with hydrogen. Although the calculated reaction surfaces gave activation energies which are considerably higher than the experimental values, these surfaces were used to obtain the partition function of the activated state. The absolute reaction rates which are obtained using the experimental values of the activation energy and these calculated frequency factors are quite good. It is well to note, however, that in the semi-empirical treatment all valence electrons are treated as if they were in s states; this error was retained throughout the calculation and the degeneracy of the p state was neglected. Thus their rate should contain the factor $\frac{1}{3}$ to weight the activated state properly. When this correction is also made the calculated value of the frequency factor for H_2+Cl is slightly too small and that for H_2+Br is too small by more than a factor of ten.

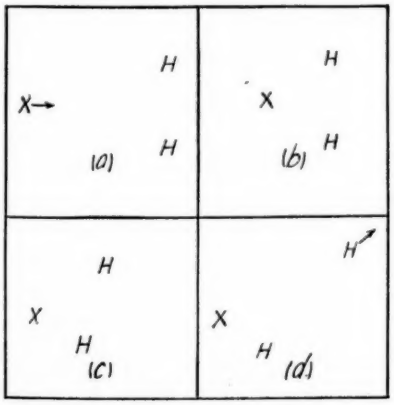

FIG. 10. A possible mechanism for the reaction $X+H_2 \rightarrow XH+H$. (a) shows the approach of X. (b) shows the stable molecule HX which should be present in a reaction mixture in fairly large concentration because of its low energy. (c) gives the activated state. In (d) the H atom is safely away from HX and the reaction is complete.

A change in the activated state from linear to triangular would change one degree of vibration to one degree of rotation. A factor

$$\frac{8\pi^2 IkT}{h^2} \prod_{i=1}^{4} \left(1-\exp\frac{h\nu_i}{kT}\right)\exp\frac{E_0}{kT}$$

is replaced by

$$\frac{8\pi^2(8\pi^3 ABCkT)^{\frac{1}{2}}kT}{h^3} \prod_{i=1}^{3} \left(1-\exp\frac{h\nu_i}{kT}\right)\exp\frac{E_0'}{kT}.$$

I is the moment of inertia of the linear activated complex; A, B, C the three moments of the nonlinear complex; the ν_i are the vibration frequencies. This change would tend to increase the frequency factor since there are more rotational than vibrational states. For example in the calculation for H_2+Br and D_2+Br the rotational partition functions ranged in value from 3 to 6 while the vibrational partition functions were from 1.0 to 1.5.

One might thus expect to obtain better agreement with experiment if a triangular activated state were used. This simple consideration is by no means conclusive and the entire potential energy surface must be calculated before the reaction is entirely understood. There is one other fact which makes the triangular activated state desirable. The calculated ratios of the rates

$$\frac{k(H_2+Br)}{k(D_2+Br)} \quad \text{and} \quad \frac{k(H_2+Cl)}{k(D_2+Cl)}$$

are smaller than the experimentally observed values. The reason that H_2 reacts more rapidly than D_2 is because the decrease in zero point energy from the initial to activated state is

more for H_2 than D_2. Wheeler, Topley and Eyring[11] suggest that their calculated vibration frequencies in the activated state are too large. The removal of one of these frequencies is thus desirable. If one degree of vibrational freedom is removed in the activated state, the rate of reaction of H_2 will be favored over that of D_2.

It was mentioned above that on considering the degeneracy introduced by the p function the factor $\frac{1}{3}$ appears in the reaction rate expression. We now proceed to explain this further and consider the other possible effects of the p valence. The theory of reaction rates gives the total rate of reaction as the sum of the rates by all possible paths. It is usually assumed that practically all of the reaction will go by one path because of the exponential dependence of the rate on activation energy. In the present example the reaction $H_2+X\rightarrow HX+H$ might be completed in an alternative way as follows. It will be simplest to consider the linear type reaction.

The X atom might conceivably approach to form a Π state and complete the reaction to form an excited HX molecule on a $^1\Pi$ state. This molecule could then radiate to form the normal $^1\Sigma$ HX molecule, giving the same result as the reaction which took the lowest path, i.e., being always Σ.

The reaction is, however, so endothermic that its occurrence can be safely neglected. The HX $^1\Pi$ molecule has no binding energy and its process amounts to the dissociation of H_2. All other possible alternative mechanisms involve the absorption of radiation and carrying out the process on still higher surfaces.

Thus the factor $\frac{1}{3}$ appears since the probability of the activated state is reduced by the additional surfaces which the degeneracy introduces. These are not capable of producing a successful reaction and serve as "blind alleys" into which reacting systems may fall. Directed valence will always introduce a factor of this type into the reaction rate expression.

In the last section the low region of the A_1 surface was shown to result from a very favorable charge distribution. It has often been noted[15] that the most stable states of molecules were generally the most symmetric. For a molecular orbital point of view this means that the total wave function usually belongs to the identical representation, i.e., it is unchanged by any symmetry operation. Coulson[16] has discussed the molecular orbitals for H_3 and has concluded that the triangular configuration is less stable than the linear because a node which of necessity appears in the orbital of the third electron introduces repulsion between two of the H atoms and tends to spend the triangular system to form a line. Of molecular orbitals built up from s atomic orbitals there can only be one belonging to the identical representation. The orbital holds two electrons and a third electron must go up into an orbital which introduces a node. This electron is "promoted" and is antibonding. For an available p atomic orbital there can be two molecular orbitals which belong to A_1 and are bonding. The valence electrons of H_2O, for example, are in such orbitals. These orbitals occur because of the greater momentum of the p electron. It can now occupy the region of low potential energy in which the hydrogen s electrons stay, whereas it would be kept from this region if it were in an s state by the exclusion principle.

The formation of stable intermediate complexes has occurred a number of times in calculations similar to this. In studying the reaction $H+CH_4\rightarrow CH_3+H_2$, Gorin, Kauzmann, Walter and Eyring[17] found a "Coulomb complex" of CH_4 and H. They attributed to this complex the effect of methane on the ortho–parahydrogen conversion. For a certain temperature range methane retards this conversion. The complex CH_5 would reduce the concentration of hydrogen atoms in the reaction system and thus slow down the rate of reaction. This complex has an activation energy for formation and therefore is effective only for temperatures higher than room temperature.

Experimental evidence for the existence of a H_2Cl complex is not easy to obtain. In a hypothetical system in which the reactions $Cl+H_2 \rightleftharpoons HCl+H$ were progressing it would of course be impossible to obtain any evidence at all, since the complex would be present in equilibrium amount and not affect the rate. In the actual H_2+Cl_2 reaction the presence of the complex

[15] For example Seitz and Sherman, J. Chem. Phys. **2**, 11 (1934).

[16] Coulson, Proc. Camb. Phil. Soc. (2) **31**, 244 (1935).

[17] Gorin, Kauzmann, Walter and Eyring, J. Chem. Phys. **7**, 633 (1939).

could have an effect. If such a radical were present in appreciable concentration and disappeared by reaction with the atoms Cl and H which carry the reaction chain, the over-all rate of reaction would tend to be independent of H_2 concentration; for the rate-determining and chain-breaking processes would be both directly proportional to H_2 concentration. It is well known experimentally that this is not true under any conditions. So under experimental conditions an H_2Cl radical must be destroyed by a process which creates a chain carrier, such as

$$H_2Cl+Cl_2 \rightarrow 2HCl+Cl.$$

At a steady state such a process could not affect the form of the reaction rate expression. A reinterpretation of the experimental data on such a scheme could hardly be profitable at present.

Note added in proof.—Since this paper was written the author's attention has been called to some work by Steiner and Rideal[18] on the exchange reactions between deuterium and hydrogen halides. Semi-empirical potential surfaces for the linear reactions of H and HX were constructed and the triatomic complex was found to be stable. These authors give as experimental evidence for the existence of the complex the acceleration of the recombination of H atoms by HCl, reported by Rodebush and Spealman.[19]

The author wishes to thank Professor Eugene Wigner for suggesting this work and for many helpful discussions. He also wishes to thank Professor Farrington Daniels and Dr. Joseph Hirschfelder for constant interest, and Miss Eleanor Gish for checking some of the calculations.

[18] Steiner and Rideal, Proc. Roy. Soc. **A173**, 503 (1939); Steiner, *ibid.* 531 (1939).

[19] Rodebush and Spealman, J. Am. Chem. Soc. **55**, 130 (1933).

SEPTEMBER, 1940 JOURNAL OF CHEMICAL PHYSICS VOLUME 8

The Mechanism of Reactions Involving Excited Electronic States

The Gaseous Reactions of the Alkali Metals and Halogens

JOHN L. MAGEE*
Princeton University, Princeton, New Jersey

(Received June 19, 1940)

In many of the reactions of the alkali metals with the halogens the reacting system changes from a homopolar to a polar state, or vice versa. The possibility of a restriction on this change is considered, and it is concluded that there will be a serious restriction only for some of the atomic reactions

$$M+X \rightarrow MX, \quad (a)$$

which are of little importance. The crossing points between the polar and homopolar states for the reactions

$$M_2+X \rightarrow MX+M \quad (b)$$

$$M+X_2 \rightarrow MX+X \quad (c)$$

are drawn in so close that the interaction is large enough to insure transition. Due to the threefold degeneracy of the initial state of *b* (which arises because X is in a *P* state) this reaction has the possibility of leading directly to the excitation of the M atom which is formed. The nature of the potential surfaces for this process are considered. The process first suggested by Polanyi, the excitation of M atoms by vibrationally excited MX molecules, is discussed. This process is possible because of a crossing of the two lowest polar states for the M_2X system. These two surfaces cross for a certain isosceles triangular configuration. Reacting systems thus easily go from the lowest to the second state in this region.

I. INTRODUCTION

EXCITED electronic states of reacting systems are frequently of considerable importance in chemical reactions. This is always true of photochemical and chemiluminescent reactions. Potential energy surfaces become increasingly more difficult to construct as systems become more complicated and as excitation is increased. For excited states there

* National Research Fellow.

are usually many surfaces which interact in various ways, cross, etc. The nature of the interacting forces are not very well known in most cases, and one frequently cannot even predict which of a number of states will be the lowest. It is important, however, to know the nature of potential surfaces because of their application in the calculation of reaction rates. In this paper a few simple reactions are considered in an attempt to explain the reaction rates and mechanisms in terms of potential surfaces.

Reactions between atoms and diatomic molecules are the most simple which can be treated. There is always the simplification which is very helpful in that the electronic states can be classified as even and odd with respect to the plane of the three atoms, and are thus separated into noncombining groups. In this paper we shall be concerned with a group of reactions which have been extensively investigated,[1] the gaseous reactions of the alkali metals and halogens. (For a discussion of the experimental results of these reactions see Section V.) These reactions involve both the change of the reacting system from a homopolar to a polar state and the excitation of atoms. Both of these types sometimes are "nonadiabatic," and occur with a small rate because of a restriction in the reaction path. We shall see that this is by no means necessarily the case for either. Reactions which lead to the excitation of atoms can take place on surfaces which are as smooth as that for the ortho–para-hydrogen conversion.

The considerations of Teller[2] on the crossing of potential surfaces in molecules explained quite satisfactorily the mechanism by which molecules lose electronic energy in nuclear motions, i.e., heat. It is clear by the principle of microscopic reversibility that the reverse process,

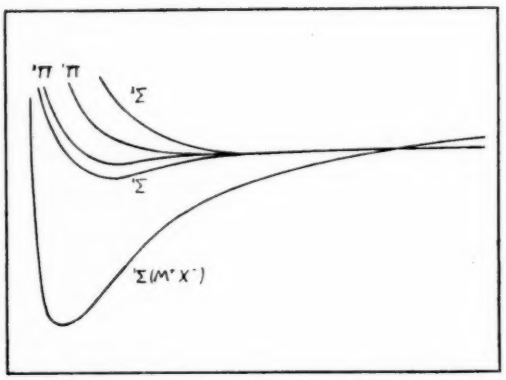

FIG. 1. Schematic potential curves for diatomic alkali halide molecules.

the transfer of kinetic energy into electronic energy, can take place. Polanyi and others[1] showed that the kinetics of the halogen alkali metal reactions seem to point to a process of this kind. The reaction

$$MX^*+M\rightarrow MX+M^*\rightarrow MX+M+h\nu$$

is said to be responsible for the observed luminescence. Here MX* designates an MX (alkali halide) molecule in its lowest electronic state with an excess of vibrational energy and M* is excited from its normal ^2S state to a ^2P state. As a rule one expects a very small probability for this sort of energy transfer, and an alternative explanation has been suggested.[3] Further consideration of the potential surfaces shows that the process is to be expected (Section VI).

The reactions to be expected in gaseous mixtures of the alkali metals and halogens are discussed in this paper.

II. The Reactions of M and X

At first we shall consider the reactions of one alkali metal atom with one halogen atom. Although these reactions are in themselves of little importance (at least in determining the mechanism of any chemical reaction), they are the simplest examples of an electron transfer which is partially restricted. It is also interesting to compare them with the atomic association reactions which involve only homopolar interaction, such as $H+H\rightarrow H_2$.[4]

In Fig. 1 schematic curves are given of the

[1] The experimental work and interpretations of the observed kinetics of these reactions are discussed in these and other papers. (a) M. Polanyi, *Atomic Reactions* (Williams and Norgate, Ltd., London, 1932). (b) G. Schay, *Hochverdunten Flamen* (Berlin Gebr. Borntrager, 1930). (c) H. Beutler and M. Polanyi, Zeits. f. physik. Chemie **B1**, 3 (1928); S. v. Bogdandy and M. Polanyi, *ibid.* **1**, 21 (1928); M. Polanyi and G. Schay, *ibid.* **1**, 30 (1928); H. Ootuka and G. Schay, *ibid.* **1**, 62, 68 (1928); H. Ootuka, *ibid.* **7**, 407 (1930). (d) M. G. Evans and M. Polanyi, Trans. Faraday Soc. **35**, 178 (1939). (e) M. Polanyi, *ibid.* **35**, 195 (1939).

[2] Teller, J. Phys. Chem. **41**, 109 (1937); for discussion of the crossing of potential surfaces see also Neumann and Wigner, Physik Zeits. **30**, 467 (1929).

[3] Wigner, J. Chem. Phys. **7**, 646 (1939).

[4] Eyring, Gershinowitz and Sun, J. Chem. Phys. **3**, 786 (1935).

lowest states of the MX diatomic molecule. Only the two lowest $^1\Sigma$ states are usually given since they are the only ones of importance in the formation of the normal MX molecule. The others will also be of interest in this work since we are concerned with the excited states. The π states arise due to the P state of the X atom. For these states the triplet is lowest because the exchange integral is positive.[5]

The reactions which we shall consider are just those which involve the dissociation of the normal molecule into the atoms

$$MX \rightarrow M+X \tag{1}$$

and the reverse reaction

$$M+X \rightarrow MX. \tag{2}$$

In the dissociation of diatomic molecules it has been recognized that the rotational state is important.[4] The angular momentum acts as an additional potential and introduces a maximum in the potential curve for the molecule. This maximum is of course the activated state for the dissociation and changes position with the rotational state. This is true of molecules which have exponential type attractions, i.e., homopolar bonds. Polar states such as M^+X^-, however, have potentials which attract as $1/r$, and the more rapidly varying angular momentum ($1/r^2$) cannot introduce a maximum. The activated state for reaction (1) is thus always at the crossing point between the polar and homopolar states. This fact materially simplifies the formulation of the rate constant, which, written in the usual manner[6] is

$$k_1' = \kappa \frac{kT}{h} \frac{\dfrac{(2\pi m_{MX} kT)^{\frac{3}{2}}}{h^3} \sum (2J+1) e^{-J(J+1)h^2/8\pi^2 \mu r_c^2 kT} e^{-D/kT}}{\dfrac{(2\pi m_{MX} kT)^{\frac{3}{2}}}{h^3} \dfrac{8\pi^2 \mu r_0^2 kT}{h^2} \dfrac{1}{1-e^{-h\nu_0/kT}}}. \tag{3}$$

μ is the reduced mass, $m_M m_X/m_{MX}$; D is the dissociation energy to M+X; r_c is the distance to the crossing point and r_0 is the equilibrium separation. The activation energy does depend upon the rotational quantum number, but we can substitute the classical rotational partition function for the activated state. This gives

$$k_1' = \kappa \frac{kT}{h} (1-e^{-h\nu_0/kT}) \left(\frac{r_c}{r_0}\right)^2 e^{-D/kT}. \tag{4}$$

Now let us consider κ. The expression k_1' without this factor gives the number of molecules which are dissociating at complete thermal equilibrium.[7] In the present example this must be corrected in two ways; so we write $\kappa = \sigma\rho$.

The factor ρ gives the fraction of the equilibrium dissociation number which comes from the normal MX molecule. Since there is a crossing of curves, some of those dissociating will have come from the excited $^1\Sigma$ state. So ρ depends upon the nature of the two states at the crossing point in the manner which Zener and Landau have given.[8] Later we shall make estimates of this factor for a number of cases. For the alkali halides it varies all the way from zero to unity, as seen below.

The factor $(1-\sigma)$ gives the fraction of dissociating molecules which have come originally from the dissociated state,[4] and are redissociating because they were not stabilized. Since a three-body collision changes the potential between the pair, the rate as we have formulated it really applies only to molecules which are stabilized by radiation. The life of an excited MX oscillator is $\sim 10^{-1}$ second.[1e] So σ is $\sim 10^{-12}$. Thus the rate of this reaction is quite slow. Actually the transfer of energy by collisions with other molecules is the most important factor in determining the rate of reaction of this

[5] Magee, J. Chem. Phys., preceding paper.
[6] Eyring, J. Chem. Phys. **3**, 109 (1935).
[7] For a discussion of this and related topics see Hirschfelder and Wigner, J. Chem. Phys. **7**, 616 (1939).
[8] Zener, Proc. Roy. Soc. **A137**, 696 (1932); **A140**, 660 (1933); Landau, Physik. Zeits. Sowjetunion **2**, 46 (1932).

type and one can use a σ which is pressure dependent. For ionic molecules a formulation of this type should be quite accurate because in the neighborhood of the activated state it is only the forces between the two ions which are important anyway.

For reaction (2) the rate constant is:

$$k_2' = \frac{1}{12}\kappa \frac{kT}{h} \frac{(2\pi m_{MX} kT)^{\frac{1}{2}} \, 8\pi^2 \mu r_c^2 kT}{\frac{h^3}{(2\pi m_M kT)^{\frac{1}{2}}} \, \frac{h^2}{(2\pi m_X kT)^{\frac{1}{2}}}}$$

$$= \tfrac{1}{6}\kappa r_c^2 (2\pi kT/\mu)^{\frac{1}{2}}. \qquad (5)$$

κ is of course the same as in 4. The factor $\frac{1}{12}$ takes into account the degeneracy of the dissociated state, fourfold for spin and threefold for orbital degeneracy. Without these factors ($\frac{1}{12}\kappa$) the rate just gives the classical number of collisions between two atoms having a collision diameter r_c.

We shall now consider in more detail the nature of the factor ρ of κ which is determined by the nature of the interaction between the two states. The potential for the ionic state can be written as:

$$V = -Z_1 Z_2/r + b/r^n. \qquad (6)$$

Here Z_1 and Z_2 are the charges on the two ions and r is their separation; b and n are constants. n varies from 6 to 10 for the alkali halides. In the region of crossing (see Fig. 1) the homopolar nteraction is small, because of the distance, and ican be taken as zero.* Equation (6) gives as zero potential the separated ions. At the crossing point this has become $I(\mathrm{M}) - E(\mathrm{X})$; $I(\mathrm{M})$ being the ionization potential of the alkali and $E(\mathrm{X})$ the electron affinity of the halogen.

$$I(\mathrm{M}) - E(\mathrm{X}) = -Z_1 Z_2/r_c + b/r_c^n, \qquad (7)$$

$$r_c \cong Z_1 Z_2/(I(\mathrm{M}) - E(\mathrm{X})). \qquad (8)$$

b/r_c^n is too small to matter. Values of r_c calculated from this formula for the alkali halides are given in Table I. Values of $I(\mathrm{M})$ and $E(\mathrm{X})$ which were used are given in Table II. The interaction between the initial and final states is approximated as follows.

$$\epsilon = \int \mathrm{M}(1)\mathrm{X}(2) H_1 \mathrm{X}'(1)\mathrm{X}'(2) d\tau. \qquad (9)$$

M(1) is the orbital of the valence electron on M. X(2) is the valence P_Z orbital on X, the Z axis being along the line of the nuclei. X′ refers to the same orbital when occupied by two electrons. H_1 is the perturbation energy operator.

$$H_1 = \frac{1}{r_{MX}} + \frac{1}{r_{12}} - \frac{1}{r_{M2}} - \frac{1}{r_{X1}} \qquad (10)$$

TABLE I. *Distance of crossing between polar and homopolar states of* M−X *as calculated from 8 (in Bohr radii, 0.53A).*

	Li	Na	K	Rb	Cs
F	22.0	27.4	144.0	933.8	—*
Cl	16.8	19.8	47.7	66.2	225.7
Br	14.8	17.0	34.6	43.1	79.6
I	12.6	14.3	24.7	29.5	41.7

* For Cs and F there is no crossing.

TABLE II. *Ionization potentials of* M *and* X⁻. *These values of I and E were obtained from Herzberg, "Atomic Spectra and Atomic Structure"; values of α from Eq. (15).*

M	I ELECTRON VOLTS	$\alpha = \frac{z^*}{n^*}$	X	E	α
Li	5.363	0.629	F	4.13	0.552
Na	5.12	0.615	Cl	3.75	0.526
K	4.318	0.565	Br	3.53	0.511
Rb	4.159	0.554	I	3.22	0.488
Cs	3.87	0.535			

* At the separations of interest here all interactions, other than ionic, are less than a large Calorie, and in most cases much less. An interaction of a Calorie would change the crossing point for Na+Cl (given in Table II) only 0.6 Bohr radii. It is doubtful whether the electron affinities are known well enough to give even a sign to the deviations to be expected for the r_c values of Table II.

and we have

$$\epsilon=-\frac{1}{r_{MX}}\int M(1)X'(1)d\tau_1\int X'(2)X(2)d\tau_2+\int M(1)X'(1)\frac{1}{r_{12}}X(2)X'(2)d\tau_1 d\tau_2$$
$$-\int M(1)X'(1)d\tau_1\int\frac{X(2)X'(2)d\tau_2}{r_{M_2}}-\int\frac{M(1)X'(1)d\tau_1}{r_{X_1}}\int X(2)X'(2)d\tau_2. \quad (11)$$

As r_{MX} is increased, the first and third terms on the right quickly become equal and cancel. The value of ϵ in the region of interest is given by the difference of the other two terms. It is difficult to say without calculation how large this difference is; both terms asymptotically approach the same value $(2/r_{MX})\int M(1)X'(1)d\tau_1$. One might guess that ϵ is roughly proportional to this quantity for a restricted region of r_{MX} values. All of the integrals which appear in (11) have been calculated for the case that all orbitals are 1s orbitals.[9] ϵ obtained from these integrals varies from $\frac{1}{3}$ to $\frac{1}{6}$ of $(1/r_{MX})\int M(1)X'(1)d\tau_1$ for distances from 3 to 12 Bohr radii. Due to the screening constant for the alkali halides, which is approximately 0.5, these distances correspond to from 6 to 24 Bohr, radii, which includes a number of the most interesting cases (see Table I). We shall approximate ϵ as

$$\epsilon\sim\frac{1}{5r_{MX}}S_{MX}, \quad (12)$$

where $S_{MX}=\int M(1)X'(1)d\tau_1$.

In order to calculate S_{MX} we use one electron atomic wave function[10] of the type

$$\psi=Nr^{n^*-1}e^{-z^*r/n^*}.$$

Here n^* is the effective principal quantum number, z^* the effective nuclear charge, N the normalization constant, and r the distance of the electron from the nucleus. We are interested in the overlap for large nuclear separations. For large r the wave equation becomes

$$H\psi\sim-\frac{1}{2}\frac{\partial^2\psi}{\partial r^2}=-\frac{1}{2}\left(\frac{z^*}{n^*}\right)^2\psi=-\frac{1}{2}\alpha^2\psi. \quad (13)$$

Atomic units are used, and α is defined by the equation. Also

$$H\psi=-I\psi, \quad (14)$$

I being the ionization potential of the electron. So that

$$\alpha^2=2I, \quad \alpha=\sqrt{2I}. \quad (15)$$

In Table II values of α calculated from Eq. (15) are given. The ionization potential for X^- is, of course, just the electron affinity of X.

Values of ϵ obtained in this manner are probably correct to within a factor of 2 to 5 for values of r_c from 5 to 15A ($\sim$10 to 30 Bohr radii). For r_c values larger than this the calculated values are too large. But at least one can obtain a semiquantitative idea as to the ease of electron transfer in these particular reactions. One can remember that values of $\epsilon\sim kT$ lead to a transition probability (ρ value)$\sim$1.

Zener and Landau[8] have given the probability in which we are interested as:

$$\rho=1-\exp\frac{(-4\pi^2\epsilon^2)}{hv|S_i-S_f|} \quad (16)$$

in which v is the velocity of motion on the poten-

TABLE III.

C	0.1	0.01	0.001	0.0001	0.00001	0.0^61
ρ	0.276	0.0531	0.00774	0.001027	0.000128	0.0^5156

$$C=\frac{4\pi^2e^2m^{\frac{1}{2}}}{(2kT)^{\frac{1}{2}}h\,|S_i-S_f|}; \quad \rho=1-e^{-\frac{4\pi^2\epsilon^2}{hv|S_i-S_f|}}.$$

TABLE IV. *Interaction energy as calculated from (12). Energy is given in small calories.*

	Li	Na	K	Rb	Cs
F	12	4	10^{-24}	*	—
Cl	228	219	10^{-3}	*	*
Br	†	†	10	1	*
I	†	†	287	170	17

* Matrix element small, $\ll$ 1 calorie.
† Matrix element large, $\sim$ 1000 calories or more.
— No crossing.

[9] Hirschfelder and Weygandt, J. Chem. Phys. **6**, 806 (1938).
[10] Slater, Phys. Rev. **36**, 57 (1930).

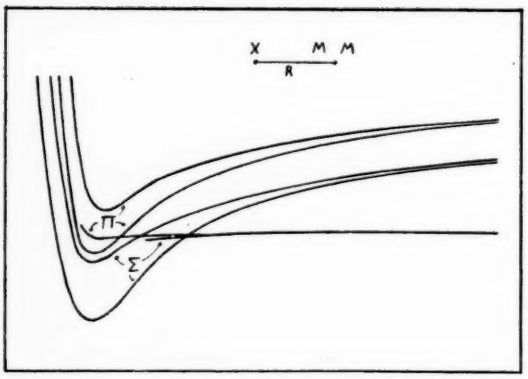

FIG. 2. Schematic curves for linear approach of X to M_2.

tial curve at the transition point, $|S_i - S_f|$ is the absolute value of the difference in slope of the two crossing curves at their crossing. Since the probability depends upon the velocity, an average must be made over all velocities. Stearn and Eyring[11] have obtained this average by graphical integration. In Table III some of their values of ρ are reproduced. They found it convenient to express the results in terms of a quantity

$$c=\frac{4\pi^2\epsilon^2 m^{\frac{1}{2}}}{(2kT)^{\frac{1}{2}}h|S_i-S_f|}.$$

For small values of c, i.e. when ϵ is small, c is the value of ρ one obtains by substituting the "most probable" velocity in Zener's formula. It is seen that the averaging process greatly increases this probability, especially for small c, because the systems with small relative velocity have so much greater probability than the average. For values of c larger than ~ 0.1 this effect is not very important.

Using the values of ϵ from Table IV one finds that, at 500°K, ρ for NaCl is 0.93, while that for Na-F is 0.008. An examination of Table IV shows that about half of the association reactions for the alkali halides should be exceedingly slow because of small ρ values. None of these rates have been measured but we shall give expressions for NaCl as an illustration.

$$k_1'=\kappa\frac{kT}{h}(1-e^{-1.08/kT})21.72e^{-D/kT}. \quad (17)$$

[11] Stearn and Eyring, J. Chem. Phys. 3, 778 (1935).

For κ we can substitute[12]

$$\kappa=0.93\frac{k_s'}{kT/h+k_s'}$$

where k_s' is the rate of the reaction

$$\text{NaCl}^*+\text{third body}\rightarrow\text{NaCl}+\text{third body}. \quad (18)$$

In a gas at total pressure 1 atmos. this would become approximately $\kappa\sim 10^{-3}$.

The rate of the reverse reaction is

$$k_2'=\tfrac{1}{6}\kappa(0.450kT)^{\frac{1}{2}}1.10\times 10^{-14}. \quad (19)$$

III. The Reactions of M_2 with X

$$M_2+X\rightarrow MX+M. \quad (20)$$

Since X is in a P state there are three potential surfaces upon which these reactions can take

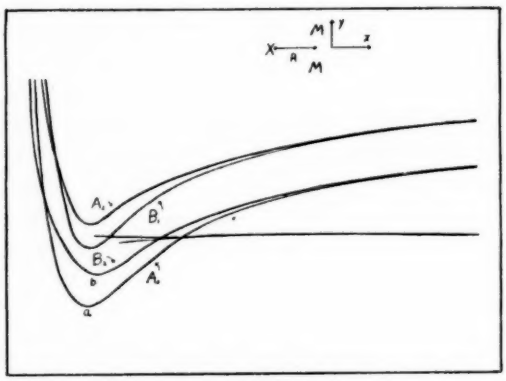

FIG. 3. Curves for the approach of X to form isosceles triangle with M_2.

place. In Figs. 2, 3 and 4 rough schematic diagrams are given to illustrate the nature of these surfaces. In Fig. 2 the linear approach of X to M_2 is shown. The abscissa is the distance from the midpoint of M_2 to X. The curves are classified as Σ and Π as in Fig. 1. The complete curves are for the polar states. The homopolar curves are discontinued after their crossing with the polar states in order to avoid unnecessary complication. The two lowest (Σ) polar states are formed from normal M_2 molecules. The lower one corresponds roughly to the M atom nearest X being ionized and the upper one to the other M atom being ionized. The upper (Π) polar

[12] This formula giving the pressure dependence of σ is due to Professor Henry Eyring. I would like to thank him for a very helpful discussion on this point.

states are formed from excited M_2 molecules, which on dissociation yield $M\ ^2S+M\ ^2P$. These correspond in the same way to one or the other of the M atoms being ionized. There are also Σ polar states of energy near these, but slightly lower, formed from the Σ states of this excited M_2 molecule. They are omitted because they are not of importance in the linear reaction.

The Σ state for the reaction system is comparable with the M+X reaction discussed in Section II. It leads directly to the formation of MX in its normal state provided the electron transfer at the crossing point is permitted. In case this is not permitted, the homopolar state is retained and the system approaches closer to another polar state crossing where it will have a better chance of changing surfaces because of the smaller separation. After this has taken place the reaction is completed to form a normal MX molecule and an excited M atom. (See discussion of Fig. 4 for mechanism of this process.) The Σ reaction may thus lead either to a normal or excited M atom depending upon the magnitude of the interactions at the various crossings.

The Π state cannot react with the lowest polar state because it is of different symmetry. In order that it may become a polar state the remaining electron of M_2^+ must be excited to leave the system in a Π state. This "symmetry restriction" is just the observance of conservation of momentum. Systems in Π linear states, if they lead to reaction at all must leave the M atom excited. We shall discuss the matrix elements for these various crossing points later.

Now let us consider the surfaces for another special case, namely, the approach of M_2 to form

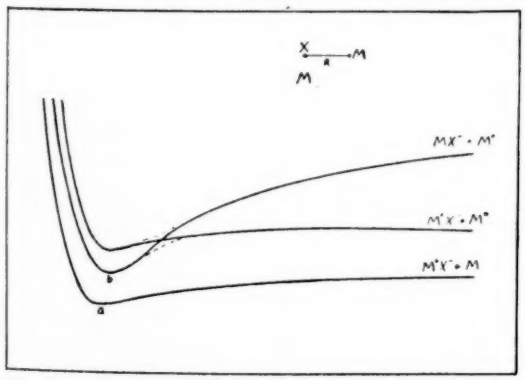

FIG. 4. Curves showing how reaction system at point *b* of Fig. 3 completes reaction yielding excited M atom.

TABLE V. *Limits (in Bohr radii) for the crossing of the ionic state and homopolar state for* M_2+X.

	Li	Na	K	Rb	Cs
F	22.0–11.4	27.4–15.4	144.0–38.6	933.8–52.2	142.5
Cl	16.8– 9.8	19.8–12.7	47.7–25.0	66.2–30.1	225.7– 47.5
Br	14.8– 9.1	17.0–11.5	34.6–20.8	43.1–24.2	79.6– 34.3
I	12.6– 8.2	14.3–10.2	24.7–16.8	29.5–19.0	41.7– 24.6

an isosceles triangle with X. For this special symmetry the states are divided into four classes. (The symmetry group is C_{2v}, Schoenfliess notation.[13]) In Fig. 3, the x and y axes are in the plane of the figure and the z axis is pointing up. The four classes of states are: A_1—totally symmetric; A_2, antisymmetric with respect to reflection in the xz and xy planes; B_1, antisymmetric with respect to rotation of 180 degrees about the x axis and reflection in the xz plane; B_2, anitsymmetric with respect to rotation about the x axis and reflection in the xy plane.

There are pairs of polar states as before, but this time they do not have the simple meaning of one or the other atom being ionized since the atoms are entirely equivalent. It is quite certain that these pairs of polar states cross at some point as shown in Fig. 3. and this will be an important point in a later discussion (see Fig. 5).

The systems which react are originally in the states A_1, B_2 and B_1. M_2 can only be totally symmetric; so the three possible symmetries are determined by the P eigenfunction of X. Naturally if they join polar states, these latter states must have the same symmetries. So only these polar states are shown in the figure. Actually there are two other pairs which have been omitted to avoid complicating the figure.

The totally symmetric A_1 state forms a normal MX molecule interacting with a normal M atom if it is successful in transferring to the polar state. The B_1 state forms directly an excited M atom interacting with a normal MX molecule. The B_2 state, on the other hand, forms a polar complex in which the excitation energy belongs more to the complex as a whole. On dissociating one knows that it should yield an excited M atom. In Fig. 4 a diagram is given to show how this is effected. The points a and b correspond to points

[13] Group theory references: Mulliken, Phys. Rev. **41**, 49 (1932); Rosenthal and Murphy, Rev. Mod. Phys. **8**, 317 (1936); E. Wigner, *Gruppentheorie* (Vieweg, Braunschweig, 1931).

on Fig. 3. The abscissa gives the distance of an M atom from the MX molecule. First following the point a to the right of the figure marked M^+X^-+M we have in a rough way completed the lowest path for reaction 20. As one M is moved away it is no longer equivalent to the other, which now forms M^+X^- with X. In the higher surface, however, as M is moved away it insists on going away charged, and would dissociate into MX^-+M^+ on this curve. It crosses very soon the state which leaves MX normal and gives the excitation to M as a P state. (This third curve is one of those which have been omitted from Fig. 3.)

Thus we see that of the surfaces on which M_2+X can react one will lead to the normal electronic state of both products (with the heat of reaction in thermal motion) while two will lead to excited M atoms. There are two factors which determine which of these will take place: transition probability, and activation energies. These require further consideration.

The reactions which lead to the normal products all require the transfer of an electron from M_2 to X at a fairly large distance, but they will always have less restriction than the corresponding M+X reactions because of the larger ionization potentials for M_2. In Table V "limits" are given for the distance of the crossing point. The upper limit is that for M+X and would be correct if M_2^+ had the same binding energy as M_2; the lower limit gives M_2^+ no binding energy. For H_2^+ the binding energy is approximately half that of H_2. If such a relationship is approximately valid for the diatomic alkali molecules the midpoint of these limits should be about the true distance. On this basis the reactions of Li and Na with all the halogens should take place without restriction, i.e., having $\rho\sim 1$. One cannot be sure about these deductions but there is most likely a restriction on some of the reactions of K, Rb and Cs. This should be true especially of Rb and Cs with F, Cl and Br. It should be remembered that this "restriction" does not mean lack of reaction but that all possible reactions will lead directly to an excited M atom.

Now let us consider the absolute rate of this reaction. The reaction rate constant for this bimolecular reaction is readily written as:

$$k_{20}' = \frac{1}{3}\kappa\frac{kT}{h}\frac{\dfrac{(2\pi m^* kT)^{\frac{1}{2}}}{h^3}\dfrac{8\pi^2(8\pi^2 ABC)^{\frac{1}{2}}(kT)^{\frac{3}{2}}}{h^3}\prod_{i=1}^{3}\dfrac{1}{1-e^{-h\nu_i/kT}}e^{-E_a/kT}}{\dfrac{(2\pi m_X kT)^{\frac{1}{2}}}{h^3}\dfrac{(2\pi m_{M_2} kT)^{\frac{1}{2}}}{h^3}\dfrac{8\pi^2 IkT}{h^2}\dfrac{1}{1-e^{-h\nu_0/kT}}}. \tag{21}$$

A, B and C are moments of inertia of the activated state; $m^*=m_{M_2}+m_X$. The slow step in the reaction most likely comes at the crossing point between the polar and homopolar states. This will be true even if the ρ factor is of the order of unity. Since the homopolar interaction at such distances is small one does not expect much activation energy and we take $E_a=0$. It is consistent with this assumption to say that the motions of the activated complex are essentially classical. So we say that M_2 has its same rotational and vibrational degrees of freedom. These terms thus cancel out of the rate expression. There are two other degrees of freedom for the activated state which correspond to rotation of the complex as a whole. Thus it is seen that the assumption made is equivalent to replacing a vibrational degree of freedom by one rotational degree. For a very weak potential this is of course valid.[14]

Making these changes we have finally

$$k_{20}' = \frac{2}{3}\kappa r_c^2\left(\frac{2\pi kT}{\mu}\right)^{\frac{1}{2}}, \tag{22}$$

where $\mu=(m_{M_2}m_X)/(m_{M_2}+m_X)$; r_c is the distance from the center of M_2 to X. It is to be noted that this expression apart from the factor $\frac{1}{3}$ just gives the classical number of collisions between M_2 and X, if their collision diameter is r_c. The

[14] I would like to thank Professor Henry Eyring for discussions of the absolute reaction rate expressions used in this paper. The validity of this theory for reactions having no activation energy has not been accepted universally. See for example Wigner, J. Chem. Phys. **7**, 646 (1939). It does, however, lead to the collision theory in the limit and probably better in all cases then kinetic theory. For references on this topic see especially Eyring, J. Chem. Phys. **3**, 107 (1935).

derivation by means of the rate theory does, however, lead to a better understanding of what assumptions are involved when one says that a reaction proceeds "at every collision."

Now let us consider the reactions of M_2+X which lead to the excitation of M. First the question of activation energy. For the states which are odd with respect to the plane of the reaction the exchange integrals between M and X are positive.[5] This is easily seen when one notices that due to the oddness of the state only that part of the exchange integrals does not vanish which involves repulsions between electrons. Activation energies arise because of large negative exchange integrals. The sign of the interaction is determined for M_2+X as attractive, and thus there cannot be an activation energy at all. The only restriction on the reaction is possibly the matrix element. Now we shall examine that.

The eigenfunctions for the initial and final states are:

$$\psi_i=(a(1)b(2)+a(2)b(1))c(3) - (a(2)b(3)+a(3)b(2))c(1), \quad (23)$$
$$\psi_f=a^*(1)c'(2)c'(3)-a^*(3)c'(2)c'(1).$$

The atoms are designated as $\underset{a}{M}\ \underset{b}{M}\ \underset{c}{X}$. a^* denotes the P state of M and $c'(2)$ the proper orbital of X^-. All of the integrals vanish, for the odd state, except

$$\int \frac{a(1)a^*(1)c(3)c'(3)}{r_{13}} d\tau_{13} \times \int b(2)c'(2)d\tau_2 = KS_{MX}. \quad (24)$$

K is defined by the equation. This integral has been calculated for excited H_2 by Kemble and Zener.[15] For the alkali halides it will certainly be larger than that for H_2; and so this may be taken as a lower limit for the matrix element. The values are given in Table VI. R is the distance between the centers and α the scale factor which was discussed in the previous section. The energy is in atomic units (624 Calories).

TABLE VI.

αR	1	2	3	4
$RK(\alpha R)$	0.204	0.246	0.189	0.112

[15] Kemble and Zener, Phys. Rev. **33**, 512 (1929).

To get an idea as to the correct value to take for the crossing we take

$$r_c=\frac{1}{I^*(M)-E(X)+\frac{1}{2}E_{M_2}}. \quad (25)$$

$I^*(M)$ is the ionization potential of excited M, $E(X)$ is the electron affinity of X and E_{M_2} is the binding energy of M_2. This is, of course, a guess and is neither an upper nor lower limit (*vide infra*). For Na_2+Cl this distance is 8.8 Bohr radii. For an isosceles triangle having NaCl distances this value, the calculated matrix element is ~ 1000 calories. Our previous discussion of transition probabilities tells us that this reaction should occur. For linear configurations, however, it is not so large and the system might easily approach closer on the same homopolar curve and finally go to a state for higher excitation of M than $2P$. In fact one might reasonably expect all states of excitation for which there is enough energy.

The other reaction which leads directly to excitation of M takes place easier than this odd reaction. It goes on the surface which (in Fig. 3) for isosceles triangle symmetry is designated as B_2. The only restriction would come for the homopolar-polar transition and this occurs easier than the lowest (A_1) mechanism.

Since we expect these last two mechanisms to take place without activation energy it is reasonable to assume classical motions in the activated state as we have done for the first case. We are led to the same rate expression as before, Eq. (21), for the rates of these reactions the only difference being that other values of r_c are to be used.

Polanyi[16a] has given the rates for the reactions of Na_2 with Cl, Br and I. He has shown that they go without activation energy and more rapidly than he calculates, using kinetic theory diameters, for reaction at every collision. We shall calculate these rates using the rough r_c values obtained in the manner we have discussed above.

For $Na_2+Cl\rightarrow NaCl+Na$

$$k'=\underset{3}{1}\times 9.25\times 10^{14}+\underset{3}{2}\times 3.04\times 10^{14} = 5.11\times 10^{14}\ \frac{\text{milliliters}}{\text{moles sec.}}. \quad (25a)$$

The experimental value is 1.5×10^{14}.

Due to the roughness of the calculation one cannot say why the calculated value is too large by a factor of three. Probably the value taken for r_c for the first mechanism is too large. One of the mechanisms may be excluded for reasons which are not apparent from our discussion. Nonclassical behavior of the activated states would also make the rate smaller, as well as the actual existence of a restricted transition.

For Na_2+Br and I we have

	calc.	exp.
Na_2+Br	2.98×10^{14}	1.5×10^{14}
Na_2+I	2.10×10^{14}	0.26×10^{14}.

IV. The Reaction of X_2 with M

$$M+X_2\rightarrow MX+X. \tag{26}$$

For this reaction there is one surface which is definitely lowest. The original reacting system is nondegenerate; so we only have one reaction to consider. This reaction does involve going from a homopolar state to a final polar state. However, one does not expect a restriction at all in this transition. The crossing is brought in even closer than that for $X+M_2$ because of the lessened electron affinity of X_2. The electron affinity of the halogen diatomic molecule is not known. We may guess at this in the following way. For M_2 we attributed the binding energy to the two electrons equally. In molecular orbital language the binding is due equally to the two valence electrons in bonding orbitals. The extra electron for X_2^- must go to the antibonding orbital corresponding to the bonding orbital, and we may expect that it is in a state which is just about as repulsive as a bonding state is attractive. In the same manner as used in Section II we obtain

$$r_c\sim\frac{1}{I(M)-E(X)+\frac{1}{2}E_{X_2}}. \tag{27}$$

Here atomic units are used. For $Na+Cl_2$ the calculated value is 10.4 Bohr radii which is much too small a separation to expect a restricted transition. This, of course, assumes small homopolar interaction and is, like the other values of r_c given above, just a reasonable guess.

Using the previous arguments about the classical nature of the activated state we obtain again Eq. 21 for the rate constant except that the factor $\frac{1}{3}$ is omitted. The calculated rate for $Na+Cl_2$ is 4.48×10^{14} milliliters (moles sec.)$^{-1}$. The observed rate is 4.1×10^{14}. This agreement is better than one has reason to expect.

For $Na+I_2$ the calculated rate is 5.98×10^{14} to be compared with the experimental value 6.1×10^{14}.

V. The Reactions in Highly Dilute Flames of Alkali Metals and Halogens

An extensive amount of experimental work has been done on the gaseous reactions of various halogen containing compounds with alkali metal vapors at very low pressures, $\sim10^{-6}$ atmosphere. In this paper we shall only be concerned with that of Polanyi, Beutler, Schay and others[1] in which the reactions of the halogens themselves were studied. The alkali metals used were chiefly sodium and potassium. The mechanism which these authors give to explain the experimental facts appears to be in excellent agreement with them. We shall consider it briefly.

Under the conditions of the experiment ($\sim500°K$ and 10^{-6} atmos.) the alkali metals exist chiefly as atoms. The halogen diatomic molecules react first with them.

$$M+X_2\rightarrow MX+X. \tag{28}$$

The halogen atom then reacts with an M_2 molecule.

$$M_2+X\rightarrow MX+M. \tag{29}$$

The reaction $M+X\rightarrow MX$ has a negligibly small rate because of the low pressure, but a wall reaction accompanies these

$$M+X+Wall\rightarrow MX. \tag{30}$$

There is a very bright luminescence observed for this series of reactions. It has been proved to be radiation from the M atoms and to be excited in homogeneous gas reactions. Reaction (28) is not exothermic enough as a rule to excite an M line. Reaction (29), releases most of the energy and Polanyi *et al.* attribute the luminescence to it in this manner: the heat of reaction goes into MX in the form of vibrational energy; these vibrationally excited MX molecules transfer their excitation to an M atom on collision. Quenching experiments have been used to prove that in certain cases the excitation must exist for a time in the MX molecules; the radiation is

quenched more strongly by foreign gases than could be possible if M were excited directly. The luminescent yields have been estimated as ~ 1 for ideal conditions. Polanyi did not consider the possibility of direct excitation such as we have done above.

Let us now consider the luminescence yields to be expected on the basis of the calculated rate constants for the reaction of chlorine with sodium. The rate constants (see Eq. (25a) above) for the two reactions which lead directly to the excitation of the sodium are both given as $\frac{1}{3}\,3.04\times10^{14}$ and the other reaction which does not excite the sodium, has a constant of $\frac{1}{3}\,9.25\times10^{14}$. If we assume that a fraction n of the NaCl molecules which are formed in the third reaction are capable of exciting a sodium atom later (by a mechanism which will be discussed in the next section), the luminescence yield will be

$$\frac{\frac{2}{3}\cdot 3.04\times10^{14}+\frac{n}{3}\cdot 9.25\times10^{14}}{\frac{2}{3}\cdot 3.04\times10^{14}+\frac{1}{3}\cdot 9.25\times10^{14}}=\frac{2.03+3.08n}{5.11}. \quad (31)$$

This neglects the possibility of quenching the excited sodium atoms before they emit light, which is usually not very important. We must now make an estimate of n.

It takes 48.2 Calories to excite the sodium D line and the reaction is exothermic approximately 74 Calories. If we assume that every NaCl molecule which retains 48 Calories of this heat of reaction in *vibrational* energy can exite an M atom (neglecting for the present a discussion of this possibility) we can estimate n as follows. The triatomic reaction system Na_2Cl has nine degrees of freedom. Because of the conservation of the translational and rotational energy of the complex as a whole there are only three degrees of freedom into which the heat of reaction is allowed to go. A little consideration shows that these are: (1) the relative translation of the products, (2) one rotational degree for NaCl, (3) the vibration of NaCl. One cannot actually calculate how much energy goes into each of these degrees without knowing the complete potential surface for the reaction, but it seems reasonable in this case to expect a distribution quite close to thermal equilibrium. In order for the products of a reaction to have a very special sort of distribution of the reaction energy the potential surface must be very restricting—i.e., only systems can react which have a very special set of initial conditions. It is difficult to imagine a system of this sort having a zero or even low activation energy. So it seems consistent with previous assumptions regarding the classical nature of the motions in the activated state to assume a classical distribution of energy in the products. The probability that an oscillator in equilibrium with two degrees of freedom shall have 48 or more of 74 calories is $(74-48)/74=0.35=n$. This gives $l=0.61$. The observed yield is somewhat higher than this, ~ 0.8. Our calculated rate constant was too large and this result probably means that the value of r_e for the first mechanism is too large.

The main point to be made in this discussion is that the light yield is probably shared by the two mechanisms. This would account for the quenching results, and also the high yields of the halogen reactions as compared to others having equal exothermicity but lower yields because they lack the possibility for direct excitation. Consider as an example the reaction of $HgCl_2$ with Na. The reactions which occur are:[1d]

$$HgCl_2+Na\rightarrow HgCl+NaCl, \quad (32)$$

$$HgCl_2+Na\rightarrow NaCl+Hg. \quad (33)$$

There is no possibility for direct excitation of an Na atom in this sequence and yet there is luminescence. The yield is much lower than that given above, ~ 0.11. The heat of the second reaction is ~ 63 Calories while that of the first is less than the sodium excitation energy. From our previous discussion we might expect a yield as high as $(63-48)/64=0.23$. This confirms our suspicion that the calculation gives a value of n much too high, and every NaCl molecule with 48 Cal. vibrational energy cannot excite an Na atom.

The yields for all the mercury halides, cadmium halides, etc., which react as $HgCl_2$, are an order of magnitude lower than those for the halogens themselves. Most of these have yields much less than 0.01.

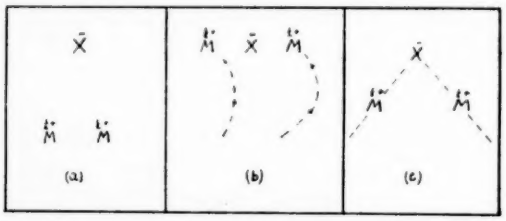

FIG. 5. Comparison of the A_1 and B_2 states shown in Fig. 3. In (a) A_1 is lower than B_2. In (b) B_2 is the lower of the two. A system having gone from configuration a to b always remaining isosceles triangular would have retained its symmetry and thus gone from the lower to the higher surface or vice versa. If it went by a path such as indicated by the broken lines, however, it would stay on the lower or higher surface on which it originally was. At some configuration such as shown in (c) the two surfaces have equal energy. They intersect in a line in configuration space, the configuration corresponding to the M's being on the broken lines of (c).

The yield for the reaction $Na_2+I\rightarrow NaI+Na$ is to be contrasted with that for $HgCl+Na\rightarrow NaCl+Hg$. The former has a heat of reaction only one Calorie in excess of the excitation energy and has a light yield of 0.4; the latter has a heat of reaction of fifteen Calories in excess of the excitation energy with a light yield of only 0.1. This is because the former has the possibility of a direct excitation of the Na atoms in the reaction while the latter does not.

Very accurate quenching experiments for these reactions would be interesting. One might determine experimentally the relative importance of the various mechanisms for M_2+X. These should be quite different for Rb and Cs than for Na and K. For the reaction of Cs and Cl, for example it is quite certain that there could only be direct excitation of the Cs since the crossing point is much too far to expect a successful transition at the first crossing.

VI. The Transfer of Vibrational to Electronic Excitation

$$(MX)^*+M\rightarrow MX+M^*. \qquad (34)$$

In this reaction the system is originally in its lowest state and finally in its first excited state. In order for this to take place with an appreciable rate there must be some configuration for which these states actually have equal energy. Otherwise there cannot be an appreciable probability for the process to occur. The general features of the crossing of potential surfaces have been discussed by several authors.[2] We shall consider the matter as follows (see Fig. 5). For general configurations the states of M_2X are classified as even and odd with respect to the plane of the atoms. The initial state (on the left of 34) is even and thus must remain even. For general configurations all one can say is that the system initially in its lowest state should remain there. For the special configuration of isosceles triangle, however, the first and second states are noncombining and can cross rigorously.

In Fig. 5(a) the state symmetric in the two M atoms (or ions) is the lowest. One is sure of this because the M's are close together and their energy is lowest when they attract. For 5(b) the state which is antisymmetric in the M's is lowest. It can gain more energy from interaction with the X^- ion than the symmetric state having that configuration. If one turns an isosceles configuration having a small angle to a linear complex there is always one point at which these two lowest states are equal. Thus a system in this neighborhood can change from the first to the second surface quite easily. After the system gets to the second surface the excitation of M occurs as indicated in Fig. 4.

The rate of this reaction brings in an interesting point. The activated state for 34 is at the crossing of the two surfaces discussed above. This is true because we are considering only those systems which have enough energy to complete the reaction, and the slowest step will be in changing to the proper surface. If we were considering the rate of this reaction for an NaCl gas at thermal equilibrium with an Na gas, the activated state would be at the point of highest energy. It would contain no property at all of the surface in the neighborhood of our present activated state.

It is not worth while to attempt an estimate of the rate of this reaction. Since the motions of the activated state cannot be taken as classical and the distances are somewhat smaller than those of the other complexes discussed, the rate will probably be smaller but certainly of the same order of magnitude.

I would like to thank Professor Eugene Wigner for calling my attention to this problem and for a number of very helpful discussions. Thanks are also due Professor H. Eyring, Professor S. Glasstone and Dr. K. J. Laidler who read the manuscript and gave valuable suggestions.

The Fundamental Frequencies of Certain Trihalomethanes

G. GLOCKLER AND G. R. LEADER[1]
School of Chemistry, University of Minnesota, Minneapolis, Minnesota
(Received May 2, 1940)

The Raman spectra of dibromochloro-, bromo-dichloro-, dichlorofluoro-, chlorodifluoro-, dibromofluoro- and bromochlorofluoro-methane have been studied. Their fundamental frequencies have been correlated and systematized. Simple graphical means were used to predict the Raman frequencies of $CHBrF_2$ and CHF_3. It was found that the C−X bond will show a "characteristic" frequency whenever the halogen X is the only and lightest of this type in a halomethane.

I. INTRODUCTION

IN this paper we discuss the relation of the Raman spectra of the following compounds: $CHBr_3$, $CHBr_2Cl$, $CHBr_2F$, $CHBrCl_2$, $CHBrF_2$, $CHBrClF$, $CHCl_3$, $CHCl_2F$, $CHClF_2$, CH_2ClF, CCl_3F and CHF_3. From the point of view of symmetry there are only five classes of halomethane derivatives although the number of individual halomethanes which are possible is very large. The individual symmetry classes are characterized by the following elements of symmetry: T_d (e.g., CCl_4); C_{3v} (e.g., $CHCl_3$); C_{2v} (e.g., CH_2Cl_2); C_s (e.g., $CHCl_2F$) and C_1 (e.g., CHBrClF).

A great deal of work has already appeared on the modes of vibration of compounds of the first two classes. Because of degeneracy, the Raman spectra of such molecules show relatively few lines and, moreover, the high degree of symmetry which they possess simplifies the problem of applying to them the theory of small vibrations, permitting one to calculate values for their vibrational frequencies and thus facilitating assignment of the observed Raman lines to given vibrational modes.[2–5] In the third class, there is no longer any degeneracy and hence nine distinct frequencies are to be expected for such molecules, all of them active in the Raman effect. Because of the reduced symmetry, the problem of calculating these nine frequencies is considerably more difficult than in classes 1 and 2. The vibrational modes of most molecules of class 3 are therefore less well established than those for the first two classes, especially with regard to the assignment of the Raman lines of specific compounds to their fundamental vibrations. However, the excellent paper recently published by J. Wagner[6] giving new measurements, polarization studies and calculations on methylene halides has greatly improved the situation.

In the present paper molecules of the type CHX_2Y and CHXYZ which belong to classes four and five will be considered. Molecules of class four possess only a plane of symmetry and hence it is difficult to calculate the vibration frequencies of such molecules by the conventional methods. However, the Raman spectrum of the molecule CHX_2Y, where X and Y are different halogen atoms, bears a much more apparent relationship to the spectrum of the symmetrical molecule CHX_3, from which it may be considered derived, than is the case with $CHCl_3$ and CH_2Cl_2, for example, since the relative change in mass produced by substituting one halogen for another is much less than the change produced by substituting a halogen for a hydrogen atom. Hence the generic relationship between the Raman lines of molecules in the series $CHX_3-CHX_2Y-CHY_2X-CHY_3$ can be traced fairly readily, and the inner consistency of such a set of data, if achieved, constitutes a fairly strong argument for the correctness of the Raman lines chosen. Our attack on the present problem has been based largely on this consideration. A sufficient amount of data has been gathered to make this procedure possible. If the fundamental vibrations

[1] This article is based upon a thesis presented to the faculty of the Graduate School of the University of Minnesota by Gordon R. Leader in partial fulfillment of the requirements for the degree of Doctor of Philosophy.
[2] H. Urey and C. Bradley, Phys. Rev. **38**, 1969 (1931).
[3] J. Rosenthal, Phys. Rev. **45**, 538 (1934).
[4] J. Rosenthal and H. Voge, J. Chem. Phys. **4**, 134–143 (1936).
[5] J. Wagner, Zeits. f. physik. Chemie **B40**, 36 (1938).
[6] J. Wagner, Zeits. f. physik. Chemie **B45**, 70 (1939).

of the molecules CHX_2Y and CHZ_2Y have been correctly chosen, then the problem of selecting the fundamental vibrations of the molecule CHXYZ becomes fairly simple since each of its Raman lines should lie between the corresponding lines of the other two compounds as shown in Fig. 4.

II. Symmetry Properties of the Normal Modes of Vibration

Molecules of the type CHX_2Y belong to the symmetry class C_s. The predictions of group theory concerning the symmetry properties of the normal modes of vibration of pentatomic molecules of this type are given in Table I.[7] The numbering of the lines corresponds to that employed by Kohlrausch for $CHCl_3$.[7b] The vibrations are either symmetrical or antisymmetrical to the molecule's one plane of symmetry. Molecules of the type CHXYZ have no symmetry and hence should show nine distinct fundamental vibrations, all of them polarized.

III. Experimental Results

Data on the Raman spectra of all the compounds discussed in the present paper (with the exception of CHF_3 and $CHBrF_2$) have already appeared in the literature.[8–12] We have repeated determinations on three of these compounds in an effort to settle a few remaining doubtful points about their Raman spectra. Results obtained are as follows (cm^{-1}):

$CHBrCl_2$: 214.6 (9) (*a*, *b*, *c*), 220.4 (10) (*a*, *b*, *c*), 329.6 (8) (*a*, *b*, *c*), 601.7 (9) (*a*, *c*); 718.8 (4, broad) (*a*, *c*); 760.0 (3, diffuse) (*a*, *c*); 1170.8 (2) (*c*); 1214.3 (1) (*c*); 3020.5 (5) (*a*, *b*, *c*).

$CHClF_2$: 369.1 (4) (*c*); 410.5 (3) (*c*); 415.4 (10) (*a*, *c*); 595.1 (9) (*a*, *c*); 793.8 (4) (*a*, *b*, *c*); 804.7 (4) (*a*, *b*, *c*); 1088.4 (1, diffuse) (*c*); 1310.2 (2) (*a*, *c*); 1350.0 (2) (*a*, *c*); 3035.0 (6, broad) (*a*, *c*).

$CHBr_2F$: 171.4 (10) (*a*, *b*, *c*, *d*); 296.5 (5) (*a*, *b*, *c*); 340.7 (1) (*a*, *c*); 359.0 (9) (*a*, *c*); 620.4 (10) (*a*, *b*, *c*, *d*); 656.7 (0) (*c*); 704.9 (4, broad) (*a*, *c*); 1064.0 (2, diffuse) (*c*); 1169.6 (1) (*a*, *c*); 1293.2 (3) (*a*, *c*); 3017.2 (6) (*a*, *b*, *c*). [$a=4046$; $b=4077$; $c=4358$; $d=4347$].

$CHBr_2F$ was prepared by treating $CHBr_3$ with SbF_3 and Br_2, according to the procedure of Swarts.[13] Seven cc of material boiling at 65–66° at 740 mm was used for the Raman study. It was vacuum distilled into the Raman tube, and the tube was finally sealed under vacuum. No filters were used. The material discolored only slightly during exposure. No lines appeared in its Raman spectrum that could be attributed to any likely impurity.

$CHBrCl_2$ was prepared by refluxing together for 12 hours $CHBr_3$ and $CHCl_3$ with a small amount of anhydrous aluminum chloride and a drop of bromine as catalyst. Interchange of the halogen atoms between $CHBr_3$ and $CHCl_3$ molecules occurs under these conditions, and a mixture is finally obtained containing $CHCl_3$, $CHBrCl_2$, $CHBr_2Cl$ and $CHBr_3$. These substances can be readily separated by fractional distillation after separating the crude product from the catalyst by a preliminary distillation. This procedure as a method for preparing $CHBrCl_2$ and $CHBr_2Cl$ appears to be quite satisfactory and the yields are good. Four fractionations using an ordinary Clark flask gave a 15-cc sample of $CHBrCl_2$ boiling at 89–90° at 742 mm. Its Raman spectrum did not show any lines that could be attributed to the probable impurities, $CHCl_3$ and $CHBr_2Cl$. The material discolored slightly during exposure to the mercury lamps.

$CHClF_2$ used for the present study was furnished by the E. I. duPont de Nemours Company and is the same sample that was used in obtaining the results already published by Glockler and Bachmann.[9] The present run was made in order

Table I.

Type	σ_z	State of Polarization	No. of Lines	Notation
A'	s	p	6	$\nu_1\nu_2\nu_4\nu_6\nu_7\nu_8$
A''	a_z	dp	3	$\nu_3\nu_5\nu_9$

[7] K. W. F. Kohlrausch, *Der Smekal-Raman Effekt, Ergänzungsband* (J. Springer, Berlin, 1938), p. 43. (b) page 150.
[8] C. Bradley, Phys. Rev. **40**, 908 (1932).
[9] G. Glockler and J. Bachmann, Phys. Rev. **55**, 669 (1939).
[10] G. Glockler and J. Bachmann, Phys. Rev. **54**, 970 (1938).
[11] G. Glockler and G. R. Leader, J. Chem. Phys. **7**, 553 (1939).
[12] G. Glockler and G. R. Leader, J. Chem. Phys. **8**, 125 (1940).
[13] Swarts, Bull. Acad. Roy. de Belgique 113–23 (1910).

to obtain a more intense spectrum than was previously obtained. The repetition of the experiment permits us to conclude that in the Raman spectrum of $CHClF_2$ two of the fundamentals lie so close together as to be nearly coincident. The further assumption that the sample used is contaminated with about 1 percent CHF_3 enables us to account satisfactorily for all of the Raman lines observed in its spectrum. The $CHClF_2$ was run at an average temperature of $-60°$ in the low temperature apparatus previously described.[14]

IV. Discussion of Experimental Data

The Raman lines of $CHCl_3$ and $CHBr_3$ used in the present paper are taken from the compilation "Effet Raman" by M. Magat.[15] The Raman lines of $CHBr_2Cl$ have been previously reported by us.[11] The lines reported are all fundamentals, $CHBrCl_2$ has been run by Bonino and Brüll and by Kohlrausch and Köppl.[16] The latter obtained only eight lines, whereas nine Raman lines are to be expected from a compound of this type. We also obtained only eight distinct lines for this compound. However, the line at 220 cm^{-1} reported by Kohlrausch as being of intensity 10 is unusually broad. The Stokes and anti-Stokes lines of this value from λ4358 cannot be made to appear as two distinct lines, even on short exposure. However, the corresponding Stokes line from λ4046 which falls on a portion of the plate where the dispersion is greater does show slight resolution of the two components of the line. Hence in the present study this broad Raman line has been treated as two Raman lines of approximately equal intensity lying very close together at 215 and 220 cm^{-1}. A similar situation has been encountered with $CHClF_2$ and has been handled in the same way. This procedure of treating as two lines certain broad Raman lines not clearly resolved into two components seems to us justifiable in the present cases, through there might be some danger in its general use, because the Raman spectra of these two unusual compounds are thereby made consistent with the Raman spectra of related compounds whose behavior is normal. (See Figs. 1 and 2.)

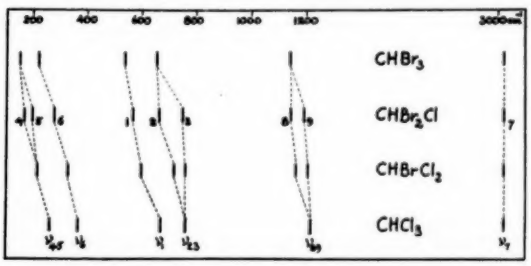

FIG. 1. The spectral sequence $CHBr_3-CHCl_3$.

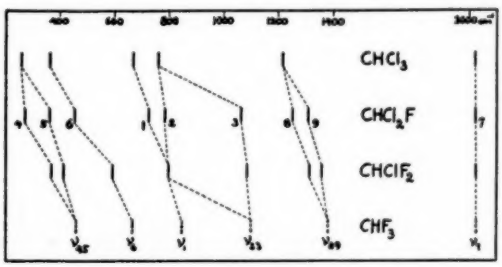

FIG. 2. The spectral sequence $CHCl_3-CHF_3$. (Values for CHF_3 are predicted.)

The Raman spectrum of $CHCl_2F$ has been reported by Bradley.[8] He found only eight lines. A comparison of the Raman spectrum of this substance with the results for a similar molecule (CHBrClF) shows that the missing line should lie near the line reported at 1305. All molecules of the type CHX_2Y where X or Y may be Br, Cl or F have been found to show a pair of lines in their Raman spectrum in the region 1100–1400 cm^{-1}. Such molecules also have in common a fundamental at 3020 cm^{-1} and the Raman line of this value from λ4046 would be $\Delta\tilde{\nu}=1250$ if considered as a Stokes line from λ4358. Hence, when mercury radiation is used the 3020 line from λ4046 falls in the same region on the plate as does a pair of lines from λ4358. Ordinarily it causes no interference. However, in CHBrClF, the lower of the aforementioned group of two lines falls at $\Delta\tilde{\nu}=1205$. In $CHClF_2$ it falls at 1310. It is reasonable to suppose that in $CHCl_2F$ which is a compound of intermediate mass it falls at about 1250 in which case it would be hidden by the 3020 line from λ4046. This assumption furnishes a satisfactory explanation of why the 1250 line was missed by Bradley, despite the fact that he detected the 1065 line which is usually the weakest line in the Raman spectrum

[14] G. Glockler and M. M. Renfrew, Rev. Sci. Inst. **9**, 306 (1938).
[15] M. Magat, "Effet Raman," No. 15 of *Tables Annuelles de Constantes et Donnees Numeriques* (Paris, 1937).
[16] K. W. F. Kohlrausch and F. Köppl, Monatshefte **65**, 185 (1935).

of compounds of this type. Bradley did not observe any line which could be interpreted as $\Delta\tilde{\nu}=1250$ from $\lambda 4046$. However any such line would be very faint and might easily have failed to appear. On the basis of the above argument, it has been assumed in the present study that the ninth Raman line of $CHCl_2F$ lies at $\Delta\tilde{\nu}=1250$.

$CHClF_2$ has been run by Glockler and Bachmann.[9] A new set of data for this compound, determined on the same sample of $CHClF_2$, is reported in the present paper. These new results agree quite well with the previous set, so far as most of the lines are concerned. However certain changes have been made which require explanation. The line reported by Glockler and Bachmann at 800 cm^{-1} is an unusually broad line. Even when only moderately exposed so that there can be no broadening of the line due to halation it extends from about 788 cm^{-1} to 810 cm^{-1}. A comparison of the Raman spectrum of this compound with the spectra of closely related haloforms (see Fig. 2) indicates that two of the Raman lines of $CHClF_2$ should fall at approximately 800 cm^{-1}. Hence we interpret the broad line at 800 as due to two neighboring Raman lines too close together to be resolved, and in making measurements, the line was treated accordingly. This procedure leads to values 794 and 805 for the two components of the line. In place of the two lines 1085 and 1128 reported by Glockler and Bachmann, we report only the line 1088 in the present study. The Raman line appearing on our plate at this point is again unusually broad, extending from about 1078 cm^{-1} to 1119 cm^{-1}. The line expected at this point should, by analogy to the corresponding line for similar compounds, be broad and diffuse, but its unusual width in the present case suggests that we are again dealing with two neighboring lines, the second line in this case being due to an impurity CHF_3 whose presence we suspect in the sample of $CHClF_2$ which we used. This second line we estimate as being at 1109 cm^{-1}. Its intensity should of course be much less than that of the 1088 line of $CHClF_2$, and actually the intensity in the broad line which we are discussing is appreciably less on the higher wave-length side. The very weak line reported by Glockler and Bachmann at 436 cm^{-1} was not observed in the present study. Three lines were found at 459.5, 667.3 and 830.8 cm^{-1} (two of these had been previously reported by Glockler and Bachmann) which are evidently not fundamentals of $CHClF_2$ nor (with the exception of 830.8) can they be explained as combinations or overtones of the fundamentals of the latter compound. It is interesting to note that these three lines fall almost precisely at the points where by extrapolation of a diagram such as is shown in Fig. 2, one would expect certain Raman lines of CHF_3 to fall. Moreover, CHF_3 is the impurity most likely to be present in $CHClF_2$, and hence it seems reasonable to attribute these extra lines to CHF_3 present in small amount as an impurity in the $CHClF_2$. As mentioned previously our plate also showed some evidence of the presence of a fourth CHF_3 line at 1109 cm^{-1}, which is also a position at which Fig. 2 would lead one to expect to find a line for this compound. It might at first glance seem more reasonable to call the line 830.8 an overtone of the strong fundamental at 415.4 since the numerical relationship is so satisfactory. However, if one assumes the lines at 459.5 and 667.3 due to CHF_3, then one must also consider the line 830.8 as due to CHF_3. The line expected for CHF_3 at this point is ν_1, the symmetrical "valence" vibration, and should be the strongest line in the CHF_3 spectrum. Hence if any of the other CHF_3 lines appear, the ν_1 Raman line should appear also. Moreover, ν_1 for CHF_3 must almost certainly lie somewhere between 810 and 900 cm^{-1}. The line at 830 is the only one which appears on our plate in this region, and hence if the assumption that CHF_3 is present as an impurity is valid, then this line must be the ν_1 line for CHF_3. The possibility that the overtone of 415.4 of $CHClF_2$ also falls at this point is, of course, not excluded. But it seems to us unlikely that the line at 830 is only the overtone of 415 because its intensity relative to the 415 line is too great. The two lines reported at 410.5 and 415.4 appear distinctly on the plate as two lines despite their closeness together. Both are sharp lines, the 415.4 line being about 4 times as intense as the 410.5 line. It seems probable that the 415.4 line corresponds to the vibration of $CHCl^{35}F_2$, and that the weaker companion is due to the corresponding vibration of $CHCl^{37}F_2$ molecules.

The Raman spectrum of $CHBr_2F$ has been previously reported by Glockler and Bachmann.[10]

The results there given are incomplete, and contain several superfluous lines. No evidence was found in the present study for the lines previously reported by Glockler and Bachmann at 93.2, 559.7, and 3059 cm^{-1}. A line actually appears on the plate which would be 559.7 cm^{-1} if excited by λ4358, but it is more probable that this is the strong line 620 excited by λ4347. The longer exposures used for this study, brought out five lines not previously reported which lie at 340, 657, 1064, 1169 and 1293 cm^{-1}. The first of these is probably the overtone of 171, the second is a combination frequency (359+297=656) and the last three correspond to fundamental vibrations.

The Raman lines of CHBrClF have already been reported by us.[14] Of the eleven lines listed, all correspond to fundamental vibrations with the exception of 649 and 735 which are combination frequencies (225+425=650; 313+425=738).

V. Graphic Correlation of Results

The data discussed in the present paper are graphically presented in Figs. 1–4. As mentioned previously, the inner consistency of these graphs argues for the correctness of the choice of Raman lines that has been made. It is to be noted that the change in mass between successive members of a given series is constant. Hence if the spacing of the horizontal lines on which the successive Raman spectra of a given series are drawn is uniform, then these charts are essentially graphs of the positions of the Raman frequencies *versus* the mass of the molecule. By making such a graph on an enlarged scale for the series in Fig. 1., it was found that the dotted line connecting the positions of corresponding Raman shifts in the four compounds was nearly a straight line. In the intermediate two compounds there are two Raman lines corresponding to each of the degenerate vibrations of the symmetrical haloforms. The mean of these two lines was used on the graph. A similar enlargement of Fig. 2 was used in predicting the Raman lines of CHF_3. The large shift in the vibration ν_3 caused by the introduction of a fluorine atom causes difficulty in this case. However, it was found that the ν_2 frequencies of $CHCl_2F$ and $CHClF_2$ lie on a straight line with ν_{23} of $CHCl_3$. The extrapolation to find ν_{23} of CHF_3 was made on the assumption that it would lie on a straight line with the ν_3 Raman frequencies of $CHCl_2F$ and $CHClF_2$. It is evident from Fig. 2 that the extrapolation to find ν_{89} of CHF_3 can be made quite accurately since the trend of this vibration is so regular. We have assumed that the vibration ν_7 would have the same value (3035) for CHF_3 as it has in $CHClF_2$, since this vibration has the same value (3020) in the Raman spectra of both $CHCl_3$ and $CHCl_2F$. The lower four Raman lines of CHF_3 given in Fig. 2 are experimental values for the impurity lines observed in the Raman spectrum of $CHClF_2$. Since all four of them fit so well the predictions which Fig. 2 makes for the Raman lines of CHF_3, it seems highly probable that these impurity lines are actually Raman lines of CHF_3. Figures 1, 2 and 3 illustrate well the usefulness of charts of this sort in correlating the Raman spectra of closely related molecules and thereby facilitating the assignment to them of their fundamental vibrations.

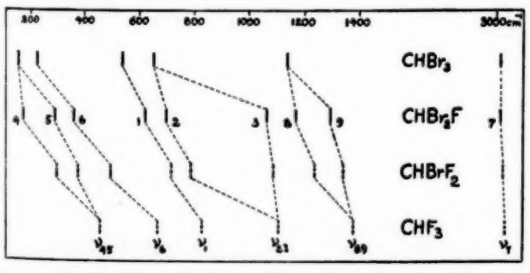

Fig. 3. The spectral sequence $CHBr_3-CHF_3$. (Values for $CHBrF_2$ and CHF_3 are predicted.)

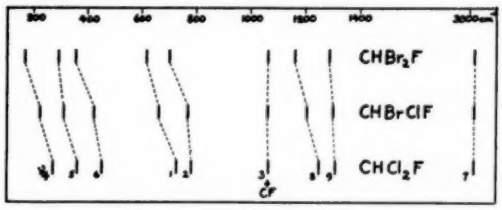

Fig. 4. The spectral sequence $CHBr_2F-CHCl_2F$.

VI. Prediction of Raman Lines

In addition to affording a check on the correctness of experimentally determined fundamentals, the use of Raman data on a series of closely related molecules arranged graphically as in Fig. 1 or Fig. 4 can serve in certain cases to predict the location of the Raman lines of compounds on which no experimental data are available. Such predicted Raman lines, although subject to

rather large errors, may have value for certain purposes. We have previously mentioned the use of this method in predicting the Raman lines of CHF_3, in which case such predictions check satisfactorily with lines of CHF_3 which were possibly observed as impurity lines in the Raman spectrum of another compound. By similar use of the sequences $CHBrCl_2-CHBrClF-CHBrF_2$ and $CHBr_3-CHBr_2F-CHBrF_2-CHF_3$ one can predict values for the Raman lines of $CHBrF_2$, as yet undetermined experimentally. The Raman lines of this compound used in Fig. 3 and in Table III were obtained in this way. For prediction of Raman lines, it appears to be advantageous to arrange the compounds considered as in Fig. 4, where, it will be noted, the change in mass from one molecule to the next is constant. Under these conditions the dotted vertical lines connecting corresponding Raman lines in successive molecules are most regular.

VII. The Characteristic C–X Vibrations

In all the trihalomethanes the vibration ν_7 remains practically constant at about 3020 cm^{-1}. This vibration corresponds to an oscillation of the lone hydrogen atom with respect to the rest of the molecule. It is evident in Fig. 4 that the three molecules there considered have in common a Raman line at 1065 cm^{-1}. They also have in common a lone fluorine atom. Hence the line at 1065 cm^{-1} is probably characteristic of the C–F bond in the same way that the line at 3020 cm^{-1} is characteristic of the C–H bond. One might expect to find a similar constant line corresponding to the C–Cl bond in the series $CHBr_2Cl$, $CHBrClF$ and $ChClF_2$. But this is far from being the case. It should be noted, however, that in this series the chlorine atom is no longer always the lightest halogen atom as is true of the fluorine atom in the series shown in Fig. 4. In order that a trihalomethane molecule shall show a valency vibration characteristic of a given halogen atom which it contains, it appears necessary that the halogen in question shall be the only one of that kind present in the molecule and shall be also the lightest halogen atom in the molecule. When this condition is fulfilled, any halomethane containing that halogen atom will show its characteristic Raman line. This fact is graphically illustrated for the C–F bond in Fig. 5. The dotted lines which connect corresponding vibrations in the different molecules are drawn in accordance with the work recently published on the nature of the spectral sequence $CX_4 \rightarrow CY_4$ by Kohlrausch and Wagner.[17] Similar constant vibrations character-

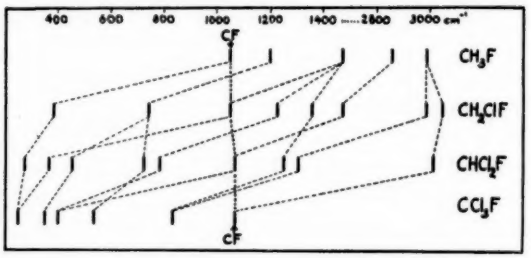

Fig. 5. The spectral sequence CH_3F-CCl_3F.

Table II. *The characteristic* C–X *vibrations.*

C–F		C–Cl		C–Br		C–I	
CH_3F	1048	CH_3Cl	732	CH_3Br	610	CH_3I	532
CH_2ClF	1046	CH_2ClBr	726	CH_2IBr	616	—	—
$CHCl_2F$	1065	$CHBr_2Cl$	750	CHI_2Br	—	—	—
CCl_3F	1067	CBr_3Cl	734	—	—	—	—

[17] K. W. F. Kohlrausch and J. Wagner, Zeits. f. physik. Chemie **B45**, 93 (1939).

Table III. *The fundamentals of certain trihalomethanes.*

Compound	ν_4	ν_5	ν_6	ν_1	ν_2	ν_3	ν_8	ν_9	ν_7
$CHBr_2Cl$	168.3(8)	201.1(7)	279.4(10)	568.9(8)	658.7(5)	749.5(3)	1145.5(1)	1193.8(1)	3022.6(7)
$CHBrCl_2$	214.6(9)	220.4(10)	329.6(8)	601.7(9)	718.8(4)	760 (3)	1170.8(2)	1214.3(1)	3020.5(5)
$CHCl_2F$	274 (7)	366 (4)	454 (7)	723 (9)	786 (4)	1065 (1)	1250	1307 (3)	3019 (5)
$CHClF_2$	369.1(4)	415.4(10)	595.1(9)	793.8(7)	804.7(7)	1088 (1)	1310.2(2)	1350 (2)	3035 (6)
$CHBr_2F$	171.4(10)	296.5(5)	359.0(9)	620.4(10)	704.9(4)	1064.0(2)	1169.6(1)	1293.2(3)	3017.2(6)
$CHBrF_2$	300	380	500	720	790	1090	1240	1340	3030
$CHBrClF$	225.0(10)	313.0(9)	425.0(9)	658.7(10)	773.4(5)	1062.6(3)	1204.6(4)	1301.7(5)	3017.8(7)
CHF_3*	459.5		667.3	830.8	1109.0		1380		3035

* *Note added in proof.*—We have since determined experimentally the following Raman lines of CHF_3: 508.1, 669.7, 936.8, 1116.5, 1376.2 and 3062.0 cm^{-1}.

istic of the remaining carbon halogen bonds occur in other series analogous to that shown in Fig. 5. These constant vibrations for each of the halogens are shown in Table II. The Raman lines listed in a given horizontal row of this table[18] are in each case corresponding vibrations of their respective molecules.

In Table III are tabulated the fundamental vibration frequencies of the molecules which we have discussed. The numbers in parentheses which follow the experimentally determined values denote the relative intensities of the corresponding Raman lines.

[18] Values used in this table are from the following sources: CH_3F, CH_3Cl, CH_3Br, CH_3I—H. Sponer; *Molekülspektren I* (J. Springer, Berlin, 1935), p. 84; CH_2ClF—Glockler and Bachmann, Phys. Rev. **55**, 1273 (1939); CH_2ClBr and CH_2IBr—J. Wagner, Zeits. f. physik. Chemie **B45**, 69 (1939); $CHCl_2F$—C. Bradley, Jr., Phys. Rev. **40**, 908 (1932); $CHBr_2Cl$—this paper; $CFCl_3$—Glockler and Leader, J. Chem. Phys. **7**, 278 (1939); CBr_3Cl—Volkringer, Lecompte and Tchakirian, J. de phys. et rad. **9**, 105 (1938).

SEPTEMBER, 1940 JOURNAL OF CHEMICAL PHYSICS VOLUME 8

The Near Ultraviolet Absorption Spectrum of Heavy Benzene

H. SPONER
Department of Physics, Duke University, Durham, North Carolina

(Received June 12, 1940)

The absorption spectrum of heavy benzene at 2700–2300A has been analyzed. As in light benzene it represents a forbidden transition $^1A_{1g} \rightarrow B^1_{2u}$ made allowed through the interaction of vibrations of type ϵ_g^+. Interpretations have been given for the majority of the bands. The measured bands together with the assignments are exhibited in Table I.

INTRODUCTION

THE near ultraviolet absorption spectrum of heavy benzene extends from 2700 to 2300A. Its analysis has been carried out[1] in connection with the analysis of the corresponding system in light benzene[2] and the main results have been briefly used in the discussion of the analysis of C_6H_6. Here the experimental data for C_6D_6, together with the detailed interpretation, is presented.

EXPERIMENTAL

The heavy benzene used was a sample prepared by Dr. C. K. Ingold and collaborators. The spectrum showed that it was very pure. While the absorption spectrograms were taken the heavy benzene was kept in temperature baths varying from $-50°$ to $+25°$C, covering pressures from 0.2 to 100 mm. The 75-cm long quartz absorption tube was at room temperature. As light source a hydrogen discharge lamp of the ordinary type was employed and as spectrograph a 3-m grating instrument (Eagle mounting) was used in the first order. With Eastman spectroscopic plates I O, II O and III O exposure times varied between 1 and 4 hours. Most spectra were taken with II O plates. The iron lines were used as comparison spectrum.

RESULTS

Figure 1 exhibits part of the absorption spectrum of C_6D_6 taken at $-33°$C, which corresponds to a pressure of about 1.3 mm. Above it is the corresponding spectrum of C_6H_6 taken for comparison at about the same temperature and with the same spectrograph. Both spectra in Fig. 1 have been enlarged equally. A relative displacement of the spectra by 180 cm^{-1} has been introduced into the figure in order that the strongest bands of the first strong groups are exactly above one another. This arrangement enables a convenient and instructive comparison of both spectra.

The first weaker group which lies on the red side of the intense groups in Fig. 1, the strongest

[1] Preliminary report in Phys. Rev. **55**, 683A (1939).
[2] H. Sponer, G. Nordheim, A. L. Sklar and E. Teller, J. Chem. Phys. **7**, 207 (1939).

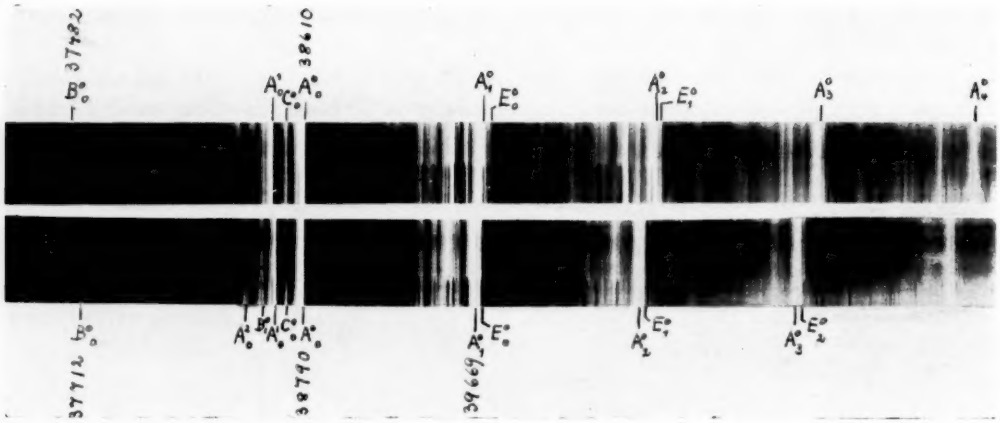

FIG. 1. Absorption spectra of C_6H_6 and C_6D_6.

band of which can barely be seen, is reproduced separately in Fig. 2. It appears only at higher pressures. Figure 2 corresponds to a temperature bath of 0°C giving a benzene pressure of about 25 mm.

In Table I are collected the frequencies of the edges of all measured bands. The intensities were obtained visually from the plates and hence represent only rough estimates. The last column mentions the experimental conditions. Most strong bands which are not diffuse are probably correct to within 1 or 2 wave numbers, while the weaker bands have a larger error, particularly the diffuse ones which may be off by as much as 5–10 wave numbers. The letters in the column Intensity mean *e w*=extremely weak, *v w*=very weak, *w*=weak, *m–w*=medium to weak, *m*=medium, *st*=strong, *v st*=very strong, *d*=diffuse. For notations the same letters are introduced as have been used in the analysis of light benzene. The column Assignment should be understandable from the text.

ANALYSIS OF THE SPECTRUM

As in light benzene the near ultraviolet absorption system represents an electronic transition[3] $^1A_{1g}\rightarrow{}^1B_{2u}$ which is forbidden by symmetry.[4] If the sixfold symmetry is destroyed by a vibration of type[5] ϵ_g^+ the system can appear with weak intensity. Since a general theoretical discussion has been given for light benzene[2] we need present only a very brief summary here. Once the inhibition against transition is lifted by an interacting ϵ_g^+ vibration we expect superimposed on such transitions progressions with totally symmetrical vibrations. The length of these progressions is governed by the Franck-Condon principle. Other superimposed transitions which involve nontotally symmetrical vibrations will correspond to changes $\Delta v=0, 2, \cdots$ in the respective quantum numbers. There may also occur bands whose appearance is not made possible through the interaction of a single ϵ_g^+ vibration but by simultaneous excitation of

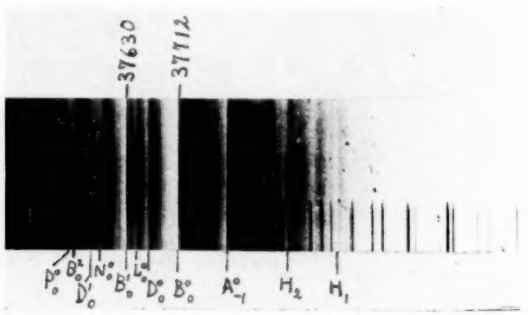

FIG. 2. First weak group of the absorption spectrum of C_6D_6.

[3] Contrary to the custom for diatomic molecules where the upper state is always mentioned first in the transition the lower (initial) state is put first throughout this paper and the arrow indicates the direction of the transition. This was done in order to be in agreement with the notation used for light benzene.[2] Since the spectra of most polyatomic molecules are and will be absorption spectra, the initial state in the transition will then be the first in the symbol. But there is the question whether the assignment customary for diatomic molecules would not be more appropriate in order to avoid different types of notations.

[4] A. L. Sklar, J. Chem. Phys. **5**, 669 (1937).

[5] Symmetry symbols for vibrations are denoted with small Greek letters.

several like or different frequencies provided their direct product contains ϵ_g^+. These bands would, however, be very much weaker. With these few rules in mind we shall proceed now with the analysis.

Two main progressions can be followed throughout the spectrum, one beginning with the strongest band, denoted by A_0^0, in the first strong group and the other beginning with the corresponding band B_0^0 in the weak group at longer wave-lengths. The difference between A_0^0 and B_0^0 is $38790.2-37712.0=1078.2$ cm^{-1}. Interpreting A_0^0 and B_0^0 as vibrational transitions $0\rightarrow1$ and $1\rightarrow0$ of the small carbon ϵ_g^+ vibration which makes the electronic transition allowed, and taking its fundamental value as 579.5 cm^{-1}, this gives for this frequency in the excited state the value 498.5 cm^{-1}. These figures are not as accurate as the number of significant figures would indicate. They were chosen so as to obtain the best possible fit to two other progressions C and D whose first members C_0^0 and D_0^0 are distant from A_0^0 and B_0^0 by 80.5 and 81.5 cm^{-1} and are interpreted as transitions $1\rightarrow2$ and $2\rightarrow1$ of the same ϵ_g^+ vibration. The reported Raman frequencies[6] for this vibration are 577, 582, and 579.3 cm^{-1}. The four mentioned bands represent the first members of progressions with distances of 879 cm^{-1} between successive bands. This separation represents the frequency of the totally symmetrical carbon vibration α_{1g} in the excited state. Its value in the ground state is 946 cm^{-1}. The spacing of 879 gives the whole spectrum its characteristic division into groups, as does the 923 spacing in light benzene.

In the first weak group has been found a band which corresponds to a threefold excitation of the ϵ_g^+ vibration in the lower and twofold excitation in the upper state. Since, because of its weakness, no series in connection with it could be discovered, no new notation was introduced, but it is simply stated as D_0^0-81.

In all four major progressions the spacing of 879 cm^{-1} is not quite constant. In the A and C progressions it is slightly decreasing, while in the B and D progressions it seems more irregular. Hence the distances between successive bands A_0^0 and C_0^0, A_1^0 and C_1^0 etc., B_0^0 and D_0^0, B_1^0 and D_1^0 etc. are also not constant, but show a slight increase. Of course, the higher groups are measured with less accuracy. But if these effects are real, they are due to anharmonicity and coupling between the vibrations α_{1g} and ϵ_g^+. They have not been considered in Table I where assignments 1×879, 2×879 etc. have been used for simplicity.

As is obvious from the foregoing, the subscripts attached to the capital letters of the progressions refer to the change in quantum numbers of the totally symmetrical carbon vibration of 879 cm^{-1} in the upper state. This vibration occurs also in the ground state in the bands $36{,}765=B_0^0-947$, $36{,}686=D_0^0-945$, $37{,}845=A_0^0-946$, $37{,}766=C_0^0-944$ and is then (see Table) denoted by a negative subscript.

The superscripts refer to frequency *differences* of 140 cm^{-1}. The corresponding bands appear on the long wave-length side of each member of the main progression. This difference, which is 160 cm^{-1} for C_6H_6 has of course the same explanation as in light benzene and has been discussed there[2] at some length: it corresponds to $n-n$ transitions of the ϵ_u^+ carbon vibration. The observed difference varies from 136 to 143 cm^{-1}, for which 140 has been taken as an average. In light benzene the 160 difference means a drop from 400 in the ground state to 240 cm^{-1} in the excited level. This seemingly abnormal drop of 40 percent had been shown not to be unexpected for this vibration. Its restoring force is due to the π electrons, and in the excited state this restoring force is weakened. To find the corresponding frequencies in C_6D_6 we remember, from investigations of the Raman effect in deuterated benzenes,[7] that a value of 350 cm^{-1} has been estimated for the ground state by extrapolation. This, together with our observed 140 decrease, would give 210 cm^{-1} for the upper state. Now in light benzene a weak series, denoted by G, was found in which this frequency occurred twice excited in the upper level. This suggests looking for a similar series in heavy benzene. The bands at 39,199 and 39,208 are both possible first members of a G series. The first band is 409 and the second

[6] C. K. Ingold and collaborators, J. Chem. Soc. (1936), 971; K. W. F. Kohlrausch, *Der Smekal-Raman Effekt, Ergänzungsband*, p. 160; A. Langseth and R. C. Lord, Det Kgl. Danske Videnskab. Selsk. Mathem.-fys. Meddelelser **16**, 6 (1938).

[7] A. Langseth and R. C. Lord, Det Kgl. Danske Videnskab. Selskab. Mathem.-fys. Meddelelser **16**, 6 (1938).

418 cm^{-1} apart from A_0^0. If this distance is interpreted as double excitation of the ϵ_u^+ vibration in the upper state it gives for its frequency 205 or 209 cm^{-1}. It is quite possible that both bands belong together, the violet one representing the weaker branch. In Table I they have been bracketed under G_0^0 and the mean value of 207 was used. Subtracting 140 from both bands leads to the extremely weak bands 39,056 and 39,067 cm^{-1}. The bands do not, however, start 879 progressions as was observed in light benzene. This weakens somewhat the proposed interpretation.

In all series discussed so far an interpretation was possible without the knowledge of the 0,0 band. In the H series of light benzene, however, the 0,0 position must be known. This weak series owes its existence to the excitation of an ϵ_u^+ vibration in both the ground and excited states. (Direct product $\epsilon_u^+ \times \epsilon_u^+$ contains ϵ_g^+.) The 0,0 band which does not occur, is readily calculated from A_0^0 and B_0^0: $38{,}790.2-498.5=37{,}712.0+579.5=38{,}291.6$ cm^{-1}. The H series would then have the formula $38{,}292-n\times140$ and the corresponding bands have indeed been found.

Particularly interesting is the first group of the spectrum. It is of much weaker intensity since the bands start from the vibrating ground level. It is likely that most of the bands which have not already been included in the discussed series will contain $n-n$ transitions of non-totally symmetrical vibrations superimposed upon allowed transitions. One of the prominent unexplained bands is denoted by N_0^0 in Fig. 2. Its separation from B_0^0 is 207 cm^{-1} which is interpreted as drop in a $1-1$ transition superimposed on the allowed B_0^0. It has a companion displaced by 140 toward the red and a corresponding band M_0^0 occurs in the first strong group shifted from A_0^0 by 209 to long wavelengths. Progressions with 879 are not obvious. The band at 39,455 may correspond to $A_0^0-209+879$ if some anharmonicity in connection with the coupling of the different vibrations is assumed. It is interesting to note that light benzene has also a band in the region of N_0^0 but which lies on the red side of D_0^1 instead of the violet side. This band which previously has not been explained is 263 cm^{-1} apart from B_0^0 and a corresponding band is 265 cm^{-1} apart from A_0^0. The intensity of the bands both in C_6H_6 and C_6D_6 suggest a Boltzmann factor of a magnitude about that to be expected for D_0^1. Moreover, N_0^0 and D_0^1 appear both displaced to the red by 946 at high pressures, but were too weak for measurement. All this points to a vibration with a frequency of about 600–700 cm^{-1}. The only carbon vibration available for such a transition

TABLE I. *Bands of* C_6D_6.

Wave Number	Intensity	Notation	Assignment	Remarks
36,487	v w	B_{-1}^2	$B_0^0-946-2\times140$	Intensities refer to plates taken at 25°C. Bands lie on red side of first (weak) group
present	v w	D_{-1}^1	$D_0^0-946-140$	
present	v w	N_{-1}^0	N_0^0-946	
36,626.2	m	B_{-1}^1	$B_0^0-946-140$	
36,657	v w	L_{-1}^0	L_0^0-946	
36,686	w	D_{-1}^0	D_0^0-946	
36,764.6	st	B_{-1}^0	B_0^0-946	
37,278	w	P_0^1	P_0^0-140	Bands from 37,280 to 37,720 constitute first (weak) group. Intensities refer to plates taken at 0°C.
37,294	w	B_0^3	$B_0^0-3\times140$	
37,340	v w		P_0^0-82	
37,348	v w	D_0^2	$D_0^0-2\times140$	
37,358	v w			
37,365	v w	N_0^1	N_0^0-140	
37,371	v w			
37,419.6	m	P_0^0	B_0^0-292	
37,432.1	m	B_0^2	$B_0^0-2\times140$	
37,460.9	w	L_0^1	L_0^0-140	
37,488.4	m	D_0^1	D_0^0-140	coincides with $B_0^0-2\times113$.
37,504.6	m	N_0^0	B_0^0-207	
37,508.8	w			
37,540	v w			
37,548.8	w	D_0^0-81	$3\times579.5\rightarrow2\times498.5$	
37,572.2	st	B_0^1	B_0^0-140	
37,599.3	m	L_0^0	B_0^0-113	
37,630.5	m	D_0^0	$2\times579.5\rightarrow498.5$	
37,656.0	w			
37,674.4	w			
37,712.0	v st	B_0^0	$579.5\rightarrow0$	
37,720	v w			
37,730	v w	H^4	$0,0-4\times140$	Bands from 37,730 to 38,242 lie on red side of second group which is first strong group. Intensities refer to plates taken at 0°C.
37,765.8	w	C_{-1}^0	C_0^0-946	
37,797	v w			
37,844.6	st	A_{-1}^0	A_0^0-946	
37,872	v w	H^3	$0,0-3\times140$	
37,939	w d			
37,986.2	m–w			
38,001.8	m		$0,0-206-82$	
38,010.5	m–w	H^2	$0,0-2\times140$	
38,044.0	w d			
38,085.9	m		$0,0-206$	
38,095.1	w			
38,126.7	m			
38,150.3	st	H^1	$0,0-140$	
38,185.1	m			
38,205	m			
38,220.0	m			
38,242	m			
(38,291.6)			$0,0$	not observed.
38,494.5	w	O_0^0	A_0^0-292	Bands from 38,495 to 38,790 belong to first strong group. Intensities refer to plates taken at −37 and −33°C.
38,505.1	w	A_0^2	$A_0^0-2\times140$	
38.514	v w	D_1^0	D_0^0+879	
38,533	v w	K_0^1	K_0^0-140	
38,564	w	C_0^1	C_0^0-140	
38,574	v w			
38,580.6	w	M_0^0	A_0^0-209	
38,588.1	w			
38,591.9	w	B_1^0	B_0^0+879	
38,592.5	w			
38,647.1	st			
38,653.7	w	A_0^1	A_0^0-140	
38,676.1	m–w	K_0^0	A_0^0-114	coincides with A_0^0 of C_6D_5H.
38,705.3	m	C_0^0	$579.5\rightarrow2\times498.5$	
38,709.7	m			
38,736	v w			
38,760.3	w			
38,787.5	v st	A_0^0	$0\rightarrow498.5$	
38,790.2	v st			
39,056	e w	G_0^1	G_0^0-140	Bands from 39,056 to 39,706 belong to second strong group. Intensities refer to plates taken at −37 and −33°C.
39,067	e w			
39,118	e w			
39,190	e w			
39,199	v w	G_0^0	$A_0^0+2\times207$	
39,208	v w			
39,263	v w d			
39,324	e w d			

is the β_{2g}, all others giving too small Boltzmann factors. Unfortunately the vibration is not known in the ground state but can only be estimated to be somewhere around[7] 700 for C_6H_6 and 600 for C_6D_6. The large drop in frequency could be explained in a manner similar to that[2] for ϵ_u^+.

It is not impossible, however, that the 207 difference involves an H vibration. However, this interpretation is less satisfactory because of the large drop in frequency which seems unlikely for an H frequency. The possibility becomes less remote if one considers a band shifted from the 0,0 band by 206 cm^{-1} in C_6D_6 and by 263 cm^{-1} in C_6H_6 toward longer waves. The bands may, of course, not be related to the aforementioned bands, but if they are, it would mean that the 207 (263) cm^{-1} difference represents a square combination of symmetry ϵ_g^+ as does the 140 (160 in C_6H_6) difference (H series). One can see that the ϵ_g^- 664 and ϵ_u^+ 700 remain as only possibilities. In light benzene both vibrations have a frequency of about 850 cm^{-1}. If we take for C_6H_6 a decrease 850→587 and for C_6D_6 a decrease 664→457, this is much the same percentual drop, but the 700 would also be possible. The large drop seems astonishing for both vibrations. It is felt that at present no definite preference can be given to one of these possible explanations.

In connection with this, attention may be called to another fairly prominent band of the discussed first group at 37,599 cm^{-1} and denoted by L_0^0 in Fig. 2. Its separation from B_0^0 is 113 cm^{-1}. A similar band occurs in the first strong group called there K_0^0. The L and K series include bands shifted by 879 and 140 cm^{-1} to the violet and red, respectively, but some of these bands cannot be verified because of overlapping. There are no analogous bands to L_0^0 and K_0^0 in light benzene, at least none of comparable intensity. A faint band appears there 117 cm^{-1} apart from A_0^0 toward the red, but if these bands in heavy and light benzene should correspond to each other they must have quite different Boltzmann factors. This would point to a 1−1 transition of a hydrogen vibration. On account of the many possibilities in this case no definite suggestion is made.[8]

The band at 37,420 represents probably a 1−1

TABLE I.—*Continued.*

Wave Number	Intensity	Notation	Assignment	Remarks
39,334	e w	B_2^1	$B_0^0+2\times879-140$	
39,372.8	w	O_1^0	O_0^0+879	
39,385.4	w	A_1^2	$A_0^0+879-2\times140$	
39,402.9	w			
39,455.0	w	M_1^0 ?	M_0^0+879 ?	
39,470.4	w	B_2^0	$B_0^0+2\times879$	
39,502.9	w			
39,526.6	st	A_1^1	$A_0^0+879-140$	
39,533.8	w			
39,546.2	w d			
39,553	w	E_0^1	E_0^0-140	coincides with K_1^0.
39,566.4	m−w			
39,587.7	m	C_1^0	C_0^0+879	
39,609.3	v w d	F_0^0	E_0^0-82 ?	
39,669.0	v st	A_1^0	A_0^0+879	
39,693.4	st	E_0^0	$0,0+\frac{1401}{1414}$	
39,706.1	m			
39,953	e w	U_0		Bands from 39,953 to 40,663 belong to third strong group. Intensities refer to plates taken at −37 and −33°C.
39,973	e w			
40,093	e w			
40,120	e w			
40,146	e w			
40,181	e w	C_2^2 ?	$C_0^0+2\times879-2\times140$	
40,213	e w d	B_2^1	$B_0^0+3\times879-140$	
40,271	e w d	A_2^2 ?	$A_0^0+2\times879-2\times140$	
40,280	m−w d	E_1^2	$E_0^0+875-2\times140$	
40,303	e w d			
40,325	e w d	C_2^1	$C_0^0+2\times879-140$	
40,351.9	m−w d	B_2^0	$B_0^0+3\times879$	
40,375	w			
40,406	w	A_2^1	$A_0^0+2\times879-140$	
40,421.2	m			
40,426	e w	E_1^1	$E_0^0+875-140$	coincides with K_2^0.
40,436.8	m−w			
40,441.7	v w			
40,461.8	w	C_2^0	$C_0^0+2\times879$	
40,480.3	w	F_1^0 ?	$E_0^0-82-140$	
40,498.4	v w			
40,545.5	v st−st	A_2^0	$A_0^0+2\times879$	
40,566.6	st	E_1^0	E_0^0+875	
40,580.9	m			
40,610.5	w			One of these may be $A'_0{}^0 = A_0^0$+totally symmet. H vibration.
40,630.8	v w			
40,663	e w			
40,852.8	w	U_1		Bands from 40,853 to 41,555 belong to fourth strong group.
40,969	e w			
40,995	v w			
41,083	v w			
41,151	w d			Intensities refer to plates taken at −37 and −33°C.
41,200	w d	C_2^1 ?	$C_0^0+3\times879-140$	
41,233	w d	B_2^0	$B_0^0+4\times879$	
41,295	m−w	E_2^1	$E_0^0+2\times875-140$	
41,310.6	m−w			
41,318.5	m−w			
41,332	e w d	C_2^0 ?	$C_0^0+3\times879$	
41,357.1	w d	F_2^0 ?	$F_0^0+2\times875$	
41,417.6	m−w	A_2^0	$A_0^0+3\times879$	
41,440.7	st	E_2^0	$E_0^0+2\times875$	
41,453.6	m			
41,480.5	m−w d			One of these may be $A'_1{}^0 = A'_0{}^0+870$.
41,502.5	v w d			
41,530	e w d			
41,555	e w d			
41,728	v w d	U_2		Bands from 41,728 to 42,390 belong to fifth strong group. Intensities as before.
41,773	e w d			
41,961	e w d			
42,198	e w d			
42,326.2	m d	E_3^0	$E_0^0+3\times875$	
42,348.6	m d			
42,373	e w d			One of these may be $A'_2{}^0 = A'_0{}^0+2\times870$.
42,390	e w d			
43,195	w d	E_4^0	$E_0^0+4\times875$	Sixth strong group.
43,220	v w d	$A'_2{}^0$?	$A'_0{}^0+3\times870$	Intensities as before.

[8] It should also be mentioned that Kistiakowsky and Solomon (J. Chem. Phys. **5**, 609 (1937)), comparing their results with unpublished measurements of Bowman, Benedict, Kirkpatrick and Taylor, give the value 38,679 cm^{-1} as origin of a band progression of $C_6D_4H_2$. The figure of the latter authors is 38,676 and agrees exactly with the band K_0^0 of this paper. But it does not seem very probable that this would be the explanation of our K_0^0 because of the occurrence of the band L_0^0 displaced by 1078 towards the red, furthermore the occurrence of bands shifted by 140 to the red. The 879 progression cannot be taken as proof because some members coincide with other bands. The wave number 38,746 given by Kistiakowsky and Solomon as another band progression origin (probably for C_6D_5H) does not coincide with any value in this paper.

transition of a hydrogen vibration. It has no analog in light benzene in the corresponding spectroscopic region. According to its intensity it may contain a vibration that would give a Boltzmann factor of the magnitude of that for B_0^2. There are indeed enough possibilities for such a vibration. Also here the drop in the frequency would be rather large.

The totally symmetrical hydrogen vibration which was believed[2] to be 2565 cm^{-1} in the upper state of C_6H_6 seems also to occur in C_6D_6. If a similar drop as in light benzene (3062→2565) is assumed for heavy benzene we would expect a frequency of 1920 cm^{-1}. There are three bands in heavy benzene each of which could be correlated with this hydrogen frequency. They lie at 40,611, 40,631 and 40,663 cm^{-1} and could be interpreted as due to the totally symmetrical H vibration superimposed on A_0^0. All three start a progression with 870 cm^{-1}. All three, when subtracting 1078, lead to already explained bands of comparable or even larger intensity instead of smaller intensity so that the corresponding bands superimposed on the B progression must be masked in all three cases. The frequency of the possible hydrogen vibration in the upper state would be 1821, 1841 or 1873 cm^{-1}, respectively. The band 40,611 is the strongest of the three and therefore seems the best choice when comparing intensities in the two benzenes; the band 40,663 is the weakest but gives the largest frequency and in this respect seems preferable, but the intensity argument is perhaps somewhat stronger.

There are a number of other weak and very weak bands for which unambiguous interpretations cannot be given. It is for example not impossible that the band 39,118 corresponds to the excitation of the lower ϵ_g^+ H vibration. Its value is 869 in the ground state and from the just mentioned band 826 cm^{-1} would follow for the upper state. The series denoted by U_0, U_1, U_2 is interesting. The distance of U_0^0 from the 0,0 band is 1661/1681 cm^{-1} while the corresponding bands in C_6H_6, 39,777/39,795, are 1688/1706 apart from the 0,0 band. No satisfactory explanation could be found for these bands.

The E series in light benzene was attributed to the excitation of the other carbon ϵ_g^+ vibration of 1596 cm^{-1} in the ground state. Two bands at 39,561 and 39,569 were taken as the first member of this series. Now in heavy benzene there appear two corresponding bands at 39,693 and 39,706. As in C_6H_6 the one at longer wave-lengths is the stronger of the two, but the distance between them is here larger. Assuming the same explanation would mean that in C_6D_6 the ϵ_g^+ 1553 drops to 1401/1414 cm^{-1} in the upper state while in C_6H_6 the 1596 decreased to 1472/1480. The drop is larger for heavy than light benzene contrary to the behavior of the other discussed carbon vibrations. But the differences between the two benzenes are not large enough to make the interpretation seem very unlikely. For further support one may look for a band displaced by 1553 toward the red from the 0,0 band but none was detected. This is, however, no disproof of the discussed interpretation because the band may be too weak for detection. Its appearance in C_6H_6 was due to an intensification by the interaction with the combination vibration 992 $+606=1598$ cm^{-1}. However, there is the possibility that both or one of the bands at 39,693 and 39,706 in C_6D_6 have another explanation. If this should be true it seems more satisfactory to make the same assumption for the corresponding bands in light benzene. Several interpretations were tried but none of them is very satisfactory. Therefore, in Table I the bands are simply bracketed under E and the same explanation as in light benzene is added. As can be seen the E bands start 140 and 875 progressions. An 82 progression, which would mean a transition $580=498$ superimposed on E, is somewhat doubtful.

Since a comparison of the absorption with the fluorescence spectrum of C_6D_6 was already included in the paper on light benzene[2] no such discussion will be given here. We refrain also from a closer consideration of the structure of the bands. Most bands look as if they were double-headed which perhaps is due to R and Q branches as was concluded for light benzene. But much higher dispersion spectrograms are needed before more definite conclusions about the rotational structure can be drawn.

In conclusion, I want to thank Professor C. K. Ingold very sincerely for the loan of the heavy benzene made available to me through the courtesy of Professor D. H. Andrews. I also want to acknowledge the assistance of Mr. S. H. Wollman in taking some of the spectrograms.

The Vibration Frequencies and Thermodynamic Functions of Long Chain Hydrocarbons

KENNETH S. PITZER
Department of Chemistry, University of California, Berkeley, California

(Received February 28, 1940)

A method is developed for calculating thermodynamic functions for long chain molecules with particular attention to normal paraffins. In this connection the infinite chain approximation method for calculating vibration frequencies is considered. Starting with the results of Kirkwood, a modification is made which improves the agreement with the exact values for the simpler cases. In addition this method of attack is extended to out of plane motions. This vibrational analysis shows that all skeletal frequencies for molecules of the normal paraffin type can be put into two groups, one fairly narrow band near 1000 cm^{-1}, and a broader band extending from 0 to 460 cm^{-1}. The partition function is then set up on the assumption that motions in the low frequency group can be treated classically, and that the high frequency band can be replaced by a suitable number of 1000 cm^{-1} frequencies. Contributions from hydrogen atom vibrations are added on later. A formula is finally obtained which is quite simple, considering the complexity of the molecules. The calculated entropies can be brought into agreement with experimental values on the basis of very reasonable internal rotation restricting barriers.

THE writer has recently measured with considerable accuracy the entropies of *n*-heptane and of 2,2,4 trimethyl pentane.[1] In calculating statistical entropies for comparison, it became apparent that the existing methods are not very satisfactory for such molecules.[2] By making extensive use of the integral form of the partition function, a somewhat different method is presented below which has certain advantages. Considerable use also is made of the interesting scheme for calculating vibration frequencies recently described by Kirkwood[3] and in somewhat different form by Thomas and Whitcomb[4] and by Barriol.[5] Kirkwood's formulation will be used with, however, one important modification and with an extension to include out of plane vibrations.

Let us consider the vibration frequency problem first. With Kirkwood we shall separate the motions of the hydrogen atoms from those of the carbon skeleton, and shall consider the latter to lie at equilibrium in a planar, zigzag chain. The interesting step is treatment of the problem as one of an infinitely long chain after which those modes of vibration which are approximately correct for the molecule in question are selected. We shall consider first the motions within the plane, i.e., bond stretching and bending but not internal rotation, and shall take Kirkwood's nomenclature. He finds in his Eq. (7):

$$\begin{aligned}\omega^2&=\omega_0^2\pm[\omega_0^4-\omega_1^4]^{\frac{1}{2}},\\ \omega_0^2&=\alpha(1+\cos\gamma\cos\lambda)\\ &\quad+2\beta(1+\cos\lambda)(1-\cos\gamma\cos\lambda),\\ \omega_1^4&=8\alpha\beta(1+\cos\lambda)\sin^2\lambda,\end{aligned}\tag{1}$$

where α and β are the ratios k_1/m and k_2/m, of the bond stretching and bending force constants to the effective mass m of a CH_2 group, γ is the C−C−C bond angle, and ω is 2π times the frequency. The motion of the nth particle is given in terms of ω and λ as follows:

$$\xi_n=Ae^{i(\omega t+n\lambda)},\quad \eta_n=(-1)^nBe^{i(\omega t+n\lambda)},\tag{2}$$

where ξ is the displacement from equilibrium along the length of the chain and η is the displacement perpendicular to the chain. The wave-

[1] Pitzer, J. Am. Chem. Soc. **62**, 1224 (1940).
[2] Most recently Huggins (J. Chem. Phys. **8**, 181 (1940)) has published calculations of the entropies of the normal paraffins using a method quite different from that given below. The molecular picture assumed by Huggins is, in the writer's opinion, not as detailed and specific as that assumed below. Consequently the latter method is likely to give more molecular structure information. From an empirical point of view the formula given below is linear in the number of carbons while Huggins' contains also a logarithm term. While the available experimental values are probably not accurate enough to decide this point, they seem to be better fitted by the simpler linear formula which was also extensively used by Parks and Huffman (reference 13).
[3] Kirkwood, J. Chem. Phys. **7**, 506 (1939).
[4] Thomas and Whitcomb, Phys. Rev. **56**, 383 (1939).
[5] Barriol, J. de phys. et rad. **10**, 215 (1939).

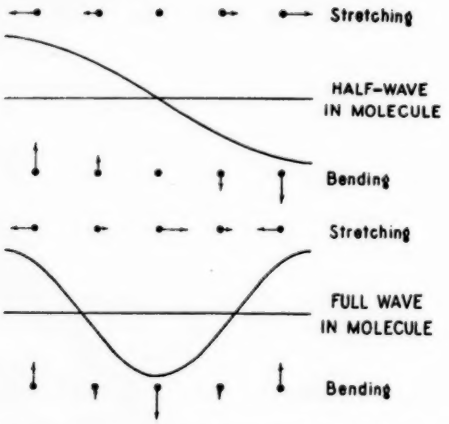

FIG. 1. Illustration of the longitudinal and transverse (stretching and bending) modes of motion for a linear pentatomic molecule with half-wave and full wave in the molecule length.

length of the longitudinal motion is thus $2\pi/\lambda$ in terms of a chain link as a unit. The transverse motion has the wave-length $2\pi/(\pi-\lambda)$.

The next step is to select values of λ so as to approximate the motion of a finite chain of N elements. Kirkwood followed Born and Karman in using the condition:

$$\lambda = 2\pi l/N, \tag{3}$$

which the writer does not believe to be quite correct.* In Eq. (3) l is to have integral values from 0 or 1 to $N-1$. In this form the maximum wave-length is N or the length of the molecule for the fundamental longitudinal mode. However, in the true fundamental stretching mode of vibration, the half-wave-length corresponds to the chain length. The better requirement is that an integral number of half-wave-lengths must be completed within the molecule, or:

$$\lambda = \pi l/N \qquad l = 1, 2, 3, \cdots N-1. \tag{4}$$

On this basis the bending modes also fit more satisfactorily. The mode of longest wave-length closely approximates a rotation of the molecule in the plane and is to be discarded on that basis, as was stated by Kirkwood. The next mode closely approximates the actual fundamental bending mode of vibration of the molecule. Some of the higher bending modes include slight rotations of the molecule. However, the error from this source is very small and seems to be inherent in this approximation method. Certainly this error is less serious than taking modes of vibration that fail to qualitatively correspond to the true ones. Figure 1 illustrates for a straight chain the motions just discussed.

It is interesting to note that this correction removes the peculiar degeneracy found by Kirkwood. The correspondence with the true frequencies is greatly improved, especially for the smaller molecules. This is shown in Table I. Here we have compared for ethane, propane, butane, and pentane, the frequencies calculated by Kirkwood's method, those calculated by the modification of it just discussed, those calculated with the accurate equations of Kassel,[6] and the experimental values. Kassel's equations approximate the CH_2 group as a unit and assume the same forces and equilibrium configuration, but are exact solutions for the molecules in question. Thus a comparison of the columns headed "Kirkwood" and "This Research" with that headed "Kassel" offers a good test of the approximations of the two infinite chain methods. Comparison of the latter with the "observed" tests the remaining approximations. The force constants are the same for each method of

TABLE I. *The skeletal vibration frequencies of some simple hydrocarbons* (cm^{-1}).

	Calculated by Method of:			
	Kirkwood	This Research	Kassel	Observed
Ethane	1120	970	970	993
	1034(?)	(408)		
Propane	1057	1057	1050	1053
	1057	934	915	867
	208	447	375	375
	(208)	(208)		
n-butane	1120	1087	1082	1058
	1034	970	970	954
	970	960	945	835
	970	408	359	326
	408	380	288	?
	408(?)	(142)		
n-pentane	1102	1102	1090	1073
	1102	1025	1020	1033
	933	983	977	900
	933	933	937	837
	460	460	394	334
	460	317	320	?
	90	304	190	?
	(90)	(90)		

* This error is entirely trivial for the applications to crystals which interested Born and Karman.

[6] Kassel, J. Chem. Phys. **3**, 326 (1935).

calculation but differ slightly from those used by Kirkwood and Kassel.*

The higher or stretching frequencies are surprisingly well approximated by the infinite chain method. The more serious approximations appear to be rather in the separation of the hydrogen vibrations and possibly in an oversimplified expression of forces.

The infinite chain method is less satisfactory for the lower or bending modes. However, the results are always of the correct general magnitude. It is pleasing that the spurious frequency which is a rotation of the individual molecule, takes a value much smaller than the other bending frequencies.

The assignment of observed frequencies[7] for butane and pentane is quite an arbitrary procedure at present, since the planar configuration here assumed is only one of many possible ones.

We may give as equations for calculation the following:

$$\begin{aligned}
&\nu_{\pm}(l)=\bar{\nu}[\tfrac{1}{2}\eta(l)\pm\tfrac{1}{2}\zeta(l)]^{\frac{1}{2}}, \quad l=1, 2, \cdots, N-1\\
&\bar{\nu}=(\tfrac{1}{2}\pi)(2k_1/m)^{\frac{1}{2}}, \quad \epsilon=k_2/k_1\\
&\eta=1+\cos\gamma\cos(\pi l/N)\\
&\qquad +2\epsilon[1+\cos(\pi l/N)]\\
&\qquad\qquad \times[1-\cos\gamma\cos(\pi l/N)],\\
&\zeta^2=\eta^2-8\epsilon[1+\cos(\pi l/N)]\sin^2(\pi l/N).
\end{aligned} \tag{5}$$

For the values in Table I, γ was given the tetrahedral angle, $\bar{\nu}$ was given the value 970 cm^{-1} and ϵ, the bending to stretching force constant ratio, was given the value 0.088. These seemed to give the best all-around agreement.

* The writer wishes to express his appreciation to Professor Kirkwood for his comments after reading this section. There is no absolutely correct criterion for selecting those modes most closely approximating the true ones in a finite molecule. Kirkwood suggests the requirement of zero acceleration for the center of mass, and states that either the Born-Karman condition or the one suggested above is sufficient. Thus further considerations are necessary. Besides the wave-length criterion for qualitative similarity to the true modes suggested in the text, one may also mention that a requirement of the proper number of different modes of vibration would lead definitely to the new condition, for molecules with N odd. For N even the latter argument does not lead to a definite result, however, the same condition might be selected by analogy. In any event the results in Table I justify a claim of superiority for the new condition; and Professor Kirkwood states definitely his agreement with this conclusion.

[7] Kohlrausch and Köppl, Zeits. f. physik. Chemie **B26**, 209 (1934).

TABLE II. *Out of plane vibration frequencies* (cm^{-1}).

	EXACT*	INFINITE CHAIN
n-butane	140	198
n-pentane	156	214
	121	157
n-hexane	172	210
	148	198
	86	121

* The equations for these frequencies are as follows:
n-butane $\omega^2=4k_3/m$
n-pentane $\omega^2=3k_3/m,\ 5k_3/m$
n-hexane $\omega^2=3k_3/2m,\ 9k_3/2m,\ 6k_3/m.$

Kirkwood considered only motions of the atoms within the plane of the molecule. We shall find some interest in the modes of motion where the atoms move perpendicular to this plane and will treat this problem in an analagous manner. These motions are the beginnings of internal rotations, but if of small enough amplitude they may be treated as harmonic oscillations. If the potential energy is connected with rotation about bonds, we may take an increase of energy of $\frac{1}{2}k_3(\Delta Z)^2$ when of four successive atoms one is a distance ΔZ from the plane of the other three. In these terms the equation of motion of the nth atom is:

$$\begin{aligned}
m\ddot{Z}_n+k_3(4Z_n-Z_{n-1}-Z_{n+1}-2Z_{n-2}\\
-2Z_{n+2}+Z_{n-3}+Z_{n+3})=0
\end{aligned} \tag{6}$$

where the Z's are perpendicular distances from the plane of the infinite chain at equilibrium. Then making the usual substitution:

$$Z_n=Ae^{i(\omega t+n\lambda)}, \tag{7}$$

we find:

$$\begin{aligned}
&\omega^2=(k_3/m)(4-2\cos\lambda-4\cos 2\lambda+2\cos 3\lambda).\\
&\lambda=\pi l/N, \quad l=1, 2, \cdots, N-1, \quad \nu=\omega/2\pi.
\end{aligned} \tag{8}$$

Of these solutions the ones with $l=1$ and $l=N-1$ should be discarded as corresponding to rotations. The latter approximates rotation about an axis along the chain, the former about an axis perpendicular to the chain.

In Table II the frequencies calculated by this method are compared with exact values calculated for each of the molecules using the same forces. For the simpler molecules the exact equations are easily obtained by the usual methods.

It is seen in Table II that the infinite chain method is even less satisfactory for the out of plane vibrations. However, it may still be of value in a statistical sense for very long molecules.

It is interesting to note that the success of the infinite chain method is closely connected with the range of the principal forces involved. Thus the bond stretching depends on two atoms, the bond bending on three, and the out of plane bond rotations on four.

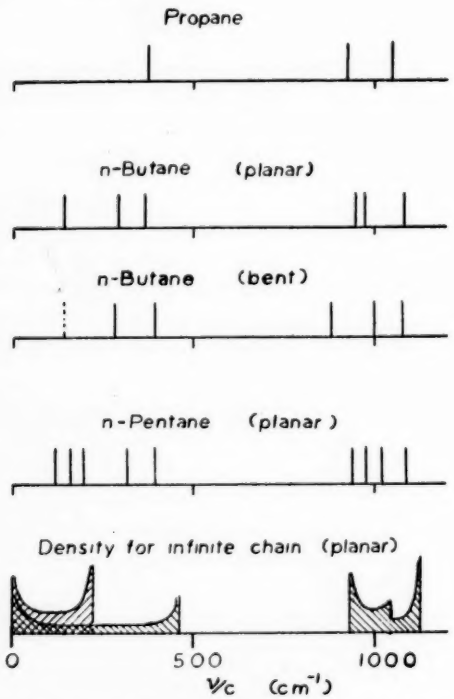

FIG. 2. Skeletal vibration frequencies for simple hydrocarbons and the infinite chain. The lowest (torsional) frequency for "bent" n-butane was estimated and is shown dotted. The lowest band for the infinite chain is for the torsional motions; the broader band extending to 460 cm^{-1} is for bending motion in the plane.

METHODS OF CALCULATING PARTITION FUNCTIONS

Before actually setting up the partition function for the chain molecules, it seems desirable to discuss general methods briefly. It would be very desirable, if possible, to obtain a general formula for the n atom chain. The usual methods do not permit this generalization, except possibly on an empirical basis after calculating a number of specific examples. Approximations which would be undesirable in simple cases are worth while here if they simplify the complex problem, particularly since only relatively rough molecular data are available for these molecules. This work aims at an accuracy of a few tenths cal. per degree.

If we consider the distribution of skeletal vibration frequencies in these molecules, as summarized in Fig. 2, the possibility immediately suggests itself of replacing the high frequency band by a suitable number of 1000 cm^{-1} frequencies. This approximation will be reasonably satisfactory for all lengths of chain from propane up. Also if we may generalize from n-butane, it will be satisfactory for various bent configurations in addition to the planar one. On the other hand similar approximations for the low frequency group would not be satisfactory, particularly when one considers that these bands extend to zero frequency.

Another possibility which arises is that the low frequency group may be treated by the classical or integral partition function. Although results obtained thereby will necessarily fail at low enough temperatures, this is not necessarily a serious limitation for practical purposes. It will be shown below that the classical formula allows the separation of a factor for each additional atom in the chain. This, combined with the approximation of a number of 1000 cm^{-1} frequencies permits the desired type of formula.

Our fundamental equation can then be taken as:

$$Q = Q^{\text{classical}}_{(\text{trans, rot, tors, bend})} Q^{n-1}_{(1000\ \text{cm}^{-1}\ \text{vib})}, \qquad (9)$$

where the first term is a classical partition function for translation, rotation, torsion, and bending and the second term accounts for $(n-1)$ vibrations of frequency 1000 cm^{-1}. For convenience in calculation we make the transformation:

$$Q = \{Q^{\text{classical}}_{(\text{trans, rot, tors, bend})} [Q^{\text{classical}}_{(10{,}000\ \text{cm}^{-1}\ \text{vib})}]^{n-1}\} \times [Q(1000\ \text{cm}^{-1}\ \text{vib.})/Q^{\text{classical}}_{(1000\ \text{cm}^{-1}\ \text{vib})}]^{n-1}. \qquad (10)$$

Now the factors in the braces comprise a complete classical partition function which can be set up more easily than one wherein only the low frequency skeletal motions are considered. This interpretation depends upon the fact established above, that the molecules will have $(n-1)$ motions of approximately 1000 cm^{-1} frequency.

The form of Eq. (10) suggests the possi-

bility of including similar factors for the low frequency bands to correct for small deviations from the classical formula in these cases. In order to investigate this possibility, we make the following expansions which are valid when $(h\nu/kT)$ is less than about 1.7. This includes the low frequency bands at or above room temperature.

$$Q_{(\nu)}=1/(1-e^{-h\nu/kT}),\quad Q_{(\nu)}{}^{\text{class}}=kT/h\nu,$$

$$[Q(\nu)/Q_{(\nu)}{}^{\text{class}}]=(h\nu/kT)/(1-e^{-(h\nu/kT)})$$
$$=1+\tfrac{1}{2}(h\nu/kT)+1/12(h\nu/kT)^2+\cdots,$$

$$[(F/T)-(F/T)^{\text{class}}]$$
$$=-R[\tfrac{1}{2}(h\nu/kT)-1/24(h\nu/kT)^2+\cdots],$$

$$[(H/T)-(H/T)^{\text{class}}]$$
$$=-R[\tfrac{1}{2}(h\nu/kT)-1/12(h\nu/kT)^2+\cdots],$$

$$[S-S^{\text{class}}]=R[1/24(h\nu/kT)^2+\cdots],$$

$$[C-C^{\text{class}}]=-R[1/12(h\nu/kT)^2+\cdots].$$

Under these conditions, the equations show that the use of the arithmetic mean for even a broad band of frequencies would give the correct leading terms in (F/T) and (H/T). These leading terms may be regarded as corrections for zero point energy in $(H_0{}^0)$ and therefore of little practical value, as is indicated by their disappearance in S and C. For the square terms which lead in S and C, a root mean square frequency should be used in approximating a band. This will not differ grossly from the ordinary mean if the band has a definite upper limit even though it continues to zero. On the other hand the computation of the partition function itself requires, in the classical case, the geometric mean frequency which would be grossly affected by the continuance of a band to zero. Thus other methods must and will be used to calculate the classical function itself. If $(h\nu/kT)$ is about one, the second-order corrections are about 0.1 cal. per degree or less and are consequently almost negligible.

We may summarize this section as follows. A partition function may be calculated as a product of the complete classical function and correcting factors for the higher frequencies provided one of the following conditions is fulfilled: (1) the exact frequencies are used in the corrections: (2) mean frequencies are used for narrow bands: (3) mean frequencies are used when $(h\nu/kT)$ is less than about 1.7. In any case force constants must be used in the classical function which are consistent with the vibration frequencies.

The Partition Function for the General Normal Paraffin

Following the method outlined above we first calculate the complete classical partition function.[8]

$$Q=\frac{1}{h^{3n}}\int_{-\infty}^{\infty}\cdots\int_{-\infty}^{\infty}\int_{0}^{X_0}\cdots\int_{0}^{Z_0}$$
$$\times e^{-(\text{P.E.}+\text{K.E.})/kT}\,dp_{x_1}\cdots dp_{z_n}\,dx_1\cdots dz_n. \quad (11)$$

Here P. E. and K. E. are the potential and kinetic energies, respectively, p_{x_1}, etc., are momenta and x_1, etc., the corresponding coordinates. This form of the partition function means a great simplification because it does away with all consideration of how a single system would move under a given set of conditions. Moments of inertia do not need to be calculated, nor is a normal coordinate treatment necessary, but only an expression of the potential and kinetic energies in terms of coordinates and momenta. As before we approximate CH_2 (or CH_3 or CH) groups as single units in this treatment and discuss the hydrogen motions separately. Considering the momenta first we write for the kinetic energy:

$$\text{K.E.}=\sum_{i=1}^{n}\tfrac{1}{2}m(p^2{}_{x_i}+p^2{}_{y_i}+p^2{}_{z_i}),$$

where the mass m is the same for all n particles. The partition function now takes the form:

$$Q=\left(\frac{2\pi mkT}{h^2}\right)^{3n/2}\int_{0}^{X_0}\cdots\int_{0}^{Z_0}$$
$$\times e^{-(\text{P.E.})/kT}\,dx_1\cdots dz_n. \quad (12)$$

For the potential energy the expression will be the same as in the preceding section for bond stretching and bending motions. For internal rotations, however, a three-peaked sinusoidal barrier will be used: $\frac{1}{2}V_0(1-\cos 3\phi)$. It is also necessary to assign a high energy to those configurations which involve serious steric repulsions.

[8] Fowler, *Statistical Mechanics* (Cambridge University Press, second edition, 1936), p. 56 ff.

Since we assume a perfect gas state, the first atom of a molecule may be placed anywhere in the container, and the second may be oriented in any direction with respect to the first. A potential energy term $[\frac{1}{2}k_1(r-r_0)^2]$ must be included for the distance between these atoms. Integrating for these atoms we have:

$$Q=\left(\frac{2\pi mkT}{h^2}\right)^{3n/2}V(4\pi r_0^2)\left(\frac{2\pi kT}{k_1}\right)^{\frac{1}{2}}\int_0^{X_0}\cdots\int_0^{Z_0}\times e^{-(\text{P.E.})/kT}dx_3\cdots dz_n, \quad (13)$$

where r_0 is the C−C distance, V the volume, and k_1 the stretching force constant.

The motion of the next atom involves another bond stretching term, a bond bending term $[\frac{1}{2}k_2\delta^2]$, where δ is the distance from equilibrium position, and a third rotation. The circumference of the allowed circle is $2\pi r_0 \sin\gamma$ where γ is the C−C−C angle. We then have:

$$Q=\left(\frac{2\pi mkT}{h^2}\right)^{3n/2}V(8\pi^2 r_0^3\sin\gamma)\frac{(2\pi kT)^{\frac{1}{2}}}{(k_1^2k_2)^{\frac{1}{2}}}\int_0^{X_0}\cdots\int_0^{Z_0}e^{-(\text{P.E.})/kT}dx_4\cdots dz_n. \quad (14)$$

All atoms along a normal chain after the third have bond stretching and bending motions and a restricted internal rotation. If one assumes three equal maxima and minima and the usual sinusoidal shape, the factor in the partition function is:

$$r_0\sin\gamma\int_0^{2\pi}e^{-(V_0/2kT)(1-\cos 3\varphi)}d\varphi.$$

With long chain molecules it seems certain that some configurations will involve considerable steric repulsion and that as a result the assumption of three equal minima for each rotation will not be satisfactory. In order to account for these steric effects without too great complexity, the following procedure was adopted. By some means the energy for each configuration corresponding to all internal rotations at minimum points was decided upon. This special "steric" energy was then assumed to remain a constant addition to the internal rotation potential energy for oscillations about a given position as far as the potential peaks. Thereafter energies appropriate to new minimal positions apply. Mathematically this procedure involves changing the upper limit of integration in each [I. Rot.] factor from 2π to $2\pi/3$, and the introduction of a factor:

$$F_{\text{steric}}=\sum e^{-E_i/kT}, \quad (15)$$

where E_i is the energy of the ith configuration. The partition function is not sensitive to changes in the shape of the potential peaks, where this assumption would err most.

We shall assume that the most stable configuration is the planar, zig-zag one discussed above and observed in solids. Rotation about one bond by $(2\pi/3)$ always involves the same interaction which probably increases the energy. Let us call this energy a. By the use of models it was found that rotation about several bonds led either to that number of these same interactions, or else to an impossible configuration from the steric point of view. By assigning a numerical value to a, and counting the number of each kind of position, the sum in Eq. (15) can be calculated easily.

We may now write the complete classical partition function as follows:

$$\begin{aligned}
Q^{\text{class}}&=\tfrac{1}{2}F_{0(T)}[C-C_{\text{str}}]^{n-1}[C-C_{\text{bend}}]^{n-2}\times[\text{I. Rot.}]^{n-3}F(\text{steric}),\\
F_{0(T)}&=(2\pi mkT/h^2)^3V(8\pi^2r_0^3\sin\gamma),\\
[C-C_{\text{str}}]&=(2\pi kT/h)(m/k_1)^{\frac{1}{2}},\\
[C-C_{\text{bend}}]&=(2\pi kT/h)(m/k_2)^{\frac{1}{2}},\\
[\text{I. Rot.}]&=(2\pi mkTr_0^2\sin^2\gamma/h^2)^{\frac{1}{2}}\times\int_0^{2\pi/3}e^{-(V_0/2kT)(1-\cos 3\varphi)}d\varphi,\\
F_{(\text{steric})}&=\sum e^{-E_i/kT}.
\end{aligned} \quad (16)$$

The molecule symmetry number 2 (which appears as the factor $\frac{1}{2}$ above) has been introduced since both ends are the same. For N_0 identical molecules the partition function is raised to that power and divided by $(N_0/e)^{N_0}$ which approximates $(N_0!)$.

Recalling now the results of the preceding section, we wish to add factors of the type $[Q_{(\nu)}/Q_{(\nu)}{}^{\text{class.}}]$ for $(n-1)$ 1000 cm^{-1} frequencies and similar factors for the low frequency bands. For these we take $(n-2)$ 290 cm^{-1} frequencies

TABLE III. *Hydrogen vibration frequencies* (cm^{-1}).[9]

(NUMBERS IN PARENTHESES ARE DEGENERACIES)

	(1)	(2)	(1)	(2)	(2)	
CH_3F	2900	2990	1460	1476	1200	
CH_3Cl	2920	3050	1355	1460	1020	
CH_3Br	2910	3060	1305	1450	957	
CH_3 adopted	3000 (3),		1400 (3),		1000 (2)	
CH_2Cl_2	2985	3045	1266	1420	1060	900
CH_2O	2900	2800	1460	—	1039	917
$(CH_2)_2$	3019	3069	1342	—	950	940
	2988	3107	1444	—	950	1100
CH_2 adopted	3000 (2),		1400 (2),		1000 (2)	
$CHCl_3$	3018		1216 (2)			
$CHBr_3$	3021		1144 (2)			
CH adopted	3000 (1)		1200 (2)			

and $(n-3)$ 120 cm^{-1} frequencies. The justification of using mean frequencies for these broad bands was explained above. It was also pointed out that these latter corrections are very small so that they might even be omitted without very serious error.

It is interesting to note that the factor $[C-C_{str}]$ in Eq. (16) is not just the classical factor for a 1000-cm^{-1} vibration but is somewhat larger. The difference may be thought of as a contribution to mass and moment of inertia terms in the usual formulas because of the additional atom in the molecule. This effect can be easily traced through in the simpler cases by comparing with the usual type of calculation. The situation is, of course, similar with $[C-C_{bend}]$ and [I. Rot.].

Finally the contributions of the hydrogen vibrations must be considered. This will be done by selecting frequencies characteristic of the CH_3 and CH_2 (and for branch chain compounds CH)

TABLE IV. *Formula for calculating thermodynamic functions of paraffin hydrocarbons.*

Th. F. $= [F_0(T)] + n_1[C-C_{str}] + n_2[C-C_{bend}] + n_3[\text{I. Rot.}] + F_{(\text{steric})} + F_{(\sigma)} + n_4[CH_3] + n_5[CH_2] + n_6[CH]$

	$-F/T$	H/T	C
$F_0(T)$	$R\ln\left(\frac{64\pi^5 m^3 r_0^3 k^3 \sin\gamma R}{h^6 N_0}\right)+4R\ln T-R\ln P=4.274+4R\ln T-R\ln P$	$4R$	$4R$
$[C-C_{str}]$	$R\ln(2\pi\nu_1(m/k_1)^{\frac{1}{2}})+\text{Ein.}(h\nu_1/kT)=0.75+\text{Ein.}\left(\frac{hc1000}{kT}\right)$	Ein. $(h\nu_1/kT)$ $(\nu_1/c=1000\ cm^{-1})$	Ein. $(h\nu_1/kT)$
$[C-C_{bend}]$	$R\ln(2\pi k m^{\frac{1}{2}}/hk_2^{\frac{1}{2}})+R\ln T+(R/2)(h\nu_2/kT)-(R/24)(h\nu_2/kT)^2=-11.275+R\ln T+413/T-14200/T^2$	$R-(R/2)(h\nu_2/kT)+(R/12)(h\nu_2/kT)^2=R-413/T+28400/T^2$	$R-(R/12)(h\nu_2/kT)^2=R-28400/T^2$ $(T>250)$
[I.Rot.]	$R[-1.267+\frac{1}{2}\ln T+\frac{1}{2}\ln(mr_0^2\sin^2\gamma\times10^{40})-\ln 3]-\frac{(F-F_f)}{T}\left(V_0/RT,\frac{n^2}{IV}=0\right)+\frac{h\nu_3}{2T}$ $=\frac{1}{2}R\ln T-0.55+\frac{170}{T}-\frac{(F-F_f)}{T}\left(\frac{3600}{RT}\right)$	$\frac{H}{T}\left(\frac{V_0}{RT},\frac{n^2}{IV}=0\right)-\frac{h\nu_3}{2T}=\frac{H}{T}\left(\frac{3600}{RT}\right)-\frac{170}{T}$	$C\left(\frac{V_0}{RT},\frac{n^2}{IV}=0\right)=C\left(\frac{3600}{RT}\right)$
$F_{(\text{steric})}$	$R\ln Q$ $Q=\Sigma e^{-Ei/kT}$	$R(Q'/Q)$ $Q'=\Sigma(Ei/kT)e^{-Ei/kT}$	$R[Q''/Q-(Q'/Q)^2]$ $Q''=\Sigma(Ei/kT)^2e^{-Ei/kT}$
$F_{(\sigma)}$	$-R\ln\sigma$	0	0
$[CH_3]$	Σ Ein. $(h\nu/kT)+R(-1.267+\frac{1}{2}\ln T+\frac{1}{2}\ln I_R\times10^{40}-\ln 3)-(F-F_f)/T_{(V_0/RT)}$ $\nu/c=3000\ (3), 1400\ (3), 1000\ (2)$	Σ Ein. $(h\nu/kT)+H/T_{(V_0/RT)}$ $V_0=3600$ cal.	Σ Ein. $(h\nu/kT)+C_{(V_0/RT)}$ $I_R=5\times10^{-40}$
$[CH_2]$, $[CH]$	Σ Ein. $(h\nu/kT)$ $CH_2-\nu/c=3000\ (2), 1400\ (2), 1000\ (2)$ $CH-\nu/c=3000\ (1), 1200\ (2)$	Σ Ein. $(h\nu/kT)$	Σ Ein. $(h\nu/kT)$

For a normal paraffin of N carbon atoms: $n_1=N-1$, $n_2=N-2$, $n_3=N-3$, $n_4=2$, $n_5=N-2$, $n_6=0$, $\sigma=2$, summations in $F_{(\text{steric})}$ are over 3^{N-3} terms.

Ein. refers to an Einstein function for one degree of freedom and of the proper type, i.e., $-F/T$, H/T, or C. $(F-F_f)/T$, H/T, C in [I. Rot.] and $[CH_3]$ are the restricted rotation functions calculated by the writer[10] in 1937.

[9] All data are from Sponer, *Molekulspektren* (Julius Springer, Berlin, 1935) except for CH_2Cl_2 from Corin and Sutherland, Proc. Roy. Soc. London **A165**, 43 (1938), and $(CH_2)_2$ from Bonner, J. Am. Chem. Soc. **58**, 34 (1936).

[10] Pitzer, J. Chem. Phys. **5**, 469 (1937).

TABLE V. *Numerical values for some of the terms in Table IV (units: cal. per degree).*

T	$F_0(T)$	[C−C$_{str}$]	[C−C$_{bend}$]	[I. Rot.]	[CH$_3$]	[CH$_2$]	[CH]	ISOBUTANE* CORR.	NEO-PENTANE* CORR.
				CONTRIBUTIONS TO $(H_0^0-F_T^0)/T$					
298.1	49.55	0.76	1.27	2.86	0.89	0.04	0.01	0.00	−1.39
400.	51.89	.80	1.57	3.35	1.39	.14	.05	− .19	−1.80
500.	53.67	.86	1.84	3.76	1.91	.30	.13	− .32	−1.95
600.	55.11	.93	2.07	4.10	2.47	.52	.23	− .36	−2.05
800.	57.40	1.11	2.50	4.64	3.60	1.08	.50	− .45	−2.20
1000.	59.17	1.29	2.85	5.07	4.79	1.71	.81	− .60	−2.30
1500.	62.40	1.71	3.51	5.81	7.54	3.37	1.63	− .59	−2.16
				CONTRIBUTIONS TO $(H_T^0-H_0^0)/T$					
298.1	7.95	0.08	0.91	1.57	1.38	0.19	0.07	−0.73	−1.39
400.	7.95	.20	1.13	1.76	2.04	.54	.23	− .60	−1.16
500.	7.95	.34	1.27	1.85	2.73	.99	.46	− .50	− .90
600.	7.95	.47	1.37	1.89	3.39	1.47	.72	− .37	− .55
800.	7.95	.71	1.51	1.91	4.62	2.40	1.18	− .27	− .11
1000.	7.95	.89	1.60	1.86	5.73	3.27	1.61	− .22	+ .11
1500.	7.95	1.19	1.72	1.70	7.82	4.94	2.46	+ .07	+ .41

* The empirical corrections for isobutane and neopentane are to be added (algebraically) whenever a carbon atom is bonded to three or four other carbons, respectively. See text discussion.

groups. These are given in Table III, together with the data from simple molecules on which they are based.

The contributions from these vibration frequencies are easily calculated by the usual methods.

Before summarizing these data again a few additional numerical values will be adopted. An effective mass of a CH_2 group was obtained by calculating the product $[M^3I_1I_2I_3]$ for propane, both neglecting and considering the hydrogens. The effective mass of 18.6 which made both products equal will be used. This value is as high as it is because of the relatively large contribution of the hydrogens to the moments of inertia. The C−C bond distance will be taken as 1.54A and the tetrahedral angles assumed. The force constants have already been given; the potential barrier V_0 will be given the value 3600 cal. per mole. This may be regarded as estimated from simple molecules[11] or determined from the experimental data considered later. The steric interaction energy a will be taken as 800 cal. and was determined from the data considered below. In order to calculate the internal rotation contribution of a methyl group, the same 3600 cal. potential will be used and a reduced moment of inertia I_r equal to 5×10^{-40} g cm.^{2}

Table IV gives the final formula. It is expressed as the sum characteristic of a thermodynamic function rather than the partition function product. The form of each term is given for the functions $(-F/T)$, (H/T), and C. The entropy S is the sum of the first two.

Numerical values for certain of the terms in Table IV are listed in Table V for a series of temperatures. In addition to their use in calculations for hydrocarbons, it seems likely that these data may be of value when the method is extended to alcohols and other molecules derivable from the hydrocarbons.

COMPARISON WITH OBSERVED NORMAL PARAFFIN ENTROPIES

We are now ready to calculate the entropies of the normal paraffins for comparison with experiment. Of all the constants appearing in Table IV only two can be regarded as adjustable to fit the data, V_0 and a. The former was actually assigned the value 3600 cal. per mole from comparison with simpler molecules, and then it was found that a value of 800 cal. for a gave a good fit with the experimental entropies of *n*-butane[12] and *n*-heptane.[1] The agreement might be slightly improved by lowering V_0 and raising a, however, this seems improbable on other grounds and the present constants give agreement within the

[11] Pitzer, Chem. Rev. **27**, August (1940).

[12] Aston, private communication, $S°_{272.6}=72.0$ cal. per degree for gaseous *n*-butane.

experimental errors. For further comparison we have the entropies of the other normal paraffins as measured by Parks, Huffman, and co-workers,[13] which involve extrapolations below 90°K. The good agreement between Parks' extrapolated entropy at 90°K and the writer's experimental value for *n*-heptane suggests that the extrapolations for the other normal paraffins are probably about right.[14] For conversion to the gas state various data were used. The values of Parks, Shomate, Kennedy, and Crawford[15] were used for butane, the heat of vaporization of Griffiths and Awberry[16] for pentane, and the vapor pressure-temperature data[17] for the others.

Table VI summarizes these results, and includes the data on steric repulsions used in the computations.

The good agreement shown in Table VI certainly gives no reason to doubt the picture here set up, and suggests that general thermodynamic functions calculated by this method for various temperatures will be of considerable value. Such results will be presented elsewhere.[11] On the other hand, approximations have been made such that the values of the various molecular constants which give correct entropies may not be exactly the true ones. The treatment is an approximate derivation from statistical mechanics based on an admittedly oversimplified picture of the molecules. However, the errors will not change greatly from one molecule to a similar one; consequently these equations can be used empirically with expectation of considerable accuracy.

TABLE VI. *Molal entropies of the normal paraffin hydrocarbons in the gaseous state.*

SUBSTANCE	NUMBER OF POSITIONS WITH E_i (STERIC): 0	a	$2a$	$3a$	$4a$	$5a$	∞	$S^0_{298.1}$ (cal./deg.) calc.	obs.*
Butane	1	2	0	0	0	0	0	74.17	73.7
Pentane	1	4	2	0	0	0	2	83.27	82.2
Hexane	1	6	8	2	0	0	10	92.41	92.3
Heptane	1	8	18	12	2	0	40	101.54	101.3
Octane	1	10	32	38	16	2	144	110.67	110.0
Δ per CH_2	—	—	—	—	—	—	—	9.13	

* These observed entropies are probably accurate to within about 1.0 cal./deg. The more accurate values for butane[12] and heptane[1] at their boiling points were used to fix a parameter in the formula for calculation. ($S^0_{371.5}$ obs. 111.78±0.3, calc. 111.6 for heptane; $S^0_{272.6}$ obs. 72.0, calc. 72.1 cal. per degree for butane.)

ENTROPIES OF BRANCH CHAIN PARAFFINS

The present lack of knowledge of force constants and vibration frequencies for the branch chain paraffins prevents calculations of even the degree of approximation attained for the normal series. Even so, it seems that the formulas developed in the preceding section should serve to give rough estimates, of value until such time as calculations of greater certainty can be made. Only one accurate experimental entropy is available, that of 2,2,4-trimethylpentane.[1] The long extrapolation from 0 to 90°K needed in all other cases appears to be a doubtful procedure, except in a series of very similar compounds such as the straight chain paraffins.

In adapting the formulas of Table IV we note that a side chain carbon atom attached in the middle of a straight chain has the usual bond stretching degree of freedom. The other two degrees of freedom are of a bond bending nature. Thus one $[C-C_{str}]$ and two $[C-C_{bend}]$ terms should be added. The force constant in the latter is not necessarily the same, however. Vibration frequencies for the hydrogen of a CH group have been given. Steric factors must be considered as before, but are not necessarily as simple. The possibility of symmetry in the skeletal internal rotations, for example of tertiary butyl groups, must also be thought about.

If an entropy is calculated for 2,2,4-trimethyl pentane using the same force constants and potential barriers as for the normal paraffins, the result is somewhat too large. However, a potential barrier well over 4000 cal. was found for the simple highly branched molecule tetramethyl methane[11] as compared to 3300 for propane and less than 3000 for ethane. Also the vibration frequencies for isobutane and tetramethyl methane suggest higher bending force constants. As a simple way of correcting for these factors, the thermodynamic functions were calculated for isobutane and neopentane (tetramethyl methane) by these approximate methods and with the more exact method and constants available for

[13] Parks and Huffman, *Free Energies of Some Organic Compounds* (The Chemical Catalog Co., New York, 1932).
[14] This refers to Parks' original values, not to possible revised ones suggested by Parks, Shomate, Kennedy, and Crawford, reference 15.
[15] Parks, Shomate, Kennedy and Crawford, J. Chem. Phys. **5**, 359 (1937).
[16] Griffiths and Awberry, Proc. Phys. Soc. London **44**, 121 (1932).
[17] Egloff, *Physical Constants of Hydrocarbons*, Vol. 1 (Reinhold Publishing Company, New York, 1939).

TABLE VII. *Molal entropies of the branch chain paraffins together with data used in their calculation.*†

SUBSTANCE	n_1	n_2	n_3	n_4	n_5	n_6	n_7	NO. OF POSITIONS WITH ENERGY: 0	a	$2a$	$3a$	$4a$	∞	σ	$S^\circ_{298.1}$ (cal./deg.) calc. (gas)	exp. (liq.)
2-methyl butane	4	4	1	3	1	1	0	2	0	1	0	0	0	1	82.0	60.8
2,2-dimethyl butane	5	6	1	4	1	0	1	1	0	0	0	0	0	1	85.7	64.4
2,3-dimethyl butane	5	6	1	4	0	2	0	1	0	2	0	0	0	2	86.5	—
2-methyl pentane	5	5	2	3	2	1	0	2	0	3	0	0	4	1	90.1	69.9
3-methyl pentane	5	5	2	3	2	1	0	2	0	2	0	2	3	1	90.0	—
2,2,3-trimethyl butane	6	8	1	5	0	1	1	1	0	0	0	0	0	1	92.3	64.8
2,2-dimethyl pentane	6	7	2	4	2	0	1	1	0	0	0	0	2	1	93.4	68.1
2,3-dimethyl pentane	6	7	2	4	1	2	0	4	0	0	0	0	5	1	98.8	72.4*
2,4-dimethyl pentane	6	7	2	4	1	2	0	2	0	0	0	2	5	2	94.7	69.7
3,3-dimethyl pentane	6	7	2	4	2	0	1	5	0	2	0	0	2	2	95.4	70.1
3-ethyl pentane	6	6	3	3	3	1	0	11	0	0	0	0	16	3	98.3	74.6
2-methyl hexane	6	6	3	3	3	1	0	2	4	3	4	0	14	1	99.5	75.3
3-methyl hexane	6	6	3	3	3	1	0	4	4	4	0	0	15	1	101.3	74.0*
2,2,3,3-tetramethyl butane	7	10	1	6	0	0	2	1	0	0	0	0	0	6	94.1	61.4 (solid)
2,2,4-trimethyl pentane	7	9	2	5	1	1	1	2	0	0	0	0	1	1	101.4	75.2

† The experimental entropies are for the liquid except as noted. All are from Parks and Huffman (reference 13) except 2,2-dimethyl butane and 2-methyl pentane which are from Stull (J. Am. Chem. Soc. **59**, 2726 (1937)). Those values designated by * are especially uncertain; the others are probably self-consistent to within one or two cal. per degree and somewhat low. The substances marked by * are, interestingly, also the two cases where optical isomers occur. The calculated values include an R ln 2 term to account for this fact.

such simple molecules.[11] The differences which are given in Table V, can then be applied as corrections whenever a carbon atom of a complex molecule is bonded to three or four other carbons respectively. On this basis the entropy of 2,2,4-trimethyl pentane is within about one cal. per degree of the observed value. Further refinements would not be justified at present.

The results for all branch chain paraffins through the heptanes and for two octanes are given in Table VII. Therein the n's refer to Table IV except n_7 which is the number of carbon atoms bonded to four other carbons, hence the number of "neopentane corrections." The number of carbons bonded to three others is n_6, also the number of *CH* groups.

The energies for the various internal rotation minima were assigned values in terms of the parameter a of the normal paraffins. This somewhat arbitrary procedure was carried out with the aid of the "Fisher-Hirshfelder" models which approximate proportional atomic sizes.

For rough comparison the available experimental entropies are listed, even though they involve uncertain extrapolations below 90°K. Values are given for the liquids since vaporization data are not available in most cases. On the whole the calculated and experimental values show remarkably similar variations and their differences are quite reasonable for entropies of vaporization.

Finally it may be mentioned that the heat capacities in the gas phase, calculated for *n*-heptane and 2,2,4-trimethylpentane, are in agreement with preliminary experimental values obtained recently by the writer.[1]

Theory of Depolymerization of Long Chain Molecules*

ELLIOTT W. MONTROLL AND ROBERT SIMHA
Department of Chemistry, Columbia University, New York, New York

(Received May 22, 1940)

A theory of depolymerization of long chain molecules is developed on a statistical basis. It is assumed that all bonds connecting monomeric elements in the system have the same probability of being broken regardless of their position in a given polymer and regardless of the size of the polymer in which they are found. Expressions are derived for the distribution of molecular sizes in the depolymerized system as a function of the initial chain length and the average number of bonds split per molecule. Also, relationships are established between the average molecular weight of the degraded product and the average number of bonds split per molecule. Experiments on the acetolytic degradation of cellulose acetate are briefly discussed.

INTRODUCTION

IN recent years several attempts have been made to analyze the mechanism of formation of high polymers[1] and that of the reverse process, the depolymerization of long chain molecules. H. Hopff, H. Mark, and K. H. Meyer[2] investigated the hydrolysis of starch and cellulose and established a first approximation for the mechanism of these reactions. K. Freudenberg and W. Kuhn[3] extended these investigations and gave the first theoretical treatment; recently P. J. Flory,[4] H. Mark and R. Simha,[5] and W. H. Durfee and Z. I. Kertesz[6] developed a series of formulae for long chain building and cutting processes, respectively, from probability considerations.

While the degradation of simple molecules can be treated as a quantum-mechanical problem,[7] the kinetics of depolymerization of very long molecules (100 or more basic units) seems to be more suited to a statistical treatment. A complete study of depolymerization has two aspects; the time variation of the degree of depolymerization and the distribution of various chain lengths at a given time for a given degree of depolymerization and a given initial chain length. Here the size distribution at a given time will be analyzed as a function of the average molecular weight of the degradation product under the following assumptions:

1. All initial molecules have the same molecular weight. This condition could be dropped by introducing a suitable distribution. However, it would not change the essential features of the following considerations.
2. The accessibility to reaction of a bond in a given chain is independent of its position in the chain and independent of the length of its parent chain.
3. All chains in the mixture are equally accessible to reaction.

The first part of assumption (2) is probably not correct for end bonds, and in short chains the second part of (2) may not be satisfied; however, in long polymers these assumptions seem reasonable. With the above restrictions Kuhn has studied the distribution problem, but he also assumed that the initial chains were infinitely long compared with the degradation products. In the following a statistical treatment for finite chain lengths will be given.

Fundamental units in a long chain molecule (for example, glucose groups in a cellulose molecule) will be called monomeric elements and t monomeric elements connected by $t-1$ bonds will be defined as a t-mer.

* Publication assisted by the Ernest Kempton Adams Fund for Physical Research of Columbia University.

[1] R. E. Burk, *Polymerization* (Reinhold Publishing Company, New York, 1937); H. Dostal, H. Mark, and R. Raff, Ind. Eng. Chem. **29**, 595 (1937).

[2] K. H. Meyer, H. Hopff and H. Mark, Ber. **62**, 1103 (1929). See also R. O. Herzog and O. Kratky, Naturwiss. **18**, 735 (1930); M. L. Wolfrom, E. N. Lassettre, D. R. Myers and J. C. Sowden, J. Am. Chem. Soc. **61**, 1072, 2172 (1939).

[3] K. Freudenberg, F. Bolz, E. Braun, W. Dürr and G. Steinbrunn, Ann. **460**, 288 (1928); Ber. **63**, 1510 (1930); W. Kuhn, Ber. **63**, 1503 (1930).

[4] P. J. Flory, J. Am. Chem. Soc. **58**, 1877 (1936).

[5] H. Mark and R. Simha, Trans. Faraday Soc. **36**, 611 (1940).

[6] W. H. Durfee and Z. I. Kertesz, J. Am. Chem. Soc. **62**, 1196 (1940).

[7] See for example C. N. Hinshelwood, *Kinetics of Chemical Change* (Oxford University Press); R. E. Burk, reference 1; C. A. Coulson, Proc. Roy. Soc. A, **164**, 383 (1938); **169**, 413 (1939); J. E. Lennard-Jones and C. A. Coulson, Trans. Faraday Soc. **35**, 811 (1939).

Mathematical Development

In this section formulae will be derived for the fraction of monomeric elements involved in t-mers and the fraction of t-mers in a degradation product as functions of the total number of bonds split and of the initial chain lengths of the depolymerized material. First the theory of the breaking of single molecules will be developed. Then using this and taking into account the distribution of breaks in the various chains, the above mentioned formulae will be derived.

Suppose a system of N long chain molecules, each of which is composed of $p+1$ monomeric elements, is exposed to a depolymerization process that breaks R bonds of the system in a given time. If r bonds of one of the molecules are broken, the breaks can occur in

$$\binom{p}{r}=\frac{p!}{(p-r)!r!}$$

different ways. Since r cuts imply the formation of $r+1$ chains and since the number of monomeric elements in a molecule is conserved during the reaction, the probability of n_1 monomers, n_2 dimers, $\cdots$, n_s s-mers, $\cdots$ being formed is

$$\frac{(r+1)!}{\prod_s n_s!}\Big/\binom{p}{r},$$

where $\sum_s n_s=r+1$ and $\sum_s sn_s=p+1$. The expected fraction, f_{tr}, of monomeric elements contained in t-mers after r cuts have been made is $tn_t/p+1$ multiplied by the probability given above and summed over all possible combinations of the n_s's and over all values of n_t compatible with the original chain length, i.e.

$$f_{tr}=\frac{t}{p+1}\binom{p}{r}^{-1}\sum_{n_t\le(p+1/t)}\sum_{\{n_s\}}\frac{(r+1)!}{(n_t-1)!\prod_s{}' n_s!}. \quad (1)$$

The summation over the set $\{n_s\}$ is subjected to the auxiliary conditions

$$n_t+\sum_s{}' n_s=r+1;\quad tn_t+\sum_s{}' sn_s=p+1$$

and the ($'$) on some of the sums and products indicates that n_t is not included in the operation. Using the expression for the sum derived in the appendix it follows that[8]

$$f_{tr}=t\binom{p-t}{r-1}\Big/\binom{p+1}{r+1}. \quad (2)$$

In the depolymerization process the original molecules may be split in any number from zero to p places, so we must now consider the distribution of splits in the original system. The number of ways of making R cuts in N chains is $\binom{Np}{R}$, and the number of ways of cutting one chain of $p+1$ monomeric elements in r places and the other $N-1$ chains in $R-r$ places is $\binom{p}{r}\binom{Np-p}{R-r}$. Therefore the probability of any particular chain being cut in r places (which is also the fraction of chains cut in r places) is

$$f_r=\binom{p}{r}\binom{Np-p}{R-r}\Big/\binom{Np}{R}. \quad (3)$$

If we let $r_0=R/N$ be the average number of cuts per molecule and apply Stirling's theorem for large factorials, $n!=n^{n+1}e^{-n}\sqrt{(2\pi)}$, neglecting p with respect to Np and r with respect to R, we have

$$f_r=\binom{p}{r}\left(\frac{p-r_0}{p}\right)^p\left(\frac{r_0}{p-r_0}\right)^r. \quad (4)$$

Hence the total fraction of monomeric elements involved in t-mers when an average of r_0 cuts per molecule has been made in N molecules of $p+1$ monomeric elements is given by

$$F_t=\sum_{r=0}^{p-t+1}f_{tr}f_r=\left(\frac{p-r_0}{p}\right)^p\sum_{r=1}^{p-t+1}t\frac{(r+1)}{(p+1)}\times\frac{(p-t)!}{[p-t-(r-1)]![r-1]!}\left(\frac{r_0}{p-r_0}\right)^r$$

or

$$F_t\left(p,\frac{r_0}{p}\right)=\frac{t}{p+1}\left(1-\frac{r_0}{p}\right)^{t-1}\times\left[\frac{2r_0}{p}+(p-t)\left(\frac{r_0}{p}\right)^2\right]\quad t\le p.$$

[8] This formula also follows implicitly from the work of Mark and Simha (reference 5), and Durfee and Kertesz (reference 6) in their treatment of depolymerization assuming that all molecules in the system have the same number of breaks at any stage of the reaction.

The fraction of monomers involved in chains of length $p+1$ is evidently

$$F_{p+1}\left(p, \frac{r_0}{p}\right)=\left(1-\frac{r_0}{p}\right)^p. \tag{5}$$

Defining the average degree of depolymerization, α, as the average fraction of bonds cut in a molecule

$$\alpha=r_0/p;$$

$$F_t(p, \alpha)=\frac{\alpha t(1-\alpha)^{t-1}}{(p+1)}[2+(p-t)\alpha] \quad t\leq p \tag{6}$$

$$F_{p+1}(p, \alpha)=(1-\alpha)^p.$$

If $p\alpha\gg 2-t\alpha$ (i.e., for high degrees of depolymerization) and if it is assumed that p is infinite (i.e., $p/p+1=1$), (6) reduces to Kuhn's[3] result; $F_t=\alpha^2 t(1-\alpha)^{t-1}$.

Since

$$F_t(p, \alpha)=tN_t(p, \alpha)/N(p+1), \tag{7}$$

where $N_t(p, \alpha)$ is the number of t-mers in the system when an average of r_0 cuts per molecule have been made in N molecules of $(p+1)$ monomeric elements,

$$N_t(p, \alpha)=N\alpha(1-\alpha)^{t-1}[2+(p-t)\alpha] \quad t\leq p$$
$$N_{p+1}(p, \alpha)=N(1-\alpha)^p. \tag{8}$$

Also, the fraction of t-mers, $n_t(p, \alpha)$, is

$$n_t(p, \alpha)=\frac{N_t}{\sum_t N_t}=\frac{\alpha(1-\alpha)^{t-1}}{(1+\alpha p)}[2+(p-t)\alpha] \quad t\leq p$$
$$n_{p+1}=(1-\alpha)^p/1+\alpha p. \tag{9}$$

Determination of Molecular Size Distribution from Average Molecular Weight of Degraded Products

Most experimental methods of determining molecular weights of macromolecular materials are incapable of detecting heterogeneity and, therefore, inevitably give average values. It can be shown[9] that the average molecular weight obtained by any procedure which in effect involves the counting of molecules (such as osmotic pressure, vapor pressure, chemical analysis, etc.) is given by the expression for the "number average" molecular weight

$$M_n=\sum N_t M_t/\sum N_t. \tag{10}$$

(M_t is the molecular weight of the tth species of which there are N_t). The average value for any experiment depending on the weights of the molecules (e.g., Staudinger's viscosity method) is given by the "weight average" molecular weight

$$M_w=\sum N_t M_t^2/\sum N_t M_t. \tag{11}$$

For a homogeneous material $M_n=M_w$ and for a heterogeneous material $M_n\leqslant M_w$, the magnitude of the difference increasing in general with the spread of molecular weights in the mixture. If M_0 is the molecular weight of a monomeric element,

$$M_n=M_0\sum tN_t/\sum N_t=M_0\sum F_t/\sum F_t/t. \tag{12}$$

Using the expressions derived in the appendix for the various $\sum_t t^n F_t$,

$$M_n(p, \alpha)/M_0=(p+1)/(1+\alpha p) \tag{13}$$

as expected, for $1+\alpha p$ is the number of segments cut on the average from a single chain. M_w can also be expressed as a function of α and p;

$$M_w(p, \alpha)=\frac{\sum N_t M_t^2}{\sum N_t M_t}=M_0\frac{\sum tF_t}{\sum F_t}, \tag{14}$$

and again applying the results of the appendix for the appropriate sums

$$\frac{M_w(p, \alpha)}{M_0}=\frac{\alpha^2(1+p)+2(1-\alpha)[(1-\alpha)^{p+1}+\alpha(p+1)-1]}{\alpha^2(1+p)}. \tag{15}$$

When αp is small

$$\frac{M_w(p, \alpha)}{M_0}=1+p(1-\alpha)\left\{1-\frac{\alpha(p-1)}{3}+O[(\alpha p)^2]\right\}, \tag{15a}$$

and when α and p are so large that $(1-\alpha)^{p+1}$ becomes negligibly small

$$\frac{M_w}{M_0}=1+\frac{2(1-\alpha)[\alpha(1+p)-1]}{\alpha^2(1+p)}. \tag{15b}$$

[9] E. O. Kraemer and W. D. Lansing, J. Phys. Chem. **39**, 153 (1935); Kern, Ber. **68**, 1439 (1935). See also Kraemer's article in *The Ultracentrifuge* (edited by Svedberg and Pedersen, Oxford Press, 1940), p. 343.

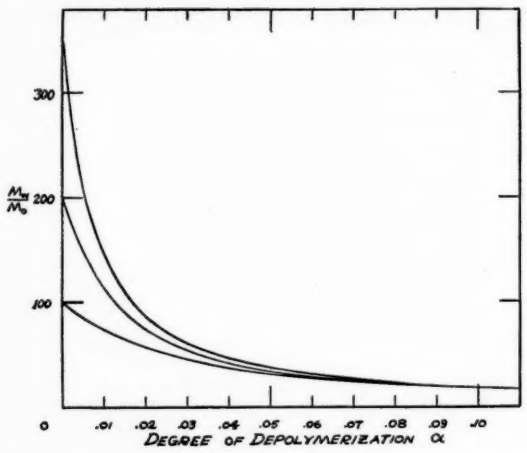

FIG. 1. Variation of degree of depolymerization with "weight average" molecular weight for various initial chain lengths.

If M_w/M_0 or M_n/M_0 can be determined experimentally and if the initial chain lengths are known, either (15) or (14) can be solved for α. Once the average degree of depolymerization, α, is known the problem of finding the molecular size distribution is completed by substitution of α into (6), (8) and (9).

If, on the other hand the number of bonds broken in the depolymerization process can be determined (as is often possible by chemical means) α is the observable quantity and M_n/M_0 (or M_w/M_0) can be predicted by (13) (or (15)).

DISCUSSION

In case M_n is a measurable quantity α is easily determined as the root of the linear Eq. (13), and when one measures M_w at very low or fairly high degrees of depolymerization the determination of α is simple algebra using (15a) or (15b). For intermediate stages of degradation an algebraic solution of (15) is tedious; however, by plotting M_w/M_0 as a function of α as is done in Fig. 1, α can be read off the graph for an observed M_w/M_0. With a knowledge of α one can follow the progress of the reaction by using the distribution curves plotted in Fig. 2.[10] These curves emphasize the fact that the distribution becomes sharper about the maximum F_t as depolymerization approaches completion.

From an experimental standpoint it is sometimes more desirable to know the number of monomeric elements which exist as components of chains with "about t links" (i.e., in chains with lengths between $t-\epsilon$ and $t+\epsilon$, where ϵ is 5 or 10, etc., depending on the experiment) than it is to know F_t. This function can easily be determined by finding the area under the appropriate F_t curve for t between $t-\epsilon$ and $t+\epsilon$, or by evaluating the integral $\int_{t-\epsilon}^{t+\epsilon} F_t dt$.

The length, $t_{\max}$, of the chains in which a monomeric element is most likely to be found is obtained by setting $(\partial/\partial t)F_t(p, \alpha)=0$, and solving the resulting equation for t. This gives

$$t_{\max}=-1/\log(1-\alpha)+(1/\alpha+p/2)\times\{1-\sqrt{1+1/[(1/\alpha+p/2)\log(1-\alpha)]^2}\}. \quad (16)$$

Since $0\leqslant 1/[(1/\alpha+p/2)\log(1-\alpha)]^2\leqslant 1$ (0 for $\alpha=1$ and 1 for $\alpha=0$) the binomial theorem is applicable and

$$t_{\max}=-\frac{1}{\log(1-\alpha)}\left[1+\frac{1}{2(1/\alpha+p/2)\log(1-\alpha)}-\frac{1}{4(1/\alpha+p/2)^3\log^3(1-\alpha)}+\cdots\right]. \quad (16a)$$

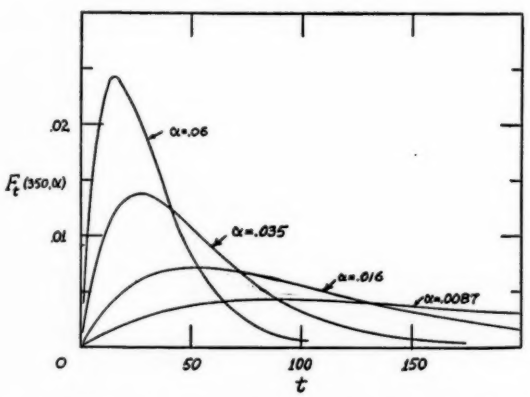

FIG. 2. Fraction of monomeric elements involved in t-mers for various α when $p+1=350$.

[10] These curves are derived from experiments on the acetolytic degradation of cellulose acetate reported by Mark and Simha (reference 5). A highly homogeneous initial material of 350 monomeric elements was depolymerized and at several stages of the reaction the mean degree of polymerization was measured by Staudinger's viscosity method to be 158, 100, 54, and 31. As previously discussed these numbers represent the fraction M_w/M_0; therefore from the $p+1=350$ curve in Fig. 1, the corresponding degrees of depolymerization are 0.0087, 0.0164, 0.035, and 0.06. Figure 2 shows the theoretical distribution of monomeric elements among the various t-mers at these degrees of depolymerization.

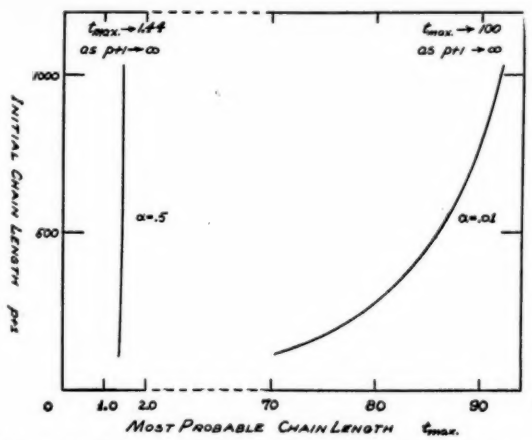

FIG. 3. Variation in $t_{\max}$ with initial chain length at constant degrees of depolymerization.

As the chain length of the initial material becomes great, i.e., as $p+1 \to \infty$,

$$t_{\max} \sim -1/\log(1-\alpha). \tag{16b}$$

As the degree of depolymerization, α, becomes small, $\log(1-\alpha) \sim -\alpha$ therefore

$$t_{\max} \sim \frac{1}{\alpha}\left[1 - \frac{1}{2\left(1+\frac{p\alpha}{2}\right)} + \frac{1}{4\left(1+\frac{p\alpha}{2}\right)^3} \cdots\right]. \tag{16c}$$

If one plots (Fig. 3) $t_{\max}$ *vs.* the number of monomeric elements in the original molecules for various values of α there is a shift of $t_{\max}$ to the left as $p+1$ decreases. However at high degrees of depolymerization this shift becomes less pronounced, thus suggesting that the distribution functions tend to become independent of the initial chain length as the degradation process nears completion.

In conclusion the authors take pleasure in thanking Professor Joseph E. Mayer for his valuable suggestions and discussions.

APPENDIX

I. **Summation of**

$$\sum_{n_t} \sum_{\{n_s\}}' \frac{(r+1)!\,t}{\Pi_s' n_s!(n_t-1)!}$$

under the restrictions

$$n_t + \sum_s' n_s = r+1 \quad \text{and} \quad t n_t + \sum_s' s n_s = p+1.$$

According to the multinomial theorem

$$\left(\sum_s x_s^s z^s\right)^{r+1} = (r+1)! \sum_{(\Sigma n_s = r+1)} \prod_s \frac{(x_s^s z^s)^{n_s}}{n_s!}.$$

Therefore

$$x_t \frac{\partial}{\partial x_t}\left(\sum x_s^s z^s\right)^{r+1} = (r+1)! \sum_{(\Sigma n_s = r+1)} \frac{t(x_t^t z^t)^{n_t}}{(n_t-1)!} \prod_s' \frac{(x_s^s z^s)^{n_s}}{n_s!}$$

$$= (r+1) t x_t^t z^t \left(\sum x_s^s z^s\right)^r,$$

and

$$\sum_{n_t} \sum_{\substack{\{n_s\} \\ \{n_t + \Sigma' n_s = r+1 \\ t n_t + \Sigma' s n_s = p+1}}' \frac{(r+1)!\,t}{(n_t-1)!\Pi_s' n_s!} = \lim_{x_s \to 1} \{\text{coeff. of } z^{p+1} \text{ in } (r+1) t x_t^t z^t \left(\sum x_s^s z^s\right)^r\}$$

$$= \text{coeff. of } z^{p+1} \text{ in } \frac{(r+1) t z^{t+r}}{(1-z)^r}$$

$$= t(r+1)\binom{p-t}{r-1}. \tag{A}$$

II. Calculation of $\overline{l^n}$ with respect to the distribution function $F_l(p, \alpha)$.
Let us define

$$\overline{l^n}=\sum_{l=1}^{p+1} l^n F_l(p,\alpha)=(p+1)^n\beta^p+\sum_{l=1}^{p}\frac{\alpha l^{n+1}\beta^{l-1}}{p+1}[2+(p-l)\alpha]$$

$$=(p+1)^n\beta^p+\frac{\alpha}{\beta(p+1)}\{(2+\alpha p)\sum_{l=1}^{p} l^{n+1}\beta^l-\alpha\sum_{l=1}^{p} l^{n+2}\beta^l\}$$

and $\beta=1-\alpha$. If

$$I_0(\beta)=\sum_{l=1}^{p}\beta^l=\frac{\beta-\beta^{p+1}}{1-\beta},$$

it is obvious that*

$$I_n(\beta)=\sum_{l=1}^{p} l^n\beta^l=\left(\beta\frac{\partial}{\partial\beta}\right)^n I_0(\beta)=\left(\beta\frac{\partial}{\partial\beta}\right)^n\left(\frac{\beta-\beta^{p+1}}{1-\beta}\right).$$

Therefore

(B) $$\overline{l^n}=(p+1)^n\beta^p+\frac{\alpha}{\beta(p+1)}\left[(2+\alpha p)-\alpha\beta\frac{\partial}{\partial\beta}\right]\left(\beta\frac{\partial}{\partial\beta}\right)^{n+1}\left(\frac{\beta-\beta^{p+1}}{1-\beta}\right).$$

Some special cases are

(a) $$n=-1,$$

$$\overline{l^{-1}}=\sum_{l=1}^{p+1}\frac{F_l(p,\alpha)}{l}=\sum_{l=1}^{p}\frac{\beta^{l-1}\alpha}{(p+1)}[2+(p-l)\alpha]+\frac{\beta^p}{p+1}$$

$$=\frac{\beta^p}{p+1}+\frac{\alpha(2+p\alpha)}{\beta(p+1)}\sum\beta^l-\frac{\alpha^2}{\beta(p+1)}\sum l\beta^l$$

$$=\frac{\beta^p}{p+1}+\frac{(2+\alpha p)(1-\beta^p)}{p+1}-\frac{1-(p+1)\beta^p+p\beta^{p+1}}{p+1},$$

or

(C) $$\overline{l^{-1}}=(1+\alpha p)/(p+1).$$

(b) $$n=0,$$

$\overline{l^0}=\sum_l F_l=1$, since F_l is the fraction of monomers in l-mers. (This can easily be verified by direct

---

* $\left(\beta\frac{\partial}{\partial\beta}\right)^n=\beta\frac{\partial}{\partial\beta}\cdot\beta\frac{\partial}{\partial\beta}\cdots\beta\frac{\partial}{\partial\beta}$; for example $\left(\beta\frac{\partial}{\partial\beta}\right)^2=\beta\frac{\partial}{\partial\beta}\cdot\beta\frac{\partial}{\partial\beta}=\beta^2\frac{\partial^2}{\partial\beta^2}+\beta\frac{\partial}{\partial\beta}$.

calculation).

(c) $n=1$,

$$\bar{l}^1=\sum lF_l(p,\alpha)$$

$$=\beta^p(p+1)+\frac{\alpha}{\beta(p+1)}\left[(2+\alpha p)-\alpha\beta\frac{\partial}{\partial\beta}\right]\left[\beta\frac{\partial}{\partial\beta}\right]\left[\frac{\beta-(p+1)\beta^{p+1}+p\beta^{p+2}}{(1-\beta)^2}\right]$$

$$=\frac{(1+p)-2\beta-\beta^2(1+p)+2\beta^{2+p}}{\alpha^2(p+1)}$$

$$(D_1)\qquad =1+2(1-\alpha)[(1-\alpha)^{p+1}+\alpha(1+p)-1]/\alpha^2(p+1)$$

$$(D_2)\qquad =1+p(1-\alpha)\left\{1-\frac{\alpha(p-1)}{3}+\alpha^2\frac{(p-1)}{3}\frac{(p-2)}{4}-\cdots\right\}.$$

SEPTEMBER, 1940 JOURNAL OF CHEMICAL PHYSICS VOLUME 8

The Role of Heat Conduction in Thermal Gaseous Explosions

O. K. Rice
University of North Carolina, Chapel Hill, North Carolina

(Received June 17, 1940)

The theory recently developed by Frank-Kamenetzky for thermal explosions in which heat is removed by conduction only, has been applied to the azomethane, ethyl azide and methyl nitrate explosions. A fairly detailed discussion has been given of the experimental results and their relation to the theory. In the case of azomethane and ethyl azide the conclusion is reached that at low pressures thermal conduction as contrasted to convection is an important, if not the exclusive, method of removal of heat from the reacting gas, with deviation appearing at high pressures. As was already concluded by Rice and Campbell, the results appear to indicate that the methyl nitrate explosion is not a thermal explosion. Certain criticisms directed by Frank-Kamenetzky against the determination of the heat of reaction from the induction period, as carried out by Rice and Campbell, have been considered and refuted.

WHEN an exothermal reaction occurs in a reaction flask heat is produced, which tends to increase the temperature of the reacting gas, thus causing the reaction to go faster and produce still more heat. On the other hand, as the temperature of the reacting substance increases, loss of heat takes place through the walls of the vessel. If conditions are such that the rate of loss of heat can become as great as the rate of production of heat, then a steady state is reached. Above a certain pressure at any predetermined temperature, however, it becomes impossible for the heat loss to catch up with the production of heat and an explosion occurs. A theory giving the dependence of the critical explosion pressure (explosion limit) as a function of the temperature, and accounting for the the induction period, i.e., the time required before explosion occurs, has been rather fully developed.[1]

There has, however, been much discussion concerning the mechanism by which heat is removed from the vessel. The question which arises is whether thermal conduction alone is sufficient to account for the rate of loss of heat, or whether convection and turbulence play an important role. It now seems possible to give at least a partial answer to this question through

[1] (a) N. N. Semenoff, Zeits. f. Physik **48**, 571 (1928), (b) A. O. Allen and O. K. Rice, J. Am. Chem. Soc. **57**, 310 (1935), (c) O. K. Rice, A. O. Allen, and H. C. Campbell, *ibid.* **57**, 2212 (1935), (d) A. Appin, J. Chariton, and O. M. Todes, Acta Physicochimica U. R. S. S. **5**, 655 (1936), (e) O. M. Todes, *ibid.* **5**, 785 (1936).

some recent, very interesting work of Frank-Kamenetzky,[2] in which he starts with the assumption that the entire heat loss is due to thermal conduction and derives equations which may be compared with the experimental results. Though he has applied his equations to various experimental data, further consideration of the matter appears to be called for.

1. Theoretical

Let us consider the flow of heat in a spherical flask, designating the distance from the center of the flask as r, and assume that the reaction taking place is unimolecular. We let λ be the heat conductivity of the gas, Q the heat of reaction per mole, n the number of moles per unit volume, and k the unimolecular rate constant (given by the usual Arrhenius equation $k=Ae^{-E/R(T+T_0)}$, where T_0 is the temperature of the furnace outside the reaction flask, and $T+T_0$ the temperature at any point of the reaction vessel). The standard equation for stationary flow (steady temperature) may be obtained by equating the heat conducted away to the heat produced per unit volume, and is

$$-\frac{\lambda}{r^2}\frac{d}{dr}\left(r^2\frac{dT}{dr}\right)=Qnk. \tag{1}$$

As T will in general be much less than T_0, we may write as a first approximation for the rate constant at any point in the flask $k=k_0e^{T/T^*}$, where $T^*=RT_0^2/E$, and $k_0=Ae^{-E/RT_0}$. We introduce the new variable $\zeta=r/r_0$, where r_0 is the radius of the flask, and define the dimensionless parameter

$$\delta=Qnr_0^2k_0/\lambda T^*. \tag{2}$$

Equation (1) can now be written in the form

$$\frac{1}{\zeta^2}\frac{d}{d\zeta}\left[\zeta^2\frac{d(T/T^*)}{d\zeta}\right]=-\delta e^{T/T^*}. \tag{3}$$

This equation must satisfy the boundary condition that $T/T^*=0$ when $\zeta=1$. Under this condition, according to Frank-Kamenetzky, the equation permits of a solution which is everywhere finite only when δ is less than a fixed value. For δ greater than this value no steady state exists, and such a condition must result in explosion. Frank-Kamenetzky has found that this value of δ is 3.32. I have checked this calculation independently and since the details of Frank-Kamenetzky's work[3] are in Russian, and since Harris[4] has recently reported a somewhat different result, it seems worth while to present the calculation.

We simplify Eq. (3) by introducing a new quantity $\phi=-a+T/T^*$, where a is the value of T/T^* when $\zeta=0$. We also set $x=(\delta e^a)^{\frac{1}{2}}\zeta$. Since δ and a are constant in any given case, Eq. (3) is converted into

$$\frac{1}{x^2}\frac{d}{dx}\left(x^2\frac{d\phi}{dx}\right)=-e^{\phi}, \tag{4}$$

which is to be solved under the conditions

$$\phi=0 \text{ when } x=0 \tag{5}$$

and

$$\phi=-a \text{ when } x=(\delta e^a)^{\frac{1}{2}}, \tag{6}$$

the latter corresponding to the condition $T/T^*=0$ when $\zeta=1$. Since ϕ has the general character of a temperature, we know it will have its greatest value at the center of the flask, corresponding to $x=0$, and will decrease uniformly with x. Hence if ϕ is set equal to zero at $x=0$ all values for other points will be negative.

If Eq. (4) is integrated once, we obtain

$$x^2d\phi/dx=-\int_0^x x^2e^{\phi}dx. \tag{7}$$

The integration constant is correct, since both sides of Eq. (7) obviously vanish when $x=0$. If we introduce $F=x^2e^{\phi}$, Eq. (7) becomes

$$(x^2/F)dF/dx=2x-\int_0^x Fdx. \tag{8}$$

This may be solved, for small x, in the usual way by expanding F as a power series (starting with a term in x, since $F=0$ when $x=0$) and equating coefficients. Coefficients of all odd

[2] D. A. Frank-Kamenetzky, Acta Physicochimica U. R. S. S. **10**, 365 (1939).

[3] D. A. Frank-Kamenetzky, Russian J. Phys. Chem. **13**, 738 (1939).

[4] E. J. Harris, Proc. Roy. Soc. London **A175**, 254 (1940).

powers of x turn out to be zero, and we obtain

$$F=b^2x^2-0.1667b^4x^4+2.222\cdot10^{-2}b^6x^6 -2.688\cdot10^{-3}b^8x^8+3.080\cdot10^{-4}b^{10}x^{10} -3.407\cdot10^{-5}b^{12}x^{12}+3.673\cdot10^{-6}b^{14}x^{14} -3.888\cdot10^{-7}b^{16}x^{16}+\cdots, \quad (9)$$

where b is an arbitrary constant. b may be evaluated from the fact that e^{ϕ} becomes equal to 1 when $x=0$. If x is sufficiently small, therefore, F becomes equal to x^2, hence b must have the value 1 in our problem, which shows that F, and hence e^{ϕ} and ϕ are uniquely determined as functions of x by the boundary conditions.

Let us now use a subscript zero to denote values of the various quantities at the surface of the reaction vessel. We have then, as was also shown by Frank-Kamenetzky,

$$F_0=x_0^2e^{\phi_0}=x_0^2e^{-a}=\delta, \quad (10)$$

the last relation coming from Eq. (6). Equation (9) gives us F as a function of x, and this relation is obviously the same as the relation of F_0, or δ, to x_0. x_0 can take any value from 0 to ∞, but no other. To solve the problem at hand, we need only find the largest possible value of F with x between 0 and ∞.

It is found that the coefficients in Eq. (9) appear to approach an almost constant ratio, the ratio of the last two coefficients given being 0.1060. We may, therefore, approximate to the remaining terms of the series by assuming that the last term is simply multiplied by the geometric series $1-0.1060b^2x^2+(0.1060b^2x^2)^2-\cdots$ or $(1+0.1060b^2x^2)^{-1}$. The calculated values, setting $b=1$, are shown as circles in Fig. 1. The crosses give $x^{-1}\int_0^x F dx$, calculated by term by term integration. Slightly beyond $x=2.8$ the series diverges, and the curve has been obtained by extrapolation. The results were verified, first, by noting that integration under the extrapolated curve for F gives the extrapolated value for $x^{-1}\int_0^x F dx$, and, secondly, by then solving for dF/dx from Eq. (8), the results thus obtained agreeing with the value obtained from the slope of the curve for F within about the accuracy with which the tangent can be measured. It is seen that F has a maximum of 3.3, in agreement with Frank-Kamenetzky, when $x=4.0$.

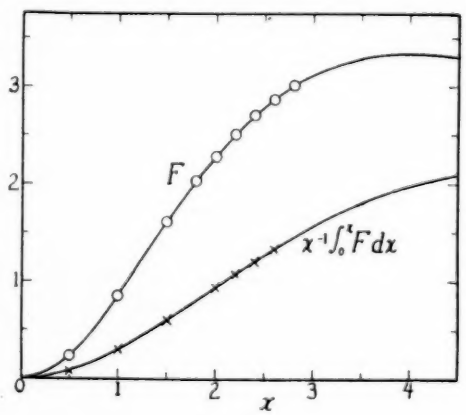

FIG. 1.

TABLE I. *Experimental determination of* δ.

SUBSTANCE AND ABS. TEMP.	P^*, MM	n, MOLES $CC^{-1}\times10^9$	Q, KCAL./MOLE	E, KCAL./MOLE	k_0, SEC.$^{-1}$	δ
Azomethane 645	28	0.696	43	51.2	0.031[a]	7.6
200-cc flask 620	102	2.64	43	51.2	0.0085[b]	8.5
Ethyl azide 553	16	0.463	55	39.0	0.028[c]	6.0
200-cc flask 533	92	2.76	55	39.0	0.0085[c]	11.8
Ethyl azide 563	18.4	0.523	55	39.0	0.053[c]	4.9
50-cc flask						
Methyl nitrate 546	16.5	0.484	6.2	39.5	0.088[d]	0.51

[a] Estimated from Table IV of reference 1c (Note: $k_0=k^*/e$).
[b] Estimated from Table III of reference 1b.
[c] Taken or estimated from Table V of Campbell and Rice, J. Am. Chem. Soc. **57**, 1044 (1935).
[d] Calculated from rate expression given in reference 1d, multiplied by 2.303.

2. APPLICATION TO EXPERIMENTAL DATA

The obvious way to test the theory is to substitute observed values of T_0 and n, corresponding to the explosion limit, in Eq. (2) and evaluate δ. If the theory is right, δ under these circumstances should turn out to be equal to about 3.3.

A number of typical cases are presented in Table I. P^* is the explosion limit, from which n is calculated. The values of Q are those determined by Rice, Allen and Campell,[1c] and Rice and Campbell,[5] or given by Appin, Chariton and Todes.[1d] For λ we have accepted Frank-Kamenetzky's estimate of 10^{-4} cal. deg.$^{-1}$ cm^{-1} sec.$^{-1}$. For a 200-cc flask, $r_0=3.63$ cm; for a 50-cc flask, $r_0=2.29$ cm. The methyl nitrate experiments were done in a 130-cc cylindrical vessel of radius 1.7 cm. The equation for an (infinite) cylindrical vessel, corresponding to Eq. (3) involves the same parameter δ, but with r_0 equal to the radius of the cylinder. According to

[5] O. K. Rice and H. C. Campbell, J. Chem. Phys. **7**, 700 (1939).

Frank-Kamenetzky the critical value of δ in this case is 2.00.

We may first note from Table I that the value of δ for methyl nitrate is about fourfold lower than the theoretical value. This appears to be in accord with the calculations of Frank-Kamenetzky, who shows a difference of about 20° between the temperature calculated for a given explosion limit and that observed. This he considers good agreement; however, although λ may be a little less than 10^{-4}, a fourfold discrepancy in δ is difficult to account for, unless, indeed, the mechanism of the quiet decomposition of methyl nitrate is not that assumed by Appin, Chariton and Todes, so that the value of Q which has been taken is incorrect.* It seems to me that the results are at least consistent with the previously published conclusion of Rice and Campbell that the explosion of methyl nitrate is not a thermal explosion. For it is clear that the theory based on thermal conduction without convection must give an absolute minimum for δ. Any other process operative in causing removal of heat from the reaction vessel can only make an explosion less likely, hence raise the value of n at the explosion limit at a given temperature, and so increase rather than decrease the experimentally determined value of δ at the explosion limit.

In the case of azomethane and ethyl azide at low pressures, the values of δ are about twice the theoretical values.[6] Since by putting δ constant, we obtain from Eq. (2) essentially the same relation for the critical explosion pressure as a function of temperature as is obtained for the simple Semenoff theory, and since azomethane and ethyl azide obey the Semenoff theory at low pressure, the first values of δ given in Table I for both azomethane and ethyl azide should be characteristic of each of these explosions at low pressures. At high pressures the value of δ goes up, as should be sufficiently illustrated by Table I; this is very probably due to increased convection at the higher pressures. The dependence on pressure of the heat loss coefficient of the simple Semenoff theory has been discussed in some detail by Rice and Campbell. The considerable effect of addition of diethyl ether on the explosion limit of ethyl azide can only be explained by an increase in convection, since it seems unlikely that change in the heat conductivity is sufficient to account for it.

The question remains as to whether the difference between the experimental values of δ at low pressures and the theoretical value is due to the effect of convection in increasing the rate at which heat is removed from the reaction vessel, whether it is due to errors in the theory, or whether it arises from errors in evaluating the quantities used in finding δ. One possibility, which is perhaps unlikely, but which should not be overlooked, is that 3.3 is not actually the greatest possible value for δ. The differential equation for a spherical flask is by no means simple, and no proof exists, as far as I am aware, that the function F has only one maximum, or that the maximum found is the largest one.[7] If it is not the largest, another type of steady state could conceivably exist, which still would not result in explosion.

On the other hand there is certainly considerable possibility of error in the values used in evaluating δ. The value used for λ is a pure estimate, and may well be in some error, though judging from other gases of similar complexity, it cannot be very far off. It is quite possible that a more accurate evaluation would give values of

* I have just noted that the rate constants given by Appin, Chariton, and Todes are smaller than those usually defined by a factor of 2.303. This changes the estimate of Q from the induction period to 30 or 40 kcal., rather than 70 or 80 kcal., as given by Rice and Campbell, but this is still much larger than the value from thermochemical data. If Q were 30 or 40 kcal., δ would agree with the theoretical value about as well as in the case of azomethane and ethyl azide, so the induction period data and the calculations given here cannot be said to give entirely independent evidence that the explosion of methyl nitrate is not a thermal explosion.

[6] The statement regarding ethyl azide is in disagreement with Frank-Kamenetzky, references 2 and 3, but apparently in agreement with Harris, reference 4.

[7] It may readily be shown, however, that the value of F at a maximum must be less than 6. Suppose F had reached the value 6 at some point, x_1. If this were true F could not have been less than $6x^2/x_1^2$ for any x less than x_1, for, otherwise, $F/x^2=e^\phi$ would not have been a uniformly decreasing function of x, as we know it is. Since F is thus greater than $6x^2/x_1^2$ for $x<x_1$, if we substitute this value for F in the integral on the right-hand side of Eq. (8) the latter becomes an inequality which may be written

$$dF/dx_1<(F/x_1^2)\int_0^{x_1}(2-6x^2/x_1^2)dx=0.$$

For any higher value of F the derivative must also be less than zero. It is clear then that any maximum value of F must lie below 6.

δ nearer the theoretical value. Also, the fact that a certain amount of gas reacts before explosion takes place, has a tendency to raise the explosion pressure, and so to raise the apparent value of δ. A correction for this effect would be in the right direction, but judging from the work of Rice and Campbell could not be very large.

Finally we must consider the value of Q. Since Frank-Kamenetzky[8] has recently criticized Rice and Campbell's determination from the induction period of ethyl azide, it seems well to review his comments in some detail, although some of these sources of error have already been discussed in our earlier papers. His criticisms, and the answers which may be made to them, are as follows:

1. Theory and experiment both break down near the explosion limit. This is undoubtedly true, but there is no evidence that the breakdown occurs before the limit is very closely approached. The estimated values of Q do not vary systematically with the excess of pressure above the explosion limit, and, in any event, in the work of Rice and Campbell there were runs at pressures considerably above the explosion limit.

2. It is claimed that it is not allowable to neglect the time required to admit the gas to the reaction vessel. The best answer to this criticism seems to be that the value of Q does not show systematic deviations for the different induction periods. It is unfortunate that very large induction periods, which might be expected to have the least error due to this cause, occur close to the explosion limit where other errors possibly enter; however, it is possible to produce appreciable changes in the induction period, even when remaining reasonably far from the explosion limit, by changing the temperature, or adding an inert gas like diethyl ether. In our experiments a two- or threefold change in the induction period was obtained in this way for pressures rather well above the explosion limit. It seems, as a matter of fact, rather probable that somewhat above the explosion limit, the time of entry of the gas becomes less important. For a considerable fraction of the gas must enter almost immediately. Since the induction period varies less rapidly with the pressure the more the explosion limit is exceeded, the delay in entrance of the last fraction of the gas should not have too much effect when the pressure is reasonably far above the explosion limit.

Changing from 6-mm to 12-mm tubing for the connection to the flask did, as noted by Rice and Campbell, change the apparent value of Q for ethyl azide from 42 to 55 kcal. per mole. We felt it probable that we had eliminated the effect of the time of entry of the gas with this larger tubing. It should be noted that complete elimination of the slowness of entry of the gas would only have the effect of further increasing the value obtained for Q, resulting in still larger experimental estimates of δ.

3. The gas is heated somewhat by passage through the tube admitting it to the reaction chamber. For this reason, Frank-Kamenetzky believes it would be better to assume that the gas as it enters the vessel is already at the temperature of the vessel, instead of calculating the time required to heat the gas up from some arbitrarily assumed temperature to the temperature of the reaction vessel, as we have done. In general the time required to heat the gas to the temperature of the flask is, according to the theory, of the same order of magnitude, but usually less than the rest of the induction period after this temperature has been attained. If our procedure were wrong in this respect, the calculated heat of reaction could be incorrect by a factor of not over 2. In defense of our procedure it may be said that runs made just below the explosion limit, with a thermocouple in the flask, quite regularly showed initial cooling. The temperatures observed, it is true, were within 10°, or at most 20°, of the temperature of the flask, but the actual readings could not be very significant as the damping period of the galvanometer used was 2.5 seconds—too large to permit accurate observations in a very short period of time. Even if our calculations overestimated the effect of the preliminary heating of the gas, I feel that the error introduced is considerably less than the factor of 2, which would result if we were entirely incorrect in allowing time for the preliminary heating.

4. Frank-Kamenetzky contends that hydraulic impact and adiabatic compression may have an

[8] D. A. Frank-Kamenetzky, J. Chem. Phys. **8**, 125 (1940).

effect in heating the gas on admission to the reaction vessel. The gases under consideration, however, have such large specific heats that it seems that such effects should be negligible.

In conclusion I may remark that no claim is made that our value of Q is a precision value, but it should be correct within 25 or 30 percent, provided, at least, that the fundamental assumption that the rate of loss of heat from the reaction vessel is proportional to the difference between the temperature inside and outside the flask is correct.

It may be remarked that Harris has also stated that the use of Todes' formula[1] for the induction period with the data on azomethane and ethyl azide yields values of Q about five times lower than those we found, from our own formula. This statement, however, I believe, arises from a misapprehension. In the first place Harris applied Todes' limiting formula which gives the limiting minimum value of the induction period for very high pressures. Our data do not conform to this condition. Also Todes' formula neglects completely the pre-induction period, i.e., the time required to heat the gas to the temperature of the reaction vessel, which, as indicated above, I do not believe to be justified.

As is to be expected, there is no essential difference between the formula obtained from our theory and that of Todes for the limiting case of high pressures, if $(C_M/Q)(RT_0^2/E)$, where C_M is the specific heat, is small, provided the pre-induction period is neglected. [In our papers $(C_M/Q)(RT_0^2/E)$ is equal to 2θ, as shown in Eq. (14) of Rice, Allen and Campbell,[1] whereas it is $(\lambda\alpha)^{-1}$ in Todes' work.] Under these circumstances, Eq. (4) of Rice and Campbell[5] reduces to Eq. (11) of Appin, Chariton, and Todes,[1d] except for a factor of $(1-e^{-2})$, which relatively unimportant factor reflects a difference in the exact time at which the induction period is assumed to end.

The application by Harris of the formula which neglects the pre-induction period to his own data on diethyl peroxide seems questionable. In a number of respects the explosion of diethyl peroxide seems to differ from those of azomethane and ethyl azide, while in other respects it is similar. Unfortunately, Harris has omitted many details in the presentation of his experimental work, which, on the whole, seems to be in disagreement with earlier work of Neumann and Tutakin[9] on the same explosion. I believe there is, perhaps, some doubt that the explosion of ethyl peroxide is a purely thermal explosion.

3. Some Remarks on the Theory of the Induction Period

In the theory of the induction period of a thermal explosion, it has generally been assumed that the rate of loss of heat from the reaction vessel is proportional to the difference between the temperature inside and outside the flask. There may be some possibility, however, that this assumption is incorrect. The complete answer to this question could be obtained, for the case where the heat is removed by conduction only, by solving the general equation for heat conduction, rather than the steady-state equation. This, however, would be extremely difficult. The steady-state equation does, at any rate, allow us to consider this question for the steady states set up with various values of δ up to the maximum, obtained, say, by varying the pressure while holding T_0 constant. These correspond to different mean internal temperatures in the flask, and the rate of flow of heat in these cases may be compared with the excess of this mean temperature over T_0.

By the mean internal temperature in the flask is meant an average temperature such that the same amount of reaction would take place if the flask were all at this average temperature. In formulating this mathematically it is convenient to consider T/T^*, which gives essentially the excess of temperature at any point inside the flask, the rate of reaction being proportional to $e^{-E/RT_0}e^{T/T^*}$, or, since the first factor is constant if T_0 is fixed, simply to e^{T/T^*}. The average value $\overline{T/T^*}$, then, will be given by setting $e^{\overline{T/T^*}}=\overline{e^{T/T^*}}$, where $\overline{e^{T/T^*}}$ is the average obtained by averaging e^{T/T^*} over all elements of volume of the flask. The volume of an element in the form of a spherical shell is proportional to $\zeta^2 d\zeta$ (where ζ is the quantity defined just before Eq. (2)), so that

$$\overline{e^{T/T^*}}=3\int_0^1 e^{T/T^*}\zeta^2 d\zeta.$$

[9] M. B. Neumann and P. M. Tutakin, Acta Physicochimica U. R. S. S. 9, 873 ff. (1938).

TABLE II.

δ	$\overline{T/T^*}$	$-x_0(d\phi/dx)_0$	$-\frac{x_0(d\phi/dx)_0}{\overline{T/T^*}}$
0.240	0.016	0.081	5.1
0.852	0.066	0.303	4.6
2.283	0.219	0.948	4.3
3.15	0.402	1.57	3.9
3.33	0.588	2.00	3.4

Introducing the quantities x, ϕ, and finally F, and noting Eq. (10)) this becomes

$$\overline{e^{T/T^*}} = 3x_0^{-3}\int_0^{x_0} e^{\phi+a}x^2dx$$
$$= 3\delta^{-1}x_0^{-1}\int_0^{x_0} Fdx. \tag{11}$$

Since the relationship between x_0, δ, and $\int_0^{x_0}Fdx$ is readily found from Fig. 1, the value of $\overline{T/T^*}$ corresponding to any δ can be found from Eq. (11).

Now the rate at which heat is conducted from the flask is proportional to $-d(T/T^*)/d\zeta$ for $\zeta=1$. This is equal to $-x_0(d\phi/dx)_0$. By Eq. (7)

$$-x_0(d\phi/dx)_0 = x_0^{-1}\int_0^{x_0} Fdx,$$

so that $-x_0(d\phi/dx)_0$ is readily evaluated from Fig. 1.

In Table II we give values of $\overline{T/T^*}$ and $-x_0(d\phi/dx)_0$ for various values of δ up to the maximum. If the rate of flow of heat were directly proportional to the excess of temperature inside the flask, or $\overline{T/T^*}$, these two quantities should show direct proportionality, and reasonable proportionality is indicated. The trend for $-x_0(d\phi/dx)_0$ is displaced somewhat toward that expected from proportionality with $(T/T^*)^{\frac{1}{2}}$. This indicates that some modification of the simple theory of the induction period would be an improvement, and suggests that we try a square-root law for the heat loss, to see the effect such a modification might have.

As a matter of fact, the theory of Rice, Allen, and Campbell can be modified readily and carried through on such a basis.[10] The greatest change comes in the estimate of the time necessary to heat the gas up to the temperature of the reaction flask, and it is not impossible that such a square-root law would increase our estimate of Q by 30–40 percent. It seems unlikely, however, that the first-power law is in error by as large an amount as this.

CONCLUSIONS

While it seems probable that neither the errors in Q due to the experimental work, the errors in Q due to the form of the theory used, nor the error in the estimate of λ could be sufficient alone to account for the high δ values of Table I, it is possible that all these together could account for them. It seems likely that at low pressures all the heat is actually removed by thermal conduction. in accordance with the views of Frank-Kamenetzky. The undoubted change in the character of the heat removal process at higher pressures is perhaps evidence in favor of this, as this could well indicate that convection first becomes important at the high pressures. On the other hand, the fact that the value of δ for ethyl azide is closer to the theoretical value for a 50-cc flask than for a 200-cc flask may indicate that there is still some effect due to convection or turbulence even at low pressures, at least in the 200-cc flask. However, the difference between the flasks of different size is sufficiently small so that no definite conclusion can be drawn.

We may summarize the principle results of the paper by saying, first, that thermal conduction is an important, if not the exclusive, means of heat removal at low pressures in the explosions of azomethane and ethyl azide, and, secondly, that the explosion of methyl nitrate is probably not a thermal explosion.

[10] H. C. Campbell, thesis, Harvard University, 1935.

The Reaction of Hydrogen Atoms with Butane

E. W. R. Steacie and E. A. Brown
Physical Chemistry Laboratory, McGill University, Montreal, Canada

(Received June 21, 1940)

The reaction of hydrogen atoms, produced by the Wood-Bonhoeffer method, with butane has been investigated over the temperature range 35° to 250°C. The activation energy is 9±1.5 kcal. The products consist solely of methane at low temperatures. At high temperatures ethane is also formed. It is concluded that the results indicate a mechanism in which a series of "atomic cracking" reactions play the main role. The main steps in the postulated mechanism are:

Primary process

$$H+C_4H_{10}\rightarrow C_4H_9+H_2.$$

Secondary processes at low temperatures

$$H+C_4H_9\rightarrow C_3H_7+CH_3$$
$$\rightarrow 2C_2H_5$$
$$H+C_3H_7\rightarrow C_2H_5+CH_3$$
$$H+C_2H_5\rightarrow 2CH_3$$
$$H+CH_3\rightarrow CH_4.$$

Additional secondary processes at higher temperatures

$$C_4H_9\rightarrow C_2H_4+C_2H_5$$
$$H+C_2H_4\rightarrow C_2H_5$$
$$C_3H_7\rightarrow C_2H_4+CH_3$$
$$H_2+C_2H_5\rightarrow C_2H_6+H$$
$$H_2+CH_3\rightarrow CH_4+H.$$

Introduction

"Atomic cracking" reactions of the type

$$H+C_2H_5\rightarrow 2CH_3,$$

first suggested by Taylor,[1] have assumed considerable importance in connection with the mechanism of the elementary reactions of the hydrocarbons.[2] Strong evidence for the occurrence of reactions of this type was furnished by the work of Steacie and Parlee[3,4] on the reaction of hydrogen atoms with propane. They found that at low temperatures the only product of the reaction was methane, and concluded that its exclusive formation could only be explained by the postulation of an initial abstraction of a hydrogen atom

$$H+C_3H_8\rightarrow C_3H_7+H_2,$$

followed by a series of atomic cracking reactions

$$H+C_3H_7\rightarrow CH_3+C_2H_5,$$
$$H+C_2H_5\rightarrow 2CH_3.$$

In view of the importance of the results with propane, it was considered of interest to extend the work to butane. The only previous work on the reaction of hydrogen atoms with butane is one run made by Trenner, Morikawa and Taylor[5] in the course of another investigation.

Experimental

The reaction was investigated by the Wood-Bonhoeffer method, atomic hydrogen being produced by an electrical discharge. The apparatus was similar to that used in a number of previous investigations.[3,4,6]

Hydrogen was taken from a commercial cylinder and passed through a tube containing platinized asbestos at 500°C. The gas then passed through a blow-off trap, a liquid-air trap to remove water and other impurities, and entered the discharge through a capillary flowmeter.

Butane was obtained from the Ohio Chemical and Manufacturing Company. It contained no impurities detectable by the analytical methods used. Variations in the flow rate of both gases

[1] H. S. Taylor, J. Phys. Chem. **42**, 763 (1938).
[2] E. Gorin, W. Kauzmann, J. Walter and H. Eyring, J. Chem. Phys. **7**, 633 (1939).
[3] E. W. R. Steacie and N. A. D. Parlee, Trans. Faraday Soc. **35**, 854 (1939).
[4] E. W. R. Steacie and N. A. D. Parlee, Can. J. Research **B17**, 371 (1939).
[5] N. R. Trenner, K. Morikawa and H. S. Taylor, J. Chem. Phys. **5**, 203 (1937).
[6] E. W. R. Steacie, Can. J. Research **B15**, 264 (1937).

TABLE I. *Reaction of hydrogen atoms with butane. Pressure = 0.35 mm.*

Run No.	Temperature, °C	Atom concentration, percent	Butane flow, moles per sec. at NTP ×10⁵	Hydrogen flow, moles per sec. at NTP ×10⁵	Products of the reaction, moles percent*			Percent of C_4H_{10} reacted
					C_4H_{10}	CH_4	C_2H_6	
1	35	5	0.332	2.03	63.8	36.2	0.0	12.2
2	35	5	0.326	2.03	65.8	34.2	0.0	11.8
3	35	5	0.332	2.03	66.2	33.8	0.0	11.3
4	100	5	0.334	2.03	73.6	19.6	6.8	10.0
5	100	5	0.306	2.03	72.4	20.2	7.4	10.4
6	100	5	0.282	2.03	72.5	20.1	7.4	10.5
7	100	5	0.277	2.03	72.0	19.2	8.8	11.5
8	100	5	0.243	2.03	70.0	23.6	6.4	11.4
9	170	3	0.325	2.03	70.2	12.9	16.9	14.5
10	170	3	0.300	2.03	71.5	10.7	17.8	13.8
11	170	3	0.303	2.03	68.2	12.5	19.3	15.5
12	170	3	0.300	2.03	71.8	12.6	15.6	12.8
13	250	(1)†	0.303	2.03	70.8	9.1	20.1	14.8
14	250	(1)†	0.282	2.03	70.6	9.2	20.2	15.1
15	250	(1)†	0.288	2.03	72.4	7.4	20.2	14.8

* Together with traces of unsaturates and higher hydrocarbons at higher temperatures.
† Roughly. The accuracy of the determination of these small values is poor.

were accomplished by varying the pressure on the supply side of the capillary flowmeter.

The hydrogen was passed through a straight Pyrex discharge tube of 2.5 cm bore, about 30 cm long, to which were sealed side tubes containing cylindrical aluminum electrodes. The electrodes were pinched on to stout platinum wires which passed out through the glass by means of capillary tubes and De Khotinsky seals. The discharge was operated with an applied voltage of 3500 across the tube and a 5000-ohm resistance. The operating current of 200 milliamperes was kept constant by means of a rheostat in the primary of the transformer.

The reaction vessel was situated as close as possible to the discharge. It consisted of a Pyrex cylinder 7 cm in diameter and 30 cm long, and had a volume of 1370 cc. It was surrounded by a removable electric furnace. Two tubes entered the reaction vessel from below, one of which served as an inlet for propane, while the other was a thermocouple well.

The walls of the apparatus were "poisoned" in the usual way with phosphoric acid. At higher temperatures, the efficiency of the poisoning fell off owing to the dehydration of the phosphoric acid. After a number of preliminary runs, it was found that although the efficiency of the poisoning had fallen off considerably, conditions were extremely stable. The system was therefore used in this condition, although the atom concentrations were thus lower than those usually employed (1–5 percent). The atom concentration was measured by means of a Wrede diffusion gauge of the usual type.

The size of the reaction vessel and the speed of the pumps were such that the contact time was of the order of one second. After leaving the reaction vessel the products passed through a liquid-air trap which removed butane and higher hydrocarbons together with most of any ethylene or ethane present. The remainder of the gas passed through a fast three-stage steel diffusion pump. After leaving this the low boiling products were removed by a trap containing silica gel at −180°C. The unadsorbed gas passed out of the system through a Hyvac pump.

TABLE II. *Average values of analyses.*

Temperature, °C	Percent Butane Converted to		Total percent reaction
	CH_4	C_2H_6	
35	11.8	0.0	11.8
100	7.9	2.8	10.7
170	5.8	8.3	14.1
250	4.4	10.5	14.9

At the end of a run, which normally lasted about two hours, the traps were allowed to warm up, and the products were pumped into a portable mercury gas holder by means of a Toepler pump. Trials showed that all the ethane and ethylene and virtually all the methane were trapped by the silica gel. A small amount of hydrogen was also retained by the gel.

The products of an average experiment amounted to about 500 cc of gas at NTP. The gas was analyzed in a low temperature distillation apparatus of the Podbielniak type. In the distillation methane and hydrogen were taken off together, and this fraction was analyzed by combustion. In addition to the distillation analysis, occasional checks on the fractions were made for unsaturates by conventional methods.

RESULTS

The experimental results of runs made at four different temperatures are given in Table I.

It is noteworthy that the sole product of reaction at room temperature is methane. There is no doubt, as shown by blank runs, that ethane

would have been detected if it had been present to the extent of 0.5 percent. Ethane is formed in considerable amount at higher temperatures, but the absence of propane over the whole temperature range is surprising. Higher hydrocarbons were not present in detectable amount, but a slight oiliness on the surface of the mercury in the Toepler pump indicated that traces must be present.

The trend of the products with temperature is best shown by the data of Table II.

Table III gives the collision yield and the activation energies calculated on the assumption that the steric factor A in the equation

$$\text{Collision yield} = Ae^{-E/RT}$$

is equal to 0.1. In the table $Z_{C_4H_{10},\,H}$ represents the number of collisions of one butane molecule with hydrogen atoms in the reaction time. In making this calculation, the diameter of the butane molecule was taken as 4.8×10^{-8} cm,[7] and the diameter of a hydrogen atom as 2.14×10^{-8} cm.[8]

In Fig. 1 the collision yields of the individual products (i.e., the number of molecules of each product produced per collision between a hydrogen atom and a butane molecule) are plotted against temperature. This gives the most unambiguous picture of the results, since the use of collision yields automatically corrects the results for variations in atom concentration, reaction time, etc.

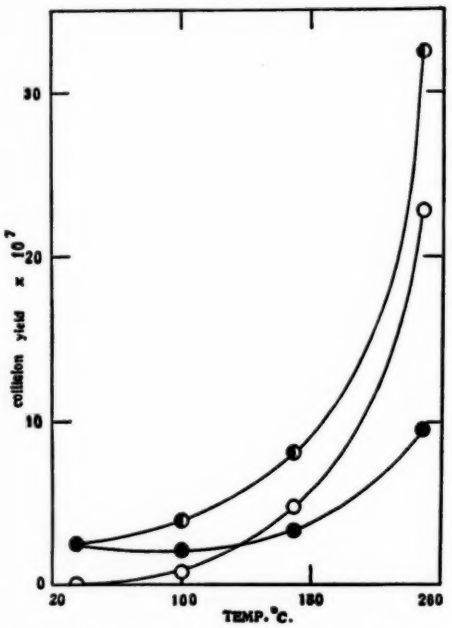

FIG. 1. Collision yields of the individual products. Methane—full black circles, ethane—open circles, total—half-black circles.

Comparison of the collision yields with those of Steacie and Parlee for propane shows that butane reacts with hydrogen atoms considerably faster than propane. This agrees with previous

[7] T. Titani, Bull. Inst. Phys. Chem. Research (Japan) **8**, 433 (1929).

[8] K. F. Bonhoeffer and P. Harteck, *Photochemie* (Leipzig, 1933).

TABLE III. *Calculation of collision yields, etc.*

RUN NO.	TEMPERATURE, °C	TOTAL FLOW, CORRECTED FOR PRESENCE OF ATOMS, MOLES PER SEC. $\times10^5$	REACTION TIME, SEC.	PARTIAL PRESSURE OF HYDROGEN ATOMS, MM	$Z_{C_4H_{10},H}$ IN REACTION TIME	PERCENT REACTION	COLLISION YIELD	ACTIVATION ENERGY, KCAL. ASSUMING $A=0.1$
1	35	2.46	1.01	0.016	4.81×10^5	12.2	2.45×10^{-7}	7.9
2	35	2.46	1.01	0.016	4.81	11.8	2.45	7.9
3	35	2.46	1.01	0.016	4.81	11.3	2.35	7.9
4	100	2.46	0.84	0.016	3.62	10.0	2.76	9.5
5	100	2.43	0.85	0.016	3.66	10.4	2.84	9.5
6	100	2.41	0.86	0.016	3.70	10.5	2.84	9.5
7	100	2.41	0.86	0.016	3.70	11.5	3.11	9.4
8	100	2.37	0.87	0.016	3.76	11.4	3.03	9.4
9	170	2.42	0.72	0.0093	1.71	14.5	8.49	10.3
10	170	2.39	0.73	0.0093	1.73	13.8	7.98	10.3
11	170	2.39	0.73	0.0093	1.73	15.5	8.97	10.2
12	170	2.39	0.73	0.0093	1.73	12.8	7.41	10.4
13	250	2.35	0.63	0.0031	4.57×10^4	14.8	3.32×10^{-6}	10.7
14	250	2.33	0.63	0.0031	4.61	15.1	3.28	10.7
15	250	2.34	0.63	0.0031	4.59	14.8	3.23	10.7

investigations which indicate increasing reaction with increasing molecular weight of the hydrocarbon.[5,9]

The present experiments show no formation of propane. This is not in agreement with the results of the run made by Trenner, Morikawa and Taylor, who reported three percent propane in the products at 110°C. In their experiments, which were made with deuterium atoms, the propane formed was not deuterized. This is difficult to understand, since the only possible way for propane to be formed and not deuterized would seem to be by the reaction

$$D+C_4H_{10}\rightarrow C_3H_8+CH_2D,$$

and all recent evidence seems to be against the occurrence of hydrocarbon chain breaking reactions of this type.

Apart from this the results are in excellent general agreement with those of Trenner, Morikawa and Taylor.

Discussion

The main facts to be explained are (a) the occurrence of methane as the sole product at low temperatures; and (b) the occurrence of ethane at higher temperatures.

The primary step

For the primary step the possibilities are

$$H+C_4H_{10}\rightarrow C_4H_9+H_2, \quad (1)$$
$$H+C_4H_{10}\rightarrow C_3H_8+CH_3, \quad (1a)$$
$$\rightarrow C_3H_7+CH_4, \quad (1b)$$
$$\rightarrow C_2H_6+C_2H_5. \quad (1c)$$

If (1a) or (1c) occurred, propane and ethane should be found even at low temperatures. Since they are not found in the products at room temperature they may be ruled out. (1b) can be ruled out by analogy with (1a) and (1c). The primary step must therefore be reaction (1).

Secondary reactions at low temperatures

The only way in which methane can be the exclusive product at low temperatures would appear to be by a set of "atomic cracking" reactions.

$$H+C_4H_9\rightarrow C_3H_7+CH_3, \quad (2a)$$
$$\rightarrow C_2H_5+C_2H_5, \quad (2b)$$
$$H+C_3H_7\rightarrow C_2H_5+CH_3, \quad (3)$$
$$H+C_2H_5\rightarrow 2CH_3, \quad (4)$$
$$H+CH_3\rightarrow CH_4. \quad (5)$$

Reactions of hydrogen molecules with radicals can be ruled out at low temperatures, since these would lead to the formation of propane and ethane. Also

$$H_2+CH_3\rightarrow CH_4+H \quad (7a)$$

does not occur measurably below 160°C.[10,11]

Radical recombination reactions can also be ruled out since they would lead to the formation of ethane and propane, and in any case the concentration of atomic hydrogen is so much greater than that of any radical that reaction (5) will outweigh other recombination reactions.

Secondary reactions at higher temperatures

At higher temperatures two additional types of reaction may be expected to make their appearance:

(a) decomposition of radicals

$$C_4H_9\rightarrow C_3H_6+CH_3, \quad (6a)$$
$$\rightarrow C_2H_4+C_2H_5, \quad (6b)$$
$$C_3H_7\rightarrow C_2H_4+CH_3. \quad (6c)$$

(b) reactions of radicals with molecular hydrogen

$$H_2+C_3H_7\rightarrow C_3H_8+H, \quad (7a)$$
$$H_2+C_2H_5\rightarrow C_2H_6+H, \quad (7b)$$
$$H_2+CH_3\rightarrow CH_4+H. \quad (7c)$$

The increasing formation of ethane is undoubtedly to be ascribed to two causes. In the first place the concentration of ethyl radicals rises due to (6b) and to the hydrogenation of ethylene produced by (6b) and (6c) by the reaction

$$H+C_2H_4\rightarrow C_2H_5. \quad (8)$$

This reaction is known to be very fast, since the presence of ethylene causes a rapid removal of hydrogen atoms. In the second place reaction (7b) comes into play at higher temperatures. It is further favored by the diminished hydrogen atom concentration which results from the occurrence of (8).

The absence of propane requires explanation, since it would be expected that (7a) would lead to its formation. Its absence is apparently due to the fact that (7a) only becomes appreciable at

[9] W. Frankenburger and R. Zell, Zeits. f. physik. Chemie **B2**, 395 (1929).

[10] H. S. Taylor and C. Rosenblum, J. Chem. Phys. **6**, 119 (1938).

[11] K. Morikawa, W. S. Benedict and H. S. Taylor, J. Chem. Phys. **5**, 212 (1937).

temperatures at which (6c) is fast enough to destroy the propyl radicals before they can react.

Any propylene formed by (6a) will presumably be immediately hydrogenated by the analog of (8).

$$C_3H_6+H\rightarrow C_3H_7. \qquad (8a)$$

It should be emphasized that the most important feature of the mechanism is the fact that the products of the reaction can only be accounted for on the assumption that "atomic cracking" reactions play the major role. This work, therefore, furnishes further strong evidence for the occurrence of such reactions as

$$H+C_2H_5\rightarrow 2CH_3$$
$$H+C_3H_7\rightarrow C_2H_5+CH_3$$

and adds to the list the reactions

$$H+C_4H_9\rightarrow CH_3+C_3H_7$$
$$H+C_4H_9\rightarrow 2C_2H_5.$$

The activation energy of the reaction

Over the temperature range of this investigation, the value of the activation energy of the over-all reaction rises from 7.9 kcal. at 35°C to 10.7 kcal. at 250°C. Since the primary process in the above mechanism is the only butane consuming step, and since practically no substances other than transitory ones are consumed in secondary processes, the above activation energy may be assumed to be that of the primary step.

The variation in E from 7.9 to 10.7 kcal. with rising temperature is presumably to be ascribed to uncertainties in the concentration of atomic hydrogen. In the first place the values of the atom concentration at 250°C are only approximate. Secondly, the measurements of atom concentrations can only be made in blank runs with no butane present. At the higher temperatures the collision yield increases and since the main steps in the process involve the consumption of hydrogen atoms, the atom concentration must be appreciably reduced. The lower value of the activation energy, therefore, is probably the more reliable one. We may therefore take the value of E as 9 ± 1.5 kcal. This is somewhat lower than the value found for propane, 10 ± 2 kcal. The difference is undoubtedly significant, since the collision yields are definitely higher for butane than for propane.

SEPTEMBER, 1940 JOURNAL OF CHEMICAL PHYSICS VOLUME 8

Molecular Structure of Nitrogen Dioxide and Nitric Acid by Electron Diffraction[1]

LOUIS R. MAXWELL AND V. M. MOSLEY
Bureau of Agricultural Chemistry and Engineering, Washington, D. C.

(Received May 13, 1940)

New electron diffraction photographs have been taken of NO_2 extending the region previously investigated to include larger angles of scattering. An interference ring was found at $(1/\lambda)\sin\frac{1}{2}\theta=0.49$ followed by another ring appearing at 0.94 as determined by visual measurements. The outer portion of the pattern consists of two rather broad rings and two well-defined minima. Theoretical intensities of scattering were computed for various nitrogen valence angles, assuming the positions of the two oxygens to be equivalent. The best fit, and probably the correct structure, gives the angle $O-N-O=130\pm2°$ with the $N-O$ distance $1.21\pm.02$A. Photographs were obtained from pure nitric acid vapor at 70°–85°C. The interference maxima were measured visually as far out as the eighth maximum at $(1/\lambda)\sin\frac{1}{2}\theta=1.83$; a prominent minimum was seen at 1.54. Theoretical intensities were computed for various likely models, disregarding the scattering by the hydrogen atom. Good agreement was obtained for a planar model having an NO_2 group with the same structure found for nitrogen dioxide. The third oxygen atom O′ is located at a distance of 1.41 ± 0.02A from the nitrogen atom and equidistant from the other oxygen atoms. A model having the nitrogen atom slightly out of the plane containing the oxygen atoms also gave good agreement with the experimental results. This model however is considered less probable in view of Raman spectra data which apparently require a planar structure for $O'-NO_2$.

INTRODUCTION

PREVIOUS electron diffraction work[2] on NO_2 showed certain nitrogen valence angles to be inconsistent with the experimental results obtained; however, sufficient data were not available to provide an accurate determination of the molecular structure. Considerable work[3] has been done on the interpretation of the infra-red

[1] For a preliminary report on this work, see Phys. Rev. **57**, 1079A (1940).

[2] Maxwell, Mosley, and Deming, J. Chem. Phys. **2**, 331 (1934).

[3] Sutherland and Penney, Proc. Roy. Soc. **A156**, 678 (1936).

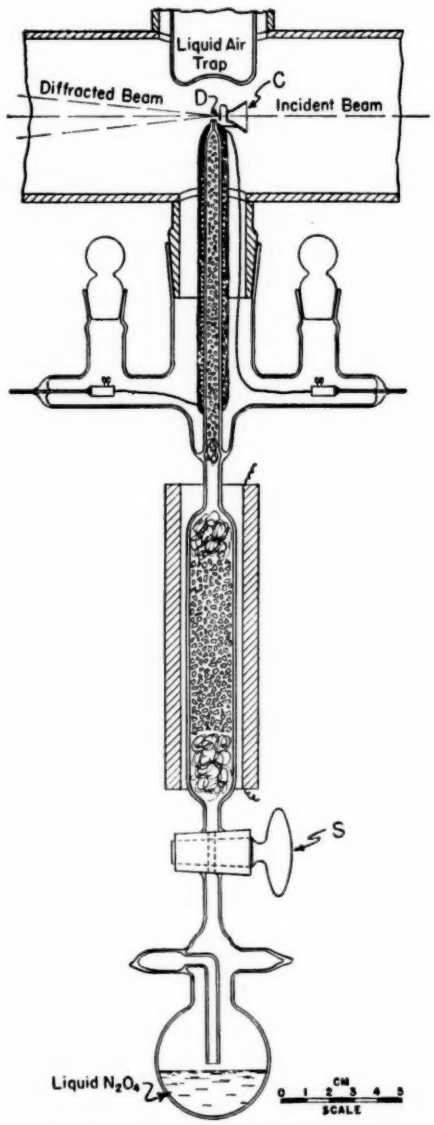

FIG. 1. A sketch showing part of the experimental arrangement used for electron diffraction from NO_2.

spectrum of NO_2 but several difficulties were encountered which made a structure determination uncertain. The product of the three principal moments of inertia of NO_2 has been determined from entropy measurements[4] so that if either the nitrogen valence angle or the N—O distance were known the other constant could be readily obtained. The present investigation extends the electron diffraction experiments to include larger angles of scattering in an effort to obtain more definite information on the structure of this molecule. Work now in progress in the spectroscopic section of this laboratory on the infra-red absorption of nitric acid vapor shows that below 80°C the rate of decomposition is so slow that it is possible to obtain electron diffraction photographs from nitric acid molecules free from products of dissociation. Structure determinations obtained from Raman spectrum data[5] on nitric acid have led to rather definite conclusions, although the complete structure is not yet known.

[4] Giauque and Kemp, J. Chem. Phys. **6**, 40 (1938).

TABLE I. *Summary of electron diffraction results obtained from* NO_2.

Description of Interference Ring	Position			
	$(1/\lambda)\sin\frac{1}{2}\theta$	x_{exp} (N—O=1.21A)	x_{theo} (O—N—O=130°)	$\frac{x_{theo}}{x_{exp}}$
1st maximum	0.49 ±.02(4)*	7.45	7.80	1.047
2nd maximum	0.940±.01(15)	14.29	14.40	1.008
Broad ring, outer edge measured	1.41 ±.02(7)	21.44	21.20	0.989
Broad ring, center measured	1.76 ±.01(5)	26.76	26.75	1.000
Minimum, well defined	1.52 ±.01(6)	23.11	23.50	1.017
Minimum, well defined	1.96 ±.01(5)	29.80	30.00	1.007

* Numbers in parentheses give number of photographs used for measurement. Variation given represents the average deviation (without regard to sign) found between separate photographs.

EXPERIMENTAL

Figure 1 illustrates the type of apparatus used for the work on NO_2. Liquid N_2O_4[6] was used for the production of the NO_2 vapor. The temperature of the source was raised to values between 43 and 95°C, depending upon the amount of electron scattering desired. Gas leaving the source passed through two tubes filled with broken glass maintained at approximately 130°C. This temperature was sufficient to shift the $N_2O_4 \rightleftarrows 2NO_2$ equilibrium to the high concentration of NO_2 necessary for the electron diffraction photographs. A diaphragm *D* was introduced to reduce background scattering from the edges of the opening in the small cone *C*.

This arrangement was also used for the work on nitric acid after removing the lower heating tube. In this case the stopcock was removed and the amount of gas entering the diffraction chamber

[5] Chedin, J. de phys. et rad. **10**, 445 (1939).

[6] The liquid N_2O_4 used in this work was kindly prepared by Mr. J. Y. Yee of this laboratory, using his special oxidizer. See Ind. Eng. Chem. **21**, 1024 (1929).

was controlled by varying the temperature of a bath surrounding the source of liquid nitric acid. Bath temperatures ranged between 70 and 85°C during the exposures and the heating column was held at 70 to 85°C. This additional heating prevented condensation of the nitric acid vapor before it entered the diffraction chamber.

Plate distances used were 10.0 cm and the de Broglie wave-length values ranged from 0.0485A to 0.0815A depending on the regions of the diffraction pattern under investigation. Lantern slide plates were used for the work on NO_2 while both lantern slide and x-ray plates recorded the patterns obtained from HNO_3.

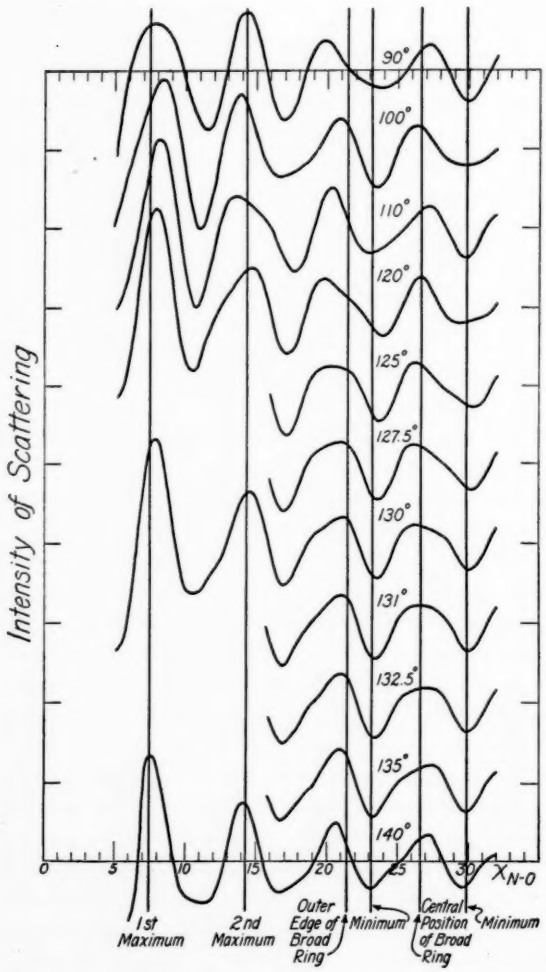

FIG. 2. Theoretical curves computed for various assumed models of NO_2. The positions of the experimental maxima and minima are also shown for comparison in terms of x_{n-0} where the N−0 distance was assumed to be 1.21A, i.e. $x_{n-0}=4\pi(1/\lambda)(l=1.21\text{A})\sin\frac{1}{2}\theta$.

RESULTS AND DISCUSSION

Nitrogen dioxide

Table I summarizes the electron diffraction results obtained from NO_2. An interference ring was obtained at $(1/\lambda)\sin\frac{1}{2}\theta=0.49$ followed by a second maximum at 0.94. A third ring was broad with a definite outer edge which in some photographs looked like a maximum. The fourth ring whose center was measured at $(1/\lambda)\sin\frac{1}{2}\theta=1.76$ was also quite broad; two well-defined minima were located at 1.52 and 1.96, respectively. Previous electron diffraction work[2] on NO_2 investigated the scattering out to $(1/\lambda)\sin\frac{1}{2}\theta=0.6$ and within this range no interference humps were obtained on the densitometer records; also it was reported that no diffraction rings could be seen on the photographic plates. A long plate distance of 26.2 cm was used in that work to permit a greater spread of the electron scattering for use with the densitometer recordings. Since a diffraction ring is now observed at $(1/\lambda)\sin\frac{1}{2}\theta=0.49$, within the limit of the range previously studied, the earlier photographs have been reexamined and it is possible to detect on these plates a diffuse ring which is probably the one now reported at $(1/\lambda)\sin\frac{1}{2}\theta=0.49$. In the present case no densitometer records have been taken, because the important molecular structure data are the outer diffraction rings which unfortunately are very difficult to detect by means of the densitometer.

TABLE II. *Summary of electron diffraction results obtained from* HNO_3.

Number of Interference Maxima	Intensity	Position $(1/\lambda)\sin\frac{1}{2}\theta$	x_{exp} N−O=1.22A	x_{theo} Model No. 2	$\frac{x_{theo}}{x_{exp}}$
1	Weak	0.298±.004(2)*	4.57	4.20	0.92
2	Strong	0.503±.01 (6)	7.71	7.60	0.986
3	Medium	0.731±.004(5)	11.21	11.40	1.017
4	Medium	0.949±.006(3)	14.55	14.50	0.996
5	Weak	1.184±.004(4)	18.15	18.20	1.003
6	Weak	1.400±.004(4)	21.46	21.50	1.002
7	Very weak	1.644±.004(2)	25.20	25.25	1.002
8	Very weak	1.83 approx. (1)	28.05	28.20	1.005
Minimum	Well defined	1.541±.002(3)	23.62	23.50	0.995

* Numbers in parentheses give number of photographs used for measurement. Variation given represents the average deviation (without regard to sign) found between separate photographs.

Figure 2 shows theoretical scattering curves computed for various nitrogen valence angles in which the atomic scattering amplitudes ψ_i were

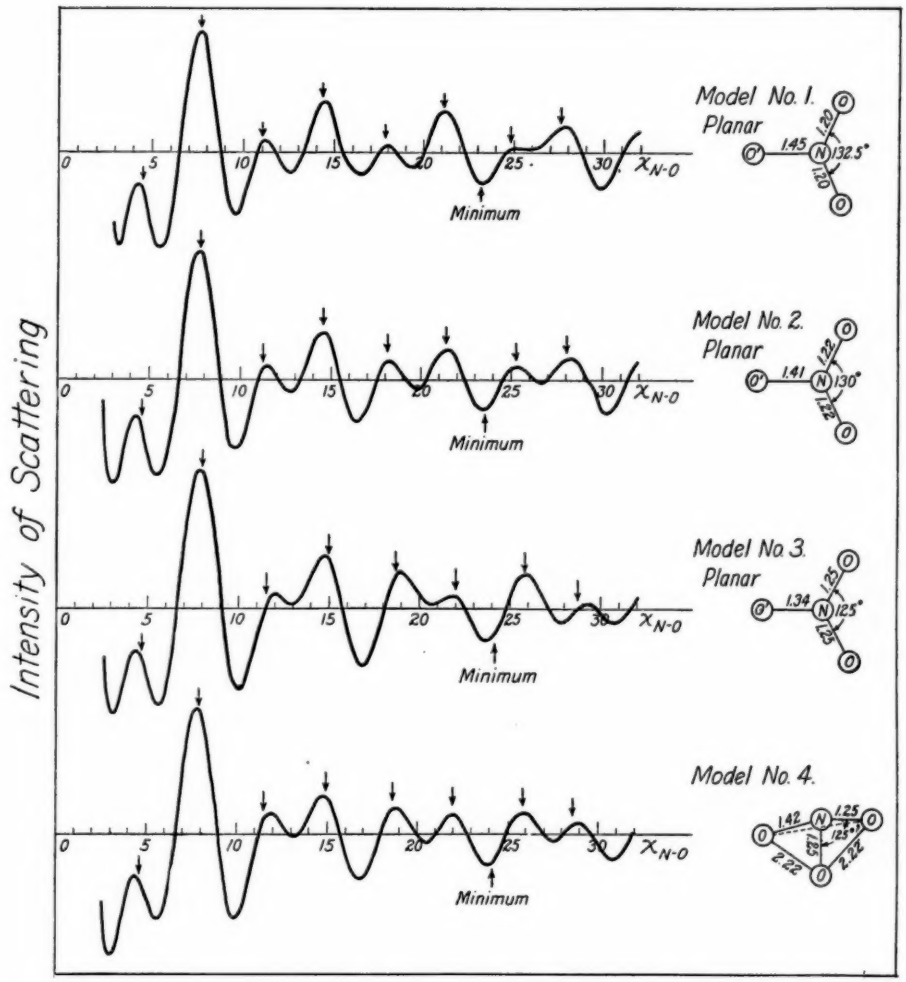

FIG. 3. Theoretical curves computed for various assumed models of HNO_3. For comparison, the positions of the experimental maxima and one minimum are indicated by arrows.

replaced by the atomic number Z_i. Some error may occur in locating the first maximum as pointed out earlier;[2] however, the correctness of this approximation can be verified for the outer rings by examining the atomic cross sections computed for nitrogen and oxygen.[7] In all cases the oxygen atoms were assumed to be located in equivalent positions. No theoretical curves were calculated for an unsymmetrical molecule although it is not improbable that such a model might give good agreement with the experimental results. Angles used range from 90° to 140° inclusive; the 60°, 150°, and 180° values were previously ruled out.[2] Theoretical curves for models in which the nitrogen valence angle is greater than 120° and less than 140° give intensity distributions in approximate agreement with the observed visual measurements described above. After considering a number of angles within this interval the best fit was found for a nitrogen valence angle of 130°. The final structure is given as follows:

$$\sphericalangle O-N-O=130\pm2°$$
$$N-O=1.21\pm0.02\text{A}.$$

Relative positions of the experimental and

[7] Theoretical values of the atomic electron scattering amplitudes for Hartree fields can be easily obtained from a table given by Mott and Massey, *Theory of Atomic Collisions* (Oxford University Press, London, 1933), p. 124. It is seen that the ratio ψ_n/ψ_0 for large values of $(1/\lambda)\sin\frac{1}{2}\theta$ approximates the ratio given by the Rutherford scattering law, i.e. Z_n/Z_0.

theoretical maxima, showing good agreement, are compared in Table I. An N−O distance of 1.21A is slightly greater than 1.18A, which is the value for the nitrogen-oxygen double bond separation obtained from revised data on covalent radii.[8] Very good agreement is found with a predicted distance of 1.20A made by Pauling[9] on the basis of a resonating electronic structure involving a nitrogen-oxygen double bond for one oxygen atom and a single plus a three-electron bond for the other oxygen. Entropy measurements[4] give an angle of 138° for this N−O distance of 1.21A, a value 8° greater than observed in the present case. Assuming the 130° valence angle, an N−O distance of 1.165A is obtained, about 0.04A less than the electron diffraction value.

Nitric acid

Electron diffraction results obtained from nitric acid vapor are summarized in Table II. The interference pattern is characterized by a weak first maximum at $(1/\lambda)\sin\frac{1}{2}\theta=0.298$, followed by a strong maximum at 0.503, then a series of rings measured to the eighth maximum at $(1/\lambda)\sin\frac{1}{2}\theta=1.83$. The positions of the interference maxima, but not the relative intensities, can be satisfactorily explained on the basis of a 2.22A distance within the molecule; thus models were chosen for computation in which all three oxygens were located approximately at the corners of an equilateral triangle, 2.22A on a side. Intensities of scattering by the approximate method $\psi_i=Z_i$, are shown in Fig. 3 for four such models. Scattering by the hydrogen atom has not been included for its contribution to the total scattering is small. Model 1 is eliminated because its seventh maximum is too weak; model 3 is also eliminated because the third maximum is too weak and the eighth is out of position. Models 2 and 4, however, give good agreement with the experimental results. It is difficult on the basis of the electron diffraction results alone to make a choice between models 2 and 4. Also, as in the case of nitrogen dioxide, equally good agreement could probably be found for a model in which the two oxygen atoms of the NO_2 group are not equivalent in position. It is therefore necessary to obtain additional information from other sources before selecting the most probable structure.

Considerable work has been done on the Raman effect in pure liquid nitric acid and recently Chedin[5] has discussed the structure of the molecule from this standpoint. He concludes that HNO_3 has the symmetry C_{2v} (hydrogen excluded) with two planes of symmetry perpendicular to each other, one plane containing all of the atoms and the other plane passing through the N−O′ bond and bisecting the ∢O−N−O. Accepting his argument as giving the correct symmetry of the nitric acid molecule, we can eliminate Model 4 mentioned above since it does not satisfy these requirements. Therefore we select Model 2 as being the most probable structure of nitric acid since it has the above symmetry. The molecular constants are as follows:

Planar (hydrogen atom excluded)

$$\sphericalangle O-N-O=130\pm5^\circ$$
$$\sphericalangle O'-N-O=115^\circ\pm2.5^\circ$$
$$N-O=1.22\pm0.02\text{A}$$
$$N-O'=1.41\pm0.02\text{A}.$$

It is seen that the structure of the NO_2 group is practically identical with that given above for nitrogen dioxide. The N−O′ distance is somewhat greater than the nitrogen-oxygen single bond distance[8] of 1.36A.

Comparable molecules studied by electron diffraction are methyl nitrate and fluorine nitrate.[10] In these the ∢O−N−O was given as 125° 16′ and 125±5°, respectively, the latter value agrees with the present data to within the experimental errors. The N−O distances found for these molecules were 1.26A and 1.29A, respectively, compared with 1.22A obtained in nitric acid. The N−O′ distance was 1.36A and 1.39A for the methyl and fluorine nitrate, respectively, as compared to 1.41A found for HNO_3. A structure for the NO_2 group in nitromethane[11] and tetranitromethane[12] of ∢O−N−O=127°, N−O=1.21–1.22A agrees very closely with the structure found in the present work.

[8] Pauling and Brockway, J. Am. Chem. Soc. **59**, 1223 (1937).
[9] Pauling, *The Nature of the Chemical Bond* (Cornell University Press, New York, 1939), p. 250.
[10] Pauling and Brockway, J. Am. Chem. Soc. **59**, 13 (1937).
[11] Brockway, Beach and Pauling, J. Am. Chem. Soc. **57**, 2693 (1935).
[12] Stosick, J. Am. Chem. Soc. **61**, 1127 (1939).

LETTERS TO THE EDITOR

This section will accept reports of new work, provided these are terse and contain few figures, and especially few halftone cuts. The Editorial Board will not hold itself responsible for opinions expressed by the correspondents. Contributions to this section should not exceed 600 words in length and must reach the office of the Managing Editor not later than the 15th of the month preceding that of the issue in which the letter is to appear. No proof will be sent to the authors. The usual publication charge ($3.00 per page) will not be made and no reprints will be furnished free.

Bond Length and Bond Strength

In a recent communication Wrinch and Harker[1] propose to extend the suggestion[2] that there is a 1–1 relation between the strengths and lengths of each bond, i.e., CN, CC, CH, etc., irrespective of the assigned numerical valencies in the various compounds considered. It has been found convenient[3] to define the term *bond strength* explicitly as the energy difference (per mole) between the lowest energy state of a compound and the summed lowest energy of the products formed by rupture of a bond.[4] There is no suggestion in such a definition of the mechanism of the decomposition; particularly there is no requirement for adiabatic dissociation. The latter requirement, however, is inherent in the term *spectroscopic heat of dissociation*.[5]

It is evident that the bond length is related to the force constant for the bond since both terms are concerned with the bond in its lowest vibrational state. Bond length is related to spectroscopic heat of dissociation less directly. There is a 1–1 relation for a particular class of bonds (e.g., CC) only if we can assume that the anharmonicity factor is constant[6] or varies in a regular manner with the bond length. Such an assumption may be approximately correct. In the employment of values derived from a "strength-length" relationship two points must be born in mind. (1) The values so obtained are approximate. Differences of 2–3 kcal. (which may be significant when it is desired to estimate relative activation energies) may not be real and may even be of the wrong sign. (2) The values so obtained are for spectroscopic heat of dissociation (i.e., the *adiabatic bond strength*) not for bond strength or bond energy as either of those two terms has hitherto been defined.

MILTON BURTON

Department of Chemistry,
New York University,
New York, New York,
August 5, 1940.

[1] D. Wrinch and D. Harker, J. Chem. Phys. **8**, 502 (1940).
[2] Cf. J. J. Fox and A. E. Martin, J. Chem. Soc. 2106 (1938); 884 (1939).
[3] Cf. (a) M. Burton, J. Chem. Phys. **6**, 817 (1938). (b) H. Henkin and M. Burton, *ibid.* **8**, 297 (1940).
[4] The term *bond strength*, so defined is to be contrasted with the term *bond energy* as used by L. Pauling (cf. *The Nature of the Chemical Bond* (Cornell University Press, Ithaca, 1939)). For polyatomic molecules whose bonds are all alike the bond energy is the average amount of energy per bond per mole required to break it into atoms.
[5] Cf. (a) G. K. Rollefson and M. Burton, *Photochemistry and the Mechanism of Chemical Reactions* (Prentice-Hall, Inc., New York, 1939). (b) G. Herzberg, *Molecular Spectra and Molecular Structure* (Prentice-Hall, Inc., New York, 1939).
[6] The assumption of such constancy was made by J. W. Ellis, Phys. Rev. **33**, 27 (1929) in some bond strength calculations and has been used repeatedly since. Cf. O. Redlich, J. Chem. Phys. **7**, 856 (1939).

The Calculation of the Heat Capacity and Entropy of Methylamine from Spectroscopic Data Alone. The Torsional Mode of Vibration

The recent paper of Owens and Barker[1] gives infra-red data from which they deduce the following frequency assignment for methylamine. $\nu(\pi)_{CH}$, 2964; $^2\nu(\sigma)_{CH}$, 2820; $\delta(\pi)_{CH}$, 1385; $^2\delta(\sigma)_{CH}$, 1470; $\nu(\pi)_{NH}$, 3410; $\nu(\sigma)_{NH}$, 3360; $\delta(\pi)_{NH}$, 1625; $\nu_{CH_3NH_2}$, 1043; $\delta_{1RR'}$, 780; $\delta_{2RR'}$, 780; $\delta_{3RR'}$, 1130; $\delta_{4RR'}$, 1150; torsion, 270.

Using these data the heat capacity has been calculated at three temperatures and compared with the experimental values of Felsing and Jesson.[2] The results are given in Table I. The experimental data have been corrected to the ideal gas state on the basis of the modified Berthelot equation which yields:

TABLE I.

TEMP. °K	C_p^0 CALC.	C_p^0 MEASURED
273.16	11.61	11.45
298.16	12.15	12.71
323.16	12.72	13.63

$$C_p - C_p^0 = 81/32 \cdot RT_c^3/T^3 \cdot P/P_c.$$

In the calculation, the torsional frequency (270 cm^{-1}) was used to evaluate the potential hindering rotation ($I_{red} = 1.82 \times 10^{-40}$, $V = 1520$ cal.), assuming three potential energy minima, using the method of Pitzer.[3] The torsional contribution to the heat capacity was then obtained from Pitzer's tables. The agreement is perhaps within experimental error.

The translational and rotational entropy of the rigid molecule, at the normal boiling point, were calculated using the moments deduced from the data of Owens and Barker ($I_1 = I_2 = 37.43 \times 10^{-40}$, $I_3 = 7.2 \times 10^{-40}$). To this result was added the entropy contribution due to the torsional oscillation (obtained from Pitzer's tables) and the vibrational entropy. The vibrational entropy was calculated on the basis of the above frequency assignment. The calculation is summarized in Table II. The sum is the

TABLE II. *Entropy of methylamine at 266.84°K.*

		CAL./DEG./MOLE
I	Translational and rotational	54.64
II	Torsional ($I_{red} = 1.82 \times 10^{-40}$, $V = 1520$)	1.84
III	Vibrational	.45
IV	Total	56.93
V	Calorimetric corrected to ideal gas	56.42
VI	Discrepancy	.51

value of the entropy of the ideal gas at the normal boiling point calculated from spectroscopic data alone. This is compared with the experimental value based upon the third law of thermodynamics.[4] According to a private communication from Professor Barker the identification of the strong band at 270 cm^{-1} with the torsional mode cannot be considered final. The comparisons may have some bearing on the point in that it would cast doubt on the assignment if we were sure of the correctness of the mathematical treatment of the torsion.

J. G. Aston
P. M. Doty

The Pennsylvania State College,
State College, Pennsylvania,
July 18, 1940.

[1] Owens and Barker, J. Chem. Phys. **8**, 229 (1940).
[2] Felsing and Jesson, J. Am. Chem. Soc. **55**, 4418 (1933).
[3] Pitzer, J. Chem. Phys. **5**, 469 (1937).
[4] Aston, Siller and Messerly, J. Am. Chem. Soc. **59**, 1743 (1937).

Hindered Rotation in Methyl Alcohol

A paper by Koehler and Dennison[1] has recently appeared in which these authors discuss the internal rotation in CH_3OH and examine the far infra-red data for this molecule; they conclude that the height of the barrier hindering internal rotation is probably 470±40 cm^{-1} (about 1340 cal./mole). It is the purpose of this letter to show that such a low barrier is not consistent with the third-law entropy data available for CH_3OH.

The heat capacity measurements of Kelley[2] may be combined with the data of Fiock, Ginnings and Holton[3] on the heat of vaporization and with vapor pressure data to give $S^0_{298}(g) = 56.63_5$ e.u.[4] Using the frequency assignment of Borden and Barker,[5] which seems to be a very reasonable one, the vibrational entropy is 0.257 e.u. (The frequencies, with their degeneracies, are 3683 (1), 2978 (2), 2845 (1), 1477 (2), 1455 (1), 1340 (2), and 1030 (2) cm^{-1}.) The entropy contribution due to over-all translation and rotation is 55.331 e.u.; the structure parameters used in this calculation were C−H distance, 1.09, C−O distance, 1.42, O−H distance, 0.96A. H−O−C angle 105°, methyl group angles tetrahedral.[6] This model does not differ significantly, for the present purpose, from that of Koehler and Dennison. The contribution of the internal rotation is thus fixed at 1.05±0.25 e.u., the estimate of error being increased somewhat over Kelley's estimate of 0.2 e.u. error in the entropy of the liquid.

An accurate calculation of the entropy of internal rotation is complicated by the fact that the moment of the CH_3 group is so large a fraction of the moment of the whole molecule about the CO bond; for this reason the interaction terms are relatively important. The parameter Ω_m [7] calculated from the assumed structure is 0.19923, and the effective moment for the internal rotation, F_m, is 0.63636 (masses being measured in atomic weight units and distances in angstroms). Using this effective moment with Pitzer's tables,[8] a barrier of 504 cm^{-1} gives a value of 1.69 e.u. for the entropy due to internal rotation. The more accurate calculation[7] including interaction terms raises this by about 0.3 e.u. Since the thermal data indicate that the torsional contribution cannot be more than 1.30 e.u., a discrepancy of at least 0.6 e.u. is present, and the barrier must be distinctly higher.

It would appear difficult to resolve this. The thermal data are apparently reliable to well within the estimated error, and it does not seem possible to change the vibrational assignment in any reasonable fashion sufficiently to eliminate this discrepancy.

Preliminary calculations based on the thermal data indicate a hindering potential of about 3400 cal./mole (1200 cm^{-1}). It is hoped that these calculations will be completed soon, and an attempt made to bring the thermal and direct spectroscopic evidence into agreement.

Bryce L. Crawford, Jr.

Sterling Chemistry Laboratory,
Yale University,
New Haven, Connecticut,
July 12, 1940.

[1] J. S. Koehler and D. M. Dennison, Phys. Rev. **57**, 1006 (1940).
[2] K. K. Kelley, J. Am. Chem. Soc. **51**, 181 (1929).
[3] E. F. Fiock, D. C. Ginnings and W. B. Holton, Bur. Stand. J. Research **6**, 881 (1931).
[4] L. S. Kassel, J. Chem. Phys. **4**, 493 (1936).
[5] A. Borden and E. F. Barker, J. Chem. Phys. **6**, 553 (1938).
[6] J. O. Halford and B. Pecherer, J. Chem. Phys. **6**, 571 (1938).
[7] B. L. Crawford, Jr., J. Chem. Phys. **8**, 273 (1940).
[8] K. S. Pitzer, J. Chem. Phys. **5**, 469 (1937).